Division of Engineering
BROWN UNIVERSITY
PROVIDENCE, R. I.

SURVEY OF METHODS OF ANALYSIS FOR PLASTIC DEFORMATION OF STRUCTURES UNDER DYNAMIC LOADING

P. S. SYMONDS

Department of the Navy
Office of Naval Research
Contract Nonr 3248(01)(X)
Naval Ship Research
And Development Center

BU/NSRDC/1-67 June 1967

Division of Engineering
BROWN UNIVERSITY
PROVIDENCE, R.I.

SURVEY OF METHODS OF ANALYSIS FOR PLASTIC DEFORMATION OF STRUCTURES UNDER DYNAMIC LOADING

BY

P.S. SYMONDS
Professor of Engineering
Brown University

Department of the Navy
Office of Naval Research
Naval Ship Research and Development Center
Contract Nonr 3248 (01)(X)

Final Report
BU/NSRDC/1-67
June, 1967

FORWARD

This survey attempts to make a critical study of methods described in the literature for the analysis of metal structures under dynamic loads leading to plastic deformations.

Analyses have now appeared in the literature of a considerable variety of structures of engineering interest. They include beams (under many conditions of loading, support, and materials), rings, arches, frames (simple rectangular bents), plates (circular and rectangular), membranes (i.e. plates with deflections greatly exceeding the thickness), and shells (axially symmetric loading on cylinders, spheres, and spherical caps). Most of these have been obtained by a rigid-plastic type of analysis (in which strain rates are assumed zero unless a yield condition is satisfied). A few have been obtained by wholly numerical approaches of finite difference type.

Experiments reported in the literature have in most cases shown that the actual permanent deflections are smaller than those predicted on the basis of plastic properties determined by quasi-static tests, the predictions often being in error by as much as 100 percent or more for mild steel, with smaller discrepancies for other metals, such as aluminum alloys or high strength steels. Strengthening under conditions of rapid straining has been considered the principal cause of such discrepancies; when it has been possible to modify the analysis to take account of the increase of yield and flow stresses at high strain rates, much better agreement has in most cases been obtained.

The mathematical approaches have depended heavily on assumptions. This is obviously true of analytical solutions such as rigid-plastic analysis.

It is also true, to a lesser extent, of the wholly numerical solutions; for example the "MIT method" (see Witmer et al (1963), (1967)*) depends on a parallel rod model of a beam or plate. Although "agreement" has often been obtained, it also has often been the case that only one or two tests were made for purposes of comparison. It is difficult to draw general conclusions unless the tests form a comprehensive series.

A plate or shell deforming plastically due to impact or shock loading behaves in an extremely complex manner which is difficult to analyze even if the laws of plasticity established for quasi-static conditions are exactly obeyed. Analytical solutions are out of the question except by rigid-plastic methods; when elastic deformations are included the solution of partial differential equations with moving boundaries is required, and in addition the equations become nonlinear if finite deflections must be considered, as is commonly the case. The fact that dynamic plastic properties are greatly different from those determined statically, for steel and some other important structural metals, increases the fundamental difficulty by orders of magnitude. Very little is known about dynamic plastic behavior except for uniaxial stress states and pure torsion. Extensions of such standard concepts of static plasticity as yield surfaces and flow rules (either in terms of stresses or of stress resultants) to conditions of rapid and variable straining have not been investigated. Mathematical solutions in the literature using such concepts whether by analytical or numerical means are speculative, and the results must be considered suspect.

---

* References are listed alphabetically in the Bibliography at the end of the report.

The present survey is limited to studies in some depth of analytical methods and experimental investigations on beams. This limitation is deliberate and believed justifiable, in view of the present absence of knowledge concerning laws of dynamic plasticity for complex stress states. A beam exhibits most of the major sources of complexity arising from mixed elastic and plastic behavior at large deflections. However the stress and strain states are relatively simple, apart from the possible influence of strain gradients. Thus the interactions between dynamic plastic stress resultants in a beam are relatively tractable. Also, and most important, for beams there are several published experimental investigations that are quite extensive and comprehensive. These make it feasible to carry out detailed analyses and interpretations of the test results, and thus to attempt to gain understanding of the basic processes and mechanisms.

It seems apparent to the writer that such basic understanding must first be reached for beams. There will then be a good chance of gaining it for general deformations of plates, membranes, shells, and other structures.

There are two important areas of dynamic plastic structural analysis, which have been developed in recent years, which have had to be treated inadequately in the survey. One is the area of numerical solutions by finite differences or finite elements. The other area is undoubtedly the major theoretical achievement in the subject in recent years, namely the development by Martin of energy techniques which furnish bounds on displacements and duration times (see Martin 1964, 1965, 1966). The study of the application of these methods and of the related mode approximation technique to analysis and design must be dealt with separately. These new methods promise to make possible the treatment in a simple but realistic way of complex structures under any

impulsive and perhaps more general classes of loading.

This survey was initiated and supported for an initial two year period by the Underwater Explosions Research Division of the Naval Ship Research and Development Center. The writer is most grateful for the helpful consideration shown by Dr. Schauer of the Underwater Explosions Research Division during the extended period of its preparation. The survey was begun as a joint project with Professor S. R. Bodner, whose valuable collaboration ended when he resigned to become Professor of Mechanics at Technion - Israel Institute of Technology. Material contributions were made at different times by Research Assistants D. P. Updike (now Assistant Professor at Lehigh University) and J. F. McNamara. Invaluable assistance was given by Miss Mary Huntsman in connection with drawings and illustrations, and by Mrs. Susan Erdmann who did most of the typing.

TABLE OF CONTENTS

Chapter I

MATERIAL PROPERTIES

1. Constitutive Laws. In analyses of structures deforming plastically under dynamic loads one must use appropriate constitutive laws, i.e. mathematical formulations of the essential features of behavior relating stress and strain tensors and their time derivatives.

The laws of plastic behavior of metals are generally defined as relations that are homogeneous in time; thus the material behavior involves no influence of times or rates. In fact, in structural metals rate effects may be of great importance, but we postpone discussion of them until a later section of this chapter. With this understanding, the main features of plastic behavior of structural metals are sketched in Figs. I 1(a), I 1(b), and summarized as follows:

(1) An elastic range governed by a yield stress or other yield conditions appropriate to the stress state.

(2) Plastic deformation with work hardening, governed by flow rules and loading conditions for three dimensional stress states.

(3) Irreversibility; unloading occurs elastically, leaving residual stresses and permanent (plastic) strains.

(4) Bauschinger effect; a reversal of loading after plastic deformations have occurred leads to plastic deformations in the reversed sense at lower stress magnitudes than those at which the previous plastic flow occurred.

In this review we shall be concerned with structures such as beams and plates where the state of stress is described by means of stress resultants such as bending moments and axial forces. The laws of plasticity concern relations between stress resultants and generalized strains such as curvature and strain at the center-line. They are derivable in general by calculation

from the stress-strain curve for simple tension or compression specimens together with yield conditions such as those of Tresca and von Mises. It is common to assume that plane sections remain plane.

2. Idealizations. Idealizations of plastic (time independent) behavior are essential to make analyses of plastic deformations tractable, in static and much more so in dynamic problems. Hence the bilinear stress-strain curve of Figs. I 1(c) is often used for elastic-plastic behavior; here the stress-strain relation has slope E_p in the plastic range $\sigma > \sigma_y$ for initial loading, while Young's modulus E governs elastic behavior. Further idealizations are indicated in Fig. I 1(d). Here the solid curve represents two drastic but often satisfactory idealizations: (1) the elastic modulus E is taken as infinite; and (2) the plastic slope E_p is taken as zero. The hypothetical material behavior is referred to as rigid-perfectly plastic. It is common to apply this type of analysis to static problems where plastic strain components greatly exceed elastic strains, and the material is very ductile. As will be discussed in detail in the review, the use of rigid-perfectly plastic analysis in dynamic structural problems makes for a very great simplification, so that it deserves careful study to determine the range of its validity.

For some problems strain hardening cannot be neglected. The idealized rigid-plastic material with work hardening is shown in Fig. I 1(d). In structural problems the need to consider strain hardening may arise not so much because strain hardening is large, but because some physical feature of the actual response disappears when perfectly plastic behavior is assumed. For example, in beams under either static or dynamic loading, large plastic deformations occur at plastic hinges. In the real structure these are short

regions (of the order of the beam depth) where intensive plastic flow occurs. If perfectly plastic behavior is assumed, the plastic hinge is a point on the beam center-line. The dependence of the size of the plastic hinge on the loads and on time can only be studied if the material is taken to have a finite degree of strain hardening. Another example is that of impact on the end of a long thin rod, when the impact is severe enough to produce stresses above the elastic yield stress σ_y. If the material is assumed to have a perfectly plastic behavior, there is no propagation of plastic stress and strain waves away from the impact end, and an infinitesimal segment of the rod at the struck end acquires infinite strains.

The point of these remarks is to emphasize that the neglect of strain hardening may be permissible in one problem but quite unrealistic in another, in each case involving the same material. In the beam problem, unless one wishes specifically to study the plastic zones (finite in a real structure) it may well be a good approximation to treat the material as perfectly plastic, but in the rod impact problem such a treatment does not lead to results of physical significance.

3. Idealized moment-curvature relations. As idealized bending moment-curvature characteristic for a given beam section can be derived, as mentioned, from the stress-strain diagram for simple tension and compression plus the Bernoulli-Euler assumption that plane sections remain plane. As an example, corresponding to the bilinear stress-strain law of Fig. I 1(c), one obtains a moment-curvature relation for a rectangular cross-section given by the following equations:

$$M \leq M_y : M = EI\kappa, \quad \text{or} \quad \frac{M}{M_y} = \frac{\kappa}{\kappa_y} \tag{3.1a}$$

$$M \geq M_y \quad : \quad \frac{M}{M_y} = \left(1 - \frac{E_p}{E}\right)\left(\frac{3}{2} - \frac{\kappa^2}{2\kappa_y^2}\right) + \frac{E_p}{E}\frac{\kappa}{\kappa_y} \qquad (3.1b)$$

where

$$\kappa_y = \frac{2}{h}\frac{\sigma_y}{E}$$

$$M_y = EI\kappa_y = \frac{2I}{h}\sigma_y = \frac{bh^2}{6}\sigma_y$$

b = width of cross-section

h = depth of cross-section

The idealization of the moment-curvature relation to two straight lines, one of elastic slope $\frac{dM}{d\kappa} = EI$, and the other with slope $E_p I$, is commonly made. The initial elastic line can be taken with good accuracy as extending to $M = M_p = \alpha M_y$, where $\alpha = \frac{M_p}{M_y}$ is the shape factor, the ratio of fully plastic moment to yield moment. For the rectangular section $\alpha = 3/2$, while for I-sections bent about the major axis α is about 1.15. Thus for this approximation the bilinear moment-curvature idealization can be written

$$M \leq M_p \quad : \quad \frac{M}{M_y} = \frac{\kappa}{\kappa_y} \quad \text{or} \quad \frac{M}{M_p} = \frac{\kappa}{\kappa_p} \qquad (3.2a)$$

$$M \geq M_p \quad : \quad \frac{M}{M_p} = 1 + \frac{E_p}{E}\frac{\kappa}{\kappa_p} \qquad (3.2b)$$

where $M_p = \alpha M_y$; $\kappa_p = \alpha\kappa_y$.

Figure I 3 shows the moment curve derived from the bilinear stress curve, and the bilinear approximation for the moment curve. It is evident that the significant quantities for treating problems of bending are the fully plastic moment M_p and the slope $E_p I$ in the work hardening range. The rigid-plastic moment-curvature idealizations are indicated in Fig. I 2(c), where the solid curve represents perfectly plastic and the broken curve linearly work hardening behavior.

As indicated in Figs. I2(b) and I2(c), it is simplest to take the elastic range, for reversed loading, as $2M_p$. There is little experimental justification for this, since phenomena involving reversed loading in bending have not had much attention despite the fact that in dynamic problems there are many cases where large bending moments of reversed direction occur and lead to reversed plastic deformation, under a unidirectional main loading. There are other uncertainties, for example concerning rate effects, which make it difficult to assess the experimental evidence concerning the Bauschinger effect in dynamic problems, at this time.

4. Plastic interactions. It has been mentioned that interactions between stress resultants in the plastic range must be considered in many structural problems. In later sections of this review more details will be given concerning recent work in constructing theoretical interaction curves, and solutions and experiments involving interactions. Here we will merely illustrate the problem.

The two most important interactions in beam problems are those between bending moment and axial force (M,N) and between bending moment and shearing force, (M,Q). Representative interaction curves of these types are shown in Figs. I 2(d) and I 2(e), in terms of ratios involving the limiting plastic values of bending moment M_p, axial force N_p, and shearing force Q_p. These curves correspond to stress-strain behavior of perfectly plastic type, and are derived theoretically from concepts of limit analysis. Thus, no plastic deformation is supposed to occur for points inside the curves, while unrestricted flow can occur for points on the curves. Curves A in Figs I 2(d) and I 2(e) are for rectangular cross-sections. Curve B in Fig. I 2(d) is for the limiting I-beam

or sandwich beam, which has negligible web area and flanges of finite area but negligible thickness. Curves for real I-sections lie between A and B. The shear interaction curve marked B' in Fig. I 2(e) is for a typical wide-flange I-section. The steeply falling portion of curve B' corresponds to reaching the limiting force in shear of the web alone, and this marks, for practical purposes in a problem of moment-shear interaction, the maximum shearing force that can be carried by the section.

Further details concerning these curves, including the corresponding relations governing deformations, will be given in the sections dealing with problems requiring them. It should be emphasized that they are theoretical, not experimental curves. Experimental evidence confirming them directly is very meagre for static problems, and almost non-existent for dynamic problems. Dynamic experiments have been performed giving some indirect evidence on their validity (Nonaka, 1964), and these will be reviewed in a later section. It can be said here that the use of interaction curves based on static plasticity behavior has useful suggestive value, indicating potential deformation patterns and magnitudes. However the details of such interaction curves, at least for dynamic problems of some common structural metals, are highly questionable because of their neglect of strain rate sensitivity. Rate effects have been studied fairly extensively for simple stress states, but knowledge of rate sensitivity in complex stress states is almost entirely conjectural.

In problems of plates and shells further interaction relations must be used, especially between bending moments and axial forces, which can be depicted as surfaces in an appropriate stress space. Techniques for establishing these and the corresponding displacement relationships have

been described in the literature. The remarks about experiments and rate effects apply to these.

5. Strain rate effects on yield stress. The most important difficulty in the way of solving problems of plastic deformation of structures under dynamic loading comes from the fact that the material behavior is not that of conventional plasticity theory. Even at the moderate strain rates in most structural problems (usually not exceeding about 100 per second) many structural metals have substantially different stress-strain characteristics than they exhibit in quasi-static tests.

The simplest way of depicting this so-called "strain-rate sensitivity" is by families of curves showing either stress versus strain at constant strain rate magnitudes, or stress versus strain rate at constant strain levels. Such curves have been obtained by experiments using techniques which vary in detail but in general involve impact on a short specimen - a rod or tube with length and diameter of comparable size - with one end constrained. Measurements are made of stress at one or both ends of the specimen and of strain and strain rate across the specimen length. Determinations of this sort are direct in the sense that it is not necessary to postulate a theory of plastic wave propagation in order to interpret the test data. However they are subject to the criticism that they determine averages of stress, strain, and strain rate over the specimen length, and because of propagation effects it is possible for these quantities to vary widely over this length. A further criticism is made that in impact tests on cylindrical specimens there is initially a three-dimensional stress and strain state at the impacted surface, rather than the uniaxial stress state of static tests; it has therefore been argued by Bell (see Bell, 1963, for example) that an apparent strain rate sensitivity in such

tests is not a material property but a purely geometrical result associated with elastic dilatation waves first excited by plane impact on the end of the specimen. Such phenomena are undoubtedly critical in very short time, high velocity tests, but while the geometrical effects are certainly always present it seems unlikely that they play an important role in tests at strain rates up to about 100 sec^{-1}, which are concerned in structural problems. One indication that the strain rate effects are real physical properties is their strong dependence on the condition of the metal; changes in heat treatment or alloy content produce large changes in the strain rate properties. A second indication is that the use of radically different techniques furnishes similar results; for example tests in which a ring specimen is expanded by an explosive pressure (see Johnson, Stein and Davis, 1963) or in which torsion or shear impact (for example D. B. C. Taylor and Tadros, 1956) are applied lead to increases in yield stresses close to those measured in tension or compression impact tests.

Here we give illustrations of strain rate dependence for mild steel and a few other structural metals. These are shown to indicate the magnitude of the changes in yield stress at moderate strain rates. Later in this survey a review of test results on beam specimens is given, and the analysis of plastic deformations of beams of strain rate sensitive materials is discussed. These problems require knowledge of strain-rate dependence of flexural properties. Recently direct measurements have been made of these (Aspden and Campbell, 1966). We defer discussion of these until later.

Figure I 4 shows a plot for mild steel of stress as a function of both strain ε and strain rate $\dot{\varepsilon}$, by means of an isometric projection diagram. This was published by Marsh and Campbell (1963). This plot shows

dramatically how, for a mild steel of given composition and treatment, subjected to a certain type of test, the stress-strain curve changes in position and shape as the strain rate is increased. Three aspects of such "dynamic stress-strain curves" are of interest:

(a) In the initial portion of the curve the stress rises elastically to an upper yield stress and then falls abruptly to a lower value, as plastic straining increases rapidly. The upper yield stress is a function of the strain rate in the elastic range, and is associated with the phenomenon of yield delay time; but both are of less interest than other features of the dynamic curve, for our purposes. Their significance for structural problems will be discussed in the following section 1.6.

(b) Plastic straining occurs at a nearly constant stress termed the lower yield stress. This stress magnitude and its dependence on strain rate are of primary importance in analyzing plastic deformations of structures under dynamic loading.

(c) The lower yield "plateau" terminates at a strain that depends on the strain rate, and is followed by a strain hardening region. The slopes of the stress-strain curves at various strain rates do not differ greatly from each other and from the slope of the static stress-strain curve, in this region.

It is seen that the dynamic stress-strain curves do not retain the same shape as the static curve (see Figs. I 5(a), I 5(b), I 5(c). Fortunately, in the applications the lower yield stress is of main importance, and it is not necessary to try to express mathematically the obviously complex features of the dynamic stress-strain curves.

Although the three-dimensional representation of stress, strain and

strain rate is of great interest, it should be accompanied by warnings. In the first place, it may give the impression that a metal has an equation of state, i.e. that a single functional relation holds between σ, ε, and $\dot{\varepsilon}$. No such relation can strictly be expected to exist, for a metal deforming plastically. It must be presumed that the plastic flow stress is a function not only of the current strain and strain-rate, but of the previous history of straining. If the effect of history is very strong, different diagrams would be obtained by different test methods. Fortunately for practical applications, however, it has been found that two quite different types of tests lead to closely similar diagrams. This question was studied by Marsh and Campbell (1963), who found in fact that tests imposing (a) a pulse of constant stress and (b) a nearly constant rate of strain led to diagrams of stress versus strain at constant strain rate with fairly good agreement as to both magnitudes and shapes. Some of these results are shown in Fig. I5(c), where stress-strain curves constructed from "constant stress" and "damped dynamic" (=constant strain rate) tests are compared.

Presuming that as a practical approximation one can make use of a functional relation $f(\sigma, \varepsilon, \dot{\varepsilon}) = 0$, one must still expect that strain rate sensitive plastic behavior of mild steel, for example, will depend on the chemical constitution and on the prior heat treatment. It is important to have an idea of the quantitative importance of these influences. Marsh and Campbell (1963) investigated the effects of changing grain size, as shown by comparison of Figs. I 5(a), I 5(b), and I 5(c). Later work of Aspden and Campbell (1966) used a different but similar mild steel, and although the apparatus was basically the same as in the earlier experiments, improved the technique for measuring strain and strain rate during a test. Figures I 5(d) and I 5(e) from Aspden and Campbell (1966) may be compared with the

"constant stress" test results, Figs. I 5(b) and I 5(c).

Figures I6 and I7 show further indications of variations in strain rate sensitivity to be expected with different mild steels and testing methods. We shall not attempt to analyze the difference in reported strain rate behavior, but will merely indicate their magnitude. As a measure of strain rate sensitivity we plot σ_y'/σ_y where σ_y is the lower yield stress in a static test and σ_y' the same quantity at a specified strain rate. In Fig. I 6 we have plotted this ratio as reported by eleven laboratories over a period of time from 1938 to 1964. This plot is not intended as a complete summary; other references can be found for example in the book by Goldsmith (1960). The collection of results in Fig. I 6 shows good agreement for most of the results at strain rates below about 100 sec^{-1}. The data of Manjoine (1944) cover a wide range of strain rate and are representative of the more recently obtained results. They have been used in analyses to interpret bending impact tests, and will be discussed later; recent data of Aspden and Campbell (1966) on strain rate sensitivity in flexure tests will also be referred to in that connection.

Massard and Collins (1958) gave results for twelve structural steels, including low carbon plate or bar stock in various treatments ("rimmed," "semi-killed," "fully killed," "annealed," etc.), some low alloy steels, and a nickel chromium steel. Their results are of interest in showing that substantial differences in strain rate sensitivity are reported even between steels of very similar chemical composition and static yield strength. A few of Massard and Collins' tabulated results are plotted in Fig. I7. Of all the carbon steels tested by Massard and Collins those designated 2SRBA and K showed the greatest and least strain rate sensitivity, respectively. The only "low alloy" steel for which strain rate data are

given is that designated Q; this has a static yield stress considerably higher than that of the low carbon steels, and the rate sensitivity curve lies below all the curves for the carbon steels.

It is striking that the curves for a single material - a semi-killed steel - with specimens cut parallel to the direction of rolling in one case, and transverse to it in the other - show differences as large as those between many of the low carbon steels and the low alloy steel designated as Q. Directional properties could arise from processes of fabrication of a welded structure, as well as from manufacturing processes. Their effects on plastic rate-sensitivity have not been investigated.

We give next some indication of what is known about strain rate sensitivity in steels of higher strength than mild steel. Higher strength carbon and alloy steels have received very little systematic investigation in regard to their strain-rate behavior. Some tests in this category are listed below. In all cases either a lower yield stress or a stress at a strain of roughly 0.01 is considered:

(a) Cold rolled steel (SAE 1020 or similar)

Smith, Pardue, and Vigness (1955) reported tests on a steel of static yield strength about 84 ksi at strain rates of about 10 sec^{-1}, and found a negligible change of the yield stress (at a strain of about 0.01). Steidel and Makerov (1960) observed an increase of yield strength of about 20 percent at a strain rate of 100 sec^{-1}; their steel had a static yield stress about 80 ksi.

(b) Low alloy carbon steel:

The report of Massard and Collins (1958) includes the ASTM A-242 steel designated Q in Fig. I 7 (static yield strength

50 ksi, with 0.19% C, 1.10% Mn), and a few others of this type. The Q steel, as indicated in Fig. I 7, has a dynamic yield strength ratio of about 1.4 at strain rates about 10 sec^{-1}. A few other low alloy steels tested by Massard and Collins apparently had strain rate sensitivity too small to be determined by their technique. Baron (1956) found for an En 12 steel (a hardened and tempered steel of 0.34% C, 0.82% Mn, static yield stress about 74 ksi) a dynamic yield strength ratio of about 1.25 at strain rate about 80 sec^{-1}.

Clark and Duwez (1950), using their tubular specimens subjected to circumferential stress due to internal pressure, tested a carbon-manganese steel (0.12 - 0.17% C, 1.25% Mn, with yield strength 55 ksi), and reported dynamic yield strength ratio averaging about 1.2, at strain rates of approximately 40 sec^{-1}.

(c) Nickel-chromium steels:

Several investigators have tested various nickel-chromium alloy steels and found either no strain rate sensitivity or a very small effect (less than 10 percent increase of yield stress), at strain rates up to about 100 sec^{-1}. Among these investigators are Brown and Vincent (1941), Clark and Duwez (1950), Baron (1956), and Massard and Collins (1958). Smith, Pardue, and Vigness (1955) found an increase of about 15 percent in tests on SAE 4340 steel (0.84% cr, 1.64% Ni, with static yield stress about 210 ksi). However, the same investigators observed a relatively large

effect in SAE 4340 steel (1.06% Cr, 0.12% Ni, 0.37% C, 0.21% Mo, 0.89% Mn, with static yield strength about 102 ksi), finding for this material a dynamic yield stress ratio of over 1.6. Finally, we may note that although no rate effect was found by Brown and Vincent (1941), the same nickel-chromium steel tested by Whiffin (1948), using the projectile compression technique devised by G. I. Taylor (1948), showed a dynamic strength rate ratio of nearly 1.8 at the very high strain rates (estimated at 15,000 sec^{-1}) of the projectile tests. This was a steel of 3.55% Ni, 0.47% Cr, with static yield stress about 110 ksi. Similarly, for "Vibrac" steel (4.05% Ni, 1.23% Cr, 0.28% Mo) the projectile impact test conducted by Whiffin showed a dynamic stress ratio of about 1.6, while previous work by Brown and Vincent (1941) showed no measurable increase at strain rates up to 855 sec^{-1}. The Taylor type test has the highest strain rates yet reported in (nominal) plane stress. The projectile impact tests involve serious difficulties of interpretation, and the assigned strain rate figure (16,500 sec^{-1} in these tests) is only a guess; however, an independent confirmation of the dynamic ratio for this material at very high strain rates was given by Costello (1957) using a plane impact wave technique.

Finally, references and remarks on non-ferrous metals will be given to complete the general picture concerning test data on rate sensitivity.

Pure aluminum has received a great deal of attention, and curves of dynamic stress versus strain or strain rate are reasonably well accepted

for annealed pure aluminum; review papers of Malvern (1965) and Lindholm (1965) may be consulted for these. Hauser, Simmons, and Dorn (1961), and Karnes and Ripperger (1966) have given similar curves for pure aluminum after prestraining. These tests are all in more or less complete disagreement with those of Bell (see Bell, 1966, for a brief review). The discrepancies are far from completely understood. Bell's tests over many years have concerned propagation phenomena in relatively long rods. He presents results that agree with rate-independent plastic wave theory, and hence are difficult to reconcile with dynamic stress-strain curves showing strain rate dependence. This may mean that wave phenomena are governed effectively by shapes rather than by magnitudes of stress-strain curves, and that there is in effect a "dynamic stress-strain curve" which somehow dominates the wave propagation problem, and which has a shape not greatly differing from that of the curve measured statically. This is certainly not a satisfactory or complete explanation, and others have been advanced; see, for example, Bell and Stein (1962) and Karnes and Ripperger (1966). Since our interest is in structural rather than pure metals, we shall not pursue this further. Obviously the disagreements are basic to the subject, and their explanation would be pertinent to investigations of other metals.

Tests on the dynamic plastic behavior of the structural aluminum alloys have been reported by a considerable number of investigators. In general, the alloys of higher static strength have smaller strain rate sensitivity. This trend has been particularly clearly shown by very recent tests of Green, Maiden, and Babcock (1966). They found, for example, that 6061-T6 in a fully strengthened condition had no measurable strain rate effect, but that in an annealed condition, and at higher temperatures, substantial rate sensitivity was determined. However, the evidence concerning

6061-T6 is not without contradictions. Hoge (1965) recently published test results showing a ratio of dynamic yield strength to static of over 20 percent at a strain rate of about 100 sec^{-1}. Earlier work includes similar contradictory reports on 6061-T6; Massard and Collins (1958) could find no rate sensitivity, but Ripperger and Turnbow (1959) reported an increase of yield stress proportional to the strain rate, with a rise of approximately 10 percent at 1000 sec^{-1}. Steidel and Makerov (1960) gave results for a number of aluminum alloys: 5154-0, 5456-0, 6061-0, 6061-T6, 7075-0, and 7075-T6, making tests at strain rates up to about 100 sec^{-1}. Unlike Green et al. they found 6061 to have no rate dependence in either the 0 or T6 condition; but 7075 was shown to exhibit about the same increase in yield stress in both 0 and T6 conditions.

The observed differences in strain rate sensitivity of 6061-T6 might well be ascribed to differences in heat treatment or aging, although the negative results just quoted of Steidel and Makerov (1960) contradict this explanation. Clearly differences in technique may be responsible for part of the discrepancies. In any case these are small effects (compared to mild steel).

Finally, Steidel and Makerov (1960) gave results for a series of titanium alloys, finding rate sensitivity of about 1.80 for alloy RS-55 (with static yield stress 43 ksi), of 1.30 for alloy RS-110B (static yield 120 ksi), and negligible rate dependence for the strongest alloy tested, namely RS-130 (static yield stress 146 ksi).

To sum up, this brief review of data concerning strain rate dependence of behavior in the plastic range of metals may suffice to show the magnitude of the effects in metals of structural interest, and at the same time some of the uncertainties in knowledge about this behavior. Th

lower yield stress of mild steel is substantially raised: strain rates in the range 10 sec^{-1} to 100 sec^{-1} can lead to an increase of 100 percent over the static value (Fig. I 6). But there is no unique curve for "low carbon steel"; Fig. I 7 shows variations of 25 percent between steels of approximately the same static strength, at a strain rate of 10 sec^{-1}. Higher strength carbon and alloy steels show in general much less rate sensitivity than mild steel, but yield stress increases (20 to 40 percent) have been reported for steels of 50 - 60 ksi static yield. Structural aluminum alloys also have much less rate sensitivity, and although yield stress increases of 25 percent have been reported, these are not consistently found; the discrepancies reflect differences both in condition of the metal and in methods of testing. Some other structural metals and alloys, notably those of titanium, exhibit rate effects comparable to those of mild steel.

6. Yield delay time. The property of yield delay time, exhibited by mild steel and some other metals, consists in a delay in the development of plastic strains when the specimen is subjected to stresses above the static (upper) yield stress. This phenomenon was noticed in very early investigations (B. Hopkinson, 1904), but was first studied systematically by Clark and Wood (1949). It has had much experimental and theoretical study since then (see, for example, Campbell and Marsh, 1962, and Krafft and Sullivan, 1959). The simplest case is that in which a pulse of stress is very rapidly applied and maintained constant. The observed delay time is a function of the excess stress applied above the static upper yield; for stresses below the static upper yield magnitude the delay time is indeterminate. It is found that a plot of the excess stress against the logarithm of the

delay time is close to a straight line, although a log-log plot gives a more linear relationship at small times.

If the loading is not a simple step pulse it is possible to compute an equivalent delay time by an assumption of proportional damage accumulation. This was done by Vigness, Krafft, and Smith (1957), with the results shown in Fig. I 8 Experiments employing constant l ad, constant rate of increase of load, and oscillatory loading were used, and the data determine a straight line in the semi-log plot, within the limits of experimental accuracy.

Examples of stress-strain curves at constant strain rate for mild steel have already been given in the isometric projection diagram of Fig. I 4 (Marsh and Campbell, 1963). These tests show a marked enhancement of the upper yield stress as the strain rate is increased; the upper yield stress is increased more rapidly than the lower yield stress. This enhancement is shown in the curves of Figs. I 5(a)-(c), from Marsh and Campbell (1963), and more strongly in those of Fig. I 5(d) from Aspden and Campbell (1966). The comparison of the two sets of curves is of interest in showing details determined by improvements in instrumentation, using essentially the same impact apparatus, and similar steels. The connection between yield delay time and upper yield stress has been recognized; see, for example, the discussion of Krafft and Sullivan (1959).

The yield delay time and enhanced upper yield stress, as observed in laboratory impact tests of mild steel, would appear at first glance to be highly significant for applications of analytical approaches to the plastic deformation of engineering structures. Clearly the transition from wholly elastic response to one with a mixture of elastic and plastic deformation might be strongly affected by such properties as yield delay time and increased

upper yield stress, and analytical predictions of plastic deformations which ignored these effects could be nonsense. Keil (1960) has discussed the inclusion of yield delay time in studies of dynamic loading of structures.

In practical structures, however, the phenomena of yield delay time and raised upper yield stress may be less important than the laboratory results discussed above would indicate. These quantities are observed in laboratory experiments in which much care is taken to eliminate stress concentrations and eccentricity of loading. It was noted by Belsheim (1954), among others, that the yield delay time and upper yield stress disappeared when a specimen inadvertently had a surface flaw or scratch. The sensitivity of the upper yield stress to these conditions has been well known in static tests. The observed enhancement of upper yield stresses in impact tests may mean a decreased sensitivity to eccentricity of loading in impact. In any event, in real structures various kinds of stress raisers are almost inevitable, and yield delay times and upper yield stresses may rarely be encountered. Hence it is conservative and realistic to ignore them in real structures.

The lower yield stress, on the other hand, has no such sensitivity to axiality of loading and absence of stress concentrations, and its dependence on strain rate clearly appears in practical engineering structures as well as in laboratory specimens. Its consideration as a factor in design is therefore justified. Considerable attention will be given in this review to evidences of rate sensitivity in experiments on beams, and to methods of including this behavior in analyses.

Figure Captions for Chapter I

Figure	Caption
I 1	Forms of nominal stress-strain diagrams: (a) [illegible] (b) as measured for structural metals; (b) and (c) are idealizations.
I 2	Moment-curvature and interaction diagrams for beams: (a) shows representative measured moment-curvature diagrams, (b) and (c) idealized moment-curvature diagrams; (c) rigid-perfectly plastic. (d) shows interaction between bending moment and axial force: curve A for a rectangle, curve B for a sandwich beam. (e) shows interaction between bending moment and shear force (limit load curves for end-loaded cantilever): curve A for rectangle, curve B' for I section, where Q_w is limit shear force for web area.
I 3	Bilinear nominal stress-strain diagram and corresponding moment-curvature diagram (full curves); approximating bilinear moment-curvature diagram (dashed curve).
I 4	Stress-strain-strain rate diagram for mild steel shown as isometric projection (from Marsh and Campbell, 1963); "constant stress" type tests, strain rates up to 20 sec^{-1}. Stress and strains are compressive, nominal values.
I 5	Comparison of results of compression strain rate tests of mild steel: (a) - (c) from Marsh and Campbell (1963); (d), (e) from Aspden and Campbell (1966). (a) Series E: "constant strain rate" tests, steel with mean grain density 2033 grains per mm^2. (b) Series C: "constant stress" tests, 2033 grains per mm^2. (c) Series B: "constant stress" tests, 773 grains per mm^2. (d) Curves of typical "constant stress" type test of Aspden and Campbell (1966). (e) Families of stress-strain curves at various rates, mean grain density 2300 grains per mm^2, for comparison with (b), showing changes with different mild steel, details of test technique.
I 6	Representative data on strain rate dependence of lower yield stress of mild steel: σ_y'/σ_y = ratio of dynamic to static lower yield stress. Tests of Marsh and Campbell (1963), Aspden and Campbell (1966), and Whiffin (1948) in compression; all others in tension; Clark and Duwez (1950) used circumferential tension in cylinder with internal pressure.

Figure	Caption
I 7	From Massard and Collins (1950): examples of yield stress dependence on strain rate for several structural steels.
I 8	From Vigness, Krafft, and Smith (1958): increase of upper yield stress over static upper yield stress as function of delay time (computed by integration so as to give the equivalent of constant-load test.) Points marked o for constant load test. Points marked + for uniformly increasing load. Points marked Δ for combined constant and oscillatory load.

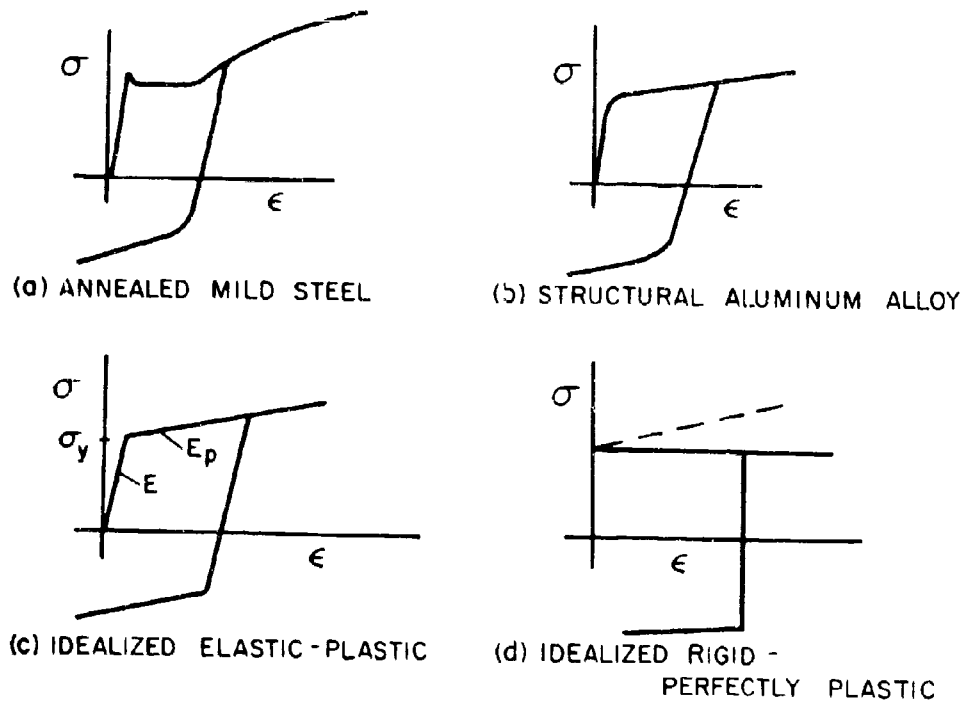
σ
ϵ
(a) ANNEALED MILD STEEL
σ
ϵ
(b) STRUCTURAL ALUMINUM ALLOY
σ
σy
Ep
E
ϵ
(c) IDEALIZED ELASTIC - PLASTIC
σ
ϵ
(d) IDEALIZED RIGID - PERFECTLY PLASTIC

FIG. I1

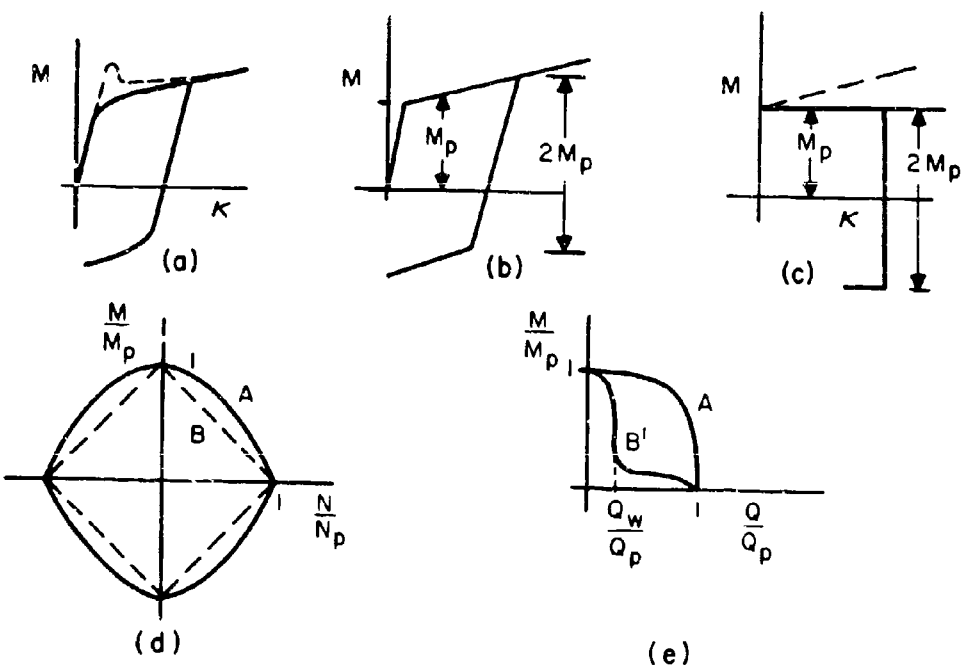
M
κ
(a)
M
Mp
2Mp
(b)
M
Mp
2Mp
κ
(c)
M/Mp
1
A
B
1
N/Np
(d)
M/Mp
1
A
B'
Qw/Qp
1
Q/Qp
(e)

FIG. I2

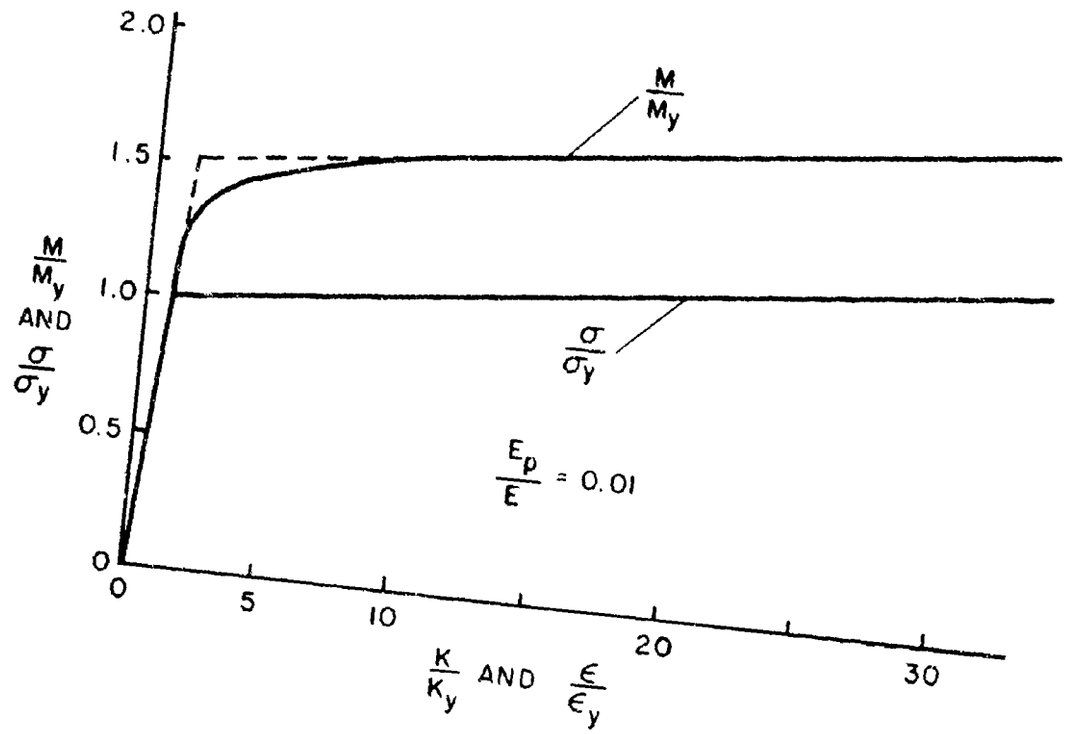

FIG. I3

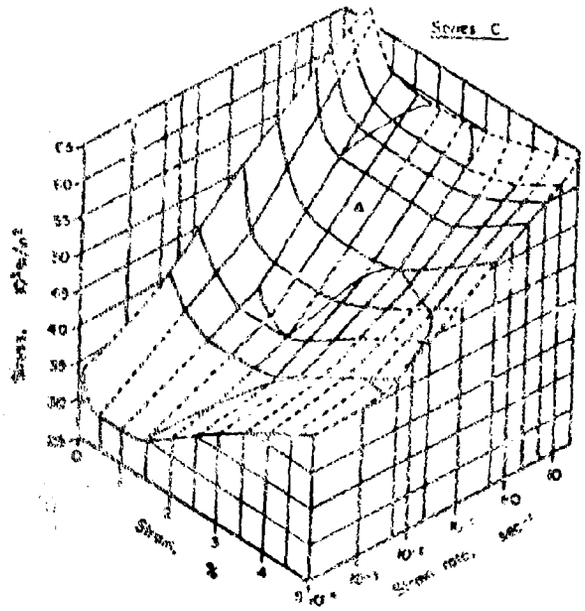

FIG. I 4

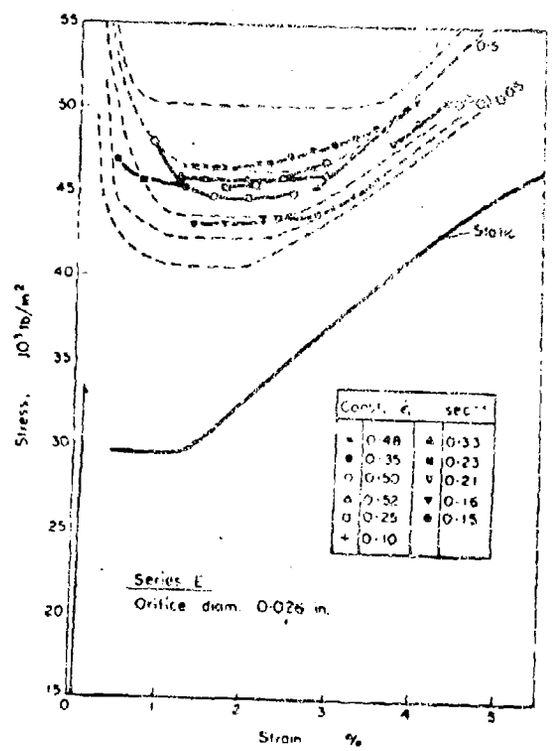

FIG. I 5(a)

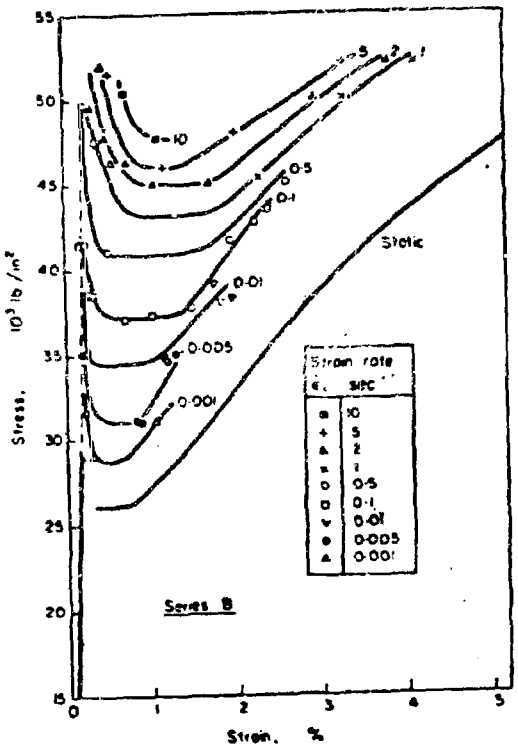

FIG. I5(c)

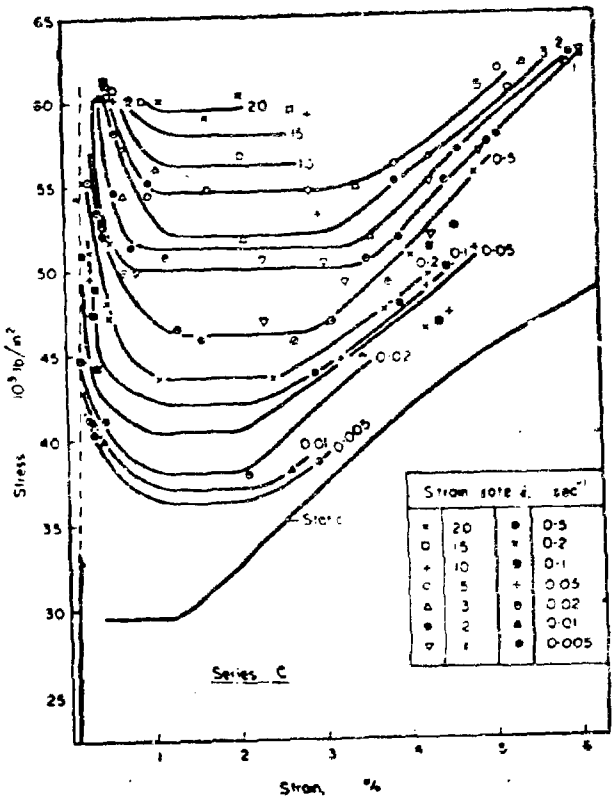

FIG. I5(b)

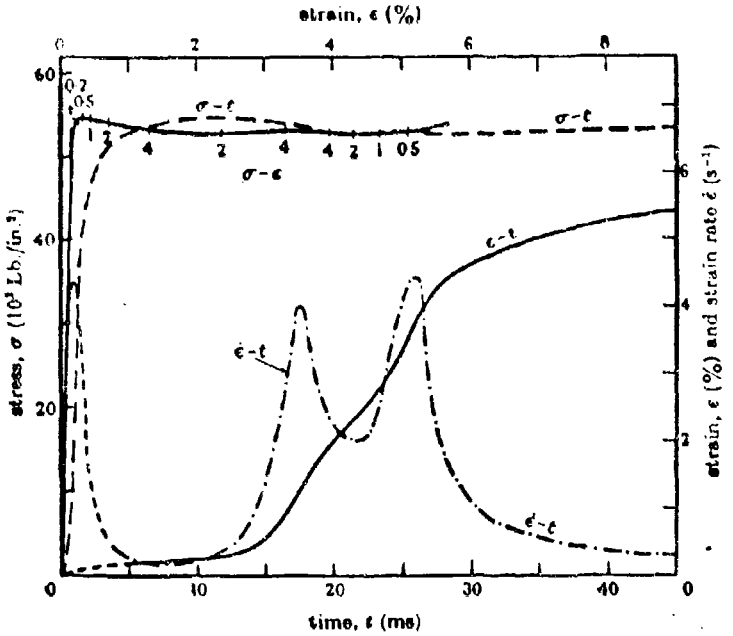

FIG.I5 (e)

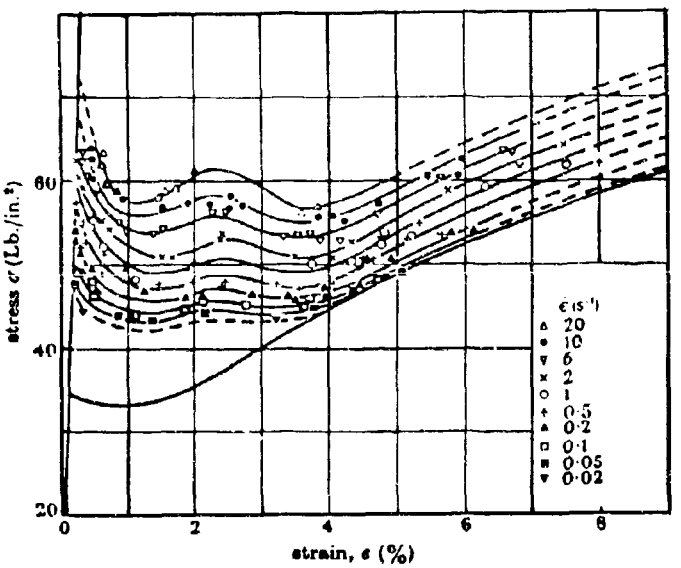

FIG.I5 (d)

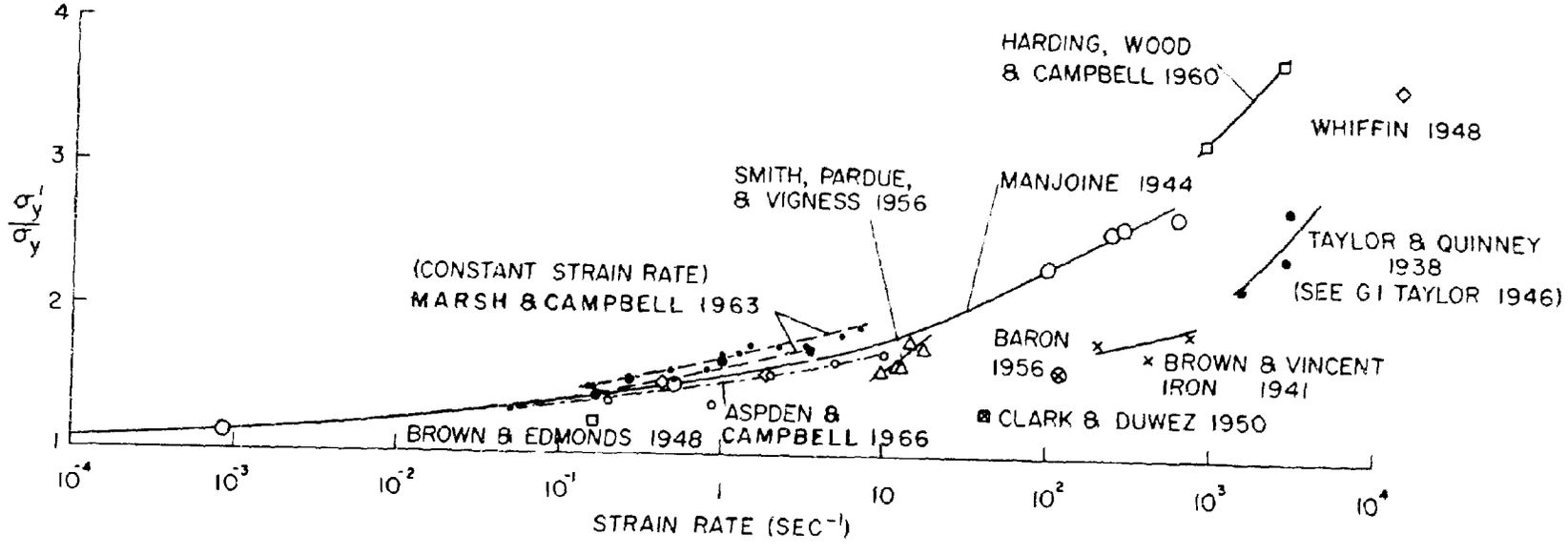
4
3
2
1
$\frac{\sigma_y'}{\sigma_y}$
HARDING, WOOD
& CAMPBELL 1960
WHIFFIN 1948
SMITH, PARDUE,
& VIGNESS 1956
MANJOINE 1944
TAYLOR & QUINNEY
1938
(SEE G I TAYLOR 1946)
(CONSTANT STRAIN RATE)
MARSH & CAMPBELL 1963
BARON
1956
BROWN & VINCENT
IRON 1941
ASPDEN &
CAMPBELL 1966
BROWN & EDMONDS 1948
CLARK & DUWEZ 1950
10^{-4}
10^{-3}
10^{-2}
10^{-1}
1
10
10^{2}
10^{3}
10^{4}
STRAIN RATE (SEC^{-1})

FIG. I 6

			σ_y (ksi)	C %	M_n %
⊖	2SRBA	RIMMED STEEL, HOT ROLLED 1" BAR STOCK, AS ROLLED	39	0.29	0.35
◇	2SSPAL	SEMI-KILLED STEEL, HOT ROLLED 1" PLATE, AS ROLLED LONGITUDINAL	33	0.27	0.51
◆	2SSPAT	SEMI-KILLED STEEL, HOT ROLLED 1" PLATE, AS ROLLED TRANSVERSE	35	0.27	0.51
○	K	FULLY KILLED STEEL, HOT ROLLED 3/4" PLATE STOCK	36	0.15	0.87
□	Q	LOW ALLOY STEEL, ASTM A-242	50	0.19	1.10

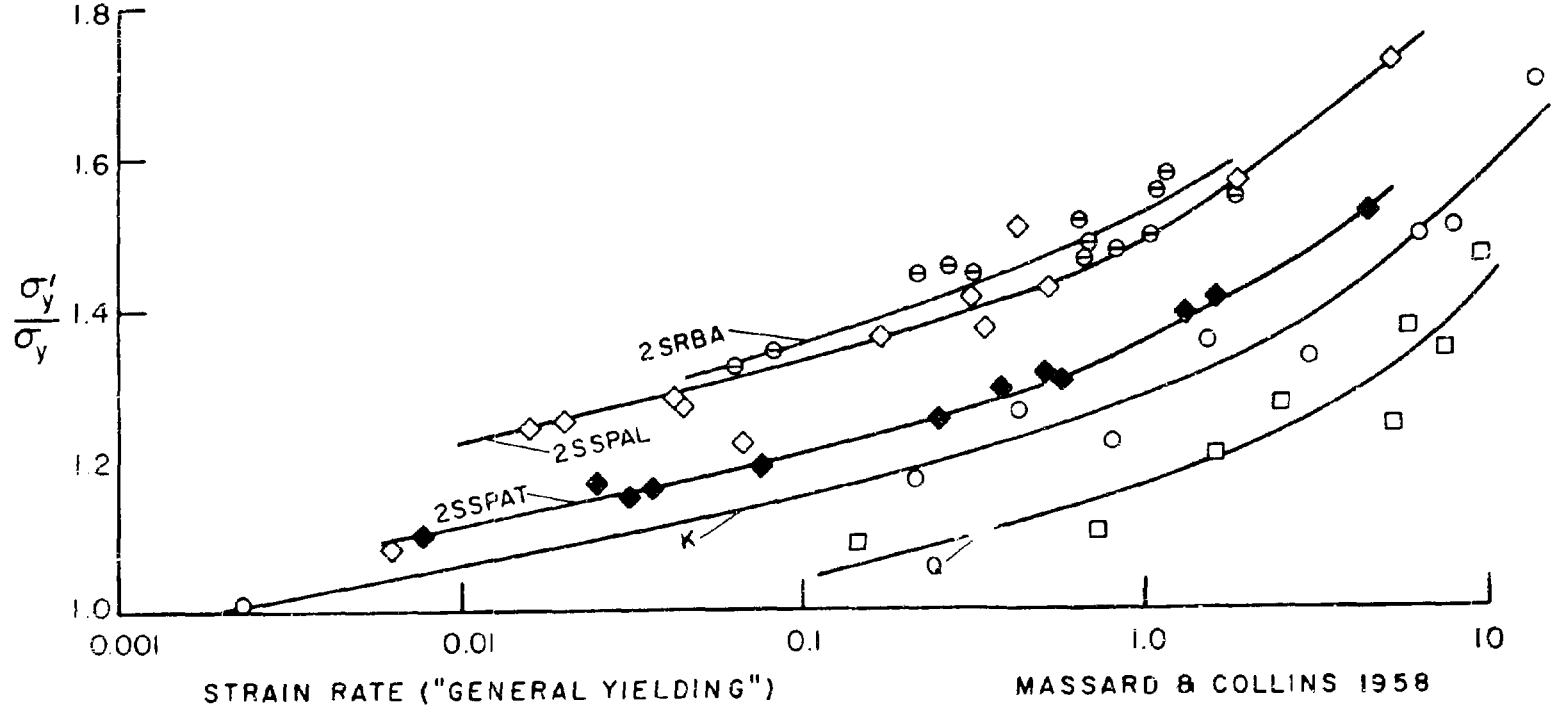

FIG. I7

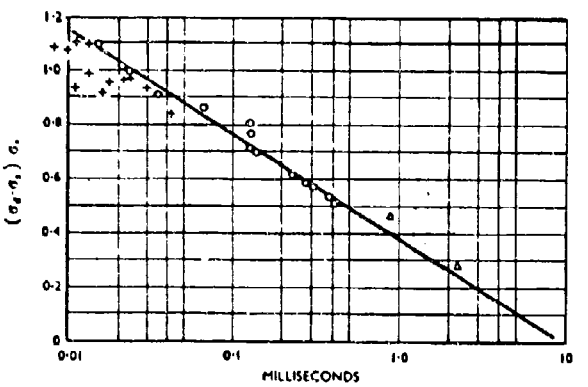

FIG. I8

Chapter II

BEAMS - ANALYTICAL METHODS

1. Basic Ideas

A beam is the simplest prototype of the general continuous engineering structure. Here "beam" means a body, one of whose dimensions is large compared to the maximum transverse dimension. The simplest case is a straight bar of uniform cross-section. This is by definition a "beam" if the loads are mainly transverse to the long axis.

A beam is a three-dimensional body, but a treatment must be given in terms of stress resultants: bending moments M, shear forces Q, axial force N and torque T; arising from normal and shear stresses acting on a cross-section plane. Effects of transverse normal stresses are generally ignored. It is convenient to use principal axes and to separate general loads into components parallel to principal planes.

The material properties of the beam, originally given by a yield function and stress-strain relations describing the elastic and plastic behavior, are translated into corresponding terms involving the stress resultants. In the simplest case of transverse loading only one bending moment M must be considered, so that a diagram of M as function of curvature κ takes the place of the simple tension-compression stress-strain diagram, as in Figs. I 2, I 3. This exhibits an elastic range with slope EI, a yield moment M_y, and a strain-hardening curve. For certain highly ductile structural metals it is a good and conservative approximation to replace the rising part of the curve by a horizontal line at a magnitude M_p; this constant moment magnitude represents the limit moment or fully plastic moment of the methods of plastic design of beams. As indicated in Sections 5 and 6 of Chapter I, most structural metals have different plastic behavior at high strain rates than they do under static conditions, and this is reflected in the $M - \kappa$ curve, which now depends

on the curvature rate $\dot{\kappa}$.

Even if the loads are parallel to one principal plane, it may not be permissible to disregard the shear force and normal force in the plastic behavior. There is in general loading always an interaction between M, Q, and N, but the importance of taking account of Q and N depends on their magnitudes relative to M. These, in turn, depend on the geometry of the beam (length-depth ratio, etc.), on the constraints, and on the loading intensity and distribution. Work of Drucker (1956) and Neal (1961), among others, has dealt with such interaction relations. Very few studies have made use of them in dynamic problems, and these will be discussed subsequently.

The response of a beam to a severe dynamic load is a complicated set of phenomena. Elastic vibrations are excited. At certain times and locations the yield moment of the beam will be reached. Then plastic deformation occurs in regions whose boundaries move, and which are separated by regions where the yield condition is not satisfied and hence elastic action continues. The problem of determining in detail the simultaneous elastic and plastic actions is obviously beyond conventional analytical techniques. It can be handled only by completely numerical procedures, with difficult questions as to stability and convergence in choosing intervals remaining to be answered, or by special analytical methods appropriate to special ranges of conditions.

The above refers to solutions in which deformations of the beam at all points along its length are determined; that is, in which the beam is treated as a continuum either by differential or by difference equations. Because of the difficulties indicated, most of the work concerned with design problems has replaced the actual beam, frame, or other structure by a model consisting of an "equivalent" mass-spring system of one degree of freedom, or a small number of degrees of freedom. This approach will be valid if there is actually one mode (or a small number of modes) of deformation (elastic and plastic) which predominates over all others. If interactions

between many modes need to be considered, this method becomes extremely cumbersome, and there is little evidence in the literature as to its reliability. However, it is essentially all that can be done in most cases of complex structure.

In the following, main attention will be given to the concepts, the main results, and the limitations as to further extensions (as they appear to the writer) of the approaches to dynamic plastic analysis of beams. A few investigations with a close combination of analysis with experiments have been published. These are mentioned at appropriate places and will be discussed more throughly in Chapter III. Little attention can be devoted to methods which treat a complex structure as a one-degree-of-freedom mass-spring system, since almost no test data is available in the open literature with which such results can be checked.

2. Elastic-plastic Analysis

There is only one "exact" theory for a material supposed to have a general elastic-plastic stress-strain characteristic. This theory was developed by H. F. Bohnenblust (Duwez, Clark, and Bohnenblust, 1950), and is based on a result obtained much earlier by Boussinesq (1885). It rests on the reduction of the partial differential equations of the beam motion:

$$\frac{\partial Q}{\partial x} + m \frac{\partial^2 y}{\partial t^2} = 0 \qquad (2.1)$$

$$Q = \frac{\partial M}{\partial x} \qquad (2.2)$$

$$M = M(\kappa) = M\left(\frac{\partial^2 y}{\partial x^2}\right) \qquad (2.3)$$

(where Q = shear force, M = bending moment, κ = curvature, y = transverse displacement) to an ordinary differential equation through the introduction of the new independent variable cx^2/t where c is a suitable constant. Bohnenblust showed that

$$\frac{y}{t} = f(\eta) \tag{2.4}$$

where

$$\eta = \frac{x^2}{4a^2 t} ; \quad a^2 = \sqrt{\frac{EI}{m}} \tag{2.5}$$

For any relation $M = M(\kappa)$ between bending moment M and curvature κ the system of Equations (2.1) - (2.3) can be reduced to an ordinary differential equation for a new dependent variable $S(\eta)$,

$$\frac{d^2S}{d\eta^2} + EI \frac{d\kappa}{dM} S = 0 \tag{2.6}$$

where

$$S(\eta) = \frac{2a^3}{EI} \sqrt{t}\, Q = \frac{2a^2}{EI} \sqrt{\eta} \frac{dM}{d\eta} \tag{2.7}$$

Formulas giving M, Q, κ, and y in terms of definite integrals involving $S(\eta)$ are easily derived, and in principle a complete solution for a general elastic-plastic material can be obtained. However, the Bohnenblust solution involves the following limitations:

1. The solution is for a <u>constant velocity</u> impact; the beam being at rest for $t < 0$, the force P required to produce the impact velocity V_o at $x = 0$, $t \geq 0$ is found to be

$$P = \frac{EI}{a^3} \frac{S(0)}{\sqrt{t}} \tag{2.8}$$

The impact velocity is related to $S(\eta)$ through

$$V_o = -\frac{1}{2} \int_o^\infty \frac{S'(\eta)}{\sqrt{\eta}}\, d\eta \tag{2.9}$$

The solution holds only for the above conditions; unloading cannot be treated.

2. The solution holds for an infinite beam struck at $x = 0$; no modification to treat finite beams seems possible.

Solutions of the Bohnenblust type have been given for semi-infinite beams under constant velocity impact with constant moment (Conroy, 1956); and a number of comparisons have been made between elastic-plastic and rigid-plastic beams ($EI \to \infty$), and between perfectly plastic and linearly work hardening materials (Conroy, 1952). These comparisons show the spread of deformations for particular conditions, but do not seem to provide any general guide-lines for other loading conditions on finite beams.

In Section 1 of Chapter III some results of Bohnenblust's solution will be compared with those obtained by simpler approximate methods for the same problem and for modified problems which may more realistically represent conditions in the experiments described by Duwez, Clark, and Bohnenblust.

An elastic-plastic theory for dynamic loading which is less exact (in general) but much more widely applicable and useful than the Bohnenblust type of analysis, is that due to Bleich and Salvadori (1955) and applied later by Thomson (1954), Allen (1955), Alverson (1956), Seiler, Cotter, and Symonds (1956) and others. The basic ideas of the method are that the motion of the beam (or other structure) is elastic during the initial instants of motion and is described by an analysis in terms of a certain set of normal modes; this initial elastic phase ends when the bending moment at some cross-section reaches the limit moment M_p. The method is simplest to apply if the beam is made of perfectly plastic material with $M = M_p$ while plastic flow occurs. If the material is assumed to be of this type, the elastic phase is succeeded by an elastic-plastic phase which again is described in terms of normal modes, but which in general requires different normal modes than those of the initial elastic phase because different end conditions must be satisfied. The

cross-section where the limit moment was first reached is assumed to remain at M_p during this phase, while on adjacent cross-sections the yield moment is not reached, so that equations of elastic beam dynamics apply. Thus, there is one cross-section at which plastic deformation occurs, all other parts of the beam behaving elastically; the section where $M = M_p$ behaves as a plastic hinge, plastic deformation in the beam being concentrated at this point. The hinge is assumed to remain stationary. Continuity of displacement and velocity exists across the hinge, but not of slope angle θ and angular velocity $\dot{\theta}$. The slope angle θ at the plastic hinge is not directly related to the moment there. The hinge remains active, and plastic deformation continues so long as $\dot{\theta} > 0$. When $\dot{\theta} = 0$ the plastic hinge disappears provided for subsequent times $M < M_p$. Further motion then obeys equations of elastic motion.

If the beam is made of a work hardening material the plastic deformation cannot be taken to occur at a single isolated cross-section, as is customarily done in theory of ideally plastic structures (ignoring the implication of infinite strains). The plastically deforming region must occupy a finite length Δx across which the slope angle change $\Delta\theta$ is

$$\Delta\theta = \int_0^{\Delta x} \frac{\partial\theta}{\partial x}\, dx = \int_{M_p}^{M_m} \frac{\kappa}{Q}\, dM \qquad (2.10)$$

where M_m and M_p are the bending moments at the ends of the plastic segment. If the length of the plastic region is assumed to be constant, an analysis of Bleich-Salvadori type can be carried out in terms of normal modes, although with much more difficulty. The method does not seem to have been applied except for an ideally plastic material. Strain hardening can, however, be taken into account very roughly by taking M_p larger than the actual yield moment, by an amount depending on the deformation.

The method is easy to describe and straightforward to apply, in principle. In practice, there is a considerable amount of labor in determining the successive sets

of normal mode functions, and the calculations of the time when $\dot{\theta} = 0$, and of the permanent angular and lateral deformations are tedious. The series for the deflection usually converges rapidly, but the series obtained after differentiations to give θ and $\dot{\theta}$ converges more slowly or may fail to converge.

Elastic-plastic solutions have been worked out in terms of normal modes for the following problems:

Table II 1

ELASTIC-PLASTIC SOLUTIONS OF NORMAL MODE-PLASTIC HINGE TYPE

CASE	END CONDITION	LOADING	REFERENCE	
(a)	free-free (span 2L)	impulsive, $\dot{y}(0,x) = \frac{V_o}{2}(1 - \cos\frac{\pi x}{L})$ (x as in Fig. II 1)	Bleich & Salvadori	(1955)
(b)		" $V_o \sin\frac{\pi x}{2L}$	Seiler, Cotter & Symonds	(1956)
(c)	simple supports	uniform load: rectangular pulse	Seiler	(1954)
(d)	simple supports	mid-point force step functions	Thomson	(1954)
(e)	clamped	mid-point force: step functions	Thomson	(1954)
(f)	cantilever	impact: base changes velocity linearly in time, then remains constant.	Alverson	(1956)
(g)	cantilever with mass at tip	same as (f)	Stallybrass	(1960)
(h)	cantilever	uniform pressure: triangular (blast) pulse	Allen	(1955)

As an illustration of the method just described the solution of case (b) above is presented. The problem to be considered is the elastic-plastic response of a prismatic beam of span 2L and flexural rigidity EI with the following initial conditions on displacement and velocity:

$$y(x,0) = 0; \qquad \frac{\partial y}{\partial t}(x,0) = V_o \sin \frac{\pi x}{2L} \tag{2.11}$$

The beam is assumed to be simply supported, and the boundary conditions are written as follows:

$$\begin{aligned} y(0,t) &= y(2L,t) = 0 \\ \frac{\partial^2 y}{\partial x^2}(0,t) &= \frac{\partial^2 y}{\partial x^2}(2L,t) = 0 \end{aligned} \tag{2.12}$$

Fig. II 1 shows the initial beam configuration and positive directions of co-ordinates and moments.

The analysis is based on the moment-curvature relationship shown in Fig. II 2, and the equation for the elastic phase of the motion is taken to be

$$EI \frac{\partial^4 y}{\partial x^4} + m \frac{\partial^2 y}{\partial t^2} = 0 \tag{2.13}$$

Solving Equation (2.13) with Equations (2.11) and (2.12), we obtain

$$y(x,t) = \frac{4V_o kL^2}{\pi^2} \sin \frac{\pi x}{2L} \sin \frac{\pi^2 t}{4kL^2} \tag{2.14}$$

where

$$k^2 = \frac{m}{EI} \tag{2.15}$$

As stated previously, the elastic phase ends when the maximum moment in the

beam reaches the limit moment M_p. This occurs at $x = L$ at a time t, such that

$$M(L,t_1) = M_p = -EI\frac{\partial^2 y}{\partial x^2}(L,t_1) \tag{2.16}$$

or, using equation (2.14), when

$$\frac{M_p}{EIkV_o} = \sin\frac{\pi^2 t_1}{4kL^2} \tag{2.17}$$

From equation (2.14), the conditions at time t_1 or the initial conditions for the elastic-plastic phase are

$$y(x,t_1) = -\frac{4V_o kL^2}{\pi^2}\sin\frac{\pi x}{2L}\sin\eta_1 \tag{2.18}$$

$$\frac{\partial y}{\partial t}(x,t_1) = V_o \sin\frac{\pi x}{2L}\cos\eta_1 \tag{2.19}$$

where

$$\eta_1 = \frac{\pi^2 t_1}{4kL^2} \tag{2.20}$$

Fig. II 3 shows the assumed shape of the beam for the elastic-plastic phase with a plastic hinge at the center where rotation is unrestricted while for the remaining half beams of length L, equation (2.13) applies. Therefore, equation (2.13) must be solved subject to the initial conditions given by equations (2.18) and (2.19) and the following boundary conditions:

$$y(0,t) = \frac{\partial^2 y}{\partial x^2}(0,t) = 0 \tag{2.21}$$

$$-EI\frac{\partial^2 y}{\partial x^2}(L,t) = M_p; \qquad \frac{\partial^3 y}{\partial x^3}(L,t) = 0 \tag{2.22}$$

The final general solution is obtained in the form

$$y = \psi(x,t) + Y(x,t) \tag{2.23}$$

where

$$\psi(x,t) = \frac{M_p L^2}{EI}\left[\frac{x^5}{40L^5} - \frac{x^3}{4L^3} - \frac{3x(t-t_1)^2}{2k^2L^5}\right] \tag{2.24}$$

$$Y(x,t) = [A_o + B_o(t-t_1)]x + \sum_{n=1}^{\infty} X_n(x)$$

$$\left[A_n \sin\frac{\lambda_n^2(t-t_1)}{k} + B_n \cos\frac{\lambda_n^2(t-t_1)}{k}\right] \tag{2.25}$$

$$X_n(x) = \sin\lambda_n L \sinh\lambda_n x + \sinh\lambda_n L \sin\lambda_n x$$

and λ_n satisfies the equation

$$\tanh\lambda_n L = \tan\lambda_n L \tag{2.26}$$

so that $\lambda_n L \cong n\pi + \pi/4$.

The coefficients A_o, B_o, A_n, and B_n, are evaluated in the usual manner by using the initial conditions given by equations (2.18) and (2.19).

For the foregoing solution to be correct, the bending moment $|M(x,t)| \leq M_o$ at all points in the range $0 \leq x \leq L$, and the sense of rotation across the plastic hinge must agree with that of the bending moment at the hinge. The latter remark indicates that the solution is invalidated at a time t_f such that

$$\frac{\partial^2 y}{\partial t \partial x}(L,t_f) = 0 \tag{2.27}$$

By solving equation (2.27) an expression is obtained for the time t_f, and

substituting this value for t in equation (2.23) the maximum deflection δ_f and slope θ_f at midspan are given as follows:

$$\frac{EI}{M_p L^2}\delta_f = \frac{48}{\pi^4} + \frac{39}{280} - \frac{9}{40} - \frac{24}{\pi^4}\eta_f'^2 + \frac{48}{\pi^4}\sqrt{2S-1}\,\eta_f'$$

$$-\pi^2\sqrt{2S-1}\sum_{n=1}^{\infty}\frac{\sin\frac{4a_n^2}{\pi^2}\eta_f'}{a_n^5\left(1-\frac{\pi^4}{16a_n^4}\right)} - \frac{\pi^4}{4}\sum_{n=1}^{\infty}\frac{\cos\frac{4a_n^2}{\pi^2}\eta_f'}{a_n^7\left(1-\frac{\pi^4}{16a_n^4}\right)} \qquad (2.28)$$

$$\frac{EI}{M_p L}\theta_f = \frac{48}{\pi^4} + \frac{39}{280} - \frac{5}{8} + \frac{48}{\pi^4}\sqrt{2S-1}\,\eta_f' - \frac{24}{\pi^4}\eta_f'^2$$

$$-\pi^2\sqrt{2S-1}\sum_{n=1}^{\infty}\frac{\sin\frac{4a_n^2}{\pi^2}\eta_f'}{a_n^4\left(1-\frac{\pi^4}{16a_n^4}\right)} - \frac{\pi^4}{4}\sum_{n=1}^{\infty}\frac{\cos\frac{4a_n^2}{\pi^2}\eta_f'}{a_n^6\left(1-\frac{\pi^4}{16a_n^4}\right)} \qquad (2.29)$$

where
$$\eta_f' = \frac{\pi^2}{4kL^2}(t_f - t_1) \qquad (2.30)$$

and
$$S = \frac{mEIV_o^2}{2M_p^2} \qquad (2.31)$$

In the above equations the approximations that $a_n = \lambda_n L = n\pi + \pi/4$, $\tanh a_n = 1$, and $\sinh a_n \gg 1$ for all n are made.

The elastic-plastic solution is plotted in Figs. II 4 for various values of S which is the ratio of the initial kinetic energy to the maximum elastic energy capacity of the beam. With the exception of Fig. II 4(a), all the other figures show a point of zero slope before the absolute maximum point of the total plot. The

Table II 2

		First max. of θ(t) curve				Absolute maximum			
S	R	$\frac{EI}{M_p L}\theta_f$	$\frac{EI\delta_f}{M_p L^2}$	$\frac{M_p\theta_f}{mLV_o^2}$	$\frac{M_p\delta_f}{mL^2V_o^3}$	$\frac{EI}{M_p L}\theta_f$	$\frac{EI\delta_f}{M_p L^2}$	$\frac{M_p\theta_f}{mLV_o^2}$	$\frac{M_p\delta_f}{mLV_o^2}$
1	0.808	0.284	0.654	0.142	0.327	0.284	0.654	0.142	0.327
2	1.24	0.62	0.998	0.155	0.249	0.82	1.168	0.205	0.292
5	4.0	2.00	2.34	0.200	0.234	2.34	2.64	0.234	0.264
13	11.9	5.96	6.27	0.229	0.241	6.30	6.59	0.242	0.254
∞	∞	$\frac{24}{\pi^4}(2S$	$- 1)$	$\frac{24}{\pi^4} =$	0.246	$\frac{24}{\pi^4}(2S$	$- 1)$	0.246	0.246
"Single-hinge" Rigid-Plastic		$\frac{1}{4}\times 2S$	$\frac{1}{4}\times 2S$	0.25	0.25				
Rigid-Plastic		$\frac{1}{6}\times 2S$	0.239 (2S)	0.167	0.239				

$$S = \frac{mEIV_o^2}{2M_p^2}; \qquad R = 2\frac{EI\theta_f}{M_p L}; \qquad \frac{M_p\theta_f}{mLV_o^2} = \frac{EI\theta_f}{2SM_p L}, \text{ etc.}$$

computation of the final angle θ_f is based on the time when the slope of the curve of θ versus time first becomes zero and, therefore, in many cases, it is likely that the theory will not give the correct maximum. No attempt was made to investigate this phenomenon, but it does indicate another elastic phase followed by an elastic-plastic phase which would require a second set of eigenfunction solutions. Results are presented in Table II 2 for both the first maximum and the absolute maximum points of the curves. It is expected that the corresponding maximum values give the range within which the actual maximum deformation occurs.

The problem under discussion was also analyzed by Seiler, Cotter, and Symonds (1956) assuming the beam to be composed of a rigid-plastic material. In this case elastic deformation is neglected, and the moment-curvature relation is as illustrated by the dotted line in Fig. II 2. It is shown that, in order to satisfy the boundary conditions at the supports and the assumed moment-curvature relation, the beam must deform with rigid segments at the supports separated by a central finite plastic zone. The plastic zone has a constant moment M_p and the plastic interfaces separating the three segments travel towards the center of the beam. In the final phase of the deformation process the central plastic zone reduces to a point hinge at the center, and the half beams rotate about this hinge until all the energy is absorbed. The final angle θ_f of the tangent line of the middle is given by

$$\frac{M_p}{mLV_o^2}\theta_f = \frac{1}{6} \tag{2.32}$$

This approach to problems of dynamic loading is outlined in greater detail in a later section of this survey, but for the purposes of comparison, results computed from equation (2.32) are included in Table II 2 under the heading "rigid-plastic."

Bleich and Salvadori suggested an "upper bound" solution which assumes that

the initial kinetic energy is completely absorbed by a single plastic hinge at midspan. This is a simplified rigid-plastic solution, and the angle of rotation at midspan is readily obtained from the following equation

$$1/2\ mLV_o^2 = 2M_p\theta_f' \tag{2.33}$$

Deformation values calculated from equation (2.33) are also given in Table II 2. It must be noted that for some problems equation (2.33) may not determine an upper bound.

Discussion

The elastic-plastic method of Bleich and Salvadori only applies when the plastic hinge is stationary and when the length of the hinge may be neglected in the analysis. Theoretically, non-uniform or unsymmetrical loading arrangements can be considered and also force pulses of various amplitudes and durations may be treated but computations may become troublesome, and some series of the solution may not converge or, at best, converge very slowly. An extension to the elastic-plastic theory has been proposed by Bleich (1956) by which many hinges at various locations may be included in the analysis. This is accomplished by using a numerical method to find the contribution of the rotations at the plastic hinges to the total deformation. The same approach is employed by Baron, Bleich, and Weidlinger (1961) in describing a completely numerical solution and is presented in Section 3 of this chapter and is, therefore, not included here.

The fundamental difficulty of a Bleich-Salvadori type of solution is that it is unable to consider "spreading" of the plastic hinge at large loads, i.e., violation of the limit condition $M_p \geq |M|$ over a finite section. In the problem under discussion, the authors (Seiler, Cotter, and Symonds) examined the plastic-moment condition at sections along the beam. By retaining only leading terms in equation (2.25) an approximate expression for bending moment is obtained as follows:

$$\frac{M}{M_p} = \frac{3}{2}\xi - \frac{1}{2}\xi^3 + \sqrt{2S-1}\,\frac{\pi^2}{\sqrt{2}}\left\{\frac{-\sin a_1 \sinh a_1\xi + \sin a_1\xi \sinh a_1}{a_1^3\left(1 - \frac{\pi^4}{16a_n^4}\right)\sinh a_1}\sin\frac{4}{\pi^2}a_1^2\eta'\right.$$

$$\left. + \frac{\sin a_2 \sinh a_2\xi - \sin a_2\xi \sinh a_2}{a_2^3 \sinh a_2}\sin\frac{4}{\pi^2}a_2^2\eta'\right\} \qquad (2.34)$$

where $\xi = \frac{x}{L}$, $a_n = n\pi + \pi/4$, $\eta' = \frac{\pi^2}{4kL^2}(t - t_1)$

Using equation (2.34), Figs. II 5(a) and II 5(b) show plots for two values of η' with M/M_p as ordinate and ξ as abscissa. These equations show, in an approximate manner, that the limit moment will be exceeded at $\xi = 0.9$ when $S > 1.2$ and at $\xi = 0.5$ when $S > 3.9$. For quite reasonable values of $S > 1$, these equations and curves demonstrate that the limit moment will be exceeded over an appreciable length of the beam.

For large energy ratios, i.e., for S approaching infinity, the elastic-plastic solution should approach the rigid-plastic solution, but referring again to the example just outlined, the values 0.246 and 0.167 given by the respective theories for $M_p\theta_f/mLV_o^2$ are in poor agreement. The "single hinge" rigid-plastic solution gives a corresponding value of 0.25 which agrees well with the limit of the elastic-plastic theory, but this agreement is to be expected since both approaches are based on the single hinge assumption. The limiting value for deflection by the elastic-plastic theory is 0.246 which shows better correlation with values of 0.239 (rigid-plastic) and 0.25 ("single hinge" rigid-plastic) than the values for angular deformations show.

It must be concluded that the elastic-plastic solution, as presented, is only strictly true for deformations occurring in the range $S \geq 1$ when elastic effects need to be considered. No experimental work has been carried out with the

specific purpose of testing the elastic-plastic solution in this range of low intensity loading. The tests results of Aspden and Campbell ('966) mentioned in Section 5 of Chapter I indicate that some caution may be required in choosing a value for the yield moment. They showed for mild steel that the transition from elastic to plastic states of deformation in bending may occur at an enhanced value of the static plastic moment where the yield curve shows a sharp peak. This increase in yield varies with the rate of loading but even for low rates the effect may be considerable. However, these effects, as noted, depend on the prior treatment of the material and on the geometry of the structure in complex ways that have received little investigation.

3. Numerical treatments

The difficulties of elastic-plastic analyses of the types outlined above are such that the analytical solutions must be replaced by schemes of numerical solution of the dynamical equations. Quite general numerical schemes have been described by Newmark (1959) and by Baron, Bleich, and Weidlinger (1961). These schemes both replace the actual structure by an assemblage of discrete masses connected by various kinds of structural elements; they approach the solution in different ways, which will be outlined. A basically different approach is that in which the partial differential equations of motion are first written and then reduced to systems of difference equations which are then solved by appropriate techniques. The only complete solution of this type for a beam seems to be that obtained by Alverson (1956) for a problem of impact of a cantilever.

More recently than Newmark and Baron et al, a group under Pian and Witmer in the Aeroelastic and Structures Research Laboratory at Massachusetts Institute of Technology has devised schemes for the numerical solution of dynamic load problems of beams, arches, plates, and shells (Witmer, Balmer, Leech, and Pian, 1963). Their numerical technique was originally programmed for the MIT 7090 computer, and is evidently

highly successful, in view of the generality of the treatment, the complexity of the problems solved, and the apparently efficient use of machine time. Witmer et al have included not only elastic deformations but finite changes of geometry, strain hardening and strain rate sensitivity in the analysis. Their finite difference scheme employs a step-by-step explicit method, the structure being replaced by a finite number of masses and connecting links. The connecting links are chosen to consist of two or more flanges carrying tension or compression stresses, separated by web material which carries shear stresses but is assumed to undergo no shearing deformation. With this model, the use of a forward difference scheme requires restrictions on the choice of the time interval Δt in relation to the space interval Δx, in order to achieve stability in the computations, i.e. in order to prevent errors from propagating with increasing magnitude. Pian, Witmer, and co-workers have not analyzed error propagation theoretically, but find empirically that $\Delta t/\Delta x = 0.7/C_o$ gave satisfactory results, where $C_o = \sqrt{E/\rho}$ is the speed of elastic waves of plane stress. This direct proportionality between Δt and Δx is apparently due to the choice of model.

We shall not attempt to describe the MIT techniques in detail, even though they are the most versatile of those that have been described. Reference will be made later to one result presented recently in discussion; this concerns the problem of a beam subjected to impulsive load at the tip, and will be described in connection with test results on beams and on the inclusion of rate sensitivity of the yield stress.

We shall summarize the approaches of Newmark (1959) and of Baron et al(1961) in order to illustrate some of the problems arising in numerical treatments of elastic-plastic problems.

Referring to Newmark's method, a distinctive feature is its viewpoint of separation of the dynamic problem from the one of structural properties. The mass of the structure is first concentrated in a finite number of mass particles. There are no rules for making this substitution; an engineer must largely depend on intuition.

At any rate, there is then a finite number of degrees of freedom, and a scalar equation of motion for each degree of freedom. Newmark writes the typical equation of motion in the form

$$P(t) - R = ma \tag{3.1}$$

where

a is the acceleration along an axis corresponding to a particular degree of freedom.

m is the mass of a typical mass particle.

P(t) is the external force component applied along the axis for which a is defined; P(t) is assumed to be known.

R is the resisting force exerted by the structure, along the axis for which a is defined.

Newmark's method depends on the concept that the complete system of resistive forces, of which R is a typical member, are all determinable at any given instant from knowledge of the current geometrical configuration, the history of deformations, and the known properties of the materials. The computation of the system of resistive forces requires the solution of equations of static equilibrium, even though viscous or other rate dependent physical effects are involved.

The integration of the equation of motion (3.1) is performed by an iteration scheme. Consider that the configuration of the structure is known at time t_n so the displacements and velocities are known at all of the mass points, together with the resistive forces R_n of the structure. Given displacement ξ_n, velocity v_n and acceleration a_n at t_n, the problem is to determine $\xi_n + 1$, $v_n + 1$ at time $t_n + 1$.

$$\text{Let } t_{n+1} - t_n = h \tag{3.2}$$

Newmark discusses the following difference formulas:

$$v_{n+1} = v_n + (1 - \gamma)\, a_n h + \gamma a_{n+1} h \tag{3.3}$$

$$\xi_{n+1} = \xi_n + v_n h + (\tfrac{1}{2} - \beta)\, a_n h^2 + \beta a_{n+1} h^2 \tag{3.4}$$

where γ and β are constants to be chosen so as to facilitate the computation.

Postponing for the moment discussion of the choice of γ and β, the iterative scheme is as follows:

1. let a'_{n+1} be a guess for a_{n+1}
2. compute v'_{n+1} from equation (3.3) and ξ'_{n+1} from equation (3.4) using a'_{n+1}, v_n, ξ_n.
3. from knowledge of the configuration of the structure (all values of ξ'_{n+1} and v'_{n+1} having been found), determine the corresponding resistive forces R'_{n+1}.
4. calculate a''_{n+1} by means of equation (3.4),

$$a''_{n+1} = \frac{1}{m}\,(P_{n+1} - R'_{n+1}) \tag{3.5}$$

The cycle is repeated, if necessary, until sufficiently close agreement is obtained between the guessed value a'_{n+1} and the computed value a''_{n+1}.

The choices of h, γ and β are governed by considerations of convergence and stability. Suppose the actual motion is that of a simple harmonic motion with radian frequency ω; then $a = -\omega^2\xi$. For a choice a'_{n+1} for a_{n+1} we have

$$\xi'_{nh} = \xi_n + v_n h + (\tfrac{1}{2} - \beta)\, h^2 a_n + \beta h^2 a'_{n+1}$$

$$a''_{n+1} = -\omega^2 \xi_{n+1}$$

$$= -\omega^2 \left[\xi_n + v_n h + (\tfrac{1}{2} - \beta)h^2 a_n\right] - \omega^2 \beta h^2 a'_{n+1}$$

The actual value a_{n+1} is given by

$$a_{n+1} = -\omega^2 \left[\xi_n + v_n h + (\tfrac{1}{2} - \beta)h^2 a_n\right] - \omega^2 \beta h^2 a_{n+1}$$

The ratio p of the error of the derived result to the error of the assumed result is

$$p = \frac{a''_{n+1} - a_{n+1}}{a'_{n+1} - a_{n+1}} = -\omega^2 \beta h^2 \qquad (3.6)$$

Convergence of the iteration scheme requires $|p| < 1$. Hence we have the result that for convergence

$$\beta\omega^2 h^2 < 1; \quad \text{or } \frac{h}{T} < \frac{1}{2\pi}\sqrt{\frac{1}{\beta}} \qquad (3.7)$$

where $T = 2\pi/\omega$ is the period of the motion. For a complex system, T must be taken as the smallest natural period of vibration, i.e. the period of the highest mode of vibration. If plastic deformation occurs, the periods of natural vibration increase; hence h can be correspondingly increased.

Stability is similarly studied under the assumption that the system is in simple harmonic motion with radian frequency ω, so that $a = -\omega^2\xi$. Appropriate equations of the type of equations (3.3), (3.4) can be combined to obtain the following difference equation in ξ:

$$\xi_{n+1} - (2 - \alpha^2)\xi_n + \xi_{n-1} + \alpha^2(\gamma - \tfrac{1}{2})(\xi_n - \xi_{n-1}) = 0 \qquad (3.8)$$

where

$$\alpha^2 \equiv \frac{\omega^2 h^2}{1 + \beta\omega^2 h^2} \qquad (3.9)$$

The last term on the left hand side of equation (3.8) is proportional to the finite difference formula for a velocity, and hence this term corresponds to a viscous damping. Since the system is assumed to be executing simple harmonic motion and to lack physical damping, the damping term in equation (3.8) is spurious. Elimination of the unwanted damping term therefore requires the choice $\gamma = 1/2$, and the difference equation for simple harmonic motion is then

$$\xi_{n+1} - (2 - \alpha^2)\, \xi_n + \xi_{n-1} = 0 \tag{3.10}$$

If one looks for a solution of form $\xi_n = \lambda^n$, one finds that

$$\alpha^2 = \frac{\omega^2 h^2}{1 + \beta\omega^2 h^2} < 4 \tag{3.11}$$

is the requirement for λ to be complex and hence for the solution to be stable.

Summarizing, in Newmark's method the iteration scheme makes use of the following difference equations relating time t, acceleration a, velocity v, and displacement ξ:

$$h = t_{n+1} - t_n \tag{3.12a}$$

$$a_n = \frac{1}{m}\left[P_n(t) - R_n(\xi)\right] \tag{3.12b}$$

$$v_{n+1} = v_n + \frac{1}{2} a_n h + \frac{1}{2} a_{n+1} h \tag{3.12c}$$

$$\xi_{n+1} = \xi_n + v_n h + (\tfrac{1}{2} - \beta)\, a_n h^2 + \beta a_{n+1} h^2 \tag{3.12d}$$

where the time interval h and the constant β are related by considerations of convergence and stability, assuming the system to be executing simple harmonic motion

with period $T = 2\pi/\omega$ as follows:

Convergence:
$$\frac{h}{T} \leq \frac{1}{2\pi} \sqrt{\frac{1}{\beta}} \tag{3.13a}$$

Stability:
$$\frac{h}{T} \leq \frac{1}{\pi} \frac{1}{\sqrt{1 - 4\beta}} \tag{3.13b}$$

The two criteria give limits as indicated in Table II, 3.

Table II 3

Convergence and Stability Limits

β	0	1/12	1/8	1/6	1/4
Limit on h/T					
Convergence h/T $\leq$	∞	0.5[illegible]	0.450	0.389	0.318
Stability h/T $\leq$	0.318	0.389	0.450	0.551	∞

The convergence and stability limits, it should be remembered, are derived from consideration of motion of the system in simple harmonic motion with period T. For an elastic system with many normal modes, T must be interpreted as the shortest natural period. In more complex problems involving plastic deformations, strain rate dependence, geometry changes, and other physical effects which preclude modal analysis, the above can only be taken as a rough guide. As a matter of fact, although Newmark's method has been applied to many problems of elastic and elastic-plastic deformation, there seem to be no published accounts of application to problems where geometry changes required changes in the equilibrium equations and in the expressions for material behavior, or to problems involving plastic deformation except of ideally

plastic nature. Because of the very general conceptual nature of the method it should in principle be applicable to such more general problems. However, question of convergence and stability remain to be investigated for these problems.

Less general but more direct and simple for many problems are finite difference methods of more conventional type. An example of such a method is that described by Baron, Bleich, and Weidlinger (1961). A typical beam problem is indicated in Fig. II 6(a). The distributed beam mass is first replaced by a number of mass particles. The notation is indicated in Fig. II 6; y_j, Q_j, and M_j being displacement, shearing force, and bending moment respectively. The intervals b_j between mass particles can be chosen arbitrarily, and the applied force per unit length q_j, mass per unit length m_j, and other beam properties can have any values but are taken as constant in each interval b_j. Thus the equation of motion for the typical mass particle is

$$\bar{m}_j \ddot{y}_j = P_j + Q_{j+1} - Q_j = P_j + \frac{M_{j+1} - M_j}{b_{j+1}} - \frac{M_j - M_{j-1}}{b_j} \tag{3.14}$$

where

$$\bar{m}_j = \frac{m_j b_j + m_{j+1} b_{j+1}}{2} \tag{3.15}$$

$$P_j = \frac{q_j b_j + q_{j+1} b_{j+1}}{2} \tag{3.16}$$

$$b_j = x_j - x_{j-1}$$

For elastic action at the typical station x_j, one introduces an effective stiffness factor K_j by writing

$$M_j = K_j \theta_j = \frac{2\,EI}{b_j + b_{j+1}} \left(\frac{y_j - y_{j-1}}{b_j} - \frac{y_{j+1} - y_j}{b_{j+1}} \right) \tag{3.17}$$

where

$$K_j = \frac{2\,EI}{b_j + b_{j+1}} \tag{3.18}$$

For the sake of illustration, let us take the simpler case of a uniform beam and let

$$m_j = m$$

$$b_j = b$$

Then the basic equations take the forms

$$b\, m\, \ddot{y}_j = P_j + \frac{1}{b}\,\delta^2 M_j \tag{3.19}$$

$$M_j = -\frac{EI}{b^2}\,\delta^2 y_j, \qquad M_j < M_p \tag{3.20}$$

where

$$\delta^2 f_j = f_{j+1} - 2f_j + f_{j-1} \tag{3.21}$$

Baron et al propose a forward integration scheme using the finite difference formula

$$\ddot{y}_j(t) = \frac{1}{h^2}\left[\, y_j(t+h) - 2y_j(t) + y_j(t-h) \,\right] \tag{3.22}$$

where $h = \Delta t$ is the interval of the time steps. This corresponds to taking $\beta = 0$ in Newmark's scheme, and hence the requirement for stability is $h/T \leq 1/\pi = 0.318$. Given values at time t, displacement at time $t + h$ can be found from

$$y_j(t+h) = 2y_j(t) - y_j(t-h) + \frac{h^2}{bm}\left[\, P_j(t) + \frac{1}{b}\,\delta^2 M_j(t) \,\right] \tag{3.23}$$

When the bending moment as computed from equation (3.20) exceeds the plastic moment M_p, at a station x_k, a plastic hinge occurs at this station. Angular rotations at constant bending moment are allowed to occur across a plastic hinge, and the

deflections are no longer related to the bending moment through elastic equations such as equations (3.17) and (3.20). If there is a plastic hinge rotation ("kink") ϕ_k at a station x_k, a deflection y_j' can be associated with this rotation. This deflection can be written as

$$y_j' = b\phi_k\psi_{jk} \tag{3.24}$$

where

$$\begin{aligned} \delta^2\psi_{jk} &= -1 \text{ for } j = k \\ \delta^2\psi_{jk} &= 0 \text{ for } j \neq k \end{aligned} \tag{3.25}$$

Thus $b\psi_{jk}$ represents the deflection curve corresponding to a kink angle unity at station k. If hinges at several stations have been operative, their total contribution to the deflection can be written as

$$y_j' = \Sigma_k\, b\phi_k\psi_{jk} \tag{3.26}$$

The total deflection at any instant t can be written as

$$y_j = y_j^e + y_j' = y_j^e + \Sigma_k b\phi_k\psi_{jk} \tag{3.27}$$

The elastic part y_j^e is related to the bending moment through equation (3.20) (or more generally, equation (3.17)), so that, using equation (3.25),

$$M_k(t) = -\frac{EI}{b^2}\,\delta^2 y_k(t) - \frac{EI}{b}\,\phi_k(t) \tag{3.28}$$

Let us write

$$\phi_k(t + h) = \phi_k(t) + \Delta\phi_k(t) \tag{3.29}$$

Then

$$M_k(t + h) = M_k^e(t + h) - \frac{EI}{b} \Delta\phi_k(t) \tag{3.30}$$

where

$$M_k^e(t + h) = - \frac{EI}{b^2} \delta^2 y_k(t + h) - \frac{EI}{b} \phi_k(t) \tag{3.31}$$

Suppose all values at time t are known; i.e. $y_j(t)$, $\phi_k(t)$, $M_j(t)$ are known for all j. To determine values at $t + h$, assume (at each plastic hinge station x_k) that $\Delta\phi_k(t) = 0$. All displacements $y_j(t + h)$ can then be calculated from equation (3.23) or its equivalent for more general cases, and the corresponding bending moments $M_k^e(t + h)$ are given by equation (3.31). Suppose at $x_j = x_k$ that $M_k^e(t + h) \leq M_p$; this is then the correct moment at x_k, and $\Delta\phi_k(t) = 0$. However, suppose it is found that $M_k^e(t + h) > M_p$. We then set $M_k(t + h) = M_p$ and compute $\Delta\phi(t)$ from the equation

$$\frac{EI}{b} \Delta\phi_k(t) = M_k^e(t + h) - M_p \tag{3.32}$$

Then we can compute

$$\phi_k(t + h) = \phi_k(t) + \Delta\phi_k(t) \tag{3.33}$$

and

$$y_j(t + h) = y_j^e(t + h) + \Sigma_k \, b\phi_k(t + h)\psi_{jk} \tag{3.34}$$

where the deflections y_j^e are those obtained by assuming that the hinge rotations are all zero in the interval from t to $t + h$.

The procedure is outlined above for "positive" hinge rotation increments, as in Fig. II 6(e). It clearly applies with obvious sign changes if hinge rotation

increments are negative. In any case, $\Delta\phi_k(t) = 0$ if $|M_k^e(t + h)| \leq M_p$. There is no difficulty about programming the method for an electronic computer so that any number of hinge rotations, of any signs, can be accounted for. However, there has apparently been no attempt to adapt the method to more complicated situtations, such as, for example, to problems where geometry changes, axial constraints, strain hardening or strain rate influences on the yield stress must be considered. An example of the application of this method will be given later for comparison with a much simpler approach.

4. Rigid-Plastic Analyses

The difficulty of obtaining a complete elastic-plastic solution, by either analytic or numerical means, has forced consideration of simplifications in the governing equations. In plasticity theory the neglect of elastic strains by comparison with plastic ones leads to a great simplification in the analysis, and this is a natural and permissible assumption when the typical plastic strains are very much larger than the largest elastic strains. This assumption, namely that strain rates are zero except at points where the plastic yield condition is satisfied, has been made in solving many problems of static plasticity. Its use in problems of dynamic plasticity seems to have begun during World War II. G. I. Taylor (1948) discussed the interpretation of dynamic compression tests in which a projectile is fired into a rigid plate by means of a rigid-plastic analysis, (Lee and Tupper (1954)). The use of the concept of rigid-plastic behavior in beam dynamics was suggested by E. N. Fox (1947). Conroy (1952) studied in more detail the application of the concept to beam problems by investigating the infinite-beam problem studied by Bohnenblust.[1] Rigid-plastic behavior must be regarded as the limiting case of elastic-plastic behavior as the Young's modulus E approaches infinity. Conroy showed that for an ideally plastic material the rigid-plastic solution of Bohnenblust's problem could be easily written

[1] See Duwez, Clark, and Bohnenblust (1950)

in simple closed form. For the same material the elastic-plastic solution was solved for a succession of values of $\sqrt{EI/m}$ where EI is the flexural rigidity, m is mass per unit length ranging from 167 to 10^6, and the results showed a satisfactory approach to those of the rigid-plastic solution, $EI/m = \infty$. Conroy attempted also to find the rigid-plastic solution for a linearly strain hardening material, but was unable to complete the solution and hence could not make the limiting comparison as for the ideally plastic case.

A discussion of the general characteristics of rigid-plastic solutions of problems of finite beams was first given by Lee and Symonds (1952). They showed that, depending on load magnitudes, plastic hinges and finite plastic regions can be expected to appear, and in general the plastic hinges and the boundaries of the finite plastic zones will move during the course of the deformation. Moving plastic hinges and interfaces between plastic and rigid regions in general involve discontinuities in the angular velocity and in the transverse acceleration.

The simplest type of rigid-plastic analysis is that in which perfectly plastic behavior is assumed (strain-hardening is neglected). A large variety of problems has been solved on this basis. These solutions are extremely simple by comparison with elastic-plastic solutions. The question that immediately arises is that of the physical validity of the results. In the following discussion of rigid-plastic solutions the main emphasis will be put on indications from theory and experiment concerning the ranges of validity of this type of analysis. It will be shown that while the ideally rigid-plastic analysis does provide a simple starting point, the conditions in which it is permissible to neglect elastic strains are often conditions in which other secondary effects become seriously influential. The most important of these secondary effects, according to indications of experimental investigations, are (1) increase of yield stress at high strain rates, and (2) change of mode of behavior caused by finite

deflections in the presence of constraints.

The great merit of rigid-plastic analysis is that the inclusion of secondary effects remains feasible in a solution of analytic type, without requiring a completely numerical scheme of integration. Apart from strain rate and geometry change effects many other secondary influences, such as strain hardening, shear deformation, and rotary inertia can be included in a rigid-plastic analysis. Any of these could be included in an elastic-plastic solution also, of course, but only in a numerical integration process which itself is by no means straightforward.

One-Degree-of-Freedom Systems

The following discussion will consider by means of simple examples the criteria for the neglect of elastic strains, and for the inclusion of the major secondary effects.

Some basic information about the relation of rigid-plastic to elastic-plastic solutions can be gained from a study of the simplest structural model, namely a simple spring-mass system.

With the notation indicated in Fig. II 7, the motion of the mass is governed by the following equation and initial conditions:

$$m\ddot{x} = P - Q(x) \tag{4.1}$$

$$x(0) = \dot{x}(0) = 0 \tag{4.2}$$

We shall consider motion due to a rectangular pulse of force as in Fig. II 8 with magnitude P_o and duration τ.

Suppose first that the spring characteristic $Q(x)$ is that of elastic-perfectly plastic behavior, so that, as indicated in Fig. II 9, curve a, there is an elastic spring constant k, a yield force Q_y, and a yield deflection x_y. The solution for the initial elastic motion involves the radian frequency $\omega = \sqrt{\frac{k}{m}} = 2\pi/T$ of the mass-spring

system, and is

$$x = \frac{P_o}{k}(1 - \cos \omega t), \qquad t \leq \tau \tag{4.3}$$

This holds while the motion is elastic, i.e. for $x \leq x_y$, $Q \leq Q_y$. If $x(t_y) = x_y$ and we assume that $t_y \leq \tau$, the solution is readily found in stages, putting the right hand side of equation (4.1) first equal to $P_o - Q_y$, for $t_y \leq t \leq \tau$, and then equal to $- Q_y$ for $\tau < t$. The maximum displacement x_m is then found by setting $\dot{x}(t_m) = 0$, solving for t_m and evaluating $x(t_m) = x_m$. The final plastic deformation is $x_p = x_m - x_y$. This result will apply to the case when $t_y \leq \tau$, i.e. when the load P_o is large enough so that the yield condition is reached during the duration of the pulse. Alternatively, if the load is small enough so the yield condition is satisfied at $t_y \geq \tau$, the maximum displacement can be found in a similar manner. The results are conveniently expressed in terms of the following dimensionless variables of the system:

$$\mu \equiv \frac{P_o}{Q_y} = \frac{\text{load magnitude}}{\text{yield force}}$$

$$\zeta = \omega\tau = 2\pi\frac{\tau}{T} = 2\pi\left(\frac{\text{pulse duration time}}{\text{natural period of system}}\right)$$

In terms of the above quantities, the results are as follows:

(1) If $\mu < \frac{1}{2}$, no plastic deformation takes place, regardless of the value of ζ.

(2) If $\zeta \leq \pi$, and $\frac{1}{\sqrt{2(1 - \cos \zeta)}} \leq \mu \leq \frac{1}{1 - \cos \zeta}$: plastic flow begins <u>after</u> the duration of the load pulse, $t_y \geq \tau$, and the final plastic deformation is given by

$$\frac{x_p}{x_y} = \mu^2(1 - \cos \zeta) - \frac{1}{2} \tag{4.4}$$

(3) If $\zeta \leq \pi$ and $\frac{1}{1 - \cos \zeta} \leq \mu$; or if $\zeta \geq \pi$, $\frac{1}{2} \leq \mu < \infty$: then plastic flow

begins during the load pulse, $t_y \leq \tau$, and the final plastic deformation is given by

$$\frac{x_p}{x_y} = \mu - \frac{1}{2} + \mu\sqrt{2\mu - 1}\,(\zeta - \phi) + \frac{1}{2}\mu(\mu - 1)(\zeta - \phi)^2 \tag{4.5}$$

where

$$\cos\phi = 1 - \frac{1}{\mu}, \qquad \phi \leq \zeta$$

and

$$\phi \equiv \omega t_y \equiv \sqrt{\frac{k}{m}}\, t_y \tag{4.6}$$

The relations between t_y, τ and μ, for $t_y \leq \tau$, are illustrated by Fig. II 10.

If $\mu(1 - \cos\zeta) = 1$, then $t_y = \tau$; i.e. the time when the yield force is first reached coincides with the end of the load pulse, and the quantity x_p/x_y is $\mu - 1/2$.

To obtain the rigid-plastic solution of the problem, we use the force displacement characteristic b of Fig. II 9, and thus assume that no deformation occurs if $P_o \leq Q_y$. If $P_o > Q_y$, the plastic deformation is easily found by integrating the equations

$$m\ddot{x} = P_o - Q_y \qquad 0 \leq t \leq \tau \tag{4.7}$$

$$m\ddot{x} = -Q_y \qquad \tau < t \tag{4.8}$$

The maximum plastic deformation occurs at time t_m when $\dot{x}(t_m) = 0$, and its magnitude is $x'_p = x(t_m)$.

The result in appropriate dimensionless form is

$$\frac{mx'_p}{Q_y\tau^2} = \frac{1}{2}\mu(\mu - 1) \tag{4.9}$$

We now compare the rigid-plastic solution equation (4.9) with the elastic-plastic one equation (4.4). We note that

$$\frac{mx'_p}{Q_y\tau^2} = \frac{mx_y}{kx_y\tau^2}\frac{x'_p}{x_y} = \frac{1}{\zeta^2}\frac{x'_p}{x_y} \tag{4.10}$$

We define the relative error as

$$e = \frac{x_p - x'_p}{x_p} \tag{4.11}$$

where

x_p = plastic deformation of elastic-plastic analysis

x'_p = plastic deformation of rigid-plastic analysis

We are interested in how the relative error e depends on the structural parameters μ = ratio of applied load to yield load, and τ/T = ratio of load pulse duration time to natural period of the system. In addition to these, an alternative parameter expressing the severity of loading is the energy ratio R,

$$R = \frac{\text{work done in plastic deformation}}{\text{maximum elastic strain energy}} = \frac{Q_y x_p}{\frac{1}{2}Q_y x_y} \tag{4.12}$$

The significance of the parameter R will be discussed later.

In Figs. II 11 and II 12 are shown curves of the deflections according to elastic-plastic and rigid-plastic theory, and of the relative error e plotted as functions of μ and R'. The quantity R' is evaluated from the result for the plastic deformation x'_p as given by the rigid-plastic theory

$$R' = \frac{Q_y x'_p}{\frac{1}{2}Q_y x_y} = 2\frac{x'_p}{x_y} = \mu(\mu - 1)\zeta^2 \tag{4.13}$$

where $\frac{1}{2}Q_y x_y$ is the maximum energy that can be stored elastically in the spring-mass system.

The results for impulsive loading are included in the Figures II 11 - II 13 showing comparisons. By definition an impulsive load is one with P(t) and τ such that

$$\tau \to 0, \qquad \int_0^{\tau} P(t)dt \to I \tag{4.14}$$

The impulse I imparts a velocity v_o to the mass, which then moves subject to the initial conditions and equation of motion

$$x(0) = 0$$

$$\dot{x}(0) = v_o = \frac{I}{m} \tag{4.15}$$

$$m\ddot{x} = -Q(x)$$

The plastic deformations are given by:

(A) Elastic-Plastic

$$x_p = \frac{m\, v_o^2}{2\, Q_y} - \frac{1}{2} x_y \tag{4.16}$$

(B) Rigid-plastic

$$x'_p = \frac{m\, v_o^2}{2\, Q_y} \tag{4.17}$$

These results are obtained readily by equating the initial kinetic energy $\frac{1}{2} m\, v_o^2$ to the plastic work $Q_y x_p$ plus (in the elastic-plastic case) the stored energy $\frac{1}{2} x_y Q_y$.

For the impulsive load case, the relative error of the rigid-plastic solution is

$$e = \frac{-1}{\frac{m\, v_o^2}{x_y Q_y} - 1} = \frac{-1}{R - 1} \tag{4.18}$$

where R is the appropriate energy ratio $\frac{1}{2} m v_o^2 / \frac{1}{2} x_y Q_y$. Note that in this case the error is always negative for R > 1, whereas for finite v/T the error may either be positive for all R in the range of significance, or may be positive in one part of the useful range of R and negative in the other part.

The results shown in the curves of Figs. II 11 - II 13 are of less interest for their numerical magnitude than for the general indications they give concerning the validity of rigid-plastic solutions. The curves show that the rigid-plastic analysis predicts a plastic deformation which approaches that of the elastic-plastic solution as the energy ratio R becomes very large. However, while the condition

$$R >> 1 \tag{4.19}$$

is necessary, it is not sufficient. The duration time of the pulse, in relation to the natural period of elastic vibration of the system, is also very important.

The criterion R > > 1 was proposed by Lee and Symonds (1952) as a possible means of estimating the validity of rigid-plastic solutions. In static problems one expects a rigid-plastic solution to be a good approximation if the plastic strains greatly exceed the largest elastic strains. Other than this, no general rules can be given for the acceptability of such a solution. The concept of the energy ratio R is particularly convenient in problems of plastic deformation of beams because in both static and dynamic problems the concept of plastic hinges is of enormous advantage. This concept implies perfectly plastic behavior, and the plastic hinge is conceived as permitting finite rotations across a plastic zone of negligible length. In fact, of course, the plastic zone is of finite length and the strains are finite. Estimates of strain magnitudes in plastic zones can be made, but the basic theory of plastic beam behavior is convenient precisely because it deals with hinge rotations and avoids direct consideration of strains. Plastic work done at hinges (stationary or moving)

is easily computed in dynamic problems, and hence the energy ratio R of the total plastic work to the maximum possible elastic strain energy is readily computed.

The comparison of solutions of the simple one-degree-of-freedom mass-spring system shows that the criterion $R >> 1$ serves best as a guide to the validity of rigid-plastic analysis for cases of short duration, high intensity loading. For these cases the error in using the rigid-plastic method will be less than, say, ten percent if R is greater than approximately ten, and the plastic deformation will be of the order of five times the yield deflection. For long pulses, for example with $\tau/T \cong 1$, in order to have agreement to within ten percent the R value must be at least 100. This implies plastic deflection such that x_p/x_y is about 50 or greater. However, when the ratio x_p/x_y is interpreted for a beam (or other structure) as the maximum plastic deflection divided by the deflection at the point of plastic collapse when the given type of load is applied statically, it becomes evident that very large values of x_p/x_y predicted by a rigid-plastic analysis will generally fail to have physical significance. This is because of the appearance at large deflections of new physical phenomena not described in the original equations of motion used in solving the rigid-plastic problem. Such phenomena may become important as catenary forces, if the ends are constrained against axial motion; strain hardening; or increases of yield stress with strain rate.

To illustrate, consider a simply supported beam with uniformly distributed load P, Fig. II 14. For simplicity, suppose this deforms as in Fig. II 15 with a plastic hinge at mid-point, final plastic deflection δ_p and rotation angle θ_1 at the support. The energy ratio is given by

$$R = \frac{2M_p\theta_1}{\frac{1}{2}\frac{M_p{}^2L}{EI}} \cong \frac{8\delta_p}{\frac{M_pL^2}{EI}}, \qquad (4.20)$$

if we take $\delta_p \cong L\theta_1/2$. In the elastic range $\delta = 5M_m L^2/48\,EI$, where $M_m = PL/8$ is the mid-point moment. If we define δ_y as the deflection just as the plastic collapse load is reached, this is for the supported beam, approximately

$$\delta_y \cong \frac{5}{48}\frac{M_p L^2}{EI} \tag{4.21}$$

$$R = \frac{5}{6}\frac{\delta_p}{\delta_y} \tag{4.22}$$

Thus for the beam, as for the simple oscillator, $R = O(\delta_p/\delta_y)$. Now the order of magnitude of δ_y/h, where h is the beam depth, can be found from equation (4.21); for example, let $\sigma_y/E = 1.5 \times 10^{-3}$, $L/h = 20$. Then

$$\frac{\delta_y}{h} = \frac{5}{24}\frac{\sigma_y}{E}\frac{L^2}{h^2} = \frac{1}{8}$$

Hence if $\delta_p/\delta_y = 50$, say, then $\delta_p/h = 50/8 \cong 6$. But at a deflection six times the beam depth, a beam with constraints against axial motions would long since have ceased to behave like a beam; in fact, as soon as the deflection exceeds the beam depth, motion would be almost completely governed by catenary rather than beam action. Hence a prediction of $\delta_p/\delta_y = 50$ on the basis of simple beam action would lack physical meaning, and an analysis for a long force pulse by rigid-plastic methods would be useless, unless it took axial forces into account.

Apart from questions of additional physical effects not considered in an elastic-ideally plastic analysis, the question of differences between the behavior of a system having a single degree of freedom and a multi-degree-of-freedom system is fundamental to a study of the prospective validity of a rigid-plastic analysis. One may accept, as reasonable on physical grounds, the postulate that when far more energy is fed into any system than can be stored as elastic strain energy, the resulting plastic

deformations can be computed to a good approximation without regard for strains of elastic magnitude. The question is whether the complex interactions between elastic and plastic deformations that may occur in a multi-degree-of-freedom system are likely to cause the approximation to be substantially worse, for a given energy ratio and ratio of force duration to fundamental period, than for a system with a single degree of freedom.

It should be possible to answer this question adequately for practical purposes by carrying out complete elastic-plastic solutions (by numerical methods, presumably) for a variety of structures and comparing results with those of rigid-plastic solutions. Here we are concerned primarily with behavior of beams as one-dimensional continuous structures. No calculations of elastic-plastic solutions for beams have been made with sufficient completeness to permit general deductions to be made about the effects of elastic-plastic interactions. The few examples for which calculations are available seem to indicate that no large differences occur between the closeness of approximation obtained for multi- and single-degree of freedom systems. Three examples of multi-degree of freedom systems will be briefly cited.

Multi-degree of Freedom Systems:

(A) System consisting of two equal masses and two similar springs (Fig. II 16(a) and (b). This is the simplest system of more than one degree of freedom, but the plastic deformations caused by an impulsive load applied to the outer mass are much more complicated when the two springs have elastic-ideally plastic characteristics than for the single mass-single spring system, (Fig. II, 16(c). As indicated in Fig. II 17, as the energy ratio R increases from zero, plastic deformation in the inner spring first exceeds that in the outer spring, while for $R > 4$ the situation is reversed. Fig. II 18 shows times at which the two springs start to yield and cease plastic flow, as functions of R. Nevertheless, the total plastic deformation differs from that

predicted by a rigid-plastic analysis by only about 10 percent of the total deformation, when R = 5. As indicated in Fig II 17, the difference between the two results is very nearly constant, so that the relative error of the rigid-plastic solution steadily decreases and is less than 3 per cent at R = 18. But the rigid-plastic analysis predicts the plastic deformation in the inner spring to be zero (the inner mass is acted on by opposing forces Q_y on each side). Hence although the <u>total</u> plastic deformation is predicted with high accuracy by the rigid-plastic solution, this analysis is incapable of accurately determining plastic deformations in the individual springs; even the prediction for the plastic deformation in the outer spring is 20 percent in error at R = 18.

(B) Simply supported beam with uniformly distributed load P(t) having exponentially decreasing time dependence

$$P(t) = P_o e^{-t/\tau} \tag{4.23}$$

The elastic-plastic solution for the case $\tau = 1/2\ T_1$, where T_1 is the fundamental period of vibration of the beam, was given by Baron, Bleich, and Weidlinger (1961) as an illustration of their finite difference method. The rigid-plastic solution was given for general "blast type" loading by Symonds (1954); the particular case of exponential loading (equation 4.23), including consideration of shearing as well as bending deformations was treated by Salvadori and Weidlinger (1957). Baron, Bleich, and Weidlinger give results of calculations for initial load magnitues P_o up to five times the static collapse load $P_c = 8M_p/L$. Formulas for the energy ratio R, and deflection δ_y at collapse have already been given, in equations (4.20), (4.21). Values of R shown in Fig. II 19 were computed from the central hinge angle $\bar{\theta}_o$ given in the numerical results presented by Baron, Bleich, and Weidlinger,

$$R = \frac{M_p \bar{\theta}_o}{\frac{M_p^2 L}{2EI}} = \frac{5}{24} \frac{\bar{\theta}_o}{\delta_y/L} \cong 77\bar{\theta}_o \tag{4.24}$$

since their calculations take $\delta_y/L \cong .0027$.

The curve marked "Simplified Elastic-Plastic" was derived by Baron, Bleich, and Weidlinger by using the fundamental mode of elastic vibrations during the elastic phase of motion, and following this by a single hinge rigid-plastic solution with initial velocity chosen so that momentum conditions are matched. This approach is a sound one only for problems in which a single mode predominates; it works well in the present problem, for example, but not in the previous example (A).

(C) Cantilever whose base is subjected to specified motion (Fig. II20), namely with displacement and velocity as follows:

$$y(x,t) = y_t(x,t) = 0, \qquad t < 0, \qquad 0 \leq x \leq L$$

$$\left.\begin{aligned} y(0,t) &= \frac{V_o t^2}{2t_o} \\ y_t(0,t) &= V_o \frac{t}{t_o} \end{aligned}\right\} \quad 0 \leq t \leq t_o$$

$$\left.\begin{aligned} y(0,t) &= V_o\left(t - \frac{t_o}{2}\right) \\ y_t(0,t) &= V_o \end{aligned}\right\} \quad t > t_o$$

This is a problem of impact which has been used in experiments. (In general it is easier to impose and measure motions of a specimen than it is to apply forces of known distribution and time history; hence problems of this type are advantageous for laboratory tests).

The elastic-plastic analysis of this problem was carried out numerically by Alverson (1958), who made use of the fact that the system of elastic beam equations (due to Timoshenko) which take account of shearing deformations and rotary inertia is a totally hyperbolic system. Motions of the beam were therefore determined by finite difference techniques based upon the network of characteristics of this hyperbolic system; the characteristics are four families of straight lines with slopes dx/dt

proportional to $\pm c_1$ and $\pm c_2$, where $c_1 = \sqrt{E/\rho}$ and $c_2 = \sqrt{kG/\rho}$ are speeds of uniaxial tension and simple shear waves, respectively, in a bar.

Alverson carried out complete calculations for several cases, of which one was chosen to have non-dimensional parameters corresponding to ranges used in experiments conducted at Brown University. Two such parameters specify the impact characteristics, namely the energy ratio R and a parameter β proportional to the base acceleration V_0/t_o during the impact. Numerical values used were

$$R = \frac{mLV_o^2}{\frac{M_p^2 L}{EI}} = 8.33$$

$$\beta = \frac{mL^2 V}{M_p t_o} = 250$$

$$\therefore \quad \frac{t_o}{T_1} = \sqrt{\frac{R}{3.28^2}} = 0.0065$$

$$\frac{L}{h} = 25$$

$$\frac{\sigma_y}{E} = 10^{-3}$$

$$\frac{c_1}{c_2} = 2$$

Alverson's results for the above case showed a remarkably complex pattern of elastic and plastic deformations. The main plastic deformation is the angle of rotation θ_o at the base. However, the numerical analysis showed that this not only took place in an intermittent manner, but was part of a region of plastic deformation at the base whose size varied in a highly irregular way; even the sign of the rate of plastic deformation was found to reverse at certain localities near the base. In addition to the main

plastic deformation near the base, there was a secondary region of plastic flow of opposite sign in the interior of the beam. This again was of an intermittent nature, and the boundaries of the plastic region moved backward and forward irregularly. Some idea of the complexity of the plastic deformation is given by Fig. II, 21(a), (b), (c), where the times and signs of plastic flow are shown for various stations along the beam length.

Fig. II20(a)shows the plastic angle at the base as a function of the parameter $\beta = mL^2V/M_p\tau$. (This solution was obtained by D. S. Green (1954), while the limiting case $\tau \to 0$ was treated by Symonds and Leth (1954). At $\beta = 250$, the rigid-plastic solution predicts a non-dimensional plastic deformation of about 0.39, whereas Alverson's elastic-plastic result is about 0.30, corresponding to a relative error of about 30 per cent. The ratio τ/T_1 should have essentially the same significance as in a problem of loading by a force pulse. In Alverson's example $\tau/T_1 \equiv .007$, so that the requirement that the time ratio be small is apparently satisfied. The agreement of the plastic-rigid solution with the complete elastic-plastic one in the case is worse than in the examples (A) and (B), and this seems attributable to a more complex interaction between elastic and plastic deformations.

5. Plastic Moment Interactions

It is never strictly correct to ignore stresses in a beam other than bending stresses. One must consider interactions of bending moments especially with axial forces and shear forces. (In a general one-dimensional structure, we would also have to consider torsion, and bending moments and shear forces in two principal planes). But in beams with loads in a principal plane, stress resultants are M and Q (shear force) plus N (axial force) if deflections are not infinitesimal. Also, in an arch or ring N would appear from the start (even for infinitesimal deflections) as well as M and Q.

Two questions: (1) when do Q and/or N have negligible effect on plastic

moment; and (2) when Q and/or N are not negligible, how can they be taken into account?

The important quantities governing shear and axial force are a shear force Q_p and an axial force N_p, which represent, respectively, the limiting magnitudes of shear and axial force in a perfectly plastic medium, in loading by "pure shear" or by simple axial force. In a beam problem, the ratio of the actual shear force Q to Q_p, and of the actual axial force N to N_p are related to the ratio M/M_p, when plastic deformation is occurring, by an effective yield condition. In other words, plastic deformation in a beam is governed by an interaction between M/M_p, Q/Q_p, and N/N_p. This interaction is always present in practice in beams. There are indications from the few problems that have been treated (mostly analytically, not experimentally) that the interaction is more serious in the case of dynamic loads than for static loads.

We may write in general

	Rectangular Section	I or Box Section
$Q_p = K_s \frac{\sigma_y}{2} A$	$K_s \cong 1$	$K_s \cong \frac{A_w}{A}$
$N_p = \sigma_y A$		
$M_p = K_b \sigma_y h A$	$K_b = 1/4$	$K_b \cong 0.4$

where A is the total section area, A_w is the web area, and h is the section depth.

There is a true "interaction relation" in sense of yield condition relating M and N at any point (cross-section) of a beam, irrespective of general loading, support, etc. But no such interaction relation in this sense exists for M and Q; we cannot consider just one cross-section of a beam, but must consider the whole beam: loading and support conditions. Published "M-Q interaction" curves all refer to a particular problem, in most cases that of a cantilever beam. (Some published M-Q curves supposed to give lower bounds on actual M, Q are wrong, since not all conditions for a lower bound are

satisfied : examples are given by Neal 1961a).

For brevity call "local" the interaction curve which is derived by considering a single typical cross-section of a beam. As stated, a local interaction curve relating M, N can exist (correct), but no such curve relating M, Q can be strictly correct. Despite this, one may derive an M-Q curve, say for a cantilever statically loaded by an end force, and use it for estimates for other static cases and for dynamic cases. This is the procedure that has been followed.

(A) Moment-Shear Interaction

Obviously any results about importance of shear forces and shear deformations in plastic deformations due to dynamic loads, obtained by using an interaction formula, are highly approximate. Hence, we should not worry too much about the exact form of the interaction curve. The best proposed curves are those of Drucker (1956) for rectangular sections and Neal (1961a) for I-sections, both for the cantilever with end force. Drucker suggested the relation

$$\frac{M}{M_p} = 1 - \left(\frac{Q}{Q_p}\right)^4 \qquad (5.1)$$

as a good approximation for a rectangular section; this interaction curve is shown in Fig. II 22(a). Since $M = QL$, where L is the length of the cantilever, and $M_p/Q_p = h/2$ where h is the beam depth, particular beams are indicated by straight lines

$$\frac{M}{M_p} = \frac{2L}{h}\frac{Q}{Q_p}$$

The lines drawn for the two cases $L/h = 1$ and $L/h = 2$ in Fig. II 22(a) show that M falls below M_p by less than two or three per cent if $L/h \geq 2$. This means that the shear effect is entirely negligible for a rectangular beam in static loading, since a requirement that $L/h < 2$ makes any treatment as a beam virtually meaningless. How-

ever, such a conclusion does not necessarily apply to dynamic loading.

For I or box-section beams shear effects are larger. Neal (1961a) obtained good lower bounds (again considering the cantilever under a static tip loading), his curve being shown in Figs. II 22(b) and II 22(c), together with appropriate straight lines for particular beam ratios L/h_1. Here the length h_1 was taken as h-t, where t is the flange thickness; and Q_p is the capacity load of the web area in pure shear. (In view of the approximations involved in using the results, obviously h_1 may as well be taken as the beam depth h.) Neal's results show that an I section or box beam has very little strength in bending when it carries a shear force greater than the shear capacity of the web, with a very abrupt drop in moment capacity at this value of shear. In the static problem shear effects are negligible for L/h greater than about 4; again this does not necessarily imply the same conclusion for dynamic problems. The conclusion that the shear capacity of an I section is essentially the shear capacity of the web ($Q_p \cong \frac{\sigma_y}{2} A_w$) was demonstrated experimentally by Hall and Newmark (1955).

In view of the uncertainties, the simplest form of interaction curve is likely to be adequate, and this is a simple square diagram as shown in Fig. II 22(d). Here the coordinates are M/M_p and Q/Q_p where M_p and Q_p are strengths in pure bending and pure shear, respectively; Q_p is the yield stress in shear $\sigma_y/2$ times the effective cross-section area, which can be taken as the total area for a rectangle and the web area for an I beam. Deformations can be assumed to be governed by the condition of normality to the yield curve, as indicated by the arrows representing the strain rate vector with components $(Q_p\dot{\gamma}, M_p\dot{\kappa})$ in Fig. II, 22(d).

Very few dynamic problems have been studied with inclusion of shear deformations and an interaction between bending and shearing strength. Two solutions have been given in which shear deformations have been computed on the basis of an interaction theory. Karunes and Onat (1960) worked out the ca of a free-free beam initially at

rest which is struck transversely at its mid-point by a concentrated force which causes the struck point to move with constant velocity V. This problem was studied by Symonds and Leth (1954) ignoring shear deformations. The shear loading is very severe; if only bending deformations are taken into account the shear force on each side of the struck section is proportional to $\sqrt{V/t}$. The treatment by Karunes and Onat therefore starts with pure shear deformation (sliding) of an element at the struck point. If the beam is sufficiently short, for a given material and section shape, only sliding occurs (Fig. II 23(a)); this requires

$$\frac{Q_p L}{M_p} \leq 4 \qquad (5.2)$$

When the above condition is satisfied very large shear deformations can occur with zero bending, as shown in Fig. II 24 by the curve marked "Shearing Deformation". If the bending strength is reduced, so that $Q_p L/M_p > 4$, then bending deformations occur together with shearing; the two ranges of $Q_p L/M_p$ are indicated in Fig. II 23(b) and (c). The curve labeled "Bending Deformation" in Fig. II 24 shows the final deformation angle as function of $Q_p L/M_p$. The straight line at $M_p \theta_f / mlV^2 = 0.425$ is the result predicted by the analysis neglecting shear deformations.

This is a problem in which extremely severe shear loads occur, and in which the large shear forces and deformations occur at cross-sections where the bending moment is large and bending deformations take place. The curves of Fig. II 24 show that the analysis neglecting shearing deformations overestimates the main bending deformation by an amount less than 20 per cent if $Q_p L/M_p$ is less than about 10. For rectangular sections this requires quite short beams, since $Q_p L/M_p = 2L/h$; serious shear effects would require $L/h < 5$. However, for I- or box-section beams a comparable influence of shear deformation would occur for much larger span-depth

ratios. For these sections, $Q_p L/M_p$ is of the order of $\frac{\sigma_y}{2} A_w L/\frac{\sigma_y}{2} Ah = A_w L/Ah$, where A_w is the web area, A the total section area. Since A_w/A can be quite small - about 1/4 for an 8WF40 - a minimum L/h of as much as 30 to 40 may be demanded, in order to keep the influence of shear on bending deformations less than about 20 per cent.

As mentioned, the case considered by Karunes and Onat is a particularly severe one in regard to shear effects. The problem first treated by Salvadori and Weidlinger (1957) and later extended by Nonaka and Symonds (1967) is perhaps more typical of practical cases. Salvadori and Weidlinger considered a simply supported rigid-perfectly plastic beam subjected to a uniformly distributed loading $P = P_c e^{-t/\tau}$ and showed that the beam may deform plastically by developing plastic slides at the supports and a plastic hinge at the mid-span. Here the maximum shear force comes at sections where the bending moment is zero, and vice versa. The square interaction curve of Fig. II 22(d) is appropriately used. In the above solution it is assumed that the plastic hinge at the midspan does not spread, whereas in the treatment presented by Nonaka and Symonds this phenomenon is included in the analysis. Also comparisons are made between deformations produced by an exponential and a rectangular load pulse and impulsive loading.

No deformation occurs unless the applied load P is of a sufficient magnitude to cause the maximum moment M_p to occur at the midspan or the maximum shear force Q_p at the supports. For a beam stronger in shear, bending takes place at a central plastic hinge for $P \geq 4M_p/L$; correspondingly, for a beam stronger in bending than shear, deformation occurs as shear slides at the supports for $P \geq 2Q_p$. The magnitudes of final deformations are functions of the parameters $\nu = P_s/P_b = Q_p L/2M_p$ and $\mu_o = P_o/P_b = P_o L/4M_p$ where $P_s = 2Q_p$ is the collapse load in shear and $P_b = 4M_p/L$ is the collapse load in bending.

It develops that motion may start in any of five different modes depending on

the values of ν and μ_o. The mode shapes and the limiting values of ν and μ_o for each particular mode are illustrated in Fig. II 25. It is noted that for $\nu < 1$ yielding in shear only takes place and the maximum bending moment in the beam does not reach M_p, regardless of the magnitude of the load. However, for $\nu > 1$ mixed modes of shear slides and a central hinge or plastic zone may occur depending on the values of ν and μ_o. As the value of μ_o tends to infinity, i.e. impulsive loading, shear motion always occurs. Types (E) and (B) motions were not considered by Salvadori and Weidlinger. The latter type of motion and type (A) motion, i.e. pure bending only, have been analyzed in detail by Symonds (1954).

In Fig. II, 26 are shown curves of final mid-point deflection relative to the support points for three different load pulse shapes, and with ν as parameter. In all cases the total impulse is the same. We see that in the case of the rectangular pulse, for μ_o greater than 10, the mid-point deflection is practically independent of μ_o and takes approximately 90 per cent of its limiting value of impulsive loading. For a corresponding exponential pulse load, i.e. with the same impulse and peak load, smaller deformations are produced and this is explained by the fact that deformation is complete before the end of the exponential pulse while for the rectangular pulse the whole impulse affects the deformation. This difference becomes more significant for small values of μ_o. For a given pulse shape, a single curve of $M_p \delta_f / \hat{I}^2$ against μ_o applies for all $\nu \geq 1.5$. It is noted also from Fig. II 26 that for certain values of $\nu < 1$ the deformation caused by shear motion alone exceeds that of the other types of motion. This fact is better illustrated by plotting deformation values against ν with μ_o as parameter as in Fig. II 27. We see that for any particular load, deformation is a minimum at $\nu = 1.0$, greatest for $\nu < 0.75$ approximately, and constant for $\nu > 1.5$. The deformation modes are lettered and indicated by the dotted lines in Fig. II 27 Figs. II 25 and II 27 are reproduced from Nonaka and Symonds (1967).

It has been mentioned that Salvadori and Weidlinger considered Type (D) motion only. A qualitative difference appears when this assumption of a single bending hinge at the center is made, instead of considering finite plastic zones at the center. Instead of there being one deformation-load curve for all $\nu \geq 1.5$ (for given pulse shape), as found in the complete solution, when the single-hinge approximation is made different curves are obtained for different values of ν, when μ_o exceeds a certain magnitude. In Fig. II 26 the "single hinge" curves are drawn for the limiting case $\nu = \infty$, for the two pulse shapes considered. It is seen that the quantitive error of the single hinge approximation is small.

To sum up, whether or not shear deformations are important depends mainly on the magnitude of $\nu = Q_p L/2M_p$. If $\nu > 1.5$, the presence of shear deformations has a negligible effect on the major deflections. For a range of ν between about 0.8 and 1.5 the shear deformation results in <u>smaller</u> deflections, but for ν smaller than about 0.8, the deflections are <u>larger</u> than predicted by the theory for bending deformation only (shear strength taken as infinite).

For a rectangular or other compact section $\nu \tilde{=} L/h$ and shear deformations are unimportant. For box and I sections, however, ν is smaller; for example, $\nu = L/7h$ for an 8 WF 40 section. For such sections, shear deformations can be important if the span is less than about 10 times the depth.

(B) <u>Moment-Axial Force Interaction</u>

The above discussion considered situations where shear forces were large but axial forces N were zero or at least very small. However, in practical problems of dynamic loading causing large deformations, axial forces must often be considered; they may play the principal role in determining the load-deformation characteristic of the structure. Consider a beam whose ends are fully constrained and which is subjected to a transverse pressure of high initial intensity. Neglecting effects of shearing deformation, suppose the loading can be approximated as of impulsive type;

the pressure imparts an initial velocity V to the whole beam. The initial response of the beam is one of elastic bending, but if V is sufficiently large, plastic deformations much larger than those in the elastic range will be produced. This problem was analyzed by Symonds and Mentel (1958). Assuming a rectangular cross-section the interaction between bending moment M and axial force N was taken as follows:

$$\frac{|M|}{M_p} + \frac{N^2}{N_p^2} = 1 \tag{5.3}$$

Deformations generally are a combination of axial extension ε_o at the centroid of the cross-section and curvature κ of the center line. The rates $\dot{\varepsilon}_o$, $\dot{\kappa}$ (or increments) of these quantities are related by

$$\frac{N_p \dot{\varepsilon}_o}{M_p \dot{\kappa}} = 2\frac{N}{N_p} \tag{5.4}$$

With these relations, the rigid-plastic analysis can be carried out without difficulty for the transition phase of the motion in which the initial bending response is replaced by one in which both bending and axial extension occur. This analysis shows that when the central deflection reaches a magnitude roughly equal to the depth h of the beam, the axial force becomes equal to N_p and the bending moment vanishes. For further deflections the beam behaves like a plastic string or membrane, carrying axial force N_p without bending. The analysis of this phase of the response is complicated by the need to satisfy the flow relation (5.4). When $N/N_p = 1$, $\dot{\varepsilon}_o$ and $\dot{\kappa}$ must satisfy the inequalities

$$-1/2 \leq \frac{M_p \dot{\kappa}}{N_p \dot{\varepsilon}_o} \leq 1/2 \tag{5.5}$$

Symonds and Mentel ignored this restriction resulting from the finite bending

strength of the section: the beam is treated in the second phase like a plastic string until the maximum deflection is reached, which is taken as the final deflection. Deflections obtained in this way are bounded above by the deflection calculated assuming plastic string behavior during the entire motion, rather than just the final stage. They are bounded below by results of an analysis continuing (beyond its proper range) the treatment for beam response with bending moment-axial force interaction. The curves shown in Fig. II 28 show the final deflection according to the complete (approximate) solution of reference, together with the upper and lower bound solutions just mentioned, and the simplest rigid-plastic solution in which axial constraints are disregarded. These are for the case L/h = 20. It is seen that for a beam as slender as this, the behavior resembles that of a string much more than that of an unconstrained beam. Thus the end constraints against axial displacements have a profound influence on the deformation.

The beam problem discussed above required consideration of axial forces as a consequence of the growth of deflections to magnitudes as large or larger than the beam depth. In other structures, such as arches, rings, and frames, axial forces are required for equilibrium of the undeformed structure, and the interaction between bending moment and axial force, and the relation between the corresponding deformation rates must be taken into account from the start.

In the foregoing discussion of interactions of bending moment, shear, and axial force in beams we have considered separately interactions between M and Q, and between M and N. This has been expedient in order to estimate orders of magnitudes of effects, and in view of the absence of true (local) interaction relations. However, it is worth mentioning that the problem of plastic interaction between the three quantities M/M_p, Q/Q_p, N/N_p has been solved for the static loading of a cantilever by an end force. As noted, the results certainly do not apply quantita-

tively even to other cases of static loading, but may give qualitative indications of the importance of the interactions. The full interaction problem for a beam of rectangular section was solved by Neal (1961b). Previously it had been shown (Drucker (1956)) that a good approximate interaction relation between M and Q is equation (5.1)

$$\frac{M}{M_p} + \frac{Q^4}{Q_p^4} = 1$$

Neal's results showed that an equally good approximate formula could be used when N/N_p is also taken into account, namely by replacing in the above equation

$$\frac{M}{M_p} \quad \text{by} \quad \frac{M}{M_p} \frac{1}{1 - \frac{N^2}{N_p^2}}$$

$$\frac{Q^2}{Q_p^2} \quad \text{by} \quad \frac{Q^2}{Q_p^2} \frac{1}{1 - \frac{N^2}{N_p^2}}$$

The suggested formula is

$$\frac{M}{M_p} \frac{1}{1 - \frac{N^2}{N_p^2}} + \frac{Q^4}{Q_p^4} \frac{1}{\left(1 - \frac{N^2}{N_p^2}\right)^2} = 1 \qquad (5.6)$$

Some of the interaction curves for constant N/N_p are shown in Fig. II 22(a).

For I-sections no such simple approximate formula can be given but Neal succeeded in obtaining lower bound curves. These are presented in the form of the surface drawn in isometric projection in Fig. II 29. The results are for an 8WF40 section.

Figure Captions for Chapter II

Figure	Caption
II 1	Problem solved as example of dynamic elastic-plastic analysis by normal modes: uniform simply-supported beam with initial velocity varying as half sine wave.
II 2	Idealized elastic-perfectly plastic moment-curvature relation used in illustrative problem.
II 3	Deflection pattern with plastic hinge at midpoint.
II 4	Slope angle at midpoint as function of dimensionless time η' and S = ratio of initial kinetic energy to maximum elastic strain energy capacity of beam. Normal mode solution is valid up to point of first maximum. (From Seiler, Cotter, and Symonds, 1956)
II 5	Plots of bending moment over half-span at two times η' and four magnitudes of energy ratio S. (From Seiler, Cotter, and Symonds, 1956)
II 6	Terminology for finite-difference treatment of Baron, Bleich and Weidlinger (1961).
II 7	Simple spring-mass model. P(t) is external load.
II 8	Rectangular load pulse of intensity P_o, duration τ.
II 9	Assumed linear elastic-perfectly plastic "spring characteristic": Q_y = "yield load" or "static collapse load", x_y = "yield deflection".
II 10	Relation between time of yield t_y and load ratio $\mu = P_o/Q_y$ when yield occurs during load duration interval ($t_y \leq \tau$).
II 11	Ddependence of final plastic deformation on load ratio $\mu = P_o/Q_y$ calculated by elastic-plastic analysis (x_p) and rigid-plastic analysis (x_p'), for several ratios of load duration τ to elastic period T.
II 12	Error of rigid-plastic analysis as function of energy ratio $R' = Q_y x_p'/\frac{1}{2}Q_y x_y$, for various load duration ratios τ/T.
II 13	Error of rigid-plastic analysis as function of load duration ratio τ/T, for various load magnitude ratios $\mu = P_o/Q_y$.
II 14	Illustrative problem for deflection estimate: simply-supported beam with uniformly distributed load P.
II 15	Deflection configuration, illustrative problem for deflection estimate.
II 16	Mass-spring model with two degrees of freedom, example (A). Load of impulsive type is applied to one mass giving initial velocity V_o.

II 17 Final plastic deflections of two-degree-of-freedom model, example (A).

II 18 Sequence of elastic and plastic deformations in example (A). At a given value of energy ratio R (or of n) the curves show times when plastic deformations start and stop in the two springs.

II 19 Illustrative problem of uniform pressure on simply supported beam, example (B); elastic-plastic solutions from Baron, Bleich, and Weidlinger (1961); rigid-plastic solution from Symonds (1954).

II 20 Illustrative problem of cantilever beam subjected to impact at its base, example (C). Elastic-plastic numerical solution from Alverson (1958); rigid-plastic solution from Green (1954). (a) shows final angle of rotation at base as function of dimensionless acceleration parameter. (b) shows notation and locations of typical "+" and "-" plastic deformation.

II 21 Patterns of plastic deformation of cantilever with base impact, example (C) from Alverson (1958), symbols "+" and "-" refer to concave downward and concave upward curvatures, respectively, as in Fig. II 20 (b). Vertical line indicates occurrence of plastic flow at the corresponding cross section. Solution was obtained by numerical integration of finite difference equations based on grid of characteristics, with 20 segments along beam.

II 22 Interaction diagrams: solutions from limit analysis for bending moment M, shear force Q, and normal force N at base of an end-loaded cantilever. M_p, Q_p, N_p are limit (fully plastic) magnitudes for corresponding individual load.

(a) Rectangular section. Full curve for N = 0 from Drucker (1956); dashed curves for N > 0 from Neal (1961b).

(b) and (c) Curves for typical I-section (8WF40). Sharp drop in M occurs at $Q = Q_w$ = approximately web area times yield stress in shear. (From Neal (1961a).

(d) Simplified interaction diagram assumed for use in dynamic problems. For I-section Q_p is taken as Q_w, as indicated for (b).

II 23 Problem of shear deformation of free-free beam treated by Karunes and Onat (1960).

II 24 Curves showing shear and bending deformations, adapted from Karunes and Onat (1960).

II 25 Types of initial deformation of simply supported beam under uniformly distributed load with initial magnitude $P_o = P(0)$, showing dependence on parameters of load magnitude M_o and of shear strength ν. (From Nonaka and Symonds, 1967)

II 26 Comparison of final midpoint deflection as function of load magnitude at constant impulse $\hat{I}$ for rectangular pulse, exponentially decreasing pulse, and impulsive load (initial velocity). Solution for "single hinge bending only" for exponential loading was given by Salvadori and Weidlinger (1957).

II 27 Dependence of final midpoint deflection at constant impulse on shear strength parameter ν, for various load magnitudes. Dashed lines separate regions of initial deformation pattern as shown in Fig. II 25. (From Nonaka and Symonds, 1967).

II 28 Deflection curves showing large influence of constraints against axial motion, from Symonds and Mentel (1958).

II 29 Approximate interaction between bending moment M, shearing force Q and axial force N for an I-section, plotted in an isometric diagram, from B. G. Neal, Report NNS/12, October, 1961, Brown University to Norfolk Naval Shipyard, Underwater Explosions Research Division.

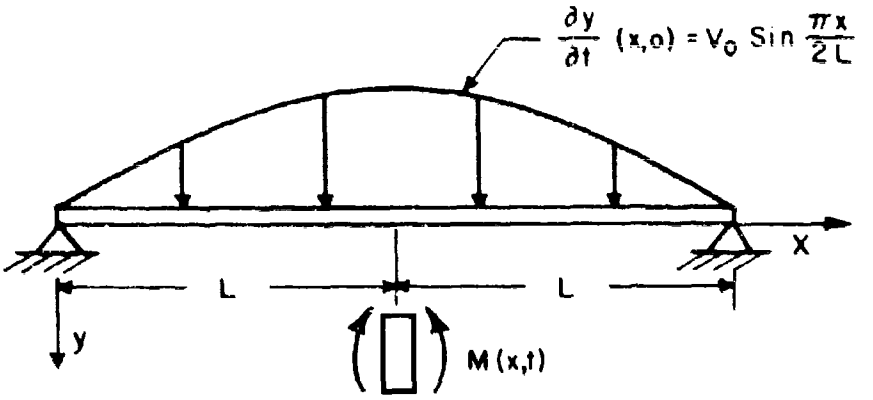

FIG. II 1

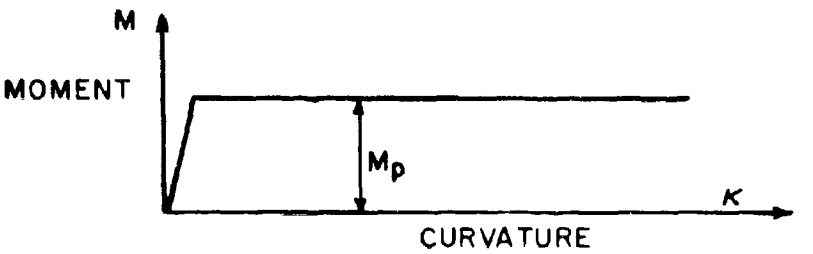

FIG. II 2

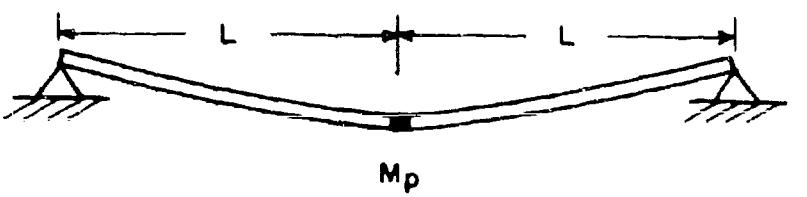

FIG. II 3

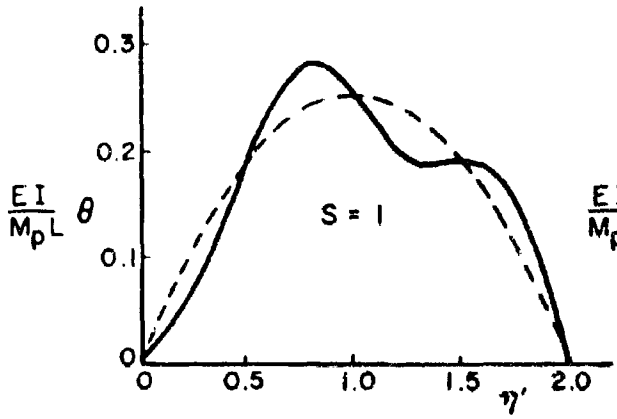

FIG. II 4(a)

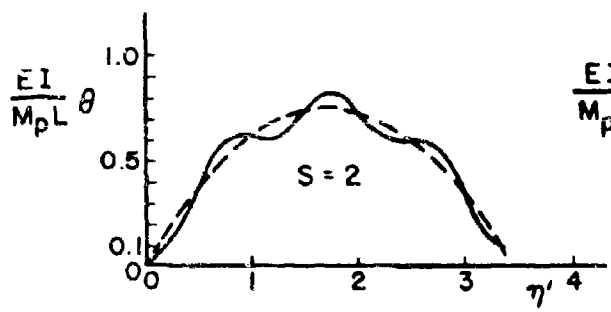

FIG. II 4(b)

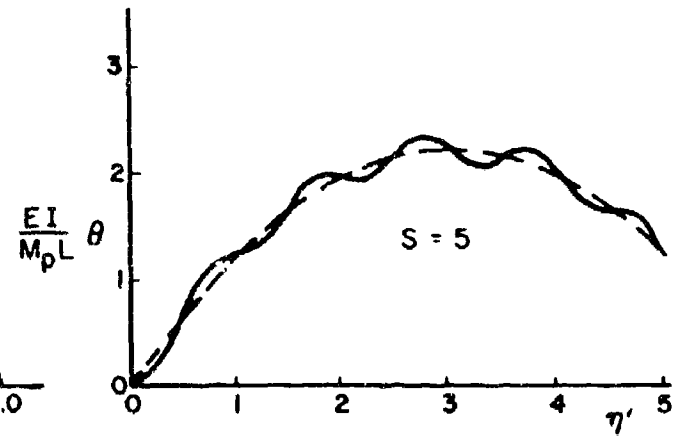

FIG. II 4(c)

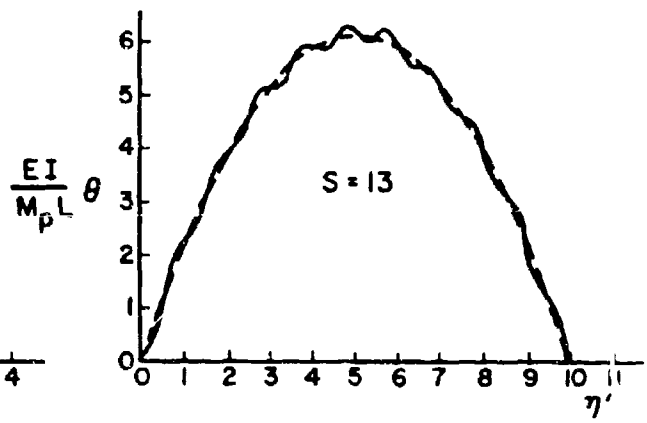

FIG. II 4(d)

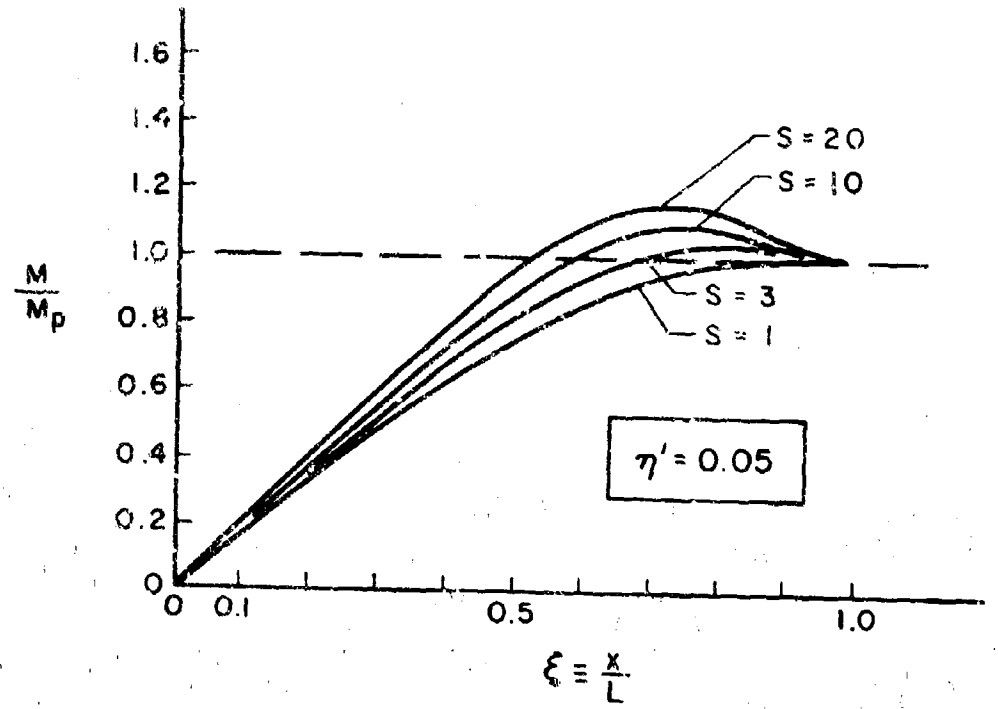

FIG. II 5(a)

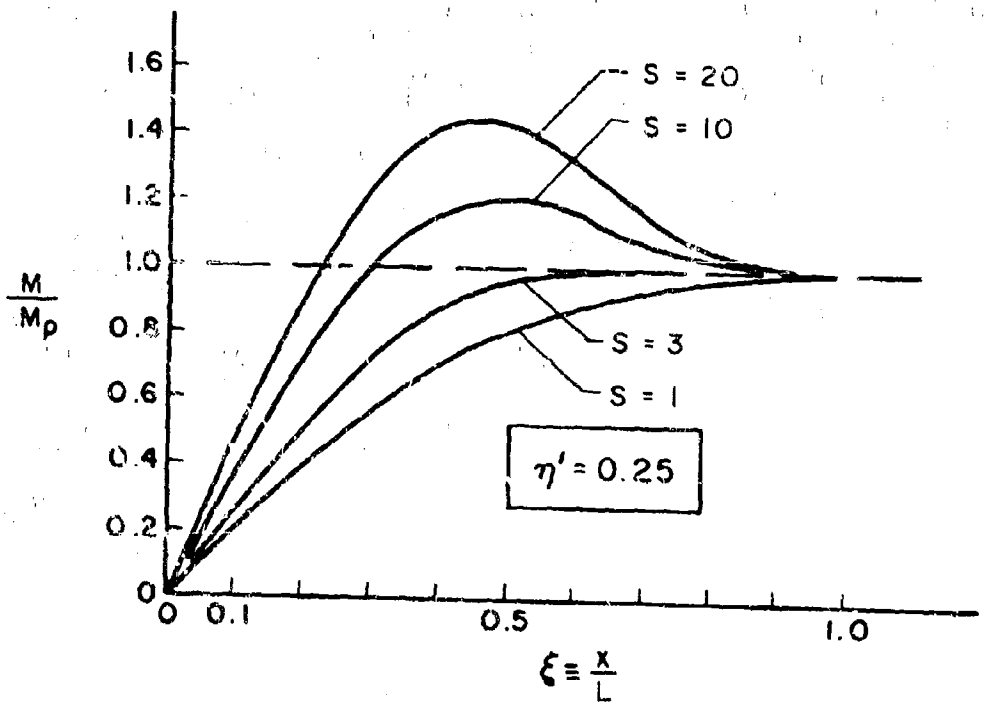

FIG. II 5(b)

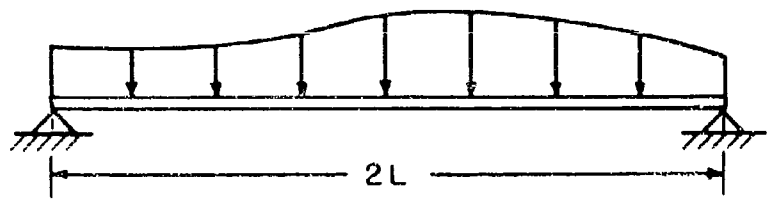

(a.)

(b.)

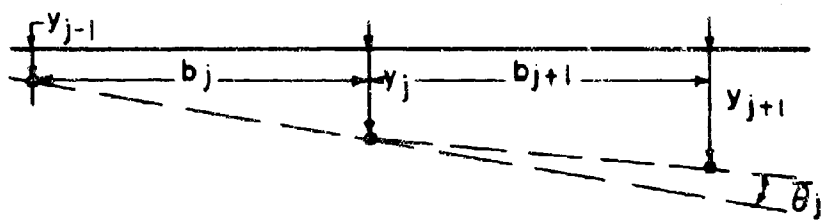

(c.)

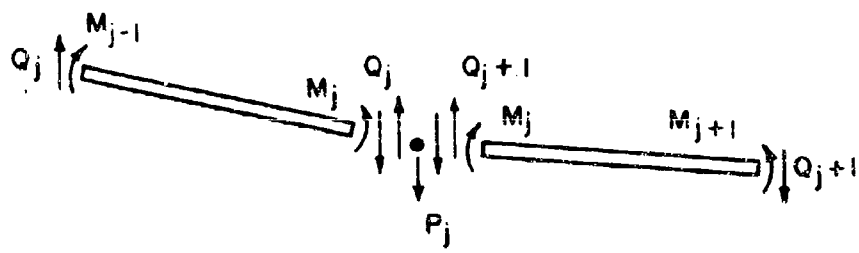

(d.)

(e.)

FIG. II 6

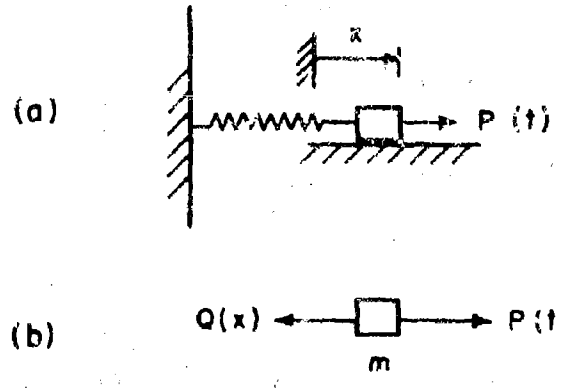

FIG. II 7

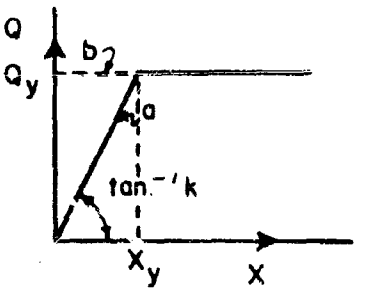

FIG. II 9

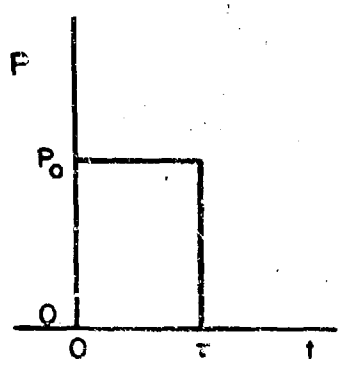

FIG. II 8

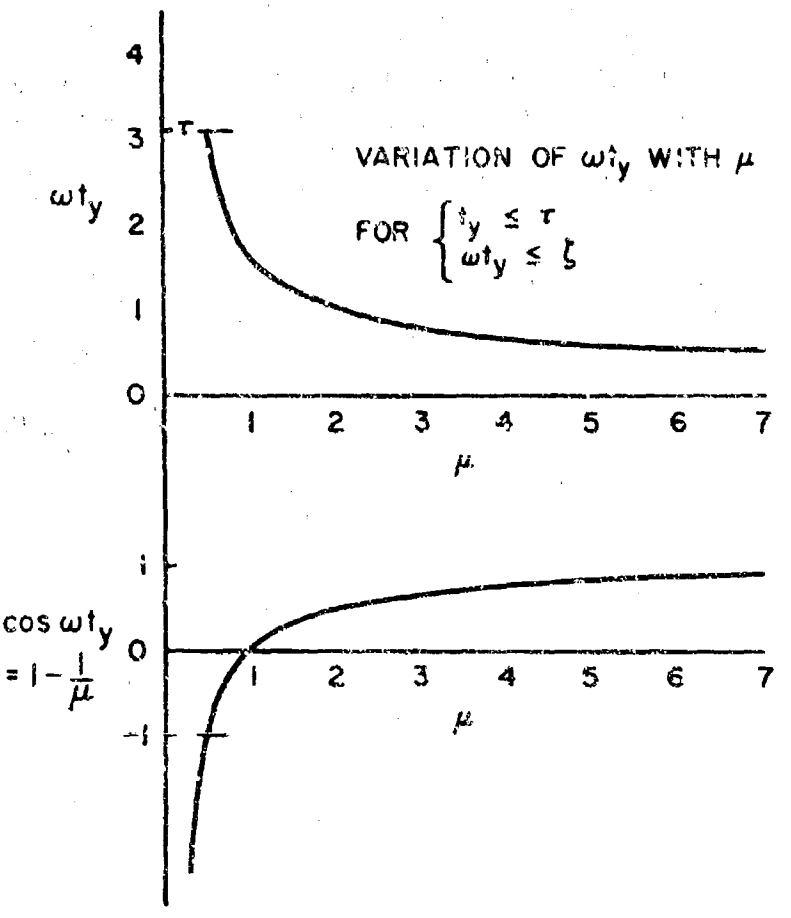

FIG. II 10

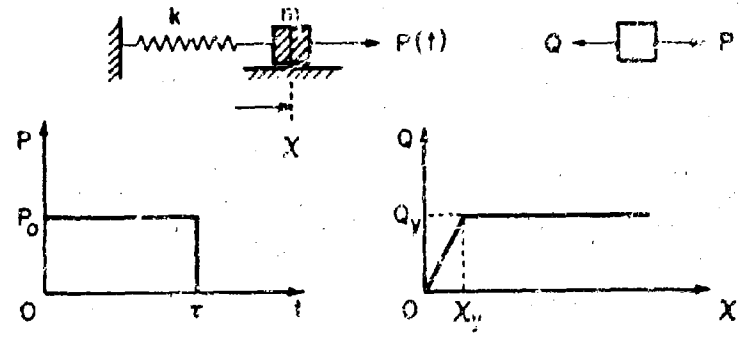

$$\mu = \frac{P_o}{Q_y}$$

$$T = 2\pi\sqrt{\frac{m}{k}}$$

$$R' = \frac{Q_y\, X_p'}{\frac{1}{2} Q_y\, X_y} = 2\,\frac{X_p'}{X_y}$$

X_p : FINAL PLASTIC DEFORMATION (ELASTIC-PLASTIC)
X_p' : FINAL PLASTIC DEFORMATION (RIGID-PLASTIC)

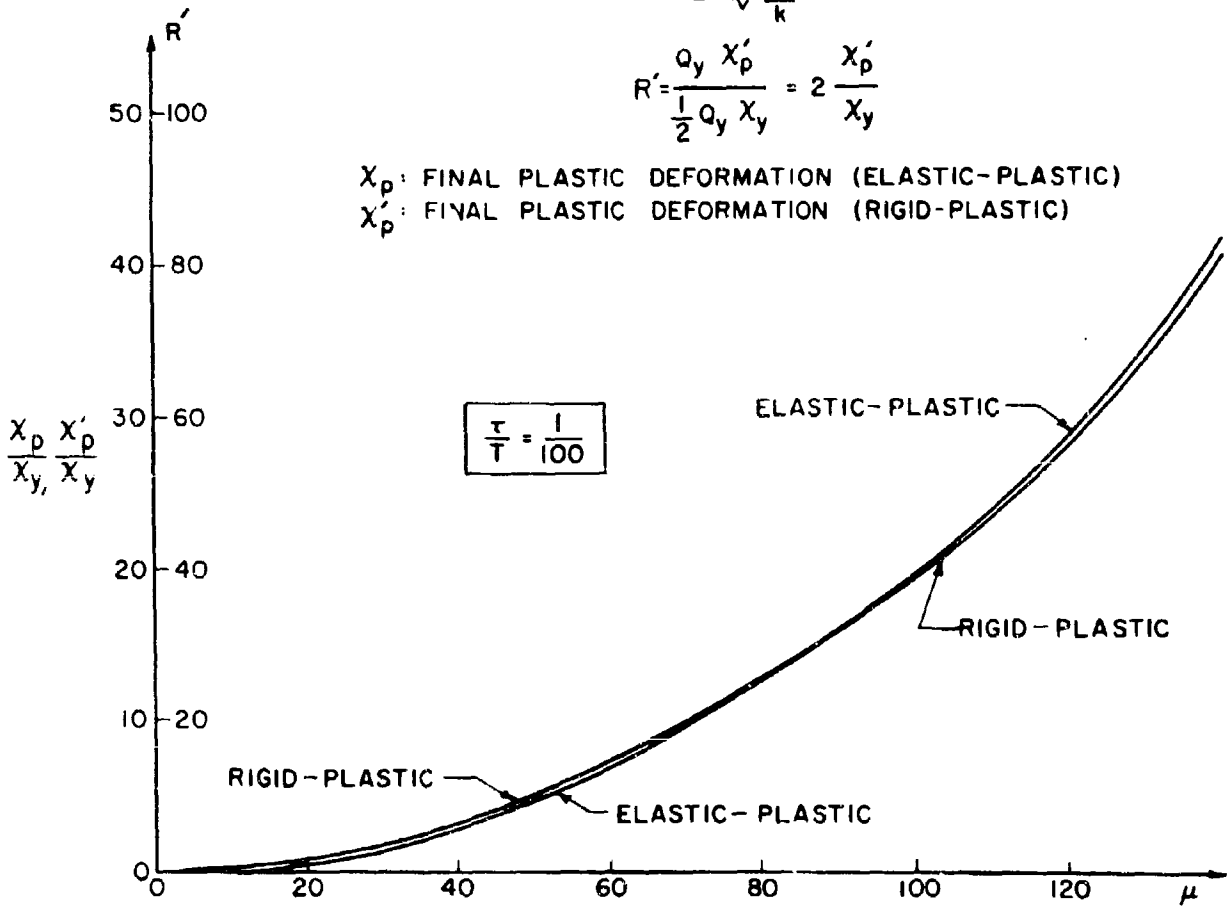

FIG. II 11(a)

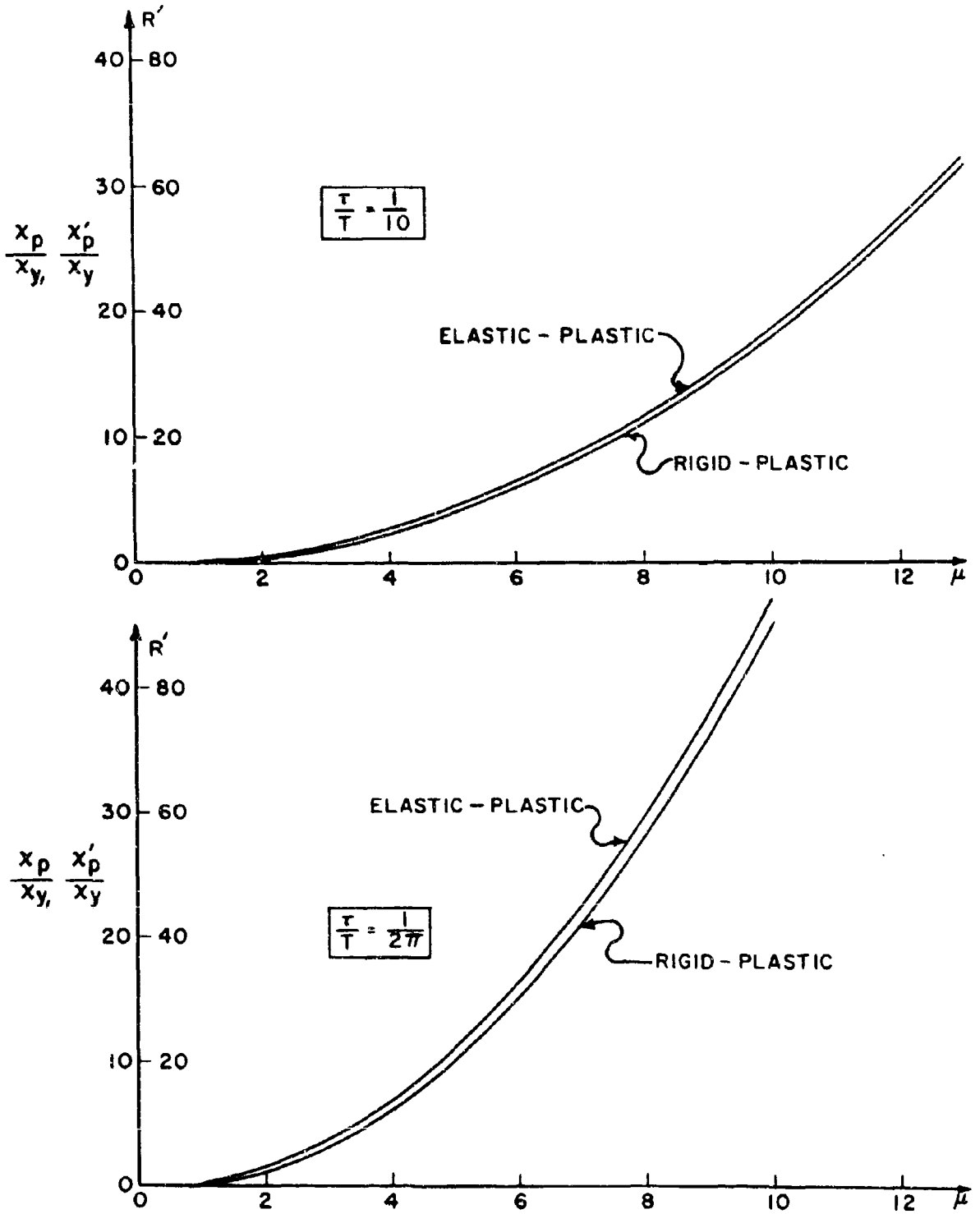
R′
40
80
30
60
20
40
10
20
0
0
2
4
6
8
10
12
μ
$\frac{x_p}{x_{y_1}}$ $\frac{x'_p}{x_y}$
$\frac{\tau}{T} = \frac{1}{10}$
ELASTIC - PLASTIC
RIGID - PLASTIC
R′
40
80
30
60
20
40
10
20
0
0
2
4
6
8
10
12
μ
$\frac{x_p}{x_{y_1}}$ $\frac{x'_p}{x_y}$
$\frac{\tau}{T} = \frac{1}{2\pi}$
ELASTIC - PLASTIC
RIGID - PLASTIC

FIG. II 11(b)

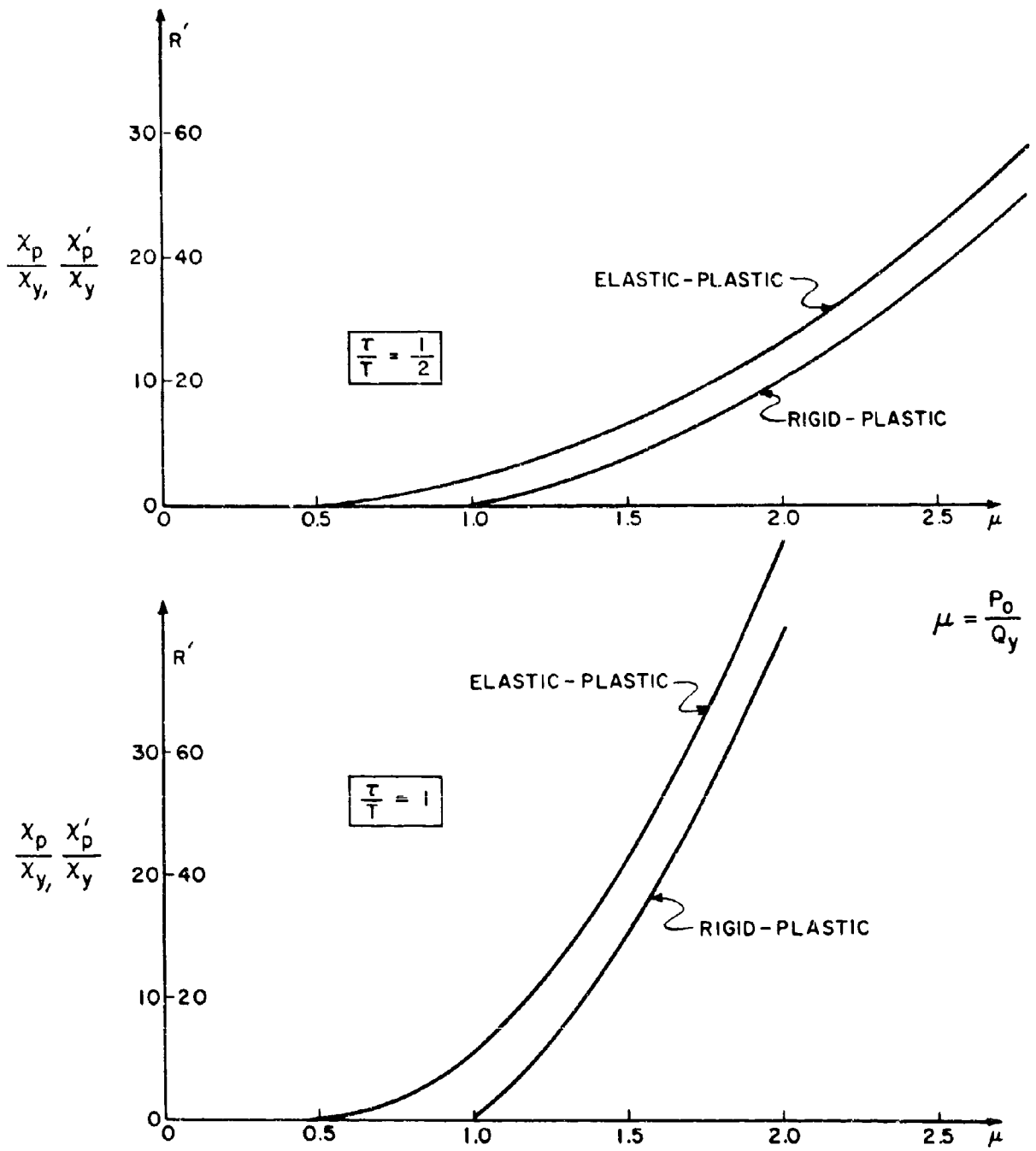
R'
30
60
20
40
10
20
0
0
0.5
1.0
1.5
2.0
2.5
μ
$\frac{x_p}{x_y}$ $\frac{x'_p}{x_y}$
ELASTIC - PLASTIC
RIGID - PLASTIC
$\frac{\tau}{T} = \frac{1}{2}$
$\mu = \frac{P_o}{Q_y}$
$\frac{\tau}{T} = 1$

FIG. III(c)

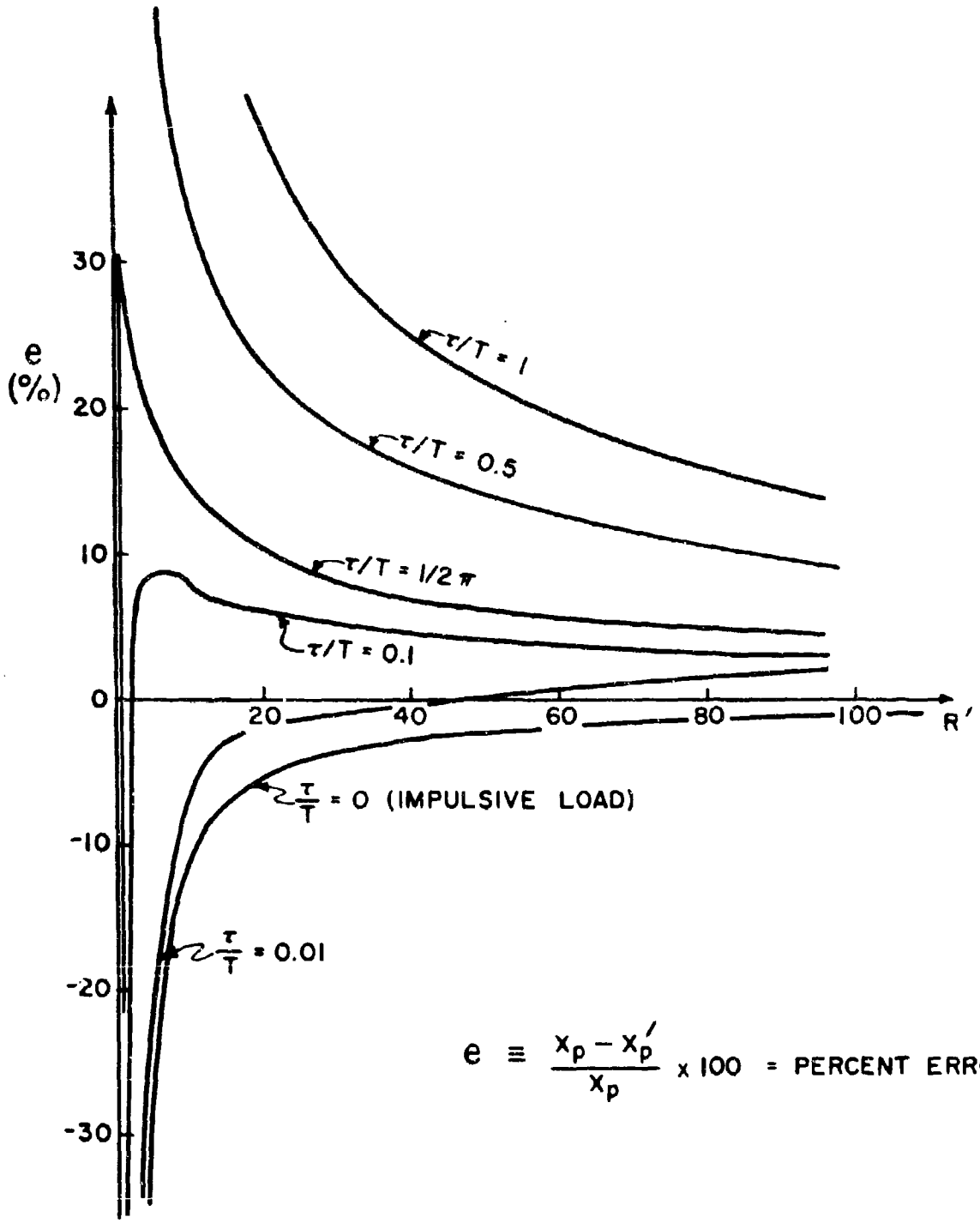

$$e \equiv \frac{x_p - x_p'}{x_p} \times 100 = \text{PERCENT ERROR}$$

FIG. II 12

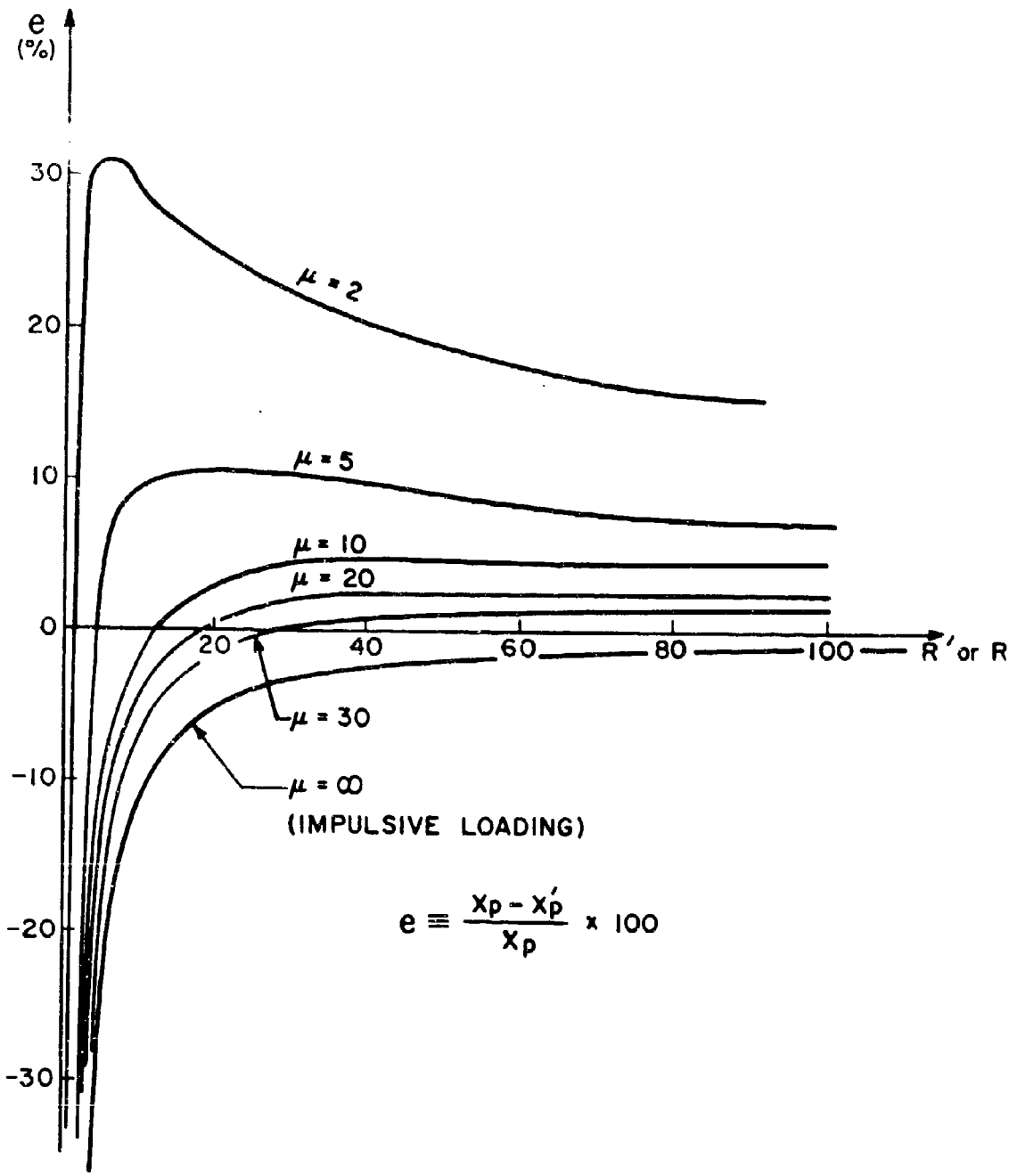
e
(%)
30
20
10
0
-10
-20
-30
20
40
60
80
100
R' or R
μ = 2
μ = 5
μ = 10
μ = 20
μ = 30
μ = ∞
(IMPULSIVE LOADING)
e ≡ (Xp - X'p) / Xp x 100

FIG. II 13

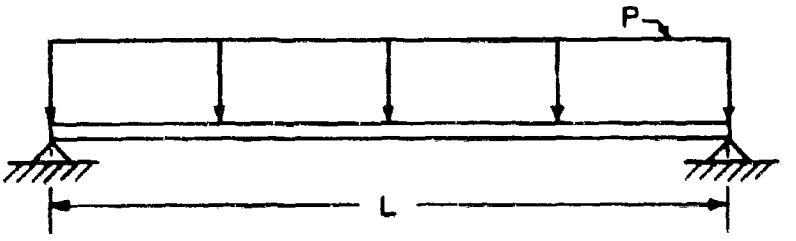

FIG. II 14

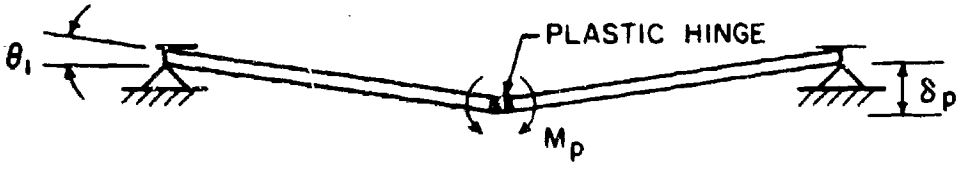

FIG. II 15

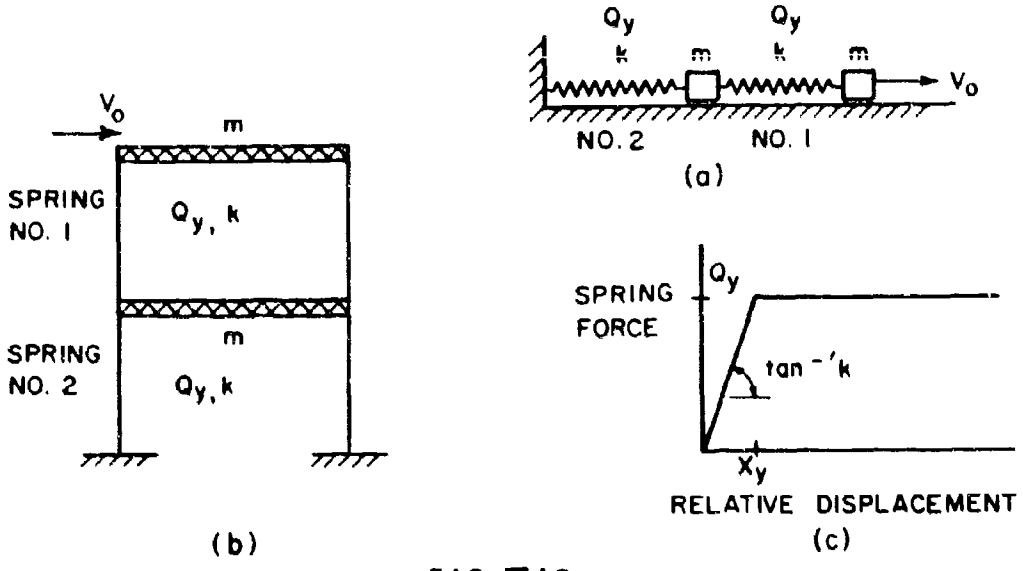

FIG. II 16

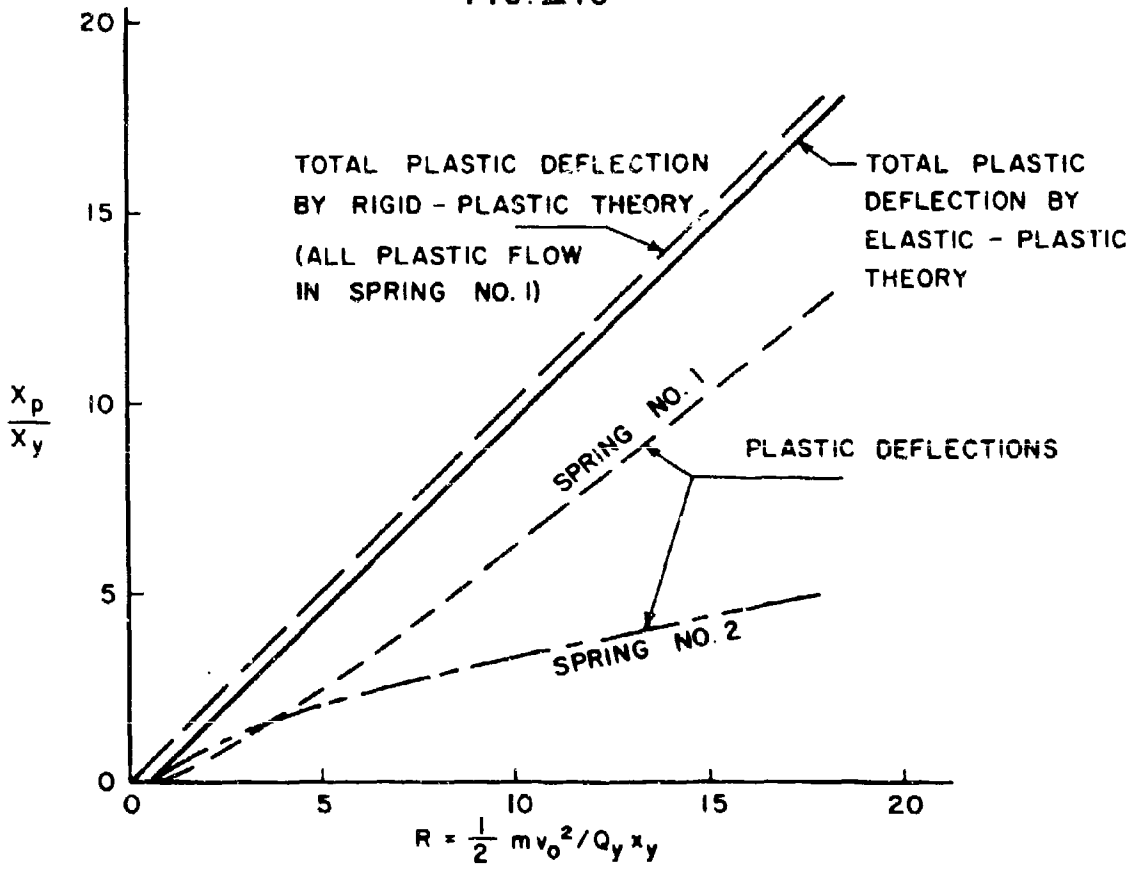

FIG. II 17

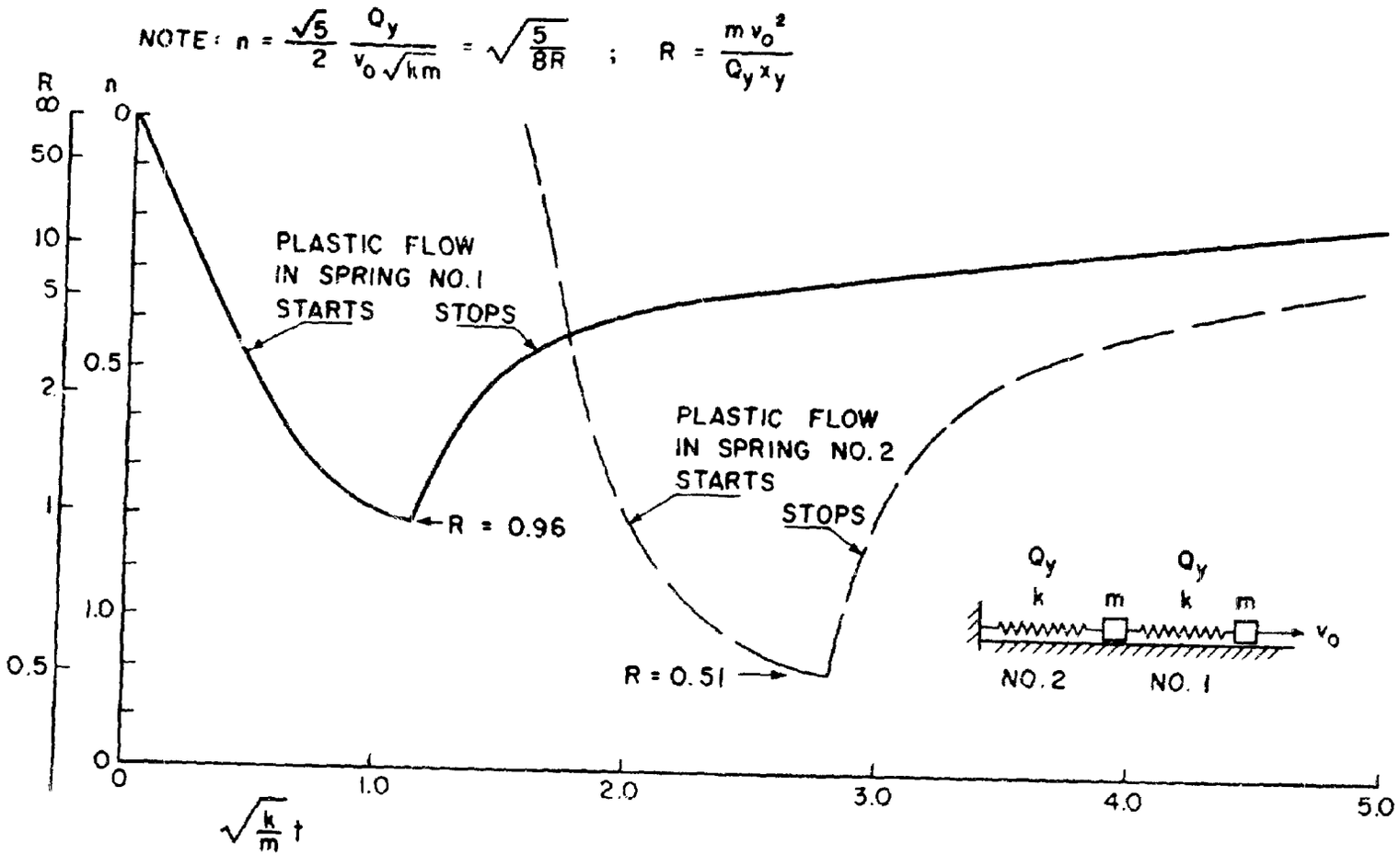
NOTE: $n = \frac{\sqrt{5}}{2} \frac{Q_y}{v_0 \sqrt{km}} = \sqrt{\frac{5}{8R}}$; $R = \frac{m v_0^2}{Q_y x_y}$
R
∞
50
10
5
2
1
0.5
n
0
0.5
1.0
0
PLASTIC FLOW IN SPRING NO.1 STARTS
STOPS
R = 0.96
PLASTIC FLOW IN SPRING NO.2 STARTS
STOPS
R = 0.51
Q_y Q_y
k m k m
v_0
NO.2 NO.1
0
1.0
2.0
3.0
4.0
5.0
$\sqrt{\frac{k}{m}}\, t$

FIG. II 18

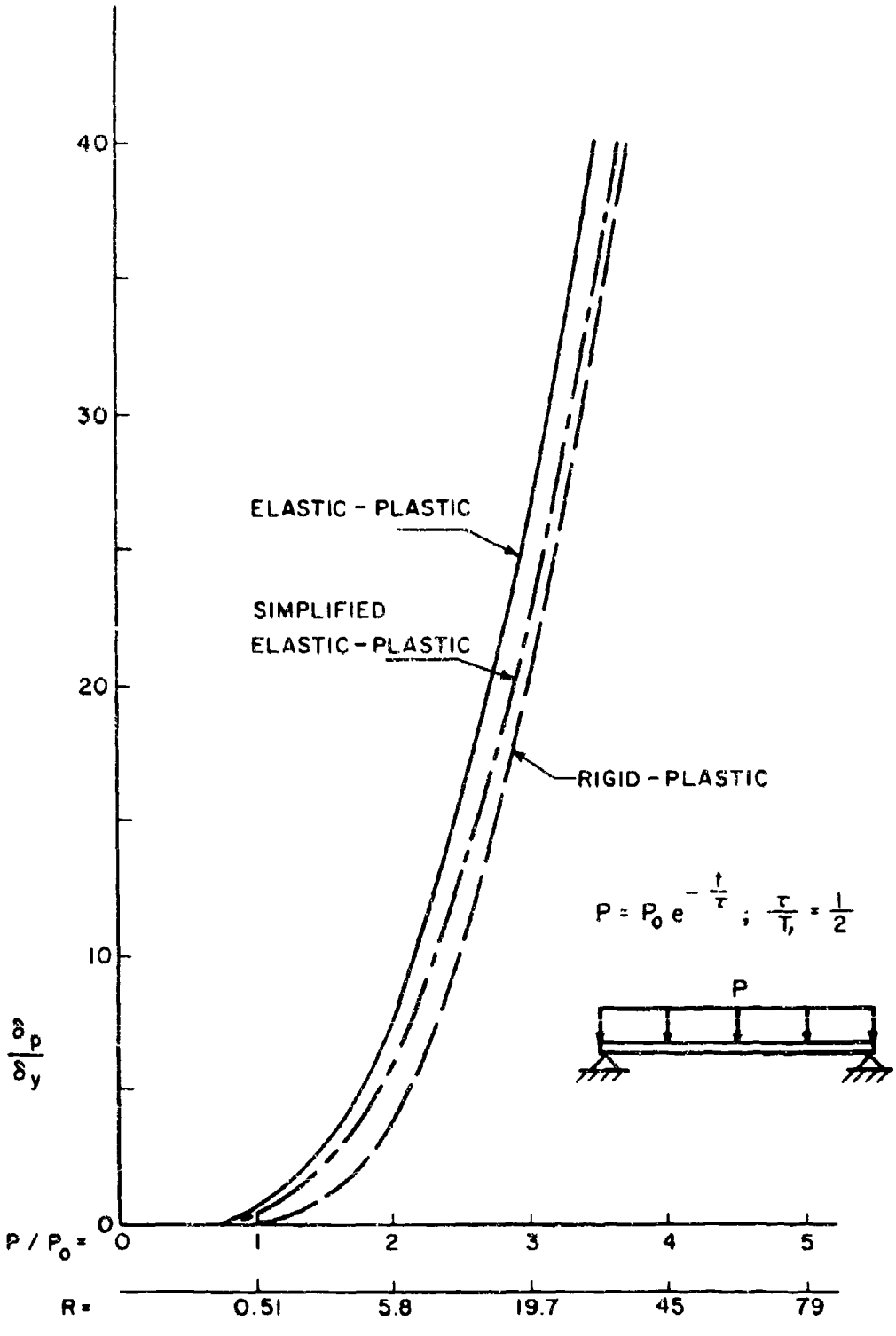
40
30
20
10
0
ELASTIC - PLASTIC
SIMPLIFIED
ELASTIC - PLASTIC
RIGID - PLASTIC
$P = P_0 e^{-\frac{t}{\tau}}$; $\frac{\tau}{T_1} = \frac{1}{2}$
P
$\frac{\delta_p}{\delta_y}$
P / P0 = 0 1 2 3 4 5
R = 0.51 5.8 19.7 45 79

FIG. II 19

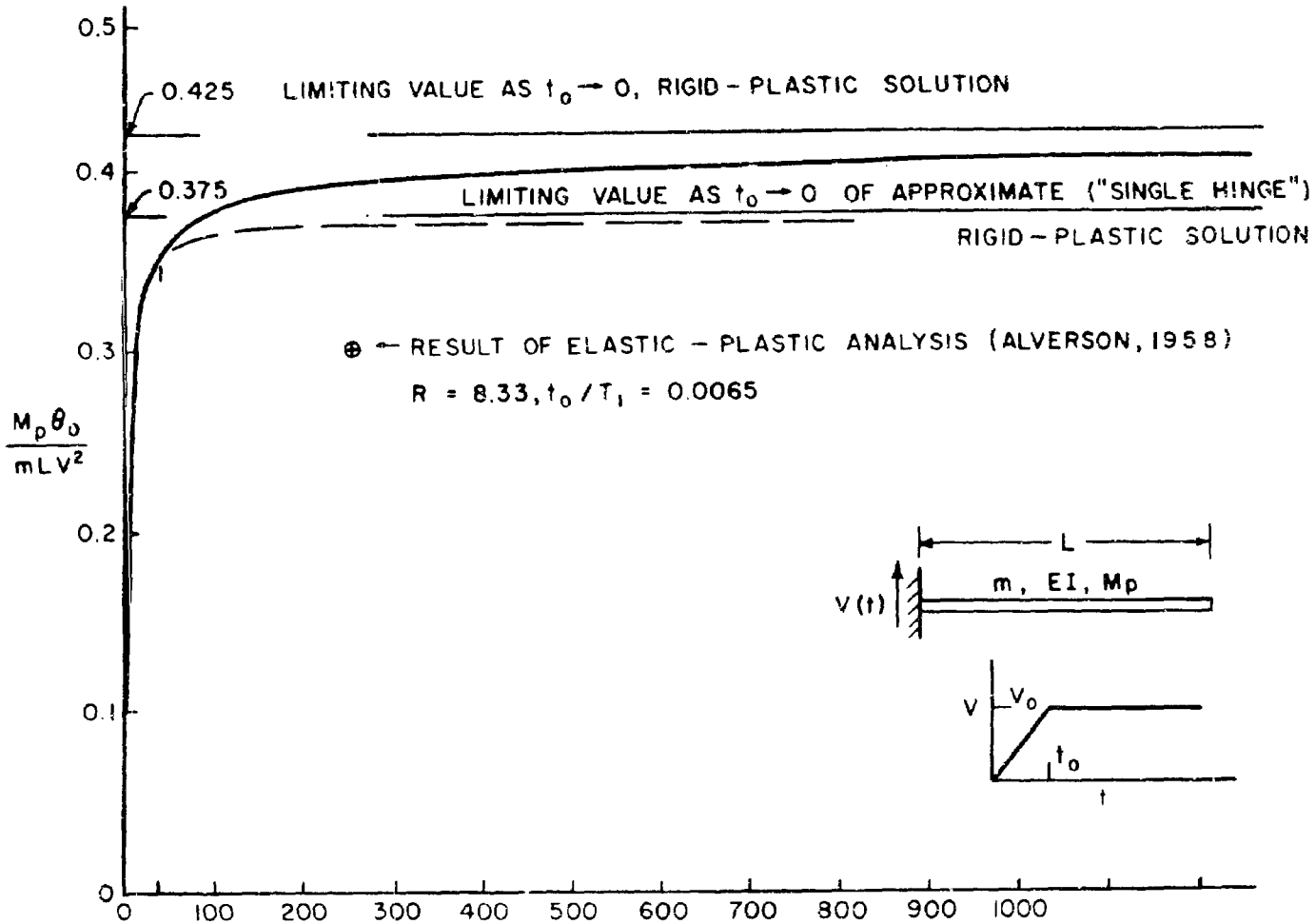
0.5
0.425
LIMITING VALUE AS $t_0 \rightarrow 0$, RIGID - PLASTIC SOLUTION
0.4
0.375
LIMITING VALUE AS $t_0 \rightarrow 0$ OF APPROXIMATE ("SINGLE HINGE")
RIGID - PLASTIC SOLUTION
⊕ ← RESULT OF ELASTIC - PLASTIC ANALYSIS (ALVERSON, 1958)
R = 8.33, t_0 / T_1 = 0.0065
0.3
$\frac{M_p \theta_0}{mLV^2}$
0.2
0.1
0
0
100
200
300
400
500
600
700
800
900
1000
$\beta \equiv \frac{mL^2V}{M_p t_0}$
L
m, EI, Mp
V(t)
V
V_0
t_0
t

FIG II 20(a)

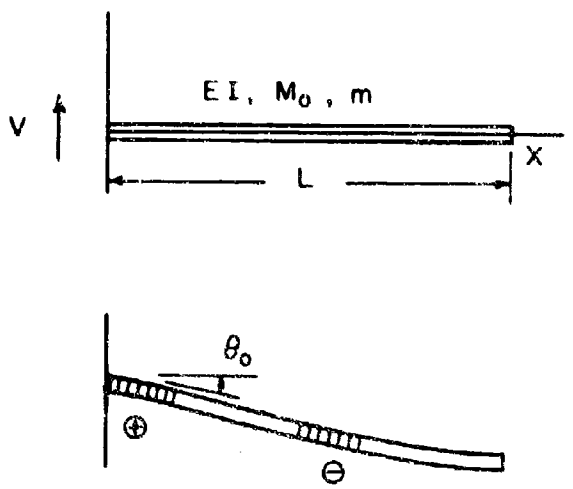

FIG. II 20 (b)

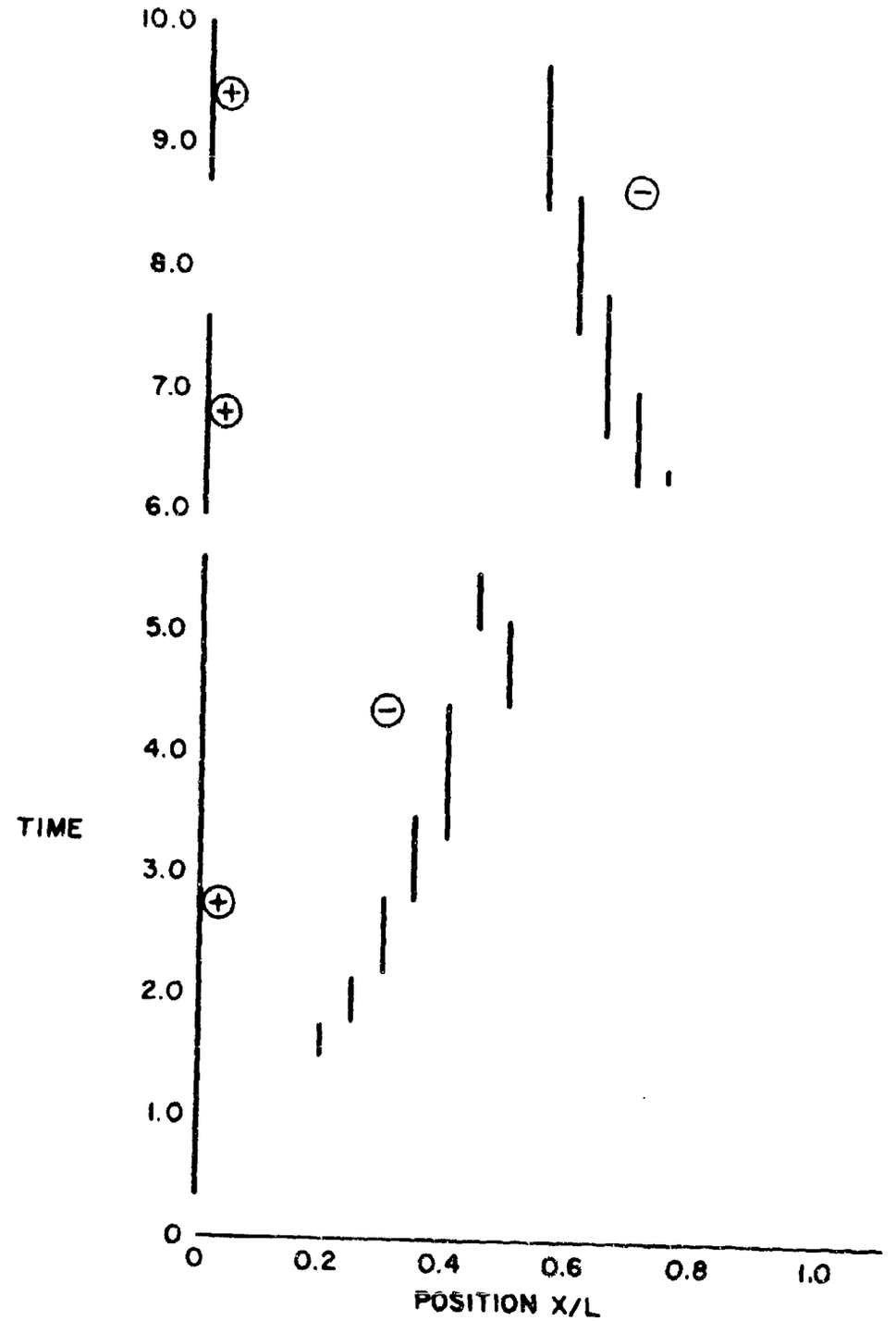
10.0
9.0
8.0
7.0
6.0
5.0
4.0
3.0
2.0
1.0
0
TIME
0
0.2
0.4
0.6
0.8
1.0
POSITION X/L
LOCATION OF PLASTIC DEFORMATIONS

FIG. II 21(a)

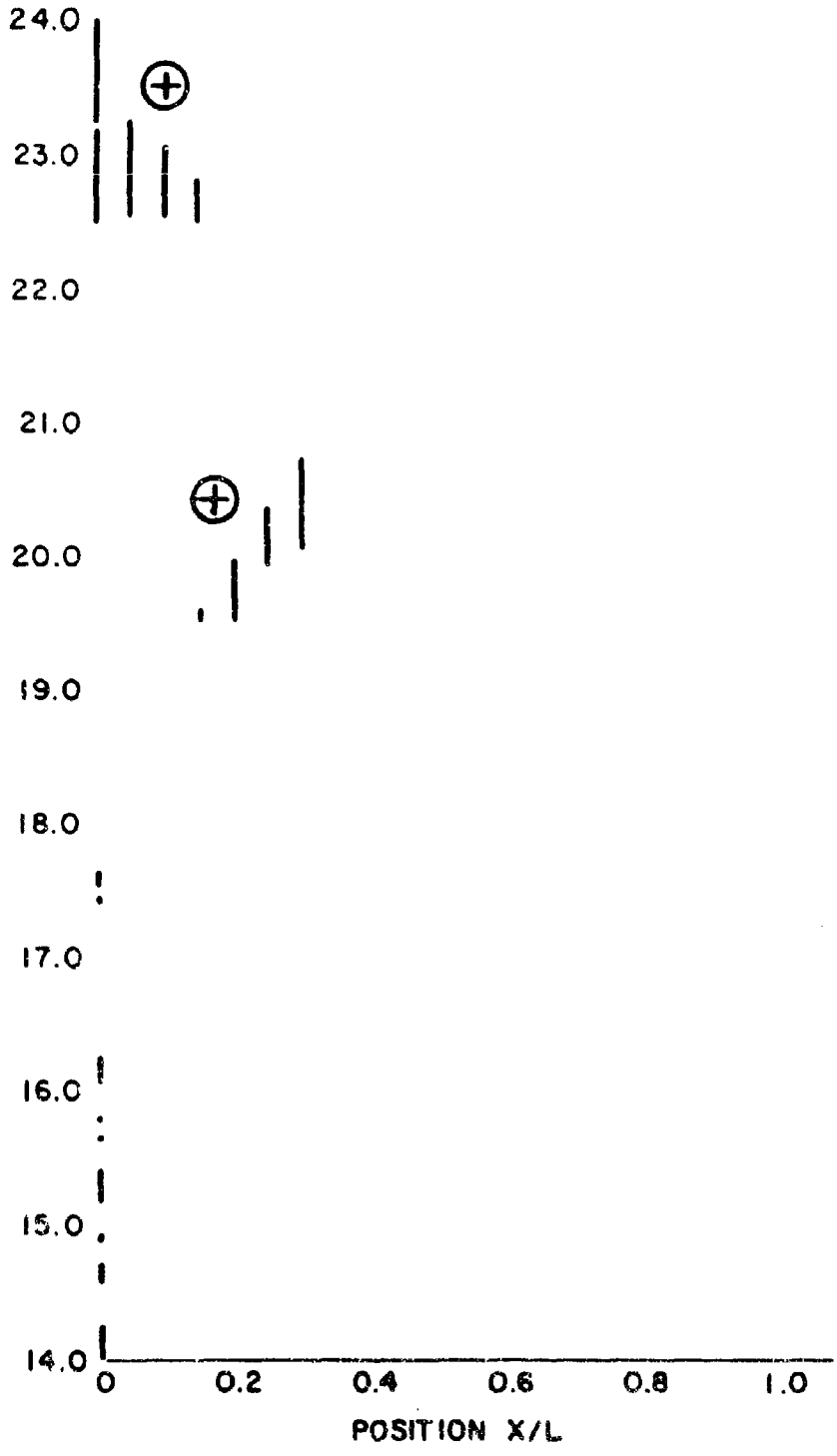

LOCATION OF PLASTIC DEFORMATIONS

FIG. II 21(b)

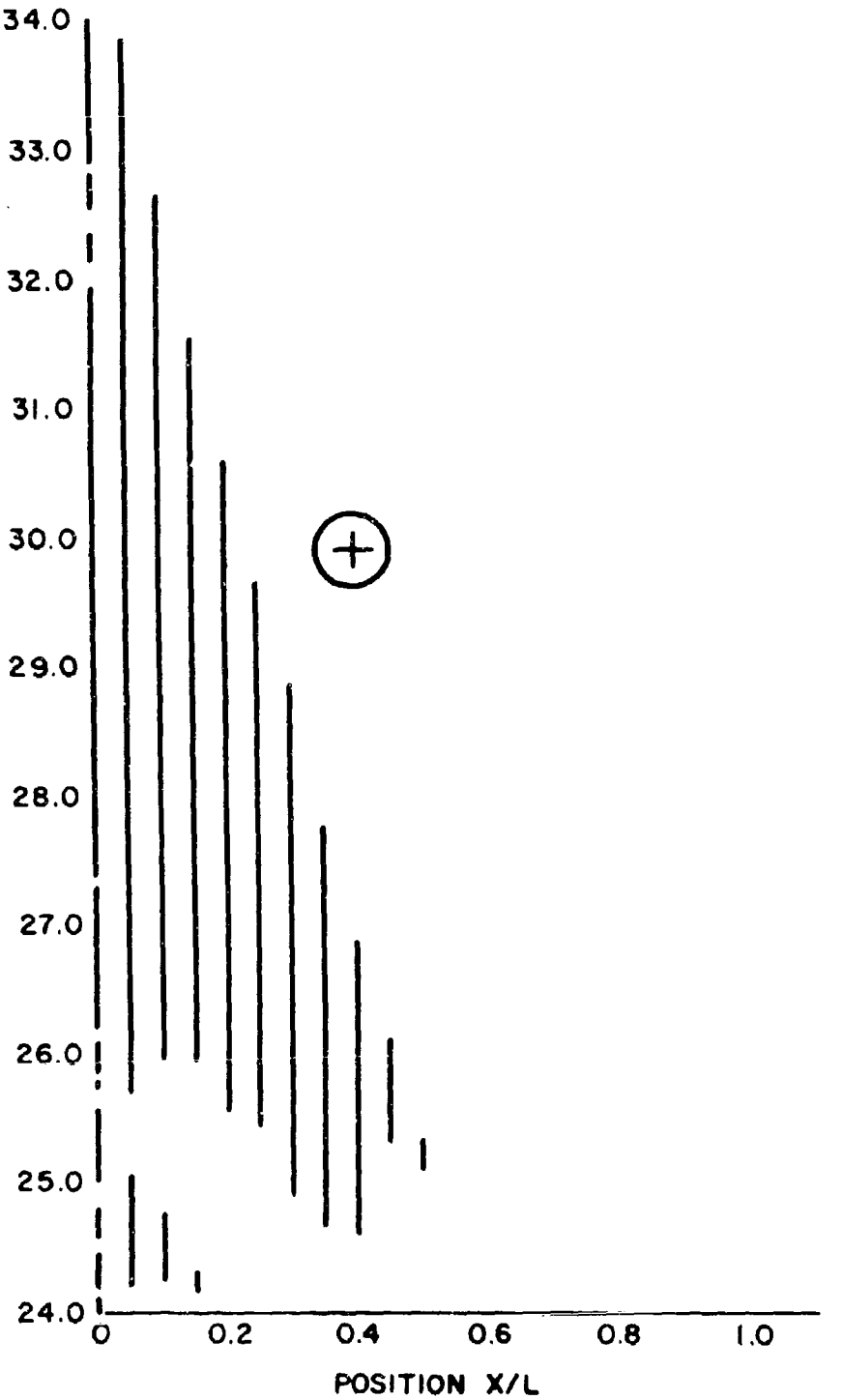
34.0
33.0
32.0
31.0
30.0
29.0
28.0
27.0
26.0
25.0
24.0
0
0.2
0.4
0.6
0.8
1.0
POSITION X/L
LOCATION OF PLASTIC DEFORMATIONS

FIG. II 21(c)

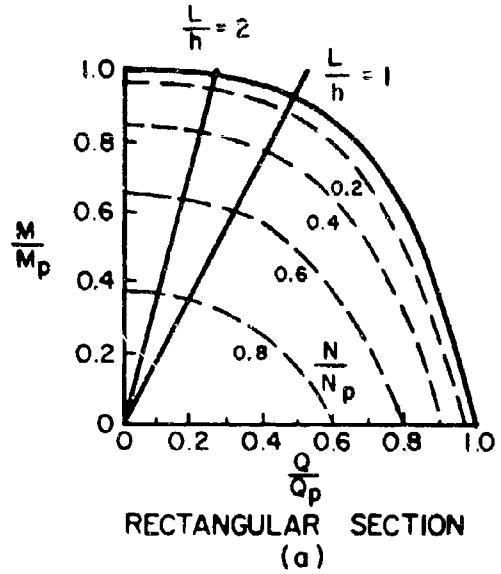

RECTANGULAR SECTION

(a)

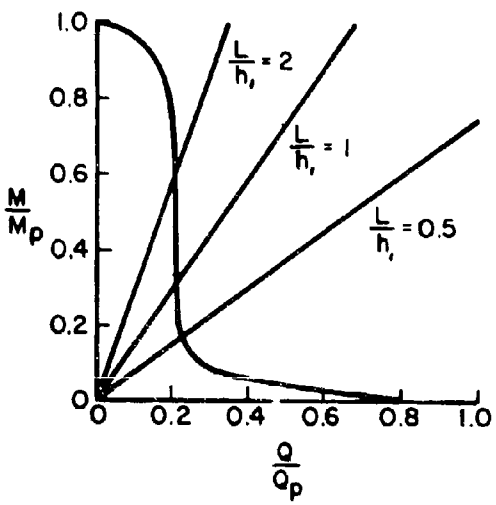

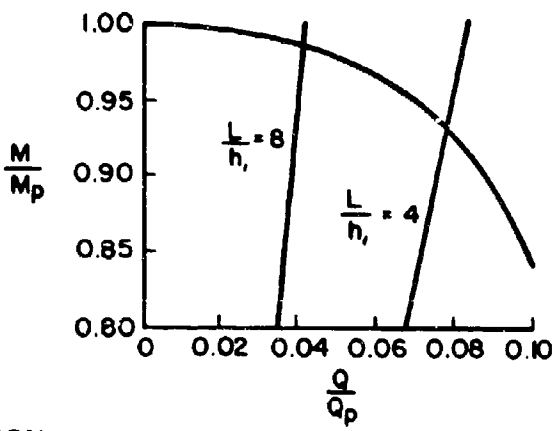

I SECTION

(b)

(c)

FIG. II 22

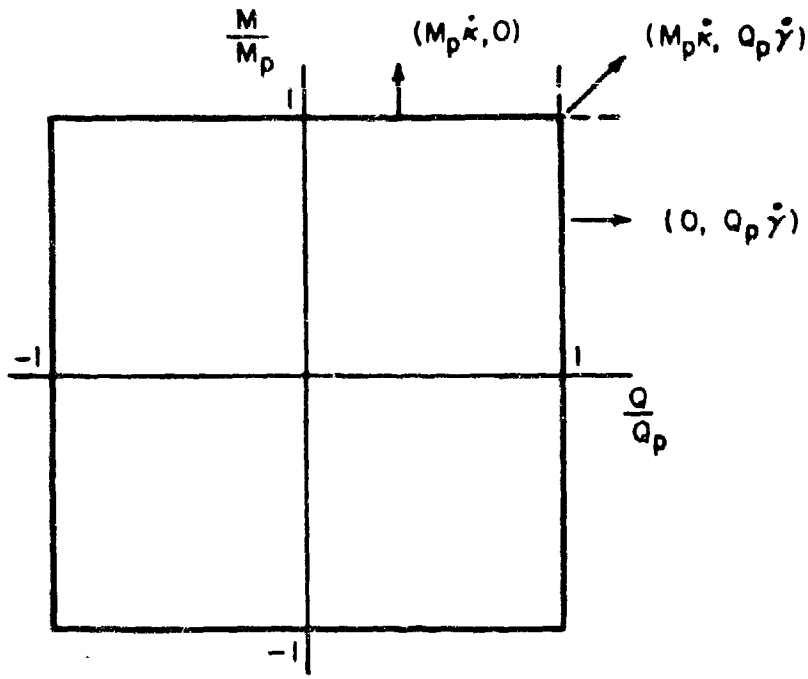

FIG. II 22(d)

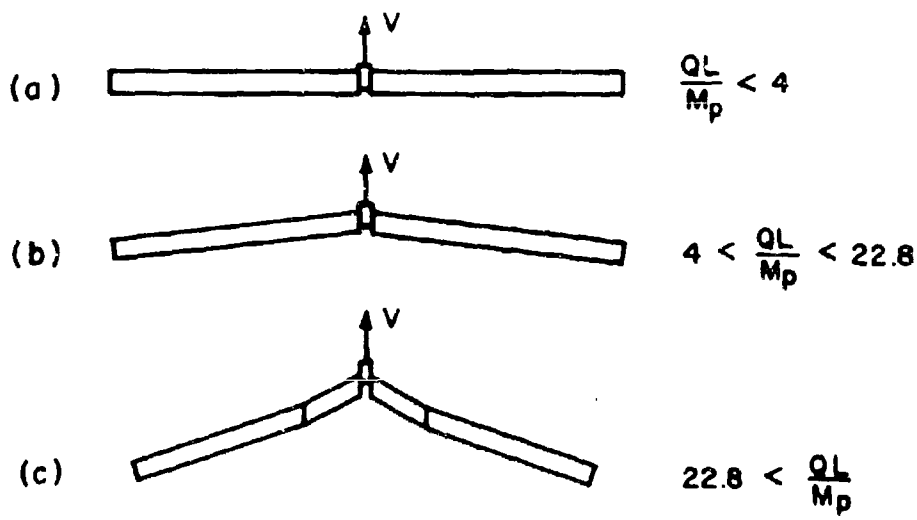

FIG. II 23

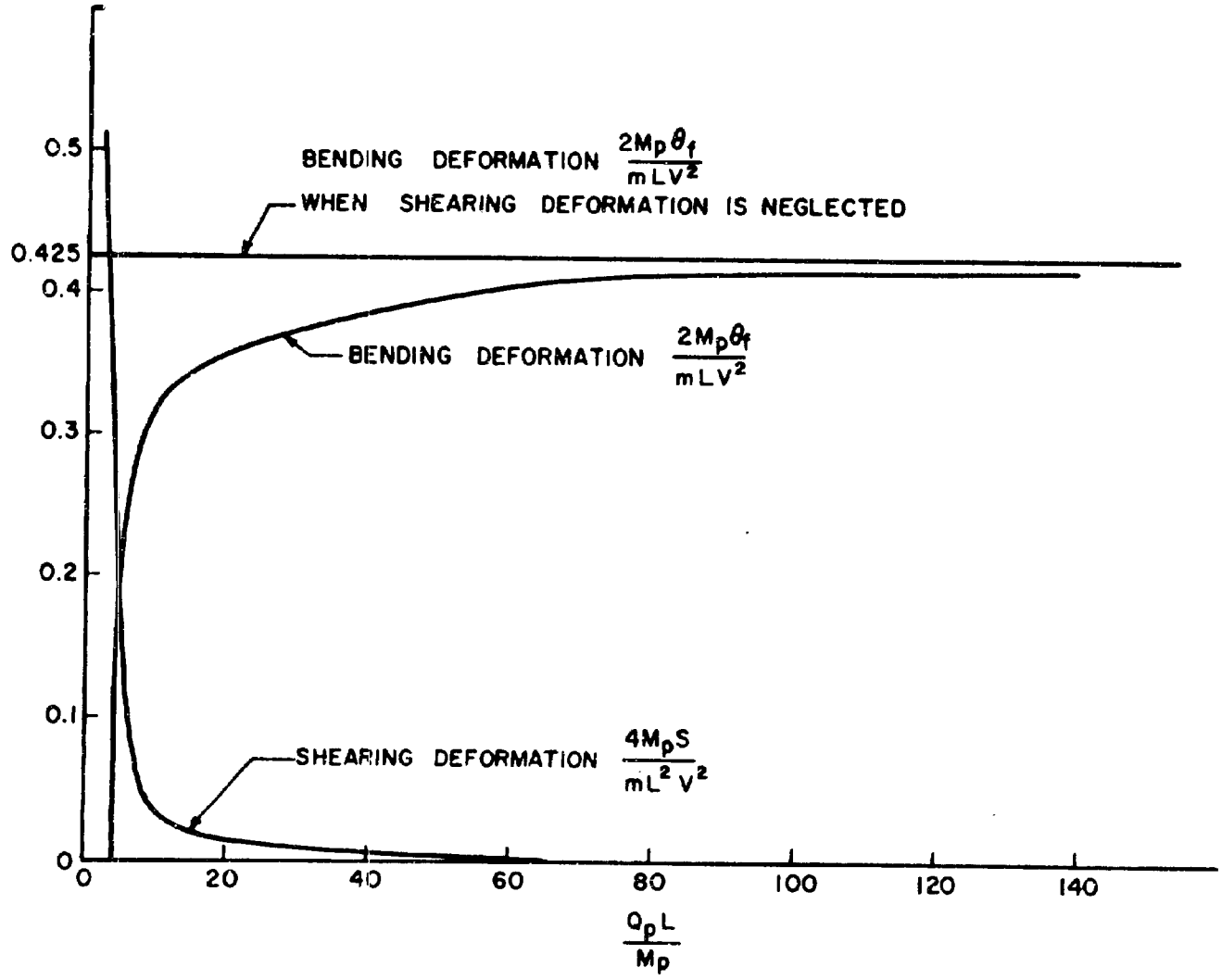
0.5
0.425
0.4
0.3
0.2
0.1
0
BENDING DEFORMATION $\frac{2M_p\theta_f}{mLV^2}$
WHEN SHEARING DEFORMATION IS NEGLECTED
BENDING DEFORMATION $\frac{2M_p\theta_f}{mLV^2}$
SHEARING DEFORMATION $\frac{4M_pS}{mL^2V^2}$
0
20
40
60
80
100
120
140
$\frac{Q_pL}{M_p}$

FIG. II 24

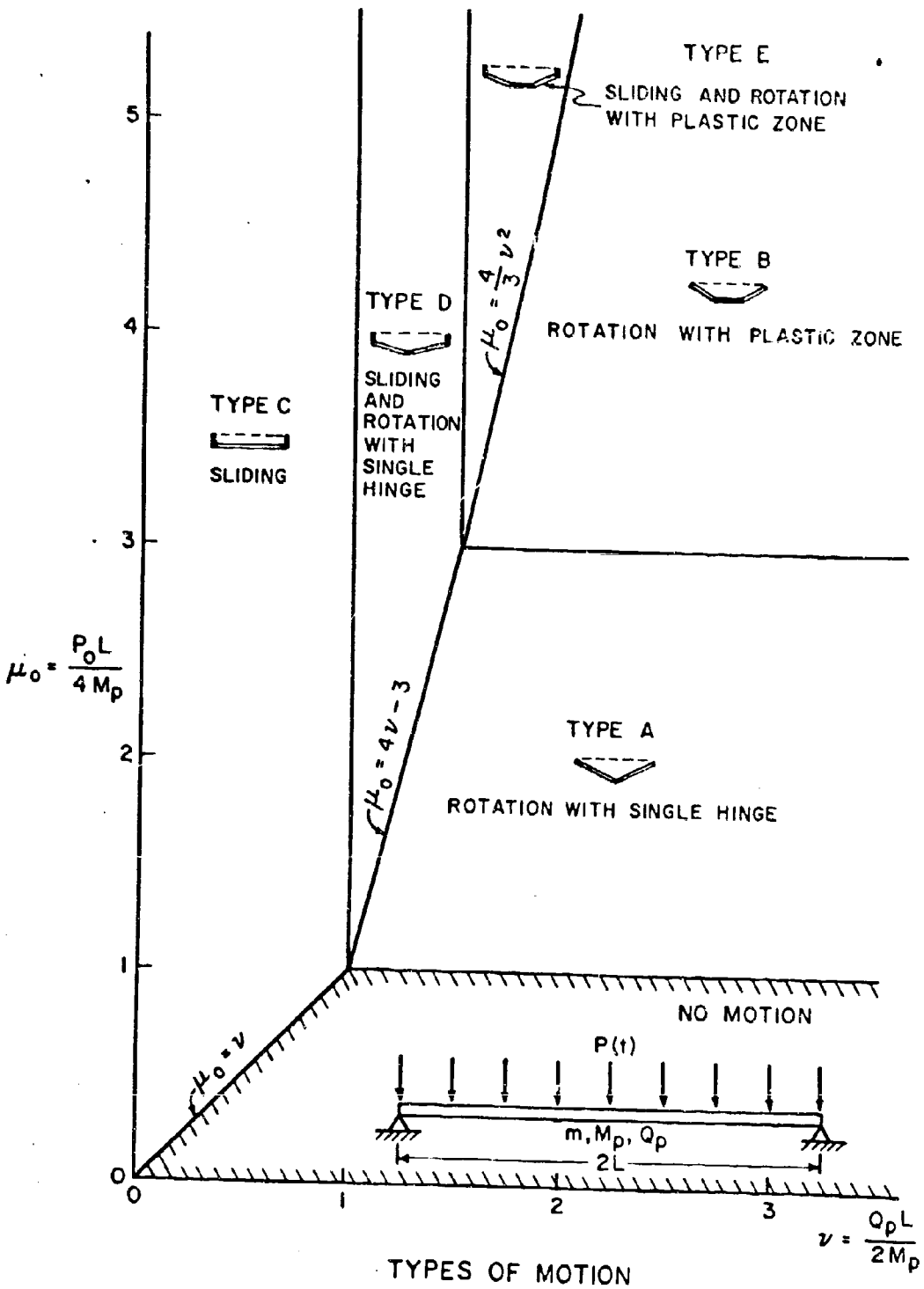

TYPES OF MOTION

FIG. II 25

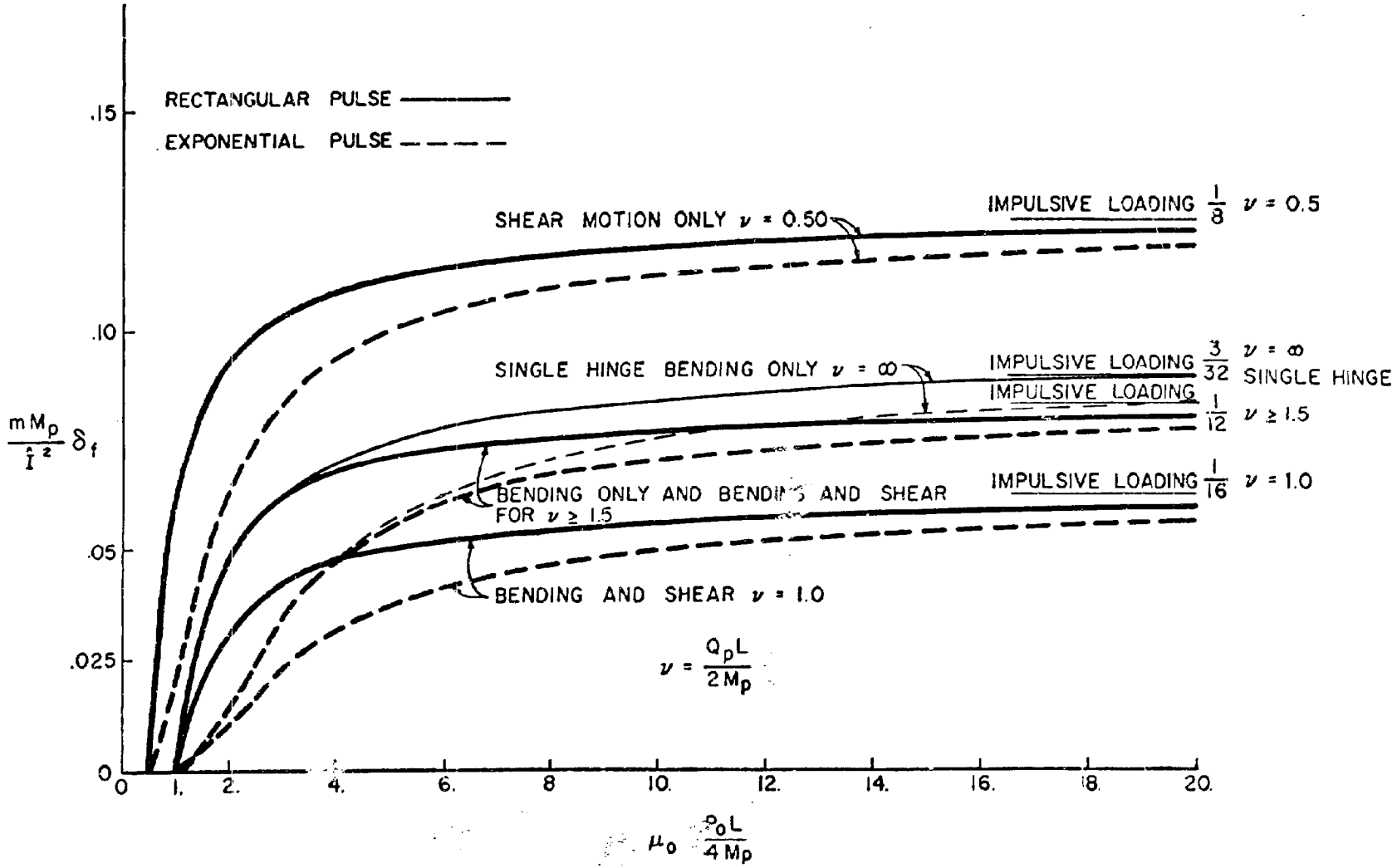
RECTANGULAR PULSE
EXPONENTIAL PULSE
SHEAR MOTION ONLY ν = 0.50
IMPULSIVE LOADING 1/8 ν = 0.5
SINGLE HINGE BENDING ONLY ν = ∞
IMPULSIVE LOADING 3/32 ν = ∞ SINGLE HINGE
IMPULSIVE LOADING 1/12 ν ≥ 1.5
IMPULSIVE LOADING 1/16 ν = 1.0
BENDING ONLY AND BENDING AND SHEAR FOR ν ≥ 1.5
BENDING AND SHEAR ν = 1.0
ν = Q_p L / 2M_p
mM_p/I² δ_f
μ_o = ρ_o L / 4M_p
.15
.10
.05
.025
0
0
1.
2.
4.
6.
8
10.
12.
14.
16.
18.
20.

FIG. II 26

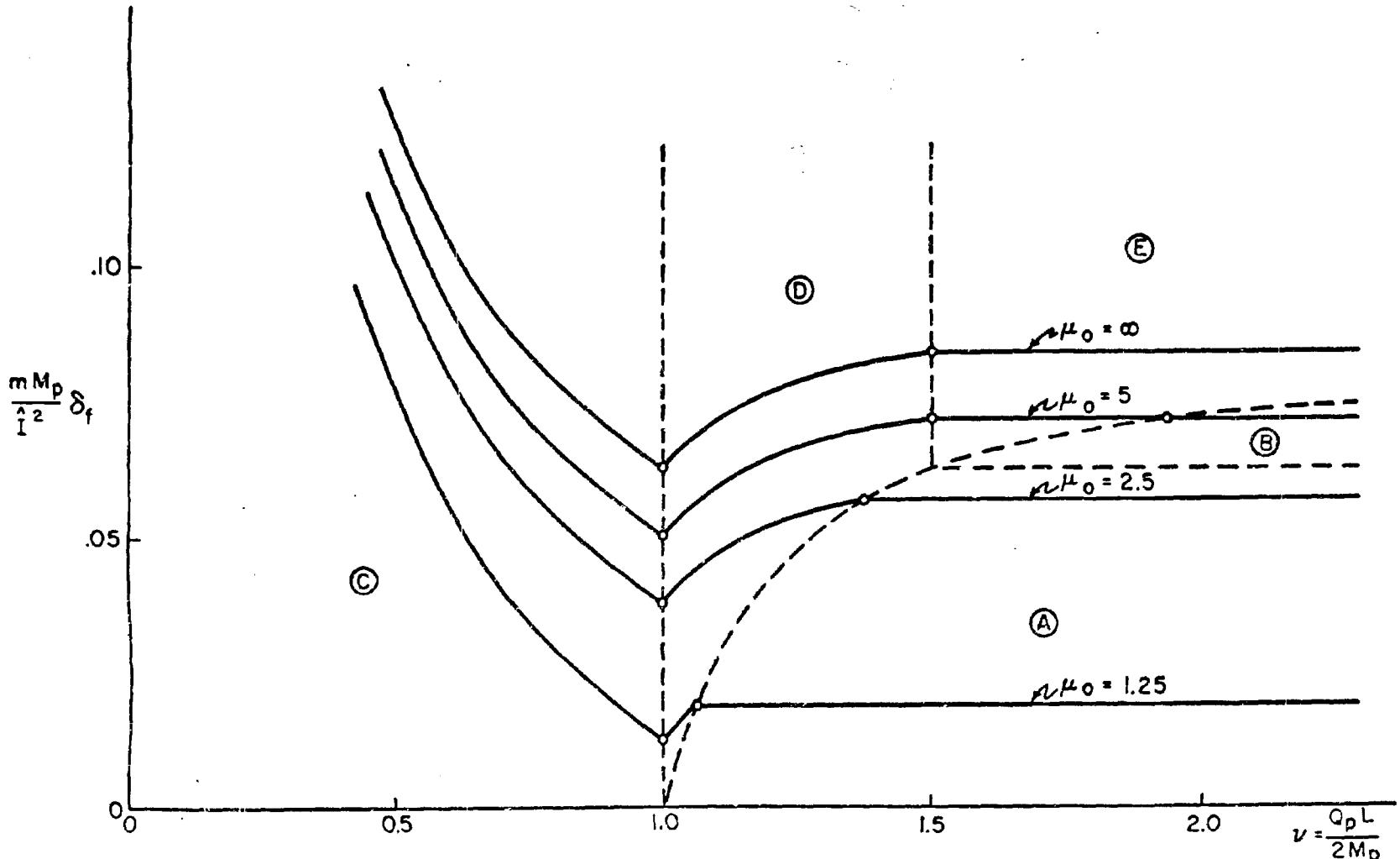

$\frac{mM_p}{\hat{I}^2}\delta_f$ FOR RECTANGULAR PULSE LOAD

FIG. II 27

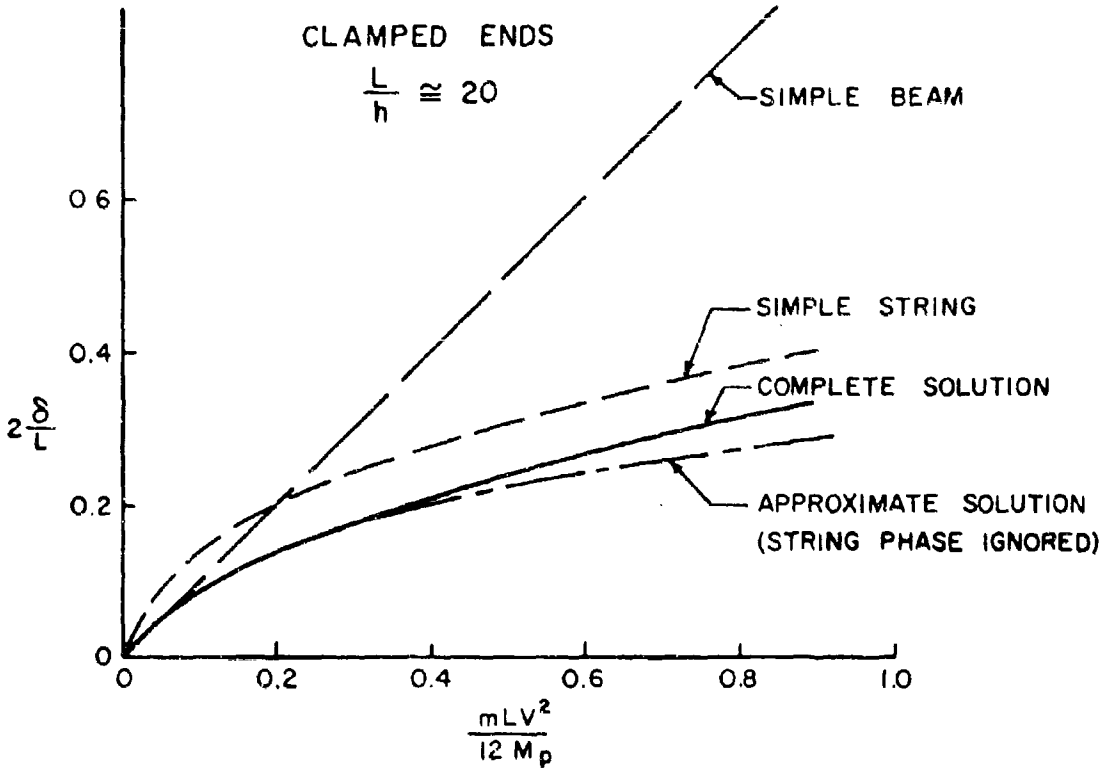
CLAMPED ENDS
$\frac{L}{h} \cong 20$
SIMPLE BEAM
SIMPLE STRING
COMPLETE SOLUTION
APPROXIMATE SOLUTION
(STRING PHASE IGNORED)
$2\frac{\delta}{L}$
0
0.2
0.4
0.6
0.8
1.0
$\frac{mLV^2}{12\,M_p}$

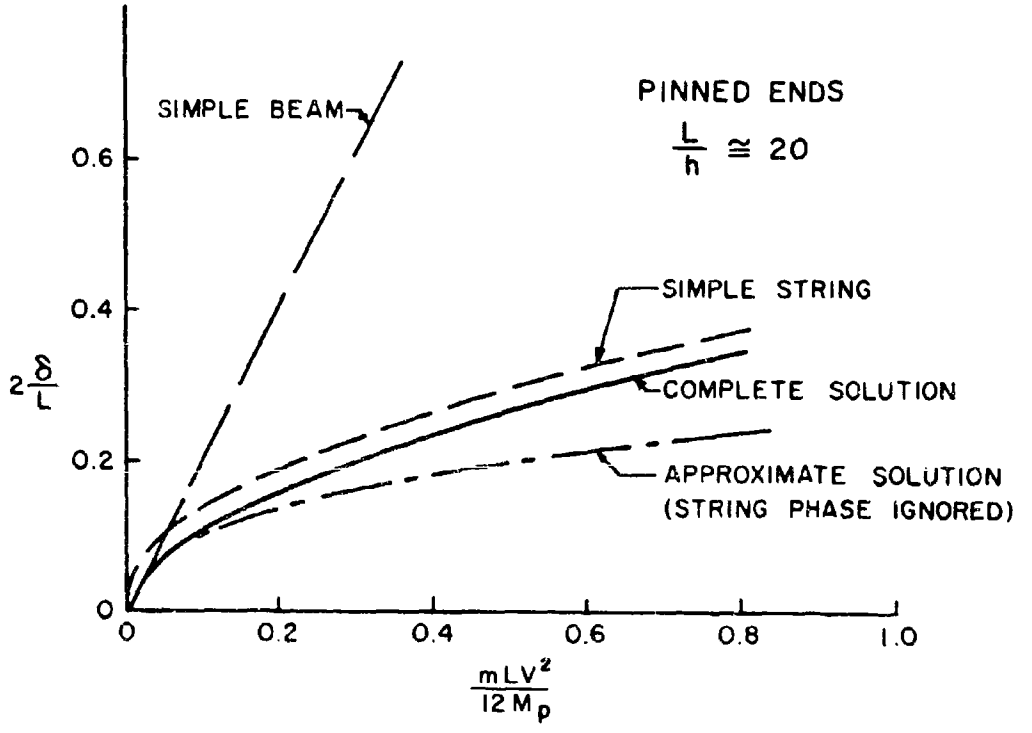
SIMPLE BEAM
PINNED ENDS
$\frac{L}{h} \cong 20$
SIMPLE STRING
COMPLETE SOLUTION
APPROXIMATE SOLUTION
(STRING PHASE IGNORED)
$2\frac{\delta}{L}$
0
0.2
0.4
0.6
0.8
1.0
$\frac{mLV^2}{12\,M_p}$

FIG. II 28

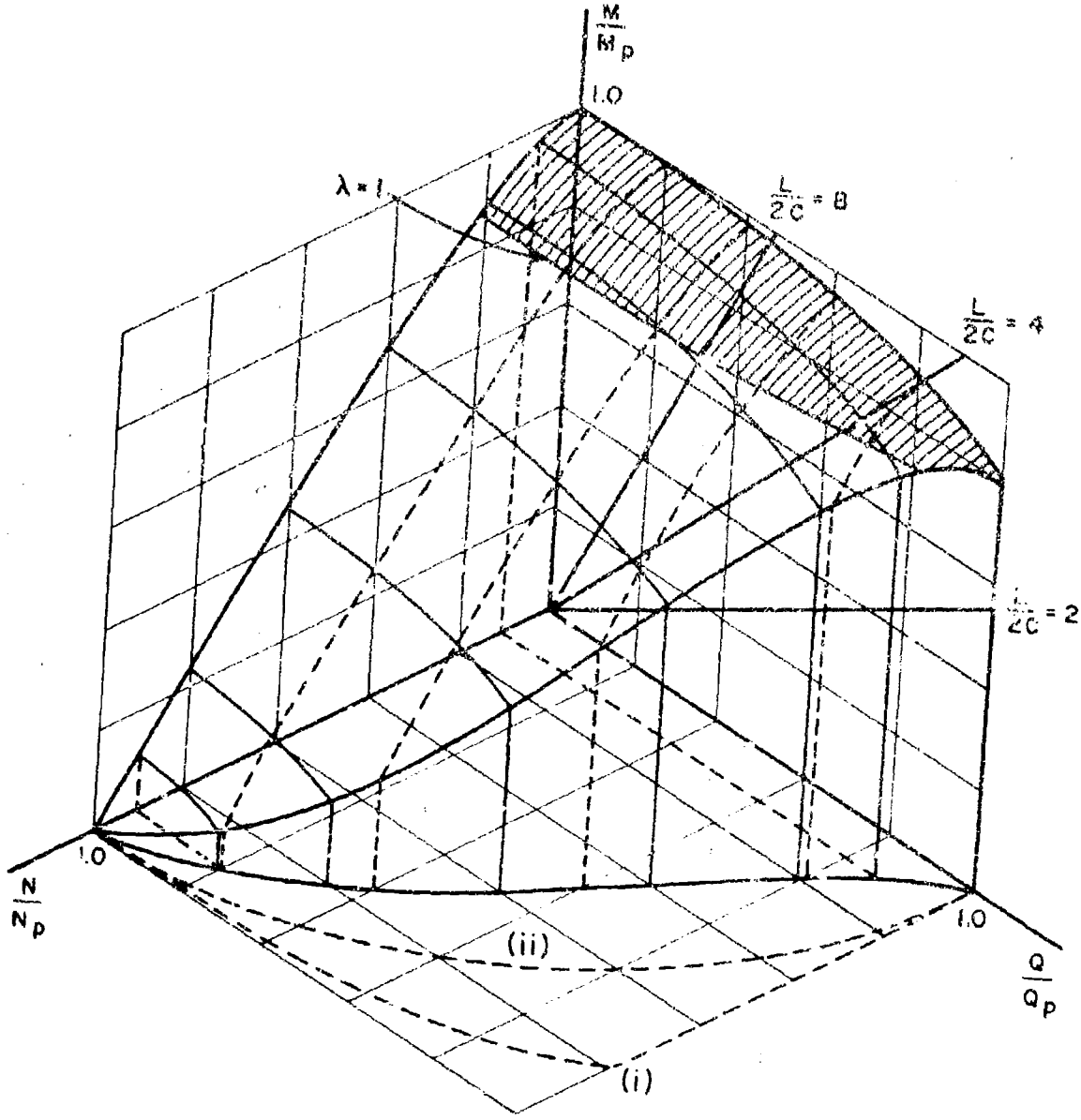

FIG. II 29

Chapter III

EXPERIMENTS ON BEAMS

Introduction

Since the beginnings of the modern interest in plastic deformation of structures under dynamic load, remarkably few experimental investigations on beams have been carried out. This is surprising, since a beam is a simple but in many ways highly representative structural element. Considerable test work has been done on more complex structures (protective structures, naval and space vessels, etc.) as an aid in design, but much of this has been done on an ad hoc basis without time to explore detailed relations between theory and test results. On the other hand, engineering scientists involved in basic research have devoted a large amount of effort to investigations, both theoretical and experimental, of longitudinal plastic wave propagation in rods. This is natural, since the theory of uniaxial stress waves is highly developed; if transverse inertia is neglected and an invariant stress-strain relation is employed, an exact elastic-plastic solution is obtainable in principle for arbitrary initial and end conditions, and for arbitrarily large strains. Similarly, a large amount of work has been done on plane waves, i.e. waves of uniaxial strain, in media with large dimensions transverse to the direction of propagation. Analyses based on invariant stress-strain relations are obviously suspect, in view of the rate dependence observed in many experiments as summarized in Chapter I. Wave experiments have unfortunately not yet been successful in resolving questions of dynamic stress-strain relations. There are basic disagreements about the wave tests and their interpretation; see for example Karnes and Ripperger (1965), Bell (1966), and Kolsky (1966).

The number of experimental investigations published on plastic deformations of beams under impact, blast, or other dynamic loads is a small fraction of the number published on longitudinal waves. The experiments on beams do show a certain degree of consistency in the general conclusions drawn from them. The summary below will try to point out these points of general agreement, but will also indicate the areas where experimental work has been neglected or is inconclusive.

The principal experimental investigations, which will be studied in what follows, are summarized in Table III 1.

We will not describe in detail the experimental investigations listed in Table III 1, but instead will attempt first to summarize the main results, show comparisons with various theoretical predictions, and then give some overall conclusions. The list of investigations is certainly not an exhaustive one, and a few other experimental studies on beams will be mentioned below at appropriate places. The most valuable investigations are those in which important parameters were varied through wide range.

1. Tests of Duwez, Clark and Bohnenblust (1950)

This investigation was concerned with impact of a mass on a long beam, the problem being that solved by Bohnenblust and discussed in Chapter II, Section 2. The authors compared the deflection curve (obtained by high speed photography) and the plastic and elastic deformations determined from it with the corresponding quantities calculated from Bohnenblust's general elastic-plastic theory and from a purely elastic theory. Both theories, it should be remembered, apply strictly to infinite beams and to constant velocity impact.

Table III 1

Investigators	Specimens		Type of Loading	Main Interest
	Materials	Type of Support Dimensions		
1. Duwez, Clark and Bohnenblust (1950).	Cold-rolled steel; copper.	Simple support length 10 ft. depth 1 in. width 3/8 in.	Impact by heavy hammer; controlled contact duration.	Comparison with general elastic-plastic theory of infinite beams.
2. Parkes (1955, 1956, 1958).	Steel, brass duralumin.	Cantilevers simple support lengths 2 in.-12 in. depth 1/4 in. width 1/4 in.	Impact by hammer or by lead bullet.	Comparison with rigid-plastic theory.
3. Mentel (1958) Bodner and Symonds (1962).	Steel Al alloy 6061-T6	Cantilevers with tip mass. lengths 2 in.-12 in. depth .12 in. width .3 in.	Impact on base; impulse at tip mass from explosive charge or bullet entering tip mass.	Comparison with rigid-plastic theory.
4. Florence and Firth (1966)	Steel CR1018 Al alloy 2024-T4 6061-T6	Simple and fixed-ended supports. length 18 in. depth 1/4 in. width 1 in.	Sheet explosive placed on the surface of the beam	Comparison with rigid-plastic theory.

The horizontal beam specimens (10 ft. by 3/8 in. wide by 1 in. deep) were supported at their ends by pins allowing rotations and horizontal displacements, and were struck at their center by a vertically moving hammer weighing 5-3/4 lb. accelerated by rubber bands to the desired velocity of impact (in the range 25 ft. per sec. to 150 ft. per sec.). The hammer struck a set of anvils a certain distance below the top of the beam, and at the instant of striking the anvils closed a circuit which fired an electric discharge tube and thus photographed a white line drawn on the beam. The various desired impact durations were controlled by the distance of the anvils below the top of the beam; the anvils permitted further downward motion of the specimen beams as a result of their inertia. Cold-rolled steel and annealed copper beams were tested. The appropriate bending moment-curvature curves were determined by computation from measured stress-strain curves for tension and compression.

For the cold-rolled steel beams the bending moment increases slowly with curvature beyond the plastic range and the curve is quite well approximated by an elastic line and a horizontal plastic line. The derived curve for the test specimens and the bilinear approximate curve are shown in Fig. III 1 (b). The plastic moment is taken as 8000 in.-lb. in the calculations. Fig. III 1 shows a summary of typical results for cold-rolled steel specimens. Fig. III 1 (a) shows a typical deflection curve together with calculated deflection curves based on Bohnenblust's elastic-plastic analysis and on the same type of treatment without consideration of plastic strains. Figs. III 1 (d) and (e) show the results of a series of tests made with common impact velocity of 100 fps, adjusting the anvils so as to obtain different impact times. These figures show that the angle of deformation θ at the struck point and the point of zero deflection x_o vary with $(\text{time})^{1/2}$ in an approximately linear manner. The numerical agreement of the θ values with the theoretical elastic-plastic curve of θ vs. $\sqrt{t}$ is quite

good, although the test points (shown in Fig. III 1 (d) by circles) fall below the theoretical curve at larger values of $\sqrt{t}$. As far as the zero-deflection point x_o is concerned, the results are completely anomalous. In Fig. III 1 (e) the test points are shown by circles, and the $x_o - \sqrt{t}$ curves predicted by various theories are drawn, the solid line being the curve predicted by Bohnenblust's elastic-plastic theory. The broken lines, as marked, are for the elastic beam corresponding to Bohnenblust's theory, and the most elementary rigid-plastic theory (discussed more fully below), both assuming that the striking mass maintains constant velocity. These two curves almost coincide, and they show much better agreement with the test results than does the curve deduced from the elastic-plastic treatment, which should be the most realistic theory. The agreement with respect to the zero deflection point between the rigid-plastic and wholly elastic theories suggests that the agreement of either of these with test results is fortuitous, and gives no indication as to the reliability of either theory in other situations.

The angle of rotation θ at the struck point is shown in Fig. III 1 (c) as a function of striker velocity V_o, the test points again shown by circles and results predicted by Bohnenblust's elastic-plastic theory by the solid curve. Evidently Bohnenblust's theory predicts the plastic deformation angles well at the smaller striker velocities, but overestimates the plastic deformation by roughly 35 percent at the highest velocity (150 ft. per. sec.)

In sum, the tests by Duwez, Clark and Bohnenblust (1950) show that for cold-rolled steel beams

(a) Bohnenblust's elastic-plastic theory predicts the plastic deformation angles, as function of impact velocity at constant impact duration time, with good accuracy over the lower part of the velocity range, but overestimates this quantity at the highest velocity by about 35 percent.

(b) Bohnenblust's elastic-plastic theory predicts the increase of angle of plastic deformation with time (at constant impact velocity) with good accuracy, although the theory overestimates this angle at the largest deformation values by about 10 percent.

(c) The shape of the deflected beam is reasonably well predicted by Bohnenblust's theory. The spread of deformation as a function of time may be studied by examining the coordinate x_o of the point where the deflection curve crosses the zero-deflection axis closest to the impact section; the predicted relation x_o = constant $\sqrt{t}$ agrees well qualitatively with the results observed in the tests.

What conclusions can be drawn from the results summarized above? "Agreement between theory and tests" should mean that the approximations and hypotheses on which the theoretical predictions were based are valid- excluding, of course, the possibility that a seriously incorrect assumption or approximation was cancelled out by some phenomenon which played a role in the tests but was omitted from consideration in the theory.

In the present case, the major assumptions and approximations in Bohnenblust's theory of elastic-plastic beam impact are as follows:

(1) The Bohnenblust form of solution applies only to constant velocity impact on a beam of infinite length.

(2) Rotary inertia and shear deflections (elastic and plastic) are neglected; in the elastic range the differential equations are those of the elementary Bernoulli-Euler beam theory.

(3) The basic material characteristics - a curve relating bending moment to curvature - are invariant properties of the material and the given beam section; in particular there is no dependence on the current strain rate or on the history of deforma-

tion rates.

(4) In applying the theory to the test specimens further approximations regarding material behavior are made, in that the moment-curvature relation was approximately represented by two straight lines; plastic behavior was represented in the case of the cold-rolled steel by a horizontal line (as in Fig. III 1 (b), and in the case of copper by a straight line at an angle with the strain axis. In both case a Bauschinger effect was assumed such that a constant elastic range exists (kinematic strain hardening)

The most important discrepancies between test results and theoretical predictions are probably those between measured and predicted plastic rotation angles at high impact velocities. The experiments must be examined to try to determine which of the listed sources of error is responsible for the observed discrepancies. This implies (in the absence of further experimentation) the need for reasonable estimates of corrections corresponding to the listed sources of error.

Rigid-plastic analysis provides a means by which some of these estimates can be made very easily. Whether or not a rigid-plastic analysis is appropriate, it seems reasonable to suppose that the qualitative importance of the correction due to plastic shear deformation, for example, is roughly the same for both the rigid-plastic and elastic-plastic treatments. We shall illustrate this use of plastic-rigid analysis in the present problem. We give first the result of the simplest possible model of the Duwez-Clark-Bohnenblust experiment. This is the case of an infinite beam of rigid-plastic material, struck at one section by a mass so large that its velocity remains unchanged; the beam is supposed to undergo plastic deformation in bending only (shear deformations neglected), to have negligible rotary

inertia, and to exhibit ideally plastic behavior, without strain rate effects on strain hardening. The results of this simplest rigid-plastic model are then compared with those obtained for models which are made successively more realistic by taking account of

(A) finite striking mass

(B) shear deformation

(C) strain rate sensitivity

Estimates of other effects such as of rotary inertia of the beam section, strain hardening, and finite deflections, could also be obtained as modifications of the elementary rigid-plastic treatment, but the calculations are more involved and only a few remarks will be made about these.

The rigid-plastic solutions are obtained from the diagrams of Fig. III 3. Sketch (b) of this figure represents the mechanism of deformation appropriate when the material is perfectly plastic, with a constant plastic limit moment M_p. As shown in (b) and (d), at the struck point there is a plastic hinge with moment $+M_p$ (assumed unaffected by the shear stress). In a segment OH of length z the bending moment changes from $+M_p$ to $-M_p$. The shear force vanishes and the bending moment has the constant value $-M_p$, at H and at all sections to the right of H. This moment diagram (d) corresponds to the velocity diagram (c), which shows velocities of beam cross-sections proportional to distance from point H in the segment OH; this segment must move as a rigid body since the bending moment has magnitude $|M| < M_p$ inside OH. To the right of H the beam is at rest.

In the "simplest solution" the impacting mass G is taken to be so large compared with the mass of the beam which is set in motion that its velocity remains unchanged at the striking velocity V_o. Neglecting shear deformations in the beam, the velocity of the beam at the struck cross-section is likewise constant at V_o. Thus the only unknown quantity of the deforming

beam is the length z. This can be found by the equation of conservation of moment of momentum about an axis at 0:

$$2M_p t = \int_0^z x\omega(z - x)\, m dx = \frac{1}{6} mz^3\omega \qquad (1.1)$$

where ω is the angular velocity of segment OH, and m is the mass per unit length of the beam. Since in the case of constant velocity impact $\omega = V_o/z$, the result for z is

$$z^2 = \frac{12M_p t}{mV_o}$$

The plot of z vs. t according to the above equation is shown in Fig. III 1 (e) for the cold rolled steel specimens tested by Duwez et al at V_o = 100 ft/sec. The agreement with the experimental values of x_o (the beam coordinate where the deflection curve crosses the horizontal axis closest to the impact point) is remarkable but seems of little significance. The angle of deformation at the impact point is

$$\theta = \int_0^t \omega dt = \frac{mV_o^2 z}{6M_p} = \frac{mV_o^3 t}{3M_p} \qquad (1.2)$$

The central angle from Equation (1.2) is shown in Fig. III 2 as curve D, plotting θ versus V_o for constant impact duration time 1.22×10^{-3} sec., using the data for the cold-rolled steel beam specimens of Duwez et al (1950). The results from Equation (1.2) agree badly with the measured values in the tests, being too large by a factor between 2 and 3. This is not surprising; apart from the corrections to be discussed, we have no reason to expect close agreement between predictions of a rigid-plastic theory and the test results (the ratio of plastic work to maximum elastic strain energy is approximately one, for the data of the test results shown in Fig. III 2). We may, however, now use the simple rigid-plastic analysis just given as a basis for estimating the

relative importance of many of the physical assumptions made, and take the results as indicative of the relative importance of the same effects in Bohnenblust's elastic-plastic theory.

(A) Finite mass. If the striking body has mass G, but is assumed to have the same velocity V(t) as the struck section of the beam, the equation of momentum of momentum Equation (1.1) must be supplemented by that of linear momentum in order to determine the additional unknown V(t):

$$GV_o = GV + mz\,V \tag{1.3}$$

Using $V = \omega z$, the following equations are obtained for V, z, and θ

$$\frac{V}{V_o} + \frac{V_o}{V} = \frac{12M_p mt}{G^2 V_o} + 2 \tag{1.4a}$$

$$\frac{mz^2}{G+mz} = \frac{12M_p t}{mV} \tag{1.4b}$$

$$\theta = \frac{mV_o^2 z}{6M_p} \frac{1 + \frac{3}{4}\frac{mz}{G}}{(1 + \frac{mz}{G})^2} \tag{1.4c}$$

The central angle θ as function of V_o according to Equation (1.4c) is plotted as curve C in Fig. III 2, taking $t = 1.22 \times 10^{-3}$ sec., and the data for G, m, etc. as given for the tests on cold rolled steel beams of Duwez et al (1950). For an initial velocity of 1200 in/sec at $t = 1.22 \times 10^{-3}$ sec., Equation (1.4a) gives the result $V/V_o = 0.71$. Thus the reduction of striker velocity is appreciable even in the first millisecond for a weight $5\frac{3}{4}$ lb. striking a 10 ft long beam of 3/8 in. and depth 1 in., and the angle of deformation is about two-thirds that which is predicted if the striker is assumed to move with unchanged velocity.

(B) Shear deformation. The rigid-plastic analyses outlined above, as well as Bohnenblust's analysis, took the shear forces in the beam as

reaction forces (doing no work), and disregarded the fact that the shear force at the struck sections is infinite initially. This result is due in part to treating the beam as a one-dimensional continuum without cross-sectional deformation due to shear or compression, and also in part to assuming that the struck portion of the beam instantaneously acquires the velocity of the striker. Since these are common assumptions in conventional beam theory, it is of interest to obtain the correction for shear deformation alone in the plastic-rigid theory.

This simple treatment of shear deformation to be outlined takes the square interaction curve of Fig. II 22 (d) as an adequate approximation. At a cross-section where $Q = Q_p$ a shear slide is permitted, (corresponding to a plastic hinge for bending); a jump in transverse velocity of the beam across the slide section must have a sign agreeing with the shear force directions so that positive work is done. In the present problem we write the velocity of the striker as V' while the velocity of each adjacent section is V. During a period after the mass strikes, the shear force at the struck section is Q_p and $V' - V > 0$. At this section the fully plastic bending moment M_p is assumed to act, without interaction between shear force and bending moment, as in the case treated by Karunes and Onat (1960) outlined above (see Fig. II 23). The equation of linear momentum replacing Equation (1.3) is

$$GV_o = GV' + mzV \tag{1.5}$$

Since the shear force at the struck section now has the known value Q_p the linear impulse-momentum equation for the half-beam is

$$Q_p t = \frac{1}{2} mVz \tag{1.6}$$

The previously written equation of angular impulse-moment of momentum still applies, and $V = \omega z$, so that

$$M_p t = \frac{1}{12} m V z^2 \tag{1.7}$$

Combining Equations (1.6), (1.7), and (1.5) we obtain

$$z = \frac{6M_p}{Q_p} \tag{1.8a}$$

$$V - V' = V_o - \left(\frac{2Q_p}{G} + \frac{Q_p^2}{3mM_p}\right) t \tag{1.8b}$$

$$\omega = \frac{V}{z} = \frac{Q_p^3 t}{18mM_p^2} \tag{1.8c}$$

Note that the hinge coordinate z is constant in this phase. The shearing deformation is completed in a time t_s determined from Equation (1.8b) by setting $V - V' = 0$. At later times the momentum conservation equations apply in their previously used forms, and the deformations are easily found by integrating beyond time t_s. The central angle of rotation computed at $t = 1.22 \times 10^{-3}$ sec. is shown as curve B in Fig. III 2. It is seen that with account taken of shearing deformation there is a further reduction of the central angle below that of curve C. The original large discrepancy between the test results and the angles predicted by the simplest rigid-plastic theory has been largely removed by the analysis taking account of the finite striker mass and shear deformations.

(C) Strain rate. Ezra (1958) has given an approximate treatment of effects of strain rate sensitivity in Duwez, Clark, and Bohnenblust's tests. We will discuss later in more detail the inclusion of strain rate sensitivity in impact problems. It will suffice here to say that Ezra's analysis introduced a corrected dynamic plastic bending moment corresponding to estimate average strain rates at the plastic hinges at successive stages of the deformation. The plastic hinges were assumed to be located at the same cross-sections as predicted by the solution for non-rate sensitive rigid-plastic material, and strains and strain rates estimated at each hinge by

assuming the length of the plastic hinge to be equal to the depth of the beam. At each step, having computed the strain rate the plastic hinge moment was determined so as to agree with the dynamic yield stress values measured by Manjoine (1944) as a function of strain rate. Using the new value of hinge moment the rotations and angular velocities across hinges were recomputed. The hinge moments were again revised, and the cycle repeated until a steady state was reached. It was arbitrarily assumed that the dynamic plastic moments were the same at all hinges. The resulting curve calculated by Ezra in this way is shown as curve (E) in Fig. III 2. Ezra's calculation takes account of the change in velocity of the striker but not of the shear deformation, and thus his curve (E) should be compared with curve (B); presumably the inclusion of shear deformation would result in an additional reduction of the final deformation angle. Ezra's curve agrees very well with test points up to about 100 ft per sec, but lies below the test values above this velocity. Apparently his method over-corrects for strain rate sensitivity in this range. However, it should be remembered that the validity of neglecting elastic deformations in this problem is questionable, as already pointed out, since the amount of plastic work is comparable to that of the maximum elastic strain energy. Moreover, the strain rate sensitivity of the mild steel tested by Manjoinewas probably considerably greater than that of the cold-rolled steel of the present tests. (See Chapter I, Section 5; some tests have shown negligible strain rate sensitivity for a cold-rolled steel). It is remarkable that curves (B) and (E) lie as close as they do to the test points, but the real interest of the various curves in Fig. III 2 is in the comparison between the curves derived from rigid-plastic theory which enable one to estimate possible corrections from various sources to the Bohnenblust treatment. There is no doubt about the need for such corrections: the striking mass is finite and its velocity must decrease; the shear force cannot attain

infinite magnitudes; and mild steel exhibits a considerable increase of yield strength at the strain rates met with in Duwez, Clark and Bohnenblust's tests. Whether the corrections for these physical effects obtained by considering rigid-plastic behavior are quantitatively applicable to the elastic-plastic treatment is not certain; however there seems no way of modifying Bohnenblust's analysis so as to obtain them.

In beam impact experiments in which final deflections considerably larger than the beam depth are produced, with ends constrained against axial motion, account must be taken of axial forces, as was pointed out. Experiments designed specifically to investigate this effect in combination with rate sensitivity have been carried out by Nonaka (1964). These confirmed the conclusion reached analytically by Nonaka (and previously by Symonds and Mentel (1958)), that membrane effects predominate over bending, with deflections a few multiples of the beam depth.

2. Parkes's experiments.

Parkes's (1955) tests were the first conducted on structures for the specific purpose of assessing the validity of a rigid-plastic analysis. These tests were performed on small cantilever beams of mild steel struck near the tip by falling weights or by rifle bullets. Subsequently results of further tests were published (Parkes 1956, 1958) in which beams clamped at both ends were struck by moving masses, the specimens in these tests being steel, brass and duralumin. The beam ends were constrained so as to prevent rotation but allow axial motions so as to freely accommodate the transverse deflections. The basic conditions of these tests are as listed in Table III 2.

Table III 2

Parkes's Test Conditions

(A) Cantilever beam specimens

Lengths: 2 in, 4 in, 8 in, 12 in.

Cross-section: 1/4 in square (nominal)

Striker masses and velocities:

Heavy strikers	1 lb at 12.7 ft/sec and	18.0 ft/sec
	4 lb at 6.4 ft/sec and	9.0 ft/sec
Light strikers	.0043 lb at 970 ft/sec	
	.0050 lb at 1580 ft/sec	

Beam material: mild steel
static plastic moment 195 lb-in

(B) Fixed-end beam specimens

Lengths: L_2 = 2 in, L_1 = 2 in, 4 in, 10 in.

L_2 = 1 in, L_1 = 1 in, 2 in, 5 in.

L_2 = 6 in, L_1 = 6 in.

Cross-section: 1/4 in square (nominal)

Striker masses and velocities:

Heavy strikers	4 lb at 19.4 ft/sec
	16 lb at 9.7 ft/sec
Light strikers	.0050 lb at 1500 ft/sec

Beam materials and static plastic moments:
mild steel and brass: both 228 lb-in;
duralumin: 256 lb-in.

The main objective of Parkes's tests was to find whether a rigid perfectly plastic analysis assuming a constant plastic moment could accurately predict final deformations, the appropriate dynamic value of the plastic moment being computed from estimates of average strain rates in the tests and published data concerning the dependence of yield stress on strain rate. The main conclusion reached was that such an analysis predicted shapes and magnitudes with good accuracy in the cases of beams struck by large masses, but gave poor predictions in the case of low mass—high velocity impact.

(A) Cantilever: The analysis for the rigid-perfectly plastic

cantilever is very simple, and follows directly from the pattern of deformation discussed above for the infinite beam struck by a mass. Let us assume, as Parkes did, that the striker with velocity V_o transverse to the beam becomes instantaneously attached to the beam at t = 0, has mass G and negligible centroidal moment of inertia. Shear deformations, strain rate sensitivity, and strain hardening, will all be neglected, for the present, although as will be seen some of these may be important in some cases. The plastic moment M_p is taken as a constant property of the section. Consider the cantilever beam case, Fig. III 5. There are two phases of deformation. In the first phase there is a segment of length z(t) in motion as a rigid body with angular velocity $\omega(z) = V/z$. Ahead of the deforming segment the beam is at rest but has constant bending moment $-M_p$ and zero shear force. Plastic deformation at an arbitrary cross-section at a distance x from the struck end occurs when z = x, i.e. when the hinge point passes through the section at x. The resulting curvature is $\kappa(x) = \omega(x)/\dot{z}(x)$.

Let $\theta(x;z)$ denote the angle of rotation at a typical cross-section at distance x from the tip, when the hinge section is at distance z from the tip. All distances may be measured along the center line of the deflected beam. The rotation angle at the tip is $\theta(0;z)$ and the relative rotation between the tip and the section at x is $\theta(0;z) - \theta(x;z)$.

Under the assumptions stated, the work-energy balance is expressed by

$$\frac{1}{2} GV_o^2 = M_p\theta(0;z) + K(z) \qquad (2.1)$$

where K(z) is the kinetic energy of the beam when the hinge is at z,

$$K(z) = \frac{1}{2} GV^2 + \frac{1}{6} mzV^2 \qquad (2.2)$$

For a beam of length L, further rotation θ_L as a rigid body occurs after the hinge section has reached the base. From the work-energy balance in this second phase we have

$$M_p\theta_L = K(L) = \frac{1}{2} GV_o^2 - M_p\theta(0,L) \tag{2.3}$$

The final angle of rotation at any section is therefore, since $\theta(x,L) = \theta(0,L) - \theta(0,x)$

$$\theta_f(x) = \theta(x;L) + \theta_L = \frac{1}{2}\frac{GV_o^2}{M_p} - \theta(0,x) \tag{2.4}$$

In particular,

$$\theta_f(0) = \frac{1}{2} GV_o^2 \tag{2.5}$$

This result for the final rotation angle at the beam tip is valid for deflections of arbitrary magnitude, for a rigid-perfectly plastic material.

Although the final angle at the beam tip can be obtained for these conditions by energy considerations alone, the angle at a generic cross-section can only be found by the use also of equations of momentum conservation. To obtain a simple solution we shall assume first that deflections are small, and obtain the solution (derived somewhat differently) by Parkes (1955). For small deflections, conservation of linear and angular momentum leads to the equations for the first phase:

$$GV_o = GV + \frac{1}{2} mzV \tag{2.6}$$

$$\frac{1}{6} mz^2V = M_p t \tag{2.7}$$

The tip velocity V and hinge position z are therefore determined by the equations

$$\frac{(V_o - V)^2}{V} = \frac{3}{2}\frac{mM_p t}{G^2} \tag{2.8a}$$

$$\frac{z^2}{1 + \frac{mz}{2G}} = \frac{6M_p t}{mV_o} \tag{2.8b}$$

The first phase ends at $t = t_1$ when $z = L$, and by Equations (2.2) and (2.6) the kinetic energy at this instant is

$$E_2 = \frac{M_p \theta_L}{\frac{1}{2} GV_o^2}; \qquad \theta_f = \theta_2 = \frac{GV_o^2}{2M_p} \frac{1 + \frac{2}{3}\beta}{(1 + \beta)^2} \tag{2.10}$$

where E_2 is the plastic work done in the second phase divided by the initial kinetic energy and $\beta = mL/2G$. In the first phase the plastic work ratio $E_1 = 1 - E_2$. If the tip mass is much larger than the beam mass most of the plastic work is done in the second phase, i.e. in the base hinge rotation. For example if $G > 3mL$, more than 80 percent of the initial energy goes into the base hinge rotation.

In the first phase the curvature may be determined as $\kappa = \omega/\dot{z} = d\theta(0;z)/dz$, using Equations (2.1) and (2.2). An element at any fixed section x acquires its curvature instantaneously when the plastic hinge reached it, $z = x$; and this curvature then remains constant. The result is

$$\kappa(x) = \frac{mV_o^2}{6M_p}\left[\frac{1}{(1+\frac{mx}{2G})^3} + \frac{1}{(1+\frac{mx}{2G})^2}\right] \tag{2.11}$$

The displacement at any instant in the first phase can be derived by virtual work (or otherwise) as

$$y(x;z) = \int_x^z \kappa(s)\,(s-x)ds \tag{2.12}$$

In particular, when $z = L$ the displacement can be written as

$$\frac{3M_p}{L}\, y(x;L) = \frac{GV_o^2}{2}\left[\frac{\beta(1-\xi)}{(1+\beta)^2} + \frac{3\xi - 2}{1+\beta} - \frac{\xi}{1+\beta\xi} + \frac{2}{\beta}\log\frac{1+\beta}{1+\beta\xi}\right] \tag{2.13}$$

where

$$\beta = \frac{mL}{2G}, \qquad \xi = \frac{x}{L}$$

The total deflection is obtained by adding to y(x,L) the displacement acquired in the second phase. Since this phase consists of a rotation θ_L, the complete deflection is

$$y(x) = y(x;L) + (L - x)\theta_L \tag{2.14}$$

where y(x;L) is given by Equation (2.13) and θ_L by Equation (2.10). For $\beta \to 0$ (large tip mass) the contribution from y(x;L) vanishes as β, and the linear deflection $(L - x)\theta_L$ predominates.

(B) Discussion: Table III 3 gives a summary of Parkes' test results with cantilever beams (Parkes (1955) and of results obtained from the rigid-plastic theory summarized above. The deformation measured and used for comparison was the angle of rotation at the base of the beam. In all of the tests there was a plastic hinge region at the base, comprising a localized plastic deformation extending a distance of the order of one inch (four times the depth) from the base. Beyond the hinge region the specimens had a fairly straight segment, and the rotation angle was presumably measured just outside the hinge. The tests with "heavy" strikers (specimens C.1-C.16 in Table III 3) resulted in specimens that were essentially straight except for the hinge region at the base. The tests with "light" strikers (specimens C.17-C.24) were strongly curved near the tip of the beam.

The experimental values of the rotation angle near the base are shown in Table III 3, column (13). These are divided by the angle predicted by the simple rigid-plastic theory to obtain the ratios listed in

TABLE III 3

Parkes (1955) Cantilevers

(1)	(2)	(3)	(4)	(5)	(6)	(7)	(8)	(9)	(10)	(11)	(12)	(13)	(14)	(15)
	Gg lb.	V_o ft/sec	L in.	β = mL/2G	$\theta_o = GV_o^2/2M_p$	$\frac{1}{L} y_{oI}$	θ_L rad.	$\bar{\varepsilon}$ sec^{-1}	$\frac{M'_p}{M_p}$	$\theta'_L = L(M_p/M'_p)$	δ_{exp} in.	θ_{exp} rad.	$\frac{\theta_{exp}}{\theta_L}$	$\frac{\theta_{exp}}{\theta'_L}$
C.1	4.0	6.4	2	.0046	0.157	0.0005	.163	2.5	1.6	.102	0.22	0.11	0.67	1.08
C.2	"	"	4	.0092	"	0.0009	.169	1.2	1.5	.113	0.42	0.105	0.62	0.93
C.3	"	"	8	.0183	"	0.0018	.183	0.6	1.4	.131	0.93	0.116	0.63	0.89
C.4	"	"	12	.0274	"	0.0027	.200	0.4	1.4	.143	1.53	0.127	0.64	0.89
C.5	"	9.0	2	.0046	0.310	0.0009	.322	3.5	1.7	.190	0.43	0.22	0.68	1.16
C.6	"	"	4	.0092	"	0.0019	.333	1.7	1.6	.208	0.90	0.227	0.68	1.09
C.7	"	"	8	.0183	"	0.0037	.362	0.9	1.5	.241	2.15	0.272	0.75	1.13
C.8	"	"	12	.0274	"	0.0054	.395	0.6	1.4	.282	3.46	0.292	0.74	1.03
C.9	1.0	12.7	2	.0183	0.154	0.0018	.152	4.9	1.7	.089	0.18	0.09	0.59	1.01
C.10	"	"	4	.0366	"	0.0035	.150	2.4	1.6	.094	0.37	0.093	0.62	0.99
C.11	"	"	8	.0732	"	0.0067	.146	1.2	1.5	.097	0.77	0.096	0.66	0.99
C.12	"	"	12	.1100	"	0.0095	.143	0.7	1.5	.095	1.11	0.093	0.65	0.98
C.13	"	18.0	2	.0183	0.310	0.0037	.305	6.9	1.7	.180	0.37	0.19	0.62	1.06
C.14	"	"	4	.0366	"	0.0071	.301	3.4	1.7	.177	0.78	0.195	0.65	1.10
C.15	"	"	8	.0732	"	0.0135	.293	1.6	1.6	.183	1.68	0.210	0.72	1.15
C.16	"	"	12	.1100	"	0.0191	.288	1.1	1.5	.192	2.43	0.202	0.70	1.05
C.17	.0043	970.	2	4.26	3.86	0.710	.537	72.	2.2	.244		0.28	0.52	1.15
C.18	"		4	8.52	"	0.530	.285	20.	1.9	.150		0.19	0.67	1.27
C.19	"		8	17.0	"	0.362	.147	5.3	1.7	.098		0.11	0.75	1.27
C.20	"		12	25.6	"	0.278	.099	2.4	1.6	.062		0.07	0.71	1.12
C.21	.0050	1580.	2	3.66	11.93	2.31	1.90	132.	2.2	.86		0.80	0.42	0.93
C.22	"		4	7.32	"	1.77	1.02	37.	2.0	.51		0.56	0.55	1.10
C.23	"		8	14.64	"	1.23	.528	9.8	1.8	.293		0.35	0.66	1.19
C.24	"		12	22.0	"	0.954	.354	4.5	1.7	.208		0.22	0.62	1.06

column (14) and plotted in Fig. III 6(a) for "heavy" strikers and Fig. III 6(b) for "light" strikers. It is seen that for both sets of tests the ratio is substantially below unity. The disagreement between experiment and theory ranges from about thirty to fifty percent.

To explain the disagreement, Parkes suggested that the strain rate sensitivity of the material must be considered, and made a semi-empirical correction of the plastic moment taking into account the dependence of the yield stress of mild steel on the rate of plastic straining. We will present and discuss this correction shortly. Before doing so we raise the question of strain hardening, which has also been ignored in the theory. Strains at the base of the cantilevers were in the range of approximately 1.5 percent to about 4 percent. (Measurements of strains are not cited in the paper, but they can be roughly estimated from the rotation angle and the observed length of the plastic region.) These are strain magnitudes in the region of appreciable strain hardening of steel. One may naturally ask: why not attribute the discrepancy between experiment and theory to the neglect of strain hardening?

An indication that strain hardening is not the source of the discrepancy is given by the plot of Fig. III 8. These are the results from the tests C.1-C.16 using heavy strikers summarized in Table III 4. In these tests, for each beam length and striker weight, two velocities were used. Thus for each value of β there are two test results. In Fig. III 8 the pair of points corresponding to each β are joined by a line. The ordinate is the rotation angle observed in the tests. Now since strain hardening is neglected in the analysis, the error due to this neglect should depend on the amount of the straining. If the error is important it should show up in the comparison of test and theoretical results. In a plot against angle of deformation (or strain) as in Fig. III 8, the

effect of strain hardening should cause the disagreement between test and theory to be greatest at the larger deformations. Thus the ratio θ_{exp}/θ_L should decrease as θ_L increases. The opposite effect is observed in Fig. III 8; the lines joining the pairs of points with common slant up, rather than down. This provides a strong indication that strain hardening is not playing a major role in the discrepancy.

The better agreement of test results with elementary theory at the larger strain magnitudes presumably is an indication that the neglect of elastic deformations is more satisfactory, i.e. that the rigid-plastic analysis is more suitable at the higher velocities than at the lower ones. The energy ratios

$$R = \frac{1}{2} G V_o^2 \Big/ \frac{M_p L^2}{2EI}$$

are doubled in the tests at the larger strain and velocity magnitudes. The actual values are listed on Table III 4. The "improvement" due to doubling R seems to depend upon R in the way that would be expected if the importance of elastic vibrations is being diminished; if R is smaller than 4 the improvement is 10 to 20 percent, while if R is 9, the improvement is less than experimental error. This provides some indication of the minimum value of R desirable for a rigid-plastic analysis: in this example it appears to be roughly $R \geq 6$, but this is clearly speculative, because effects other than elastic deformations may be playing a part.

The plastic behavior of mild steel is known to be sensitive to rate of straining, the yield stress being particularly dependent on strain rate. Parkes made use of the data on this dependence published by Manjoine (1944) to determine a correction factor applicable to his test results. He aimed at obtaining a strain rate correction that would explain his experimental results as simply as possible, rather than at

TABLE III 4

Comparison of experimental results at same β,
different R (different striker velocity and deformation)

	β =	.00457	.00915	.0183	.0274
	C1-C4 $\frac{\theta_{exp}}{\theta'_L}$ =	.675	.622	.634	.635
	R =	9.2	4.6	2.3	1.52
	C5-C8 $\frac{\theta_{exp}}{\theta'_L}$ =	.671	.682	.751	.740
	R =	18.1	9.1	4.5	3.0
	"Improvement" $\frac{\theta_{exp}\ C5\text{-}C8}{\theta_{exp}\ C1\text{-}C4} - 1$ =	$\frac{-.004}{.68}$	$\frac{0.6}{.62}$ = 10%	$\frac{.12}{.63}$ = 19%	$\frac{.10}{.64}$ = 16%
Higher Velocity Smaller Mass	C9-C12 $\frac{\theta_{exp}}{\theta_L}$ =	.592	.620	.658	.650
	R =	9.0	4.5	2.2	1.5
	C13-C16 $\frac{\theta_{exp}}{\theta_L}$ =	.610	.651	.720	.705
	R =	18.1	9.1	4.5	3.0
	"Improvement" =	3%	5%	9%	9%

obtaining a general analysis with account taken of rate dependence. Accordingly his treatment makes drastic assumptions and makes use of results obtained in his tests. It leads to a remarkable degree of agreement between test results and corrected theoretical values.

Parkes used his rigid-plastic analysis to determine the mean angular velocity at the base of the cantilever. This is θ_L/t_{f2}, where t_{f2} is the time of the second phase (rigid body rotation) and θ_L is the rotation at the base, and the result is

$$\bar{\dot{\theta}} = \frac{GV_o^2}{2M_p} \frac{1 + \frac{2}{3}\beta}{(1+\beta)^2} \Big/ \frac{GV_oL}{M_p} \frac{1 + \frac{2}{3}\beta}{1+\beta} = \frac{V_o}{2L(1+\beta)} \qquad (2.15)$$

The rigid-plastic theory does not furnish strain or strain rate magnitudes, since it deals with point hinges and instantaneous strain changes. Parkes therefore used the observation that "in all tests the hinge length was of the order of 1 in.". He thus computed the average curvature rate and extreme fibre strain rate, respectively, as

$$\dot{\kappa} = \frac{\bar{\dot{\theta}}}{h} ; \qquad \bar{\dot{\epsilon}} = \frac{d}{2}\frac{\bar{\dot{\theta}}}{h} = \frac{V_o d}{4hL(1+\beta)} \qquad (2.16)$$

and took h as 1 in. in all cases. The average strain rates in the outer beam fibres according to the formula (2.16) are shown in Table III 3, column 9, for the data of Parkes' tests. Parkes then determined "dynamic plastic moment" magnitudes corresponding to these strain rate values. The data used for this purpose, as already stated, was that of Manjoine (1944). (This data and comparable results of other experimenters has been mentioned in Chapter I; see Fig. I 6). Curves showing Manjoine's results for mild steel as a function of strain rate in tensile impact are shown in Fig. III 14. The ratio σ/σ_o is plotted in Fig. III 14, where σ_o, the static yield stress, is taken as the value of yield stress in Manjoine's curve at a strain rate of approximately 10^{-4} sec^{-1}, and is equal to

about 30,000 psi. The dynamic plastic moment M is obtained from the dynamic yield stress by an elementary calculation, assuming the compressive and tensile behavior to be identical, and that plane sections remain plane. The resulting curve for M/M_p obtained in this way by Parkes is shown in Fig. III 14. Taking the appropriate strain rate to be the average extreme-fibre strain rates as listed in column 9 of Table III 3, the dynamic plastic moment ratios are found to have the values listed in column 10 of that Table.

Figures III 6 and III 7 show the comparison between Parkes' test results and those of the rigid-plastic theory. The pair of graphs of Fig. III 6 show the angle of rotation near the base divided by that computed from the simple rigid-plastic theory, Equation (2.1''), with the plastic moment M_p corresponding to static conditions. The pair of graphs of Fig. III 7 show the same ratio of experimental to calculated angle, but replacing the static plastic moment by the estimated dynamic value. This amounts to multiplying the values plotted in the upper curves (column 14 of Table III 3) by the ratio M/M_p of column 10, to obtain the ratios listed in column 15.

The agreement between test results and rigid-plastic theoretical ones is clearly much better in the pair of graphs of Fig. III 7 especially for the heavy strikers. For these the correction factor (1.5 to 1.8) on the static plastic moment is such that the plotted ratios cluster reasonably well about the line drawn at the value unity for the light strikers; the agreement is not quite so good, the strain correction being somewhat too large, so that the plotted ratios cluster around a line drawn at about 1.15 on the ordinate scale. However the agreement is certainly better than that obtained using the uncorrected static plastic moment. Parkes noted that agreement was poor with respect to the deformation near the struck point. The test specimens had a rather different shape near the struck point than that predicted, and the zone of appreciable

curvature extended farther from the tip. However Parkes concluded that the comparison between measured and predicted angles near the root of the beam showed that a rigid-perfectly plastic analysis can give satisfactory predictions of deformations away from the point of impact, "provided due allowance is made for rate of strain effects". In making the correction for the dynamic plastic moment a result from the experiments was used, but Parkes indicated his belief that "a sufficiently accurate estimate of rate of strain could be made without much difficulty", which would suffice for practical purposes because of the insensitivity of the deformations to changes in the rate of strain.

It should be mentioned here that the computed results shown in Table III 3 and Figs. III 6 and III 7 were obtained by independent calculations from the data in Parkes' paper and that of Manjoine. Comparisons in these forms were not made in Parkes' paper which gives curves showing the theoretically predicted angle (after making the correction for strain rate influence) as function of 1/L. In the present comparisons we have used the general formula Equation (2.10) whereas Parkes used the following formula derived from (2.10) as the limiting case for very large β:

$$\theta_L = \frac{2G^2V_o^2}{3mL} \tag{2.17}$$

This gives a value of θ_L about fourteen percent too large, as compared with the result from the general formula (2.10) for the shortest beams hit by light strikers, and accounts for some of the difference in appearance of the comparisons shown in Figs. III 6 and III 7 and in Parkes' paper. Appreciable differences in the strain rate were found in some cases, but these led to insignificant differences in the dynamic plastic moment ratio.

It should also be stated here that subsequent tests by Bodner and Symonds (1962) indicate that Parkes' method of introducing the strain rate correction is satisfactory for heavy strikers, but leads to gross errors when

applied to strikers of moderate or small weight compared to the specimen weight. This conclusion was reached as a result of tests using the same basic beam-mass model, but performed in such a way that the conditions of the analytical model were approached more closely than in Parkes' experiments using lead bullets fired against the specimen tip. Before describing these tests and a theoretical treatment incorporating strain rate dependence of the plastic moment, we first complete our summary of Parkes' tests.

(C) Fixed-ended Beam

Parkes' analysis and tests with fixed-ended beams were described in two subsequent papers: the first reporting tests on steel beams (Parkes, 1956), and the second reporting tests on beams of duralumin and brass (Parkes, 1958).

The elementary rigid-plastic analysis (consideration of bending without strain hardening or rate sensitivity) can be carried through almost as easily as for the cantilever beam. The diagrams of Fig. III 3 apply in the first phase, when there are two hinge points H and H' moving out from the struck point O as shown in Fig III 9. Regions ahead of the hinge point are at the limit moment M_p. As indicated in Fig. III 9, the second phase involves one traveling hinge H' and a fixed hinge at end B. The third phase involves fixed hinges at A and B. In the first two phases the motion is defined by two kinematic quantities, for example the length z and the angular velocity ω of the segment OH'. Thus the motion in these phases can be obtained from equations of conservation of linear and angular momentum, with appropriate continuity equations. The third phase has one degree of freedom and the additional displacements are easily found either by angular momentum or work-energy equations. The momentum equations will be omitted. Solving them, the velocity V of the striking mass and hinge position z are given in implicit form by the following equations:

First phase

$$\frac{(V_o - V)^2}{V} = \frac{12M_p mt}{G^2} \tag{2.18a}$$

$$\frac{mz^2}{G+mz} = \frac{12M_p t}{GV_o} \tag{2.18b}$$

Second phase

$$V(G + \tfrac{1}{3}mL_2 + \tfrac{1}{2}mz + \tfrac{1}{6}\frac{m}{L_2}z^2) = GV_o \tag{2.19a}$$

$$mz^2V = 12M_p t \tag{2.19b}$$

Third phase

$$V = V_2 - \frac{2M_p}{G + \frac{1}{3}mL_1 + \frac{1}{3}mL_2}(\frac{1}{L_1} + \frac{1}{L_2})\,t \tag{2.20}$$

where V_2 is the velocity at the struck point at the end of the second phase. From Equation (2.19a), putting $z = L_1$, we obtain

$$V_2(1 + \frac{mL_2}{3G} + \frac{mL_1}{2G} + \frac{mL_1^2}{6L_2G}) = V_o \tag{2.21}$$

The integration to obtain final displacements is elementary, but in the case of the second phase quite lengthy. Complete formulas are given in Parkes' 1958 paper. The final displacement y_f at the struck point is given by the following formula:

$$\frac{2M_p}{GV_o^2 L_2}\, y_f = \frac{1}{12}\left[\frac{\beta}{(1+\beta)^2} + \frac{2}{\beta}\ln(1+\beta) - \frac{2}{1+\beta}\right]$$

$$- \frac{36}{\beta} K^3 \left[\phi + \sin 2\phi + \frac{1}{4}\sin 4\phi + \left(\frac{1}{3K} - 3K\right)\cos^4\phi\right]_{\phi=\tan^{-1}5K}^{\phi=\tan^{-1}K(3+2r)}$$

$$+ \frac{r\left(1 + \frac{1}{3}\beta + \frac{1}{3}\beta r\right)}{2(1+r)\left[1 + \frac{1}{3}\beta + \frac{1}{2}\beta r + \frac{1}{6}\beta r^2\right]^2} \qquad (2.22)$$

where

$$\beta = \frac{mL_2}{G}, \qquad r = \frac{L_1}{L_2}, \text{ and } \qquad K^2 = \frac{\beta/24}{1 - \beta/24}$$

The three terms correspond in order to the contributions of the three phases.

Parkes conducted experiments on beams of mild steel, duralumin, and brass, using square specimens of nominal dimensions 1/4 in. by 1/4 in. In the tests the length L_2 was held constant at L_2 = 1.0 in. or 2.0 in., and L_1 given values $L_1 = L_2$, $2L_2$, and $5L_2$. Two series were carried out, using heavy strikers and small velocities in one, and relatively very light strikers (bullets) at high velocities in the other. The experiments using bullets produced highly localized deformation near the point of striking, while those using heavy weights resulted in deformed shapes very closely linear between the struck point and the supports.

The experiments with lead bullets as strikers appear to correspond poorly to the theoretical model of a beam with attached mass. The bullet sprays out and exerts a force rather like that of a jet of fluid, with a duration of the order of $0.2/12 \times 1500 \doteq 10^{-5}$ sec. for a lead bullet of 0.005 lb. weight and 1500 ft/sec. velocity. The theoretical rigid-plastic model predicts a deformation time (considering only the first phase) of about

10^{-3} sec. Clearly the experimental situation has little to do with the problem treated theoretically, of a rigid mass striking and sticking to a beam. Although the impulse is equal to the momentum of the striking bullet, the "attached mass" is essentially the mass of the segment of beam struck by the bullet. Because of these difficulties no further discussion will be given of the experiments with bullet strikers.

The same difficulties pertain to Parkes's experiments with cantilevers, already described. For these we have outlined the test results and shown Parkes's strain-rate correction (Figs. III 6, 7). We have noted, however, that Parkes's results and conclusions for specimens with small tip mass (large β) differ importantly from those of Bodner and Symonds. The reasons for these differences will appear when the latter tests are discussed in detail.

Parkes's solution (2.22) is cumbersome to work with, but fortunately a much simpler form of solution is available, which has satisfactory accuracy in the range concerned in the tests using heavy strikers. This is an approximate solution, but in view of the approximations in any rigid-plastic analysis the further degree of approximation is acceptable in many cases. The simpler solution is obtained by assuming that the entire deformation occurs in a single mode of deformation. Such an approach is suggested by the fact that in the final deformed shape the beam segments between the ends and the struck point are essentially straight. A "mode approximation" solution is obtained by assuming that all motion occurs in a deformation having this shape, as indicated in Fig. III 10, so that motion with one degree of freedom is considered and a single quantity such as the deflection y^* of the struck point of the angle of rotation θ^* defines the motion. The equation of motion in this pattern can be found, for example by virtual work, taking the external forces as zero in the present problem of

impulsive loading:

$$-\dot{V}^*(G + \frac{1}{3}mL) = 2M_p(\frac{1}{L_1} + \frac{1}{L_2}) \tag{2.23}$$

where $V^* = \dot{y}^*$ is the velocity of the mass at any time t, in the assumed mode shape with plastic hinges at the two ends and at the struck point. The above is readily integrated to obtain the velocity and displacement at any time, assuming the initial displacement is zero and the initial velocity V_o^* in the assumed mode shape is known. To find V_o^*, suppose that in a small initial period t there are surface pressures p(x) per unit length applied to the beam and a force P applied to the mass G. These are taken to correspond to the actual initial velocities, specified in the problem:

$$\lim_{\tau \to 0} \int_o^\tau p\,dt = mv_o(x); \qquad \lim_{\tau \to} \int_o^\tau P\,dt = GV_o \tag{2.24}$$

The integral of (2.23) in the interval $0 < t \leq \tau$ is

$$-(G + \frac{mL}{3}) \int_o^t \dot{V}^* dt + \int_o^t P\,dt + \frac{1}{L_1} \int_o^{L_1} x_1 dx_1 \int_o^t p(x_1)dt$$

$$+ \frac{1}{L_2} \int_o^{L_2} x_2 dx_2 \int_o^t p(x_2)dt = 2M_p(\frac{1}{L_1} + \frac{1}{L_2})^t \tag{2.25}$$

Hence, setting $t = \tau$ and considering τ very small, we have after using Equation (2.24), and taking the initial velocity $v_o(x) = 0$ in the present problem, we obtain

$$V_o^* = \frac{GV_o}{G + \frac{1}{3}mL} \tag{2.26}$$

It may be noted in passing that the procedure used above may be

derived from a different viewpoint, according to which for any chosen mode shape the "best" initial velocity is that which minimizes the kinetic energy of the structure corresponding to the difference in velocity between the assumed mode shape and the actual prescribed initial velocity. The general philosophy of "mode solution" approximations has been discussed with several examples by Martin and Symonds (1966). In general it gives excellent results by comparison with complete rigid-plastic solutions for problems in which one pattern of deformations predominates, but even when this is not the case it may give results of practical value. Moreover it lends itself to including effects of strain rate sensitivity and work hardening (Symonds, 1965). The main advantage is the simplicity of method and calculations, as compared either with the elementary rigid-plastic theory, or with one taking account of strain rate, strain hardening, or other complicating effects.

Using the result (2.26) for the initial velocity, the solution of the present problem is immediately obtained by integration as follows:

$$V^* = \frac{V_o}{1 + \frac{mL}{3G}} - \frac{2M_p Lt}{GL_1L_2(1 + \frac{mL}{3G})} \tag{2.27a}$$

$$y_f^* = \frac{GV_o^2}{2M_p} \frac{L_1L_2}{2L(1 + \frac{mL}{3G})} \tag{2.27b}$$

$$t_f^* = \frac{GV_oL_1L_2}{2M_pL} \tag{2.27c}$$

To illustrate the accuracy possible from the simple solution, we give below the results for the final displacement y_f^* from (2.27b) and those from Parkes' solution (2.22) for two cases used in Parkes' tests. The following data relate to tests on mild steel beams with heavy strikers:

	Parkes's solution y_f Equation (2.22)				Mode Approx. y_f^* Equation (2.27b)
	First phase	Second phase	Third phase	Total	
gG = 16 lb V_o = 9.7 ft/sec	0.00039	0.0090	0.405	0.414	0.408
gG = 4 lb V_o = 19.4 ft/sec	0.00156	0.342	0.374	0.408	0.405

The curves plotted in Fig. III 11(a-d) are from calculations using Equation (2.27b). Parkes did not give results computed from his rigid-plastic solution before applying his correction for strain rate sensitivity, but judging from the example above, the curves derived from the mode approximation solution are very close to those from the full solution.

(D) Discussion: Table III 5 summarizes the test and analytical results. In Fig. III 11 (a)-(d), the test results and calculated deflections from Equations (2.27) are shown graphically in dimensional form. The deflection at the struck point is plotted as a function of the ratio $r = L_1/L_2$, the length L_2 being constant in each test series at either 1 in. or 2 in. The deflection according to the elementary rigid-plastic theory exceeds the measured deflection by a factor of approximately 1.8 in the case of mild steel, of approximately 1.3 in the case of brass, and of about 1.25 in that of duralumin. Fig. III 12 shows plots of the ratio of the test deflections to those of the simple theory, the over-estimates of the theory being indicated by the fact that the ratios of experimental to predicted values lie in the ranges 0.44 to 0.62 for

TABLE III 5

(A)Mild Steel: Parkes's Tests on Built-in Beams

M_p = 228 in-lb; Width b = 0.26 in.; Depth h = 0.253 in.

(1) L_2 in.	(2) L_1 in.	(3) $r=\frac{L_1}{L_2}$	(4) Gg lb.	(5) V_o ft/sec	(6) $\frac{GV_o^2}{2M_p}$	(7) $R=\frac{GV_o^2}{2M_p}(\frac{2EI}{M_pL})$	(8) y_f^* in.	(9) $(y_f)_{exp}$ in.	(10) $\frac{(y_f)_{exp}}{y_f^*}$	(11) $\bar{\epsilon}$ sec^{-1}	(12) $\frac{M'_p}{M_p}$	(13) $y'_f=\frac{M_p}{M'_p}y_f^*$	(14) $\frac{(y_f)_{exp}}{y'_f}$	(15) A_o	(16) $y''_f/y_f^*=(1+A_o)^{-1}$	(17) y''_f in.	(18) $\frac{(y_f)_{exp}}{y''_f}$
1	0.5	0.5	16	9.7	1.23	76	0.205			44	2.1	0.098		0.854	0.540	0.111	
"	1	1	"	"	"	57	0.308	0.13	0.43	29	2.0	0.154	0.84	0.780	0.561	0.173	0.75
"	2	2	"	"	"	38	0.410	0.20	0.49	22	1.9	0.216	0.93	0.741	0.574	0.235	0.85
"	4	4	"	"	"	23	0.491			18	1.9	0.258		0.738	0.576	0.282	
"	5	5	"	"	"	19	0.512	0.27	0.52	17	1.9	0.270	1.00	0.739	0.576	0.294	0.92
"	6	6	"	"	"	16	0.525			17	1.9	0.276		0.743	0.574	0.302	
1	0.5	0.5	4	19.4	1.23	76	0.205			87	2.2	0.093		0.980	0.505	0.107	
"	1	1	"	"	"	57	0.307	0.13	0.43	58	2.1	0.146	0.89	0.895	0.528	0.162	0.80
"	2	2	"	"	"	38	0.408	0.19	0.47	44	2.1	0.195	0.98	0.851	0.540	0.220	0.86
"	4	4	"	"	"	23	0.488			36	2.0	0.244		0.848	0.541	0.264	
"	5	5	"	"	"	19	0.510	0.25	0.50	35	2.0	0.255	0.98	0.850	0.540	0.275	0.91
"	6	6	"	"	"	16	0.521			34	2.0	0.260		0.854	0.539	0.280	
2	1	0.5	16	9.7	1.23	38	0.410			22	1.9	0.216		0.742	0.574	0.235	
"	2	1	"	"	"	29	0.615	0.35	0.57	15	1.9	0.324	1.08	0.675	0.597	0.368	0.95
"	4	2	"	"	"	19	0.818	0.53	0.65	11	1.8	0.454	1.17	0.646	0.608	0.497	1.07
"	8	4	"	"	"	11	0.980			9	1.8	0.545		0.644	0.608	0.596	
"	10	5	"	"	"	9.5	1.020	0.62	0.61	9	1.8	0.567	1.09	0.645	0.608	0.621	1.00
"	12	6	"	"	"	8.2	1.050			8.5	1.8	0.584		0.648	0.608	0.639	
2	1	0.5	4	19.4	1.23	38	0.410			44	2.1	0.195		0.854	0.540	0.221	
"	2	1	"	"	"	29	0.615	0.33	0.54	29	2.0	0.308	1.07	0.775	0.564	0.344	0.96
"	4	2	"	"	"	19	0.812	0.46	0.57	22	1.9	0.428	1.07	0.743	0.574	0.465	0.99
"	8	4	"	"	"	11	0.970			18	1.9	0.510		0.740	0.575	0.557	
"	10	5	"	"	"	9.5	1.006	0.55	0.54	17	1.9	0.530	1.04	0.741	0.575	0.578	0.95
"	12	6	"	"	"	8.2	1.032			17	1.9	0.544		0.745	0.574	0.593	

TABLE III 5 (continued)

PARKES'S TESTS ON BUILT-IN BEAMS

(B) Brass M_p = 228 in-lb; Width b = 0.260 in, Depth h = 0.253 in.

(1) L_2 in.	(2) L_1 in.	(3) $r = \frac{L_1}{L_2}$	(4) G lb.	(5) V_o Ft/sec	(6) $\frac{GV_o^2}{2M_p}$	(7) $R = \frac{GV_o^2}{2M_p}\left(\frac{2EI}{M_p L}\right)$	(8) y_f^* in.	(9) $(y_f)_{exp}$ in.	(10) $\frac{(y_f)_{exp}}{y_f^*}$	(11) $\dot{\bar{\epsilon}}$ sec^{-1}	(12) $\frac{M}{M_p}$	(13) $y_f' = y_f^*(M_p/M_p')$	(14) $\frac{(y_f)_{exp}}{y_f'}$	(15) A_o	(16) $\frac{y_f''}{y_f^*} = (1+A_o)^{-1}$	(17) y_f'' in.	(18) $\frac{(y_f)_{exp}}{y_f''}$
2	1	0.5	4	19.4	1.23	18	0.407			44	1.5	.272					
"	2	1	"	"	"	13	0.611	0.46	0.753	29	1.5	.408	1.13				
"	4	2	"	"	"	9	0.811	0.61	0.753	22	1.5	.541	1.13				
"	8	4	"	"	"	5	0.967			18	1.5	.645					
"	10	5	"	"	"	4.5	1.003	0.72	0.717	17	1.4	.716	1.00				
"	12	6	"	"	"	3.8	1.030			17	1.4	.735					

(C) "DURALUMIN" M_p = 256 in-lb, Width b = 0.260 in, Depth h = 0.253 in.

2	1	0.5	4	19.4	1.10	13	0.365			44	1.3	.281					
"	2	1	"	"	"	10	0.548	0.45	0.821	29	1.3	.421	1.07				
"	4	2	"	"	"	6	0.729	0.60	0.820	22	1.3	.560	1.07				
"	8	4	"	"	"	3.8	0.873			18	1.2	.671					
"	10	5	"	"	"	3.2	0.905	0.69	0.764	17	1.2	.755	0.91				
"	12	6	"	"	"	2.7	0.934			17	1.2	.779					

steel, 0.75 to 0.71 for brass, and 0.82 to 0.77 for duralumin.

The discrepancies between theory and experiment shown in Figs. III 11 and III 12 were attributed by Parkes to strain rate sensitivity, as in the cantilever beam tests of mild steel already discussed. It is not possible to examine these data as done in Fig. III 8 for the cantilever tests, to indicate for or against strain hardening as an alternative explanation of the discrepancies. The tests on fixed-ended beams were not performed in pairs as was done for the cantilever beam tests, with change of only the striking velocity and hence of the deformation magnitude.

The tests on mild steel beams (unfortunately not those on brass and duralumin specimens) were, however, made in pairs, such that in each pair of tests the incident energy $\frac{1}{2} GV_o^2$ was constant. The velocity was changed from 9.7 ft/sec to 19.4 ft/sec and the striking mass from 16 lb to 4 lb in each pair. The results for the ratio of measured test deflection to that calculated from elementary theory are shown in Fig. III 13, plotting against test velocity V_o. In the figure the relevant values of the energy ratio R are given, R being the ratio of incident energy to the maximum elastic strain energy

$$R = \frac{GV_o^2}{2} \frac{M_p^2 L}{2EI} = \frac{GV_o^2}{2M_p} \left(\frac{2EI}{M_p L}\right). \qquad (2.28)$$

Clearly the value of R is the same for each pair of tests.

The summary of results shown in Fig. III 13 provides some slight evidence that the discrepancy between the estimated deflection from elementary rigid-plastic theory is due to strain rate sensitivity, since there is a consistent decrease of the ratio $(y_f)_{exp}/y_f^*$ as the velocity increases. This would correspond to an increase in plastic moment at higher strain rates. There is also a consistent reduction in the degree of dependence on velocity as the

energy ratio R is increased, so that when R is about 10 there is a rather strong dependence on velocity, while at R = 57 the change with velocity is negligible. There is also a quite consistent decrease of $(y_f)_{exp}/y_f^*$ as R increases. Both these apparent dependences on R are coincidental; as R increases so does the strain rate, which seems to play the leading role. This will next be examined.

Parkes attributed the discrepancy between test deflections and elementary rigid-plastic theory wholly to the increases of yield stress with strain rate, just as in the cantilever beam tests on mild steel. He showed that remarkable agreement between measured and calculated deflection could again be achieved by the simple correction method already described for his cantilever beam tests, i.e. by replacing the static plastic moment M_p by a dynamic value M, the ratio M/M_p as a function of strain rate being derived from test results for the ratio σ/σ_c of dynamic yield stress to static yield stress as a function of strain rate. The dynamic tension test results for mild steel, already cited, of Manjoine (1943) were used for the present mild steel tests (see Fig. III 14). No data exist for duralumin and brass as complete as a Manjoine's for steel. Parkes constructed a curve for duralumin from test data of Klinger (1950) for the range of strain rate 0.01 to 1 sec $^{-1}$, of Evans (1942) for the range .01 to 10 sec^{-1}, and of Whiffin (1948) for a strain rate of about 15,000 sec^{-1}. The curve shown in Figure III 15 is the one given by Parkes for the dynamic bending moment ratio of duralumin. For brass there is even less information, but Parkes nevertheless drew the curve shown in Figure III 15, which is based on results of Jones and Moore (1940) for the strain rate range 0.1 to 10 sec^{-1}, which "suggest that the strain rate sensitivity of brass is about half that of steel."

The curves of Fig. III 15 are essentially guesswork. Moreover, their applicability to the analysis of Parkes' data is obviously questionable; the variability of strain rate sensitivity with constitution and condition of the metal

is well known (see Chapter I). Nevertheless, the use of such curves to estimate the correction due to strain rate sensitivity is of interest, if only to show the order of magnitude of strain rate sensitivity required to account for the discrepancy between test results and elementary theory.

As for the cantilever tests, Parkes' strain rate correction for the fixed-ended beams was made by estimating the strain rate in each test, and obtaining the ratio of dynamic to static plastic moment from the appropriate curve of Figures III 14, III 15. In order to estimate strain rate from velocities, the average hinge length was assumed known. This was stated as "about $\frac{1}{2}$ in. in all tests". Since the beam depth h was $\frac{1}{4}$ in. in all tests, the ratio z/h of average hinge length to beam depth was thus taken as 2. Strain rates may be estimated from the pattern of velocities in the mechanism of Figure III 10 as follows. Consider the angular velocity across the hinge at the struck point to be $\omega_1 + \omega_2$. The rate of curvature here is $(\omega_1 + \omega_2)/z$, and the rate of strain is $h(\omega_1 + \omega_2)/2z$. The average rate of strain during the deformation can be estimated as half the initial value. By writing $\omega_1 = V_o/L_1$, $\omega_2 = V_o/L_2$, the result obtained for the average strain rate is

$$\bar{\dot{\varepsilon}} = \frac{hV_o}{4z}\left(\frac{1}{L_1} + \frac{1}{L_2}\right) = \frac{hV_o}{4z}\,\frac{L}{L_1 L_2} = \frac{hV_o}{4z}\,\frac{1+r}{rL_2}\,. \qquad (2.29)$$

This is taken as an adequate estimate of the average strain rate in all three hinges. (It is the exact formula for the mean strain rate in the three hinges if the hinge lengths at the end sections are both assumed to be z/2.) The strain rates listed in Column 11 in Table III 5 are those computed by the above Column 12 of the same table were obtained by use of the curves in Figures III 14 and III 15.

The strain-rate corrected deflection, and ratio of deflection measured in the tests to the corrected magnitude are shown in Columns 13 and 14 of Table III 5. The corrected deflection curves as function of the length ratio L_1/L_2 are

plotted as dashed lines in Figs. III 11 (a)-(d). The ratio of test deflection to the strain-rate corrected rigid-plastic deflection is shown in Fig. III 16.

Agreement is seen to be very good. Considering the uncertainty of information about the strain rate sensitivity of the materials--brass and duralumin, in particular--the agreement is remarkable. Whether or not the agreement is significant is much less clear.

The good agreement in any such comparison could obviously be accidental. The elementary rigid-plastic solution (without rate effect) could be badly in error, and the strain rate correction--obviously approximate in any case--might also be erroneous, but by accident happen to just balance the other errors.

The possibility that the elementary rigid-plastic solution is grossly in error is hardly negligible. This analysis omits at least four physical phenomena which tend to reduce the deflection, i.e. lead to an over-estimate such as shown in Figs. III 11 and III 12. These are: elastic vibrations; work hardening; strengthening due to axial constraints; and load reduction due to the finite size of the striking mass. It is entirely possible that these effects together would lead to a reduction in deflection of the observed magnitude, and that the attribution of the discrepancy wholly to strain rate effects is quite incorrect.

Of the four effects listed, probably the most important in the tests on built-in beams is the effect of axial constraints. Work hardening might be important for steel, but not for the brass and duralumin beams; for the tests on these materials the plastic bending moment was chosen as the ultimate moment, rather than that computed from the yield moment (see Fig. III 17). This choice should more than compensate for work hardening. It is not certain that elastic vibrations play a negligible part. In the tests on steel beams the ratio of incident energy to maximum elastic strain energy was greater than 8 in all cases,

while in those on brass and duralumin the smallest value was 3 or 5. Figure III 12, plotting the ratio of test deflection to that of elementary theory, shows little variation of this ratio with L_1/L_2; if elastic vibrations were important, one would expect a much better agreement with theory as L_1/L_2 is decreased from 5 (R = 3) to 1 (R = 10), in the duralumin tests; but the improvement is seen to be only about 6 percent. However, the end supports, which maintained fixed angles at the beam ends, must have been massive, and may have introduced a constraint effect of appreciable magnitude. If the ends had been fully constrained so that no approach was permitted, the nature of the deformation would have been drastically altered in that bending action would have become replaced by membrane response, at the test deflections which reached two or three multiples of the beam depth. This implies a large stiffening effect, so that the deflections are a small fraction of those predicted by a theory considering bending only (see Symonds and Mentel (1958)and Nonaka (1964)).

It is difficult to feel confidence in Parkes's strain rate correction for brass and duralumin specimens because the small amount of test data in direct tension or compression shows a very small rate dependence for both metals up to a strain rate of about 10 sec^{-1}. Evans' (1942) studies included tests on mild steel, duralumin, and brass, giving curves of yield point stress and tensile strength for the three metals as functions of strain rate (Fig. III 18). In view of Parkes's use of ultimate moment values for his calculations, the dependence of tensile strength should be of particular interest. For the whole range of Evans's tests from strain rate 0.01 to 10 sec^{-1} the results for brass and duralumin show a negligible change in the tensile strength. (There seems in fact to be a slight decrease at $\dot{\varepsilon}$ about 20 sec^{-1} compared to the value at $\dot{\varepsilon}$ about 0.01, for both metals.) These results are not compatible with the strain rate corrections of 20 to 30 percent applied by Parkes, at average strain rates of

the order of 20. Only Whiffin's (1948) tests (as much higher strain rates) showed a large strain rate sensitivity for duralumin; for example, specimens with 0.2 percent static proof stress 43,000 psi were found to have dynamic yeild strengths averaging about 69,000 psi (with scatter ranging from about 60,000 psi to about 76,000 psi). These results were found from tests in which cylindrical specimens of the test metal were fired at armor steel blocks, at velocities ranging from about 600 ft/sec to about 3100 ft/sec. The analysis for the dynamic yield strength was made using the method of G. I. Taylor (1948). The computed values of the strain rates (of the order of 10^4 sec^{-1}) and dynamic yield strengths obviously depend strongly on the interpretation of the tests through an analysis that is by no means exact, and in fact demands ad hoc assumptions that affect the computed results and have no independent confirmation.

Parkes's tests on cantilevers and fixed-ended beams can be interpreted as showing that small beam specimens of mild steel, duralumin, and brass behave in impact tests as if the dynamic plastic bending moment is larger than the static value by substantial amounts, the increase ranging from about ? for mild steel to 1.2 or 1.3 for duralumin and brass. His tests appear to show also that the analysis of rigid-plastic type can be carried out as if the material were perfectly plastic, but characterized by a dynamic rather than static plastic moment, whose value can be estimated with sufficient accuracy from results given by the simple rigid-plastic treatment. This conclusion is not confirmed by tests to be described next by Bodner and Symonds, which showed instead that a correction of the elementary rigid-plastic analysis by simply correcting the plastic moment could be grossly in error in certain cases. The effect of strain rate sensitivity is in these cases to change the pattern of deformations, as well as to increase the plastic moment.

3. Bodner and Symonds's Experiments.

Experiments of Bodner and Symonds (1960, 1962) were of two kinds, termed "impulsive" and "impact", respectively. The former type made use of the same basic theoretical model as that of Parkes's (1955) tests on cantilevers, Fig. III 4. The main difference was that the tip mass was bolted to the cantilever, and was set in motion by applying an impulsive load directly to it. This was done either by detonating a small explosive charge on the tip mass, or by firing a bullet which entered and remained embedded in it. This load caused the tip mass to acquire velocity V_o in a time short compared with the time of deformation; this velocity is taken as the initial velocity in the theoretical model, analogous to the striking velocity of the falling mass in Parkes's experiments. In the second or "impact" type of test described by Bodner and Symonds, the cantilever beam specimen again carried a mass bolted at its tip, but the base of the cantilever was given a shock such that its velocity was changed in a time short compared to the time of deformation.

Since the impulse type experiments are close to those of Parkes on cantilevers, and lead to rather different conclusions, they will be described first.

(A) Impulse Tests

In Table III 6 are listed the basic conditions of Bodner and Symonds's "impulse" tests, which may be compared with those listed for Parkes's tests in Table III 2.

These tests were designed to differ from Parkes in two major respects. First, the attached mass, bolted to the beam, was an integral part of the beam. This should have eliminated uncertainties in Parkes's tests due to movement of the striking mass relative to the beam, and avoided the obvious difficulties in his tests with lead bullet strikers. Secondly, the tip masses were chosen so that the

TABLE III 6

Impulse Test Conditions: Cantilever Beams with Tip Mass, Tests of Bodner and Symonds (1960, 1962)

(1) Bullet fired into tip mass.

Length: L = 14.0 in. (mild steel specimens)
L = 6.0 in., 8.625 in. (6061-T6 aluminum alloy)

Cross-sections: depth h = 0.177 in., width b = 0.634 in. -0.695 in. (mild steel specimens)
depth h = 0.255 in., width b = 0.775 in. -0.795 in. (6061-T6 aluminum alloy)

Weight of tip mass: 0.68 lb. to 1.47 lb. (mild Steel)
0.29 lb. to 0.385 lb. (6061-T6)

Beam strength properties:

Mild steel: σ_o = 29.0 ksi, $M_p \doteq$ 146 in-lb

6061-T6 aluminum alloy: σ_o = 38.0 ksi, $M_p \doteq$ 485 in-lb

NOTE: High velocity (4000 fps) steel bullets were used, which remained embedded in the tip mass.

(2) Explosive charge detonated on tip mass.

Length: L = 4.35 in. (mild steel specimens)
L = 2.97 in., 4.34 in., 5.95 in., 7.65 in. (6061-T6 aluminum alloy)

Cross-sections: depth h = 0.053 in., width b = 0.312 in. (mild steel specimens)
depth h = 0.053 in. -0.119 in., width b = 0.210 in. -0.312 in. (6061-T6 aluminum alloy)

Weight of tip mass: 0.0115 lb. -0.0232 lb. (mild steel)
0.0056 lb. -0.0154 lb. (6061-T6 aluminum alloy)

Beam strength properties:

Mild steel: σ_o = 44.0 ksi, M_p = 9.62 in-lb

6061-T6 aluminum alloy: σ_o = 43.0 ksi, M_p = 9.42 in-lb -47.5 in-lb

NOTE: Lead azide charges in plastic cylinders were detonated in direct contact with tip mass.

mass ratio parameter $\beta = mL/2G$ had values through the range from about 0.15 to about 1.0, so that the variation of results with β could be studied. By contrast, in Parkes's cantilever tests the values of β for the heavy strikers lay in a small range from about 0.005 to 0.10, and his tests using light strikers (lead bullets) had much larger β values, roughly 4 to 26. The range of β in Parkes's heavy-striker tests is such that in all cases more than 90 percent of the initial kinetic energy is absorbed in the base hinge, according to the elementary rigid-plastic analysis. Hence these tests are not suitable for studying phenomena associated with changes of the pattern of deformation. The tests with his light strikers would have given a useful contrast with the heavy-striker tests, since for these tests less than 10 percent of the energy goes into plastic work at the base hinge. However, the significance of these tests with lead bullets must be considered doubtful, as already pointed out. In the Bodner-Symonds tests a substantial change of plastic work distribution, from over 80 percent in the base hinge to about 45 percent, was achieved without significant change in the testing technique.

In these tests, the determination of initial velocity was made by measurement of the applied impulse. In the tests where explosive charges were used, the impulse of a measured quantity of lead azide charge was held in a plastic container which disintegrated in the explosion. Care was taken that the geometry in the calibration test was closely similar to that in the test on the specimen beam. Good reproducibility of impulse was obtained for a given size of charge. In the tests using bullets fired into the tip mass the impulse was obtained from the measurement of the bullet speed by high speed photography. Again, good reproducibility of impulse was obtained for a given bullet charge. In both types of test, impulses could be reproduced with a variation of two percent or less.

A disadvantage in the tests using explosive charges, as compared with Parkes' tests, was that the magnitude of the impulse could not easily be changed by large amounts. Therefore, as shown in Table III 7(a) (mild steel) and III 7(b) (6061-T6 aluminum alloy), these tests were performed with only two magnitudes of applied impulse. The desired range of deformation angles was obtained by changing tip mass and (in the 6061-T6 tests) the beam dimensions.

The results are compared first with the prediction of the elementary rigid-plastic theory. Curves labelled A in Figures III 19(a) and 19(b) show the experimental final rotation angle near the base divided by the angle predicted by elementary rigid-plastic analysis, Equation 2.10. The results for mild steel may be compared with those of Parkes in Figs. III 6.

In plotted results from Bodner and Symonds's tests a trend appears for both mild steel and aluminum alloy 6061-T6, that is missing from Parkes's cantilever test results. This is a trend toward better agreement with tests and elementary theory as the ratio β increases, so that for $\beta \approx 0.7$ the test angle is approximately equal to the predicted magnitude, while at $\beta \approx 0.15$ the test angle is substantially less than the predicted angle--the ratio being about 0.65 for mild steel, 0.80 for 6061-T6. Thus only at the smallest β values (heaviest tip masses) is the reduction in angle of rotation as large as that found by Parkes. AT the largest β values in the Bodner-Symonds tests the final angle measured in the tests on mild steel beams was appreciably larger than the theoretical value. In other words, the elementary theory with static plastic magnitudes predicts a smaller angular deformation than that actually experienced by the specimen beam, despite the rate sensitivity of the material.

Parkes' tests at large β values fail to show the trend with β noted above; however, these tests used lead bullet strikers directly on the beam, and their validity is questionable. As already pointed out, it seems unreasonable to apply the simple analytical model with fixed end mass to these tests; and apart

TABLE III 7 (a)

Bodner and Symonds' Impulse Test: Mild Steel
Results:
Tests E: bullet fired into tip mass; Tests F: explosive charges.
Tip mass weights E1, E2: 1.46 lb; E3-E7: 0.74 lb; F1-F7: 0.023 lb; F8-F10: 0.0115 lb

	TEST DATA							QUANTITIES AVERAGED FOR EACH GROUP OF SPECIMENS								
	L in.	h in.	b in.	$\beta = \frac{1}{2K}$	I lb-sec	R	θ_{exp} degs.	θ_{exp} avg.	V_o in/sec	β avg.	θ_{rp} elem. rigid-plastic	$\theta_{vp}^{(1)}$ "complete" v-p	$\theta_{vp}^{(2)}$ Ting v-p "1st soln"	θ^*_{vp} Ting appr. formula	θ''_{rp} Parkes corr.	$\bar{\dot{\varepsilon}}$ sec^{-1}	$\frac{M}{M_p}$
E1	14.0	.176	.637	.154	.975	8.5	28.0	26.0	258	0.155	41.2	33.0	33.2	32.4	27.4	1.00	1.50
E2	"	.177	.640	.155	"	8.4	24.0										
E3	"	.178	.695	.334	"	15.0	47.0	47.0	510	0.334	61.9						
E4	"	.177	.642	.309	"	16.4	53.0	52.5	510	0.306	69.0	57.8	59.1	56.7	43.1	1.75	1.56
E5	"	.177	.647	.304	"	16.4	52.0										
E6	"	.177	.634	.302	"	16.7	51.0										
E7	"	.177	.644	.307	"	16.6	54.0										
F1	4.34	.053	.312	.442	.0481	11.5	64.0	63.8	805	0.442	71.5	57.1	59.8	55.4	39.6	8.04	1.76
F2							64.0										
F3							62.5										
F4							63.3										
F5							64.2										
F6							65.0										
F7	"	"	"	"	.0301	4.5	26.8		504	0.442	27.9						
F8	"	"	"	.890	"	9.0	45.5	43.3	1010	0.890	40.7	37.0	40.8	35.0	22.6	7.70	1.76
F9					"		39.0										
F10					"		45.5										

TABLE III 7(b)

Bodner and Symonds Impulse Test Results: Aluminum alloy 6061-T6
Tests G: bullet fired into tip mass; Tests H: explosive charges

	L in.	h in.	b in.	β	I lb-sec	R	θ_{exp} deg.	θ_{exp} avg.	V_o in/sec	β avg.	θ_{rp} deg.	"complete" θ_{vp} deg.	Approx. θ^*_{vp} deg.	$\bar{\dot{\varepsilon}}$ sec^{-1}	$\frac{M}{M_p}$	θ'_{rp} Parkes corr.
G1	6.0	0.255	0.788	0.154	0.975	8.0	35.0	33.8	976	0.154	47.0	43.6	50.8	21	1.16	40.5
G2	"	"	0.784	0.153	"	"	32.5									
G3	8.63		0.795	0.294	"	8.6	49.0	50.5	1290	0.292	53.5	58.6	63.1	13	1.19	45.0
G4			0.775	0.290	"	"	52.0									
H1		0.079	0.208	0.156	0.0301	3.5	31.1	31.2	755	0.157	38.6		42.0	20	1.21	31.9
H2	"	"	"	"	"	"	29.9									
H3	"	"	0.212	0.159	"	"	32.7									
H4	4.34	0.053	0.312	0.306	"	3.2	57.5	57.6	1010	0.306	65.4		79.0	9	1.17	56.0
H5	"	"	"	"	"	"	59.0									
H6	"	"	"	"	"	"	58.0									
H7	"	"	"	"	"	"	55.3									
H8	"	"	"	"	"	"	57.0									
H9	"	0.119	"	0.687	0.0481	3.6	24.0	23.5	1610	0.687	24.0	27.4	31.2	31	1.23	19.5
H10	"	"	"	"	"	"	22.5									
H11	"	"	"	"	"	"	24.0									
H12	5.94	0.079	0.210	0.655	0.0301	"	46.1	48.8	1570	0.654	50.9		68.8	11	1.18	43.0
H13	"	"	0.209	0.652	"	"	51.5									
H14	7.65	"	0.211	1.115	"	3.7	50.9	50.7	2080	1.115	49.4		74.3	8.4	1.17	42.2
H15	"	"	"	"	"	"	49.5									
H16	"	"	"	"	"	"	51.6									

from the fact that the tip mass is certainly not the bullet mass (as assumed), the effective impulse may be much less than the bullet momentum because of local deformation.

An unfortunate feature of the Bodner-Symonds tests was their use of beams of different lengths and cross-sections, so that changing β involved changes in several variables rather than a change only of the tip mass. Also, as β and the impulse I were changed so was the deformation magnitude. Thus it is not possible to compare the experimental deflections with theoretical predictions at constant strain magnitudes. The final angles are shown in Figs. III 19 (as average values for each set of test results at nearly constant β). There seems to be no systematic dependence on the deformation magnitude, and the correlation of deformation magnitude with ratio of experimental angle to theoretical prediction is often opposite to what would be expected if strain hardening were playing an important role. For example, the mild steel tests at $\beta = 0.15$ with $\theta_{exp} \approx 26^{\circ}$ are in worse agreement than those at $\beta = 0.3$ with $\theta_{exp} \approx 52^{\circ}$; these particular sets of tests were both made with essentially the same beam dimensions and impulse, only a change of tip mass being made. If strain hardening were the principal cause either of the discrepancy between test results and rigid-plastic theory ($\theta_{exp}/\theta_{rp} < 1$), or of the trend of test results toward better agreement as β increases, the agreement should be best at the smallest rotation angle and become worse at larger angles. The comparison of rotation angles in Fig. III 19 (a) thus leads to the same conclusion as the similar comparison in Fig. III 8 for Parkes' cantilever tests, namely that strain hardening is not mainly responsible for the differences between deflections observed in tests and those predicted by elementary rigid-plastic theory. (The indications on this point from Parkes' tests are more complete and systematic.)

Since in the cantilever tests there are no constraints arising from finite deflections, and strain hardening seems to play a negligible role, the

discrepancies between results of tests and elementary theory may be presumed due either to neglect of elastic deformations, or to neglect of strain-rate sensitivity of the plastic moment, or to both combined. We shall consider here only attempts to explain these on the basis of strain-rate sensitivity. The tests were designed so that the ratio R of incident energy to maximum elastic strain energy was large; for the mild steel tests, R was greater than 8 for all but one case, while for 6061-T6 R was greater than 3 in all cases. The influence of elastic vibrations cannot be conclusively ruled out until more systematic tests concerning their influence are reported; however, other explanations must presumably be found for the discrepancies appearing in Figs. III 19, since most of these are opposite to what would be expected if elastic deformations were playing an important role.

Further corroboration of the above statements is given by impulse tests of Bodner and Speirs (1963) on aluminum alloy 3003-H14 in a cold worked condition (static yield stress σ_o = 20,300 psi at room temperature). Tests were made on beams of depth 0.079 in., width 0.30 in. (except for some at 0.50 in.), and lengths ranging from 2.15 in. to 8.01 in., at three temperatures: 70°F, 212°F, and 400°F). The results are shown in Fig. III 20. The dependence on β is very similar to that shown in Figs. III 19 for mild steel and 6061-T6. The evidence from deformation magnitudes also is comparable to that from the results shown in Figs. III 19; in particular, strain hardening appears unable to account for the observed discrepancies.

The role of strain rate sensitivity in these tests must therefore be examined critically. The simplest way to introduce a strain rate sensitivity in that of Parkes, as described above. The dynamic yield stress is supposed known as a function of strain rate, and from this the dynamic plastic bending moment for a rectangular beam section. For the impulse tests, the average strain rate according to the formula of Equation (2.16), from the elementary rigid-

plastic analysis, thus enables a dynamic yield moment to be computed for each test. Each test result may then be compared with the predicted deformation angle reduced by the ratio M_p/M'_p, where M'_p is the dynamic plastic moment.

As shown in Table III 7, the strain rates calculated in this way for the steel tests lie in the range 1 sec^{-1} to 8 sec^{-1}, while those for the 6061-T6 tests are somewhat larger, from 8 sec^{-1} to about 31 sec^{-1}. If the test deflection is divided by that predicted by elementary rigid-plastic theory multiplied by the ratio M_p/M'_p, the result is approximately unity for the points of largest tip mass (smallest magnitudes of β). However, at the largest values of β the ratio of test deflection to the modified rigid-plastic value reaches nearly 2 for the mild steel tests, and about 1.2 for the 6061-T6 tests.

The results for mild steel indicate that the simple strain rate correction suggested by Parkes is unsatisfactory in this problem. For 6061-T6 the results point toward the same conclusion, but less positively; the maximum discrepancy after correction is about the same as that before correction, but shifted to the region of largest β.

It is obvious that at least for a strongly rate-sensitive metal such as mild steel, putting rate sensitivity in the analysis of the impulse problem cannot be done by merely increasing the magnitude of the plastic moment so as to correspond with average strain rate magnitude, and using the new constant moment magnitude in the same rigid-plastic analysis applicable to a non-rate dependent material. The failure of this simple method in the present problem is apparently related to the change of deformation pattern. Use of a constant plastic bending moment implies that the distribution of work done in plastic straining remains unchanged when strain rate sensitivity is introduced. This distribution is governed by the mass ratio parameter β. However, as β is changed over the range considered in the Bodner-Symonds tests the experiments show that the discrepancy between theory and experiment changes drastically; at

low β values the elementary theory strongly overpredicts, while at β values approaching 1 it underpredicts. Such a large qualitative difference cannot be accounted for by strain rate sensitivity if the deformation pattern retains the same dependence on β, i.e. if the analytical model used for a constant plastic moment is assumed to apply as well to the case in which M_p depends on strain rates.

The strain rate dependence in the impulse problem must therefore evidently be taken into account by a method such that the pattern of deformation as well as its magnitude is modified by the strain rate sensitivity of the material. This will presumably be the case if the plastic moment is assumed to have a functional relation to the curvature rate (or strain rate, equivalently), and regarded as a function of position and time. The first analysis of this type was presented by Cowper and Symonds (1957). This was extended and improved by Ting and Symonds (1962) and by Ting (1963, 1964).

These "viscoplastic" analyses have been reasonably successful in predicting the feature observed experimentally in the impulse tests, of a deformation less than that of the elementary rigid-plastic at small β values, and larger for $\beta \geq 1$. Qualitatively, the explanation may be as follows. Large β values correspond to small tip masses, and therefore to high strain rates in the first phase of the elementary theory, which leads to continuous deformation. These high strain rates seem to stiffen the beam in this phase, so that less energy is absorbed in it. Hence more energy must be absorbed in the second phase, with deformation mainly near the base of the beam. In this way it is seen to be possible for the deformation at the base to be larger than that predicted by the elementary rate independent solution, despite the fact that rate sensitivity is a strengthening effect.

(B) Impact Tests

Reference has been made to experiments using the "impact test" model, defined as a cantilever beam with tip mass, whose base is given a rapid change in velocity. In one type of test the specimen beam is initially in motion with constant velocity, and deformation occurs when the base strikes a massive anvil. Such tests were described by Mentel (1958) and by Bodner and Symonds (1962). Alternatively, the beam may be initially stationary and the base subjected to impact so that it acquires a velocity in a short time. This method has the advantage of eliminating vibrations of the beam specimen that may be present just before impact. Tests were reported by Gillis and Lerner (1960) using this technique. Finally, a third method which is equivalent to the others for very short acceleration times is that which uses explosive or shock wave loading applied to a fixed-base cantilever, as by Bodner and Humphreys (1964).

We will review here briefly the main experimental results of Bodner and Symonds (1962) and Gillis and Lerner (1960), these being the most complete series. The test conditions of the two investigations are summarized in Table III 8(a) - (b). The results are summarized in Table III 9(a) - (b).

The elastic-plastic treatment of this problem was discussed by Alverson (1956, 1958) and by Stallybrass (1960). We are here primarily concerned with the rigid-plastic approach, since plastic deformations are assumed large.

The rigid-plastic solution was presented by Mentel (1958) and discussed also by Ting and Symonds (1962). We outline below the essential features of this solution, since it serves as a guide for the experiments as well as for the viscoplastic analysis.

The base velocity is assumed to be $V(t) = V_o[1-f(t)]$ where $f(t) = t/t_o$ for $t \leq t_o$, $f(t) = 1$ for $t \geq t_o$. V_o is the change of velocity of

TABLE III 8 (a)

Impact Test Conditions: Cantilever Beams with Tip Mass, Tests of Bodner and Symonds (1962)

Two cantilever specimens attached transversely to carriage, accelerated by HyGe machine, propelled along track to impact with heavy mass.

Specimens:	lengths	approx. 4.5 in., 2.0 in.
	width	0.312 in.
	depth	0.125 in. (mild steel)
		0.119 in., 0.125 in. (6061-T6 aluminum alloy)
Tip mass ratios:		0, 2.0, 4.2 (mild steel specimens)
		0, 1.8, 2.0, 6.1, 4.3, 12.9 (6061-T6 aluminum alloy specimens)
Beam strength properties:		
Mild steel:		σ_o = 30.0 ksi, M_p = 36.6 in.-lb.
		σ_o = 44.0 ksi, M_p = 53.6 in.-lb.
Aluminum alloy 6061-T6:		σ_o = 43.0 ksi
		M_p = 52.4 in.-lb. or 47.4 in.-lb.
Impact velocity range:		35 ft./sec. to 100 ft./sec.
Stopping time range:		0.07 msec. to 0.37 msec.

TABLE III 8 (b)

Impact Test Conditions: Cantilever Beams with Tip Mass, Tests of Gillis and Lerner (1960)

Two cantilever specimens attached transversely to carriage, subjected to impact by mass propelled along track; specimen carriage decelerated slowly by friction brake.

Specimens:	lengths	approx. 4.5 in.
	width	0.312 in.
	depth	0.125 in., (mild steel)
		0.119 in., 0.127 in. (6061-T6 aluminum alloy)
Tip mass ratios:		0, 0.3, 0.7, 1.4, 1.9, 2.1 (mild steel)
		2.0, 3.9, 5.9 (6061-T6 aluminum alloy)
Strength properties:		
Mild steel:		σ_o = 41.0 ksi, M_p = in.-lb., 53.6 in.-lb.
Aluminum alloy 6061-T6:		M_p = 47.5 in.-lb., 56.5 in.-lb.
Impact velocity range:		53 ft./sec. to 96 ft./sec.
Stopping time range:		0.07 msec. to 0.10 msec.

TABLE III 9(a)

IMPACT TEST RESULTS - MILD STEEL BEAMS

Tests of Bodner and Symonds (1962)
Gillis and Lerner (1960)

	No.	L	K	V_o in/sec	τ μsec	R	θ_{exp} deg. rad.	θ^m_{rp} Rad.	$\frac{t^f_{rp}}{\tau}$	$\theta_{rp} = \theta^m_{rp}(1 - \frac{\tau}{t_f})$	$\frac{\theta_{exp}}{\theta_{rp}}$	Approx VP $\frac{\theta}{\theta_{rp}}$	Exact VP $\frac{\theta}{\theta_{rp}}$
BODNER AND SYMONDS	A8	4.45	2.02	694	255	43	70.0° (1.222)	2.26	106	2.24	0.543	0.55	
	A9	"	"	580	333	30	47.0 (0.821)	1.59	68	1.56	0.525	0.57	
	A10	"	"	511	319	23	42.1 (0.736)	1.23	63	1.21	0.607	0.57	
	A11	"	"	639	269	36	72.5 (1.268)	1.92	93	1.90	0.667	0.56	
	A12	"	"	589	368	31	55.0 (0.961)	1.63	63	1.60	0.600	0.57	
	A13	"	"	415	315	15	33.5 (0.586)	0.810	47	0.79	0.735	0.59	
	A14	"	"	330	356	9.5	14.5 (0.254)	0.513	36	0.50	0.508	0.60	
	A15	"	"	702	298	44	69.5 (1.213)	2.32	92	2.30	0.528	0.55	
	B1	4.46	2.00	816	202	26	78.0 (1.362)	2.13	98	2.11	0.680	0.55	
	B2	"		650	168	16	50.0 (0.873)	1 35	94	1.33	0.690	0.56	0.585
	B3	"		612	170	14	44.2 (0.771)	1.20	87	1.19	0.688	0.56	
GILLIS AND LERNER	26	4.46	2.06	631	74	32	48.8 (0.852)	1.30	294	1.30	0.654		
	27	"	"	675	83	37	55.7 (0.973)	1.49	281	1.49	0.654		
	28	"	"	739	--	44	67.8 (1.182)	1.78	322	1.78	0.664		

Specimens A8 - A15, B1 - B3 (Bodner and Symonds, 1962) Mild steel: σ_o = 30 ksi (A specimens), σ_o = 44 ksi (B specimens); Beam depth 0.125 in., width 0.312 in. M_p = 36.6 in-lb (A spec.) M_p = 53.6 in-lb (B spec.)

Specimens 26-28 (Gillis and Lerner, 1960, specimen group 56) Mild steel: σ_o = ksi, M_p = 49.6 in-lb; Beam depth 0.125 in., width 0.312 in.

TABLE III 9(b)

IMPACT TEST RESULTS ON ALUMINUM 6061-T6 BEAMS

Tests of Bodner and Symonds (1962)
and Gillis and Lerner (1960)

	Spec. No.	L in.	K	V_o in/sec	τ μsec	R	θ_{exp} deg. (rod)	$\frac{3}{8}\frac{(1+2k)^2}{1+3k}\frac{mLV^2}{M_o}$ θ^m_{rp} rod	$\frac{t^f_{rp}}{\tau}$	$\theta_{rp} = \theta^m_{rp}(1-\frac{\tau}{t_f})$	$\frac{\theta_{exp}}{\theta_{rp}}$	Approx VP $\frac{\theta}{\theta_{rp}}$	Exact VP $\frac{\theta}{\theta_{rp}}$
BODNER AND SYMONDS	D1	4.25	2.02	1040	112	5.3	43.7° (0.762)	1.230	85	1.213	0.628	.787	
	D2	"	"	1052	92	5.5	55.4 (0.968)	1.260	103	1.248	0.775	.786	
	D3	"	"	1196	101	7.0	73.2	1.628	107	1.611	0.795	.779	
	D4	"	"	1076	81	5.8	53.6 (0.936)	1.318	121	1.308	0.719	.784	
	D5	"	"	965	242	4.6	41.1	1.060	36	1.030	0.698	.794	
	D6	"	"	994	92	4.9	52.4	1.120	98	1.110	0.824	.790	
	D7	"	"	1160	73	6.7	72.3	1.530	144	1.520	0.831	.780	
	D8	"	"	1160	76	6.6	67.5	1.530	138	1.520	0.785	.780	
	D9	"	"	1168	112	6.6	60.5	1.547	95	1.530	0.690	.783	
GILLIS AND LERNER	1	4.25	2.01	935	80	4.8	35.8	0.994	105	.985	.635		
	2	"	"	880	70	4.3	34.3	0.880	113	.871	.688		
	3	"	"	970	87	5.2	40.1	1.070	100	1.060	.661		
	4	"	"	975	80	5.3	43.0	1.080	109	1.070	.700		
	5	"	"	936	84	4.8	35.8	0.995	105	.985	.635		

Specimens D1 - D9 (Bodner and Symonds, 1962) 6061-T6 Aluminum alloy = 43 ksi, density 0.098 lb/in^3
Beam depth 0.119 in., width 0.312 in., M_p = 47.4 in-lb.

Specimens 1 - 5 (Gillis and Lerner, 1960, Group A1): specimen material properties and dimensions as above.

the base (or the initial velocity of the beam due to explosive loading in Bodner and Humphreys' tests).

The initial rigid-plastic response pattern is governed by V_o/t_o and by the tip mass ratio k. Figure III 23 summarizes the situation, and shows that if $V_o/t_o \geq 24M_p/mL^2$ and $k \geq 1$ an interior plastic hinge appears with sense of bending opposite that of the base plastic zone. (Figs. III 22 (c)). The analysis leading to Fig. III 23 neglects the moment of inertia of the tip mass about its centroid. It was shown by Mentel (1958) that neglect not only of the tip mass inertia but also of the presence of the internal hinge leads to negligible errors in the main deformation at the base hinge. Thus a pattern of deformation consisting of a simple rotation about an axis at the base (Fig. III 22(d)) is a very accurate one. For this simple linear velocity distribution the elementary rigid-plastic analysis leads to the following results for the final rotation angle θ_{rp} and the time t_f at which motion stops:

$$\theta_{rp} = \theta_m\left(1 - \frac{t_o}{t_f}\right) \tag{3.22}$$

where

$$\theta_m = \frac{3}{8}\,\frac{(1+2k)^2}{1+3k}\,\frac{mLV_o^2}{M_p}; \qquad t_f = \frac{1+2K}{2}\,\frac{mL^2V_o}{M_p}$$

The test results of Bodner and Symonds (1962) and Gillis and Lerner (1960) are presented as plots of $\frac{3}{8}\theta_{exp}/\theta_{rp}$ vs. t_f/t_o. In these experiments the stopping time t_o was so short in relation to t_f that the "correction factor" $1 - t_o/t_f$ of Equation (3.22) was within 2 or 3 percent of unity. (This was intended in the design of the experiments, so as to minimize effects associated with details of the impact, such as the shape of the velocity-time curve.)

Comparisons are shown between test and theoretical results in Figs.

III 24 (a) and (b), plotting θ_{exp}/θ_{rp} as functions of velocity change V_o, where θ_{rp} is the elementary rigid-plastic result as calculated from Equation (3.22). These comparisons are made for a single mass ratio k, namely $K \doteq 2.0$. Other values of k were used in the experiments, but to keep complications to a minimum in the present comparisons, tests with only one beam geometry are considered.

In the comparison shown the energy ratio R was greater than 9 for the mild steel tests and between 5 and 7 for the aluminum 6061-T6 tests. These values are the ratio of the plastic work $M_p\theta_{exp}$ in the test to the quantity $M_p^2L/2EI$, which is taken as a measure of the maximum elastic strain energy that could be stored in the beam.

The plots in Figs. III 24 show large scatter of results, despite the restriction in each case to a single value of k and the same beam geometry. This scatter has not been explained, and the results are to some extent doubtful because of it. It is perhaps associated with elastic vibrations, despite the large values of energy ratio R. The importance of elastic deformations might have been increased by the raising of the upper yield stress, in the mild steel tests. The upper yield effect is enhanced in impact tests, and seems to be further increased in bending as compared with simple tension or compression, as shown recently by Aspden (1963); see Aspden and Campbell (1966).

Another possible source of scatter in the tests of Bodner and Symonds is the fact that the beam is in motion prior to impact. The base of the beam is moving with constant velocity, but vibrations excited by the initial acceleration of the beam are still appreciable. In the tests of Gillis and Lerner this difficulty was removed by having the beam stationary and at rest prior to impact. Some reduction in scatter was obtained by this change in

technique; average deformation values at a given velocity are about the same as in Bodner and Symonds' tests.

The plots in Figs. III 24 show that for both mild steel and 6061-T6 the measured final angular deformations were substantially smaller than those predicted by elementary rigid-plastic analysis over the range of impact velocities used, the ratios of test deformation to the value from elementary theory being approximately 0.5 to 0.7 for mild steel and 0.6 to 0.8 for 6061-T6.

The neglect of strain hardening in the elementary rigid-plastic theory again can be eliminated as a major cause for this discrepa Figs. III 24 show the deformation angles in degrees for each test. If strain hardening had been a major cause of the reduction of deformation from that predicted by the elementary theory one would expect some correlation between the discrepancy and the magnitude of the deformation, with agreement becoming worse as the deformation angle is increased. No downward trend in the ratio θ_{exp}/θ_{rp} is found in any of the test series. As far as one can judge, in view of the scatter of results, the observed deformations remain at essentially the same fraction of the values predicted by elementary theory, independent of velocity and strain magnitude.

We consider now the approach to a viscoplastic analysis.

Differential equations for the beam problems have been derived and solved, in which the plastic bending moment in excess of the static magnitude at each section is a chosen function of curvature rate. The pattern of deformation shown in Fig. III 21 is still postulated. An interface $x = z(t)$ is assumed to separate the region near the base where plastic deformation occurs at time t from the region $x > z$ which moves as a rigid body. The bending moment at the interface is M_p, the static plastic moment,

$M(x) > M_p$ at $x < z$, being governed by the strain rate. The following relation was used in the analyses by Cowper and Symonds (1957), Ting and Symonds (1962) and Ting (1963, 1964):

$$\dot{\kappa} = (\operatorname{sgn} M)\left(\frac{|M|}{M_p} - 1\right)^p, \qquad |M| \geq M_p$$

$$\dot{\kappa} = 0 \qquad\qquad |M| < M_p \tag{3.1}$$

where $\dot{\kappa}$ is the time rate of change of the curvature κ, and p and B are constants. This relation was derived from the corresponding one for simple tension or compression,

$$\dot{\epsilon} = (\operatorname{sgn} \sigma)\left(\frac{|\sigma|}{\sigma_o} - 1\right)^p, \qquad |\sigma| \geq \sigma_o$$

$$\dot{\epsilon} = 0 \qquad\qquad |\sigma| < \sigma_o \tag{3.2}$$

where σ is the stress, $\dot{\epsilon}$ the strain rate, and D is a constant of the material having dimensions of strain rate. The above simple form of non-linear viscoplastic relation can be made to fit published data with accuracy satisfactory for engineering purposes. Numbers for D and p chosen to fit Manjoine's curve for mild steel and Parkes' composite curve for duraluminum are:

Mild Steel	$D = 40\ \text{sec}^{-1}$	$p = 5$
Duraluminum	$D = 6500\ \text{sec}^{-1}$	$p = 4$

The constant B in the bending moment-curvature rate formula is related to D (by calculation assuming plane sections to remain plane) as follows:

$$B = D\,\frac{2}{h}\left(\frac{2p+1}{2p}\right)^p. \tag{3.3}$$

when $\dot{\epsilon}$ is expressed in $(\text{seconds})^{-1}$.

The pattern of deformation shown in Fig. III 21 apparently resembles

that of the first phase in the elementary rigid-plastic solution of the same problem, except that the moment in the plastic region is not constant but varies from M_p to M_m at the base. A more important difference is that instead of there being two distinct phases the configuration of Fig. III 21 applies through out the motion. During the deformation the interface moves toward the base and strain rate magnitudes decrease. When they become zero motion ceases, so that the final bending moment at the fixed end is M_p.

In order to solve the problem completely (in the framework of the conventional beam equations) it would be necessary to solve the following partial differential equation in the plastic region $0 \leq x \leq z(t)$:

$$\frac{\partial^4 \mu}{\partial x^4} + \frac{mB}{M_p} \frac{\partial \mu^p}{\partial t} = 0 \qquad (3.4)$$

where $\mu = \frac{M}{M_p} - 1 \geq 1$. This fourth-order non-linear parabolic equation must be solved subject to conditions at the boundaries $x = 0$ and $x = z(t)$; $z(t)$ defines the interface between regions $\mu \geq 1$ $(0 \leq x \leq z)$ and $|\mu| < 1$, $(z \leq x \leq L)$. The unknown function $z(t)$ must be found from the equations of momentum conservation for the whole beam and the continuity conditions at the interface. This presents a difficult problem, even for a wholly numerical analysis, and the complete solution has not been carried out. However, Ting (1963) and Ting and Symonds (1962) considered the related impact problem, where the base of the beam is impacted so that it attains a velocity V_o in a specified short time. The pattern of deformation is taken the same as in Fig. III 21. Ting (1963) obtained the complete solution of this problem by an iterative numerical technique. The approximate solution described by Ting and Symonds (1962) is based on what at first appears to be a drastic simplifying assumption, namely that in the plastic zone $0 \leq x \leq z(t)$ the inertia forces are zero. This may perhaps be argued as plausible on the grounds

that the resistance to motion in the plastic region is primarily due to bending strength, enhanced by high strain rates, rather than to inertia. In any event, this simplification was shown to be permissible in the impact problem treated, the final angles differing from those obtained in the complete solution by amounts less than one percent in two examples of mild steel beams, and by about two percent in two examples of aluminum alloy 6061-T6. The success of the approximation of neglecting inertia in the plastic zone is presumably related to the fact that during most of the deformation the plastic zone is presumably related to the fact that during most of the deformation the plastic zone is fairly small (less than one-third the beam length); the momentum of material adjacent to the base of the beam is small, and its contribution to the moment of momentum smaller still. Hence an approximate inclusion of this momentum, or its omission altogether, may lead to small errors in the final deformation.

The neglect of inertial forces means that the shear force is constant in the plastic region. Then instead of a fourth order non-linear partial differential equation with an unknown moving boundary, one has a simpler problem of coupled ordinary integro-differential equations expressing conservation of linear and angular momentum.

We shall write the equations for a viscoplastic analysis first in general forms applicable either to Parkes' problem (stationary beam with tip mass subjected to an impulse) or to the problem briefly mentioned above in which the base of the beam is given a change of velocity in a short time, i.e. the "impulse" problem and the "impact" problem respectively.

After outlining the viscoplastic approach to both problems, and showing results for the impulse problem, the impact problem will again be looked at in more detail. Experimental results are available for this problem as well, although, as will be seen, they are in some respects unsatis-

factory.

(C) Viscoplastic Analysis

We consider a beam with given initial velocity distribution $v_o(x) = v(x,0)$. In order to take approximate account of finite deformations in a simple way the velocity $v(x,t)$ is defined as normal to the deformed center-line, x being the distance from the base to a typical cross-section measured along the center-line curve (see Fig. III 21). The initial transverse momentum and angular momentum with respect to the base point B are, respectively,

$$J_o = \int_0^L mv_o(x)dx + GV_o = (\alpha mL + G)V_o \tag{3.5a}$$

$$H_o = \int_0^L mv_o x dx + LGV_o = (\tfrac{1}{2}\alpha mL^2 + GL)\, V_o \tag{3.5b}$$

where $\alpha = 0$ in the impulse (Parkes's) problem, $\alpha = 1$ in the impact problem, and m is the mass per unit length along the center-line. At time $t > 0$, with deformation of the center-line as indicated in Fig. III 21 the component of momentum parallel to the initial direction of motion is

$$J(t) = \int_0^L mv \cos\theta \, dx + GV \cos\theta_1 \tag{3.6a}$$

Where $\theta(x,t)$ is the angle of the tangent at x with the horizontal and $\theta_1 = \theta(L,t)$ is the angle at the tip. The angular momentum with respect to B is given approximately by

$$H(t) = \int_0^L mvxdx + GVL \tag{3.6b}$$

This correctly represents the moment of momentum about B for small deformations, but would do so for large deformations only if the deformed center-line curve were

a straight line. It is suggested as a good approximation for beams with a tip mass roughly equal to or greater than that of the beam by the fact that the final deformed shape of such beams has been found in experiments always to be very closely linear outside a short hinge region near the base.

The equations of conservation of momentum for the beam and attached mass are

$$-\int_0^t Q_m(\tau)d\tau = J(t) - J_o \tag{3.7a}$$

$$-\int_0^t M_m(\tau)d\tau = H(t) - H_o \tag{3.7b}$$

where Q_m and M_m are the opposing shear and bending moment at the base B; J(t), H(t) are given by Equations (3.6); and J_o, H_o are given by Equations (3.5).

Boundary conditons at the base are

$$\theta_b = \frac{\partial v}{\partial x}(0,t) = 0 \tag{3.8a}$$

$$V_b = v(0,t) = V_o\,[1 - f(t)] \tag{3.8b}$$

where for the impulse problem: $f(t) = 1$

for the impact problem: $f(t) = t/t_o$, $t \leq t_o$

and $f(t) = 1$, $t \geq t_o$

As already discussed, our solution will be simplified by neglecting inertia forces, and hence assuming that the shear force in the plastic region $0 \leq x \leq z(t)$ is independent of x, i.e. in this region $Q = Q_m(t)$. Therefore $dM/dx = -Q_m$ and the bending moment varies linearly:

$$\frac{M}{M_p} - 1 = \left(\frac{M_m}{M_p} - 1\right)\left(1 - \frac{x}{z}\right), \qquad \text{in } 0 \leq x \leq z \tag{3.9}$$

where $M_m(t)$ is the base moment and M_p is the static plastic limit moment. Using Equation (3.1), the curvature rate $\dot{\kappa}$ is

$$\dot{\kappa} = \frac{\partial^2 v}{\partial x^2} = \dot{\kappa}_m \left(1 - \frac{x}{z}\right)^p, \qquad \text{in } 0 \leq x \leq z \tag{3.10}$$

where $\dot{\kappa}_m(t) = B\left(\frac{M_m}{M_p} - 1\right)^p$.

In the region $z \leq x \leq L$ the bending moment is less than M_p, and therefore $\dot{\kappa} = \partial^2 v/\partial x^2 = 0$; this segment moves as a rigid body. Thus the assumption $Q = Q_m$ enables the curvature rate to be written as a known function of x in terms of the unknowns $\dot{\kappa}_m(t)$ and $z(t)$, and from $\partial^2 v/\partial x^2$ the velocity can be evaluated in terms of $\dot{\kappa}_m$ and z.

The evaluation of the momentum integral $J(t)$ involves the slope angle $\theta(x,t)$. This is related to $v(x,t)$ by

$$\frac{\partial \theta}{\partial t} = \frac{\partial v}{\partial x} \tag{3.11a}$$

so that

$$\theta(x,t) = \int_0^t \frac{\partial v}{\partial x}(x,\tau)\,d\tau \tag{3.11b}$$

The treatment of finite deformations is greatly simplified by the further assumption that $J(t)$ may be written for a uniform beam as

$$J(t) \equiv m \cos\theta_1 \int_0^L v\,dx + GV \cos\theta_1 \tag{3.12}$$

where θ_1 is the slope angle at the tip, $x = L$. This is strictly true only if the deformed center-line is a straight line, but it may be justified in the general case. Consider the two approximations

$$\text{(a)} \qquad m \int_0^z v \cos\theta\,dx \equiv m \cos\theta_1 \int_0^z v\,dx \tag{3.13a}$$

$$\text{(b)} \qquad m \int_z^L v \cos\theta \, dx \cong m \cos\theta_1 \int_z^L v\,dx \tag{3.13b}$$

Experiments show the final shape to be nearly straight away from a region near the beam base whose length is of the order of several beam thicknesses; this suggests that (b) is a good approximation. Although (a) is not so good an approximation, it is nevertheless permissible because $\cos\theta_1$ differs appreciably from unity only when z is small and the integral in (a) then represents a very small part of the total momentum.

Then equations of the viscoplastic problem thus simplified can be written in terms of the three variables, $\dot{\kappa}_m(t)$, $z(t)$, and $\theta_1(t)$, after putting

$$M_m = M_p[1 + (\frac{\dot{\kappa}_m}{B})^{\frac{1}{p}}]; \qquad Q_m = \frac{M_p}{z}(\frac{\dot{\kappa}_m}{B})^{\frac{1}{p}} \tag{3.14}$$

The three equations in these unknown functions are

$$-\int_o^t \frac{M_p}{z}(\frac{\dot{\kappa}_m}{B})^{\frac{1}{p}} d\tau = m \cos\theta_1 \int_o^L v\,dx + GV\cos\theta_1 - J_o \tag{3.15a}$$

$$-\int_o^t M_p[1 + (\frac{\dot{\kappa}_m}{B})^{\frac{1}{p}}] d\tau = m \int_o^L vx\,dx + GVL - H_o \tag{3.15b}$$

$$\theta_1 = \int_o^t \frac{\partial v}{\partial x}(L,\tau)d\tau \tag{3.15c}$$

The integrals in the right-hand sides of (3.15) may easily be expressed in terms of $\dot{\kappa}_m$ and z by using the expressions for $\frac{\partial^2 v}{\partial x^2}$ appropriate to the intervals $0 \le x \le z$ and $z \le x \le L$; for the first interval Equation (3.10) applies, while for the second $\frac{\partial^2 v}{\partial x^2} = 0$. We have

$$\frac{\partial v}{\partial x} = \int_o^x \frac{\partial^2 v(\xi,t)}{\partial \xi^2}\, d\xi$$

$$v(x,t) = V_b(t) + x\,\frac{\partial v}{\partial x} - \int_o^x \xi\,\frac{\partial^2 v(\xi,t)}{\partial \xi^2}\, d\xi$$

For $0 \le x \le z$: $\frac{\partial v}{\partial x} = \frac{z\dot{\kappa}_m}{p+1}\left[1 - (1 - \frac{x}{z})^{p+1}\right]$ (3.16a)

$$v(x,t) = V_b + \frac{z\dot{\kappa}_m}{p+1}\left\{x + \frac{z}{p+2}\left[(1 - \frac{x}{z})^{p+2} - 1\right]\right\} \quad (3.16b)$$

For $z \le x$: $\frac{\partial v}{\partial x} = \frac{z\dot{\kappa}_m}{p+1} = \dot{\theta}_1(t)$ (3.17a)

$$v(x,t) = V_b + \frac{z\dot{\kappa}_m}{p+1}\left[x - \frac{z}{p+2}\right] \quad (3.17b)$$

$$V(t) = V_b + \frac{z\dot{\kappa}_m}{p+1}\left[L - \frac{z}{p+2}\right] \quad (3.18)$$

Evaluating the integrals in (3.15), we obtain finally the system of equations:

$$-\int_o^t \frac{M_p}{z}\left(\frac{\dot{\kappa}_m}{B}\right)^{\frac{1}{p}} d\tau = V_o(mL+G)[1-f(t)]\cos\theta_1 - V_o(\alpha mL+G)$$

$$+ \frac{\dot{\kappa}_m mL^3}{p+1}\left\{\frac{1}{2}\frac{z}{L} - \frac{z^2}{(p+2)L^2} + \frac{z^3}{(p+2)(p+3)L^3}\right\}\cos\theta_1$$

$$+ \frac{\dot{\kappa}_m GL^2}{p+1}\left\{\frac{z}{L} - \frac{z^2}{(p+2)L^2}\right\}\cos\theta_1 \quad (3.19a)$$

$$-\int_o^t M_p\left[1 + \left(\frac{\dot\kappa_m}{B}\right)^{\frac{1}{p}}\right]d\tau = V_o\left(\frac{mL^2}{2} + GL\right)[1-f(t)] - V_o\left(\frac{\alpha mL^2}{2} + GL\right)$$

$$+ \frac{\dot\kappa_m mL^4}{p+1}\left\{\frac{1}{3}\frac{z}{L} - \frac{z^2}{2(p+2)L^2} + \frac{z^4}{(p+2)(p+3)(p+4)L^4}\right\}$$

$$+ \frac{\dot\kappa_m GL^3}{p+1}\left\{\frac{z}{L} - \frac{z^2}{(p+2)L^2}\right\} \qquad (3.19b)$$

$$\theta_1 = \theta(L,t) = \int_o^t \dot\theta_1 d\tau = \int_o^t \frac{\dot\kappa_m z}{p+1}\, d\tau \qquad (3.19c)$$

The particular forms for the impulse and impact problems will be written. By definition the impulse problem has $\alpha = 0$ and $f(t) = 1$, and the first two of Equations (3.19) become:

Impulse problem:

$$\int_o^t \frac{M_p}{z}\left(\frac{\dot\kappa_m}{B}\right)^{\frac{1}{p}} d\tau = GV_o - \frac{\dot\kappa_m mL^3}{p+1}\left\{\left(\frac{1}{2}+k\right)\frac{z}{L} - \frac{1+k}{p+2}\frac{z^2}{L^2} + \frac{z^3}{(p+2)(p+3)L^3}\right\}\cos\theta_1 \qquad (3.20a)$$

$$\int_o^t M_p\left[1+\left(\frac{\dot\kappa_m}{B}\right)^{\frac{1}{p}}\right]d\tau = GLV_o - \frac{\dot\kappa_m mL^4}{p+1}\left\{\left(\frac{1}{3}+k\right)\frac{z}{L} - \frac{\frac{1}{2}+k}{p+2}\frac{z^2}{L^2} + \frac{z^4}{(p+2)(p+3)(p+4)L^4}\right\} \qquad (3.20b)$$

where k is the mass ratio, $k = \frac{G}{mL}$.

In the impact problem we have $\alpha = 1$ and $f(t) = t/t_o$ in the time interval $0 \le t \le t_o$, and $f(t) = 1$ for $t \ge t_o$. If t_o is small it is reasonable to take $\cos\theta_1 = 1$ in the interval $0 \le t \le t_o$. Then the momentum Equations (3.19a, b) become:

Impact problem:

$$\int_0^t \frac{M_p}{z}\left(\frac{\dot\kappa_m}{B}\right)^{\frac{1}{p}} d\tau = V_o(mL+G)f(t) - \frac{\dot\kappa_m mL^3}{p+1}\left\{\left(\frac{1}{2}+k\right)\frac{z}{L} - \frac{1+k}{p+2}\frac{z^2}{L^2} + \frac{z^3}{(p+2)(p+3)L^3}\right\}\cos\theta_1 \quad (3.21a)$$

$$\int_0^t M_p\left[1+\left(\frac{\dot\kappa_m}{B}\right)^{\frac{1}{p}}d\tau = V_o\left(\frac{mL^2}{2} + GL\right)f(t) - \frac{\dot\kappa_m mL^4}{p+1}\left\{\left(\frac{1}{3}+k\right)\frac{z}{L} - \frac{\frac{1}{2}+k}{p+2}\frac{z^2}{L^2} + \frac{z^4}{(p+2)(p+3)(p+4)L^4}\right\}\right.$$

(3.21b)

Initial conditions must be stated for both sets of Equations (3.20) and (3.21). We have $\theta_1(0) = 0$ in both problems, but the starting values of z and $\dot\kappa_m$ are different. There is some arbitrariness; the choice of the assumption $\dot\kappa = \dot\kappa_m(1 - x/z)^p$ means that exact initial conditions on velocity cannot be satisfied. For the impulse problem where the disturbance originates at the tip mass, we take $z(0) = L$. For the impact problem the disturbance is felt first at the base, and we take $z(0) = 0$. The initial curvature rate at the base $\dot\kappa_m(0)$ can be taken as zero in the general impact problem where the base moves with velocity $V_o(1 - t/t_o)$ for $t \le t_o$ and is at rest for $t \ge t_o$.

The initial value $\dot\kappa_m(0)$ for the impulse problem may be chosen so as to make the initial velocity pattern give the correct angular momentum. Putting $t = 0$, $z = L$ in Equation (3.20b), this gives

$$kV_o = \frac{mL^2\dot\kappa_m(0)}{p+2}\left\{k + \frac{(p+2)(2p+9)}{6(p+3)(p+4)}\right\} \quad (3.22a)$$

Since Equation (3.20a) as it stands would not be satisfied with the above value of $\dot\kappa_m(0)$, it may be modified by replacing the expression in brackets on the right hand side by the following:

$$\{(\frac{1}{2}+k)\frac{z}{L} - \frac{1+k}{p+2}\frac{z^2}{L^2} + [\frac{1}{(p+2)(p+3)} - \frac{p+1}{6(p+4)}]\frac{z^3}{L^3}\} \qquad (3.22b)$$

With this change, the linear and angular momentum conservation equations both give the same initial value $\dot{\kappa}_m(0)$.

Equations (3.20) are essentially the same but differ in detail from those solved by Ting (1964). Ting's "First Solution" omits the momentum contributions for the plastically deforming segment in $0 \leq x \leq z$. His "Second Solution" equations include contributions from these momenta; however the contributions actually obtained from the assumption $\dot{\kappa} = \dot{\kappa}_m(1 - \frac{x}{z})^p$ were modified so that they are both somewhat simpler, and so that the two momentum equations give the same initial value for $\dot{\kappa}_m$.

Numerical solutions of the viscoplastic equations (3.19) may be carried out by a step-by-step procedure. Suppose the three functions are known at time t_j : $\dot{\kappa}_m(t_j)$, $z(t_j)$, and $\theta_1(t_j)$. To find their values at t_{j+1}, one may guess $\dot{\kappa}_m(t_j+1)$. Putting this in Equation (3.19b) one may solve the resulting equation for $z(t_{j+1})$. These values put in Equation (3.19c) enable $\theta_1(t_{j+1})$ to be calculated. The three values are then substituted in Equation (3.19a) as a check; if left and right hand sides do not agree the calculations are repeated with a revised trial value of $\dot{\kappa}_m(t_{j+1})$, and the process is continued until agreement is obtained. The deformation stops when the curvature rate $\dot{\kappa}_m$ is reduced to zero, corresponding to the bending moment at the base being reduced to M_p.

Calculations of this type were carried out by Ting (1964) for the impulse problem, using modified equations, as already described. Since errors were noticed in the published results in two of the four cases calculated, all were recalculated. Table III 7(a) gives the results from the "complete solution" (Equations 3.20) as well as from Ting's "first solution" in which

momentum contributions from the plastically deforming segment are omitted. The differences are very small in three cases, and about 10 percent in the third case.

Comparisons with test results are also indicated in Tables III 7(a)-(b), and in Figs. III 19(a)-(b). For mild steel the agreement with observed final deformations of the viscoplastic theory is improved in the specimens with large tip mass (small β) as compared with elementary rigid-plastic theory. However when the tip mass is small ($\beta \geq 1$ or larger) the viscoplastic analysis leads to an underestimate by some 20 percent. This is, however, much better agreement than that obtained by using Parkes's strain-rate correction factor, which predicts deformations that are too small by nearly 100 percent at $\beta \geq 1$. For the tests on 6061-T6, Fig. III 19(b), the viscoplastic theory leads to an over-estimate (at $\beta \geq 1$), of about the same magnitude as the error in the other direction obtained by use of a simple correction factor on the plastic moment.

To summarize, we have shown comparisons between deformations predicted by a viscoplastic analysis based on a moment-plastic curvature rate relation of simple type (Equation 3.1) and test results for a particular type of beam test, in which an impulse is applied to a mass at the tip of a fixed-base cantilever. The introduction of strain rate sensitivity into the differential equations does change the pattern of deformations substantially; the deformations are more nearly confined to a region near the base, independently of the ratio of tip mass to beam mass. Quantitative agreement of final deformations predicted by this theory with those observed in tests is only fair (Fig. III 19(a)-(b)), but is very much better than obtainable when a simple correction is applied to the statically measured fully plastic moment.

Also shown in Tables III 7 (a)-(b) and Figs. III 19 (a)-(b) are

deformations determined from a simple approximation formula suggested by Ting (1964). This formula will be discussed later and compared with other approximate methods.

(D) Approximate Expressions

The complete solutions of the viscoplastic equations (3.20) and (3.21) are lengthy, and it is natural to look for simplifications that will retain essential features.

Immediate simplifications in the momentum equations of either the "impulse" or the "impact" problem, Equations (3.20) and (3.21), are suggested from the fact that the exponent p in the strain rate law is large; commonly $p \geq 4$. In the moment of momentum integral, we may write

$$\int_0^t M_p[1+A(\tau)]d\tau = M_p(1+A_o)t \tag{3.23}$$

where

$$A(\tau) = [\frac{\dot{\kappa}_m(\tau)}{B}]^{\frac{1}{p}}$$

and A_o is a constant representing a suitable average of $A(\tau)$ in the interval $(0,t)$. Numerical solutions show the actual variations of $\dot{\kappa}_m(\tau)$ to be large during the deformation. An example of a calculated curve of $\dot{\kappa}_m(\tau)$ is shown in Fig. III 25(b). Although $\dot{\kappa}_m$ first increases from 10 to 25 and then decreases approximately linearly to zero, the change in $1 + A(\tau)$ remains relatively small (Fig. III 25(a)). Until the final instants of the motion the variation of $1 + A(\tau)$ from the starting value $1 + A(0)$ is only some 7 percent. Hence it is a quite accurate approximation to take $A_o = A(0) = [\frac{\dot{\kappa}_m(0)}{B}]^{\frac{1}{p}}$, corresponding to the initial curvature rate.

Consider the viscoplastic equations of the impulse problem, Equations

(3.20). The third term in the bracket of each equation is small compared with first. In the moment of momentum equation (3.20b), if p = 5 the third term is less than one percent of the first term under the worst circumstances when k = 0 and z = L, and still smaller when z << L and k is 1 or larger. In the transverse momentum equation the third term is less than one percent of the first if z < L/2, as is the case for most of the deformation period, Fig. III 25(b). The same remarks apply equally to the equations (3.21) for the impact problem. Hence the following simplified forms of the viscoplastic equations (3.20) and (3.21) apply with very good accuracy:

$$M_p A_o \int_o^t \frac{d\tau}{z(\tau)} = GV_o - \dot{\theta}_1 mL^2(\tfrac{1}{2} + k)\left[1 - \frac{1 + k}{(\tfrac{1}{2} + k)(p + 2)} \frac{z}{L}\right] \cos\theta_1 \tag{3.24a}$$

$$M_p(1 + A_o)t = GLV_o - \dot{\theta}_1 mL^3(\tfrac{1}{3} + k)\left[1 - \frac{\frac{1}{2} + k}{(\tfrac{1}{3} + k)(p + 2)} \frac{z}{L}\right] \tag{3.24b}$$

where

$$A_o = \left[\frac{\dot{\kappa}_m(0)}{B}\right]^{\frac{1}{p}}$$

with

$$\dot{\kappa}_m(0) = \frac{GV_o(p + 2)}{mL^3\left[k + \frac{1}{3} - \frac{1}{6(p + 1)}\right]} \tag{3.24c}$$

The complete solution for several cases determines a curve of $\dot{\theta}$ as function of time like that of Fig. III 27, the main feature of which is the straightness of the curve except near the start of the motion, t = 0. This means that a good approximation to the final value of θ can be obtained by taking the $\dot{\theta}(t)$ curve to be a straight line cutting the time axis at $t = t_f$ and having the slope of the curve at $t = t_f$. Here t_f is the instant when motion ceases, $\dot{\theta}(t_f) = 0$; $z(t_f) = 0$. From Equation (3.24b) we have

$$M_p(1 + A_o) = -\ddot{\theta}(t_f)mL^3(\frac{1}{3} + k) = \frac{GLV_o}{t_f} \tag{3.25}$$

The approximate linear solution for $\theta^*(t)$ is thus

$$mL^3(\frac{1}{3} + k)\dot{\theta}^* = GLV_o - M_p(1 + A_o)t \tag{3.26}$$

and the final angle is given approximately by

$$\theta^*_{vp} = \frac{GV_o^2}{2M_p} \frac{k}{(\frac{1}{3} + k)(1 + A_o)} \tag{3.27}$$

A formula for A_o was given in Equation (3.24c). This may be simplified and improved by dropping the term $\frac{1}{6}(p + 1)$ in the denominator. This change (slightly decreasing A_o) is in the right direction to improve the linear approximation. Hence we obtain the following solution for the final angle

$$\theta^*_{vp} = \frac{GV_o^2}{2M_p} \frac{k}{(k + \frac{1}{3})(1 + A^*_o)} \tag{3.28a}$$

$$A^*_o = \left[\frac{GV_o(p + 2)}{BmL^3(k + \frac{1}{3})} \right]^{\frac{1}{p}} \tag{3.28b}$$

This formula was derived by Ting (1964) by an essentially similar argument.

The time at which deformation ceases is given to the same approximation as

$$t^*_f = \frac{GLV_o}{M_p(1 + A^*_o)} \tag{3.28c}$$

Finally, the equation for transverse momentum conservation, together with the above expressions for A^*_o and t^*_f, furnishes an approximate formula for the length $\bar{z}^*$ of the plastic zone (averaged over the deformation time) as

$$\frac{\bar{z}^*}{L} = \frac{A_o^*}{1 + A_o^*} \qquad (3.28d)$$

How well the predictions of the simple approximations of Equation (3.28) compare with those of the complete viscoplastic solution and with experiment results is shown by curves c in Figs. III 19 (a), (b).

Considering final rotation angles, the approximate solution differs from the complete solution by about five percent at the largest β (smallest tip mass), but the difference is negligible at low β values. The complete solution is closer to the test results for the final angles than the appropriate solution. Thus, at the largest β values, the approximate theory predicts a final angle about 20 percent smaller than the test values. The hinge lengths predicted by Equation (3.28d) are larger than those evident in photographs of final deformations, which show the length of the deformed region near the base as roughly four times the beam depth, or one tenth the length. The formula predicts average z/L magnitudes of the order of 0.5 or larger for mild steel.

To sum up, it is seen that the simple approximate solution furnishes results in good agreement with those of the complete viscoplastic solution, but whose agreement with experimental deformation angles is less satisfactory. However, the agreements with experiment of both the complete viscoplastic theory and the approximate formula over the range of β tested, are very much better than that of the elementary rigid-plastic theory, either uncorrected or multiplied by a rate correction factor as in Parkes's method.

Simple approximate formulas for the impact problem can also be obtained from the complete equations, Equations (3.21).

In the same spirit as for the approximate solution of the impulse problem, immediate simplifications can be made by dropping all but the first

term in the bracket in the right hand sides of Equations (3.21) a and b. In the present case $z/L = 0$ at $t = 0$ and $t = t_f$; z remains usually less than L/2 during the deformation. A typical curve for z/L is shown in Fig. III 29(a), obtained by calculation from the complete viscoplastic equations. Fig. III 28 shows the near constancy of A over most of the time of deformation. If we again replace $A(t) = (\kappa_m/B)^{1/p}$ by a constant $\bar{A}$, the equation of conservation of angular momentum (3.21b) becomes:

$$M_p(1 + \bar{A})t = V_o mL^2(k + \tfrac{1}{2})f(t) - \dot{\theta} mL^3(k + \tfrac{1}{3}) \tag{3.29}$$

where for $t \leq t_o$ $f(t) = t/t_o$; $t \geq t_o$, $f(t) = 1$.

We have used, as before, the relation from Equation (3.19c), namely

$$\dot{\theta}(t) = \frac{\dot{\kappa}_m z}{p + 1}, \tag{3.30}$$

and we have written $\dot{\theta}$ in place of $\dot{\theta}_1$, for simplicity.

An example of a $\dot{\theta}(t)$ curve is shown in Fig. III 29(b) by calculation from the complete viscoplastic theory. For $t \geq t_o$ the curve is nearly a straight line. If we suppose t_o is small ($t_o << t_f$), it is a reasonable approximation to assume a linear variation of $\dot{\theta}(t)$ over the whole deformation time, and hence to write

$$\dot{\theta} mL^3(k + \tfrac{1}{3}) = V_o mL^2(k + \tfrac{1}{2}) - M_p(1 + \bar{A})t \tag{3.31}$$

According to this equation the deformation ends at

$$t_f' = \frac{V_o mL^2(k + \frac{1}{2})}{M_p(1 + \bar{A})} \tag{3.32a}$$

and the final angle is

$$\theta_f' = \frac{V_o^2 mL}{2M_p} \frac{(k + \frac{1}{2})^2}{(1 + \bar{A})(k + \frac{1}{3})} \tag{3.32b}$$

It remains to obtain a suitable value for $\bar{A}$ from the viscoplastic theory. We can write the linear momentum equation (3.21a) in terms of $\dot{\theta}$ and $\dot{\kappa}_m$, after eliminating z by use of Equation (3.30), and dropping the z^2 and z^3 terms in the bracket. Then the equation after differentiating with respect to t is

$$t \geq t_o, \qquad f(t) = 1,$$

$$M_p A(t)\dot{\kappa}_m(t) = \dot{\theta}\,\ddot{\theta} m L^2 (k + \tfrac{1}{2})(p + 1)$$

We may set $A(t) = \bar{A}$, and evaluate

$$\bar{A} = \left[\frac{\dot{\kappa}_m(0)}{B} \right]^{1/p}$$

Taking $\dot{\theta}$ and $\ddot{\theta}$ from Equation (3.31) and putting $t = 0$, we obtain

$$\dot{\kappa}_m(0) = \frac{1 + \bar{A}}{\bar{A}} \frac{V_o}{L^2} (p + 1) \frac{(k + \frac{1}{2})^2}{(k + \frac{1}{3})^2}$$

and

$$\bar{A} = \left[\frac{1 + \bar{A}}{\bar{A}} \frac{V_o(p + 1)}{L^2 B} \frac{(k + \frac{1}{2})^2}{(k + \frac{1}{3})^2} \right]^{\frac{1}{p}} \tag{3.32c}$$

For given V_o and beam constants the above furnishes an estimate of $\bar{A}$ that can be used in Equations (3.32a, b). Finally, from the linear momentum equation with $t = t_f$ we can obtain an average value of the plastic zone length as

$$\bar{z} = \frac{\bar{A}}{1 + \bar{A}} \frac{k + \frac{1}{2}}{k + 1}$$

Finally, it is worth noting that the approximate viscoplastic solutions written above are the same as those that would be obtained if we assumed in the beginning that the deformation is governed by an expression of type

$$v(x,t) = v^*(x)\, T^*(t)$$

This represents a deformation in a fixed pattern, or mode shape, and such a solution may be called a mode solution. The use of such forms of solution to obtain approximate solutions of dynamic loading problems has been discussed by Martin and Symonds (1966) for general one-dimensional structures of rigid-plastic material. It can be shown, for example, that for any such structure subjected to a loading of impulsive type (i.e. with prescribed initial velocities), the velocities decrease linearly to zero. Criteria were derived for choosing the mode shape so as to give the best approximation to the complete solution.

The approximate solutions derived in the foregoing discussion of viscoplastic solutions were found to be of this type. In other words, when rate sensitivity of plastic properties is included in the analysis, the deformation tends to become of modal type, in these examples. Hence these results provide some indication that the simple mode approach may give better results when applied to a rate sensitive material than for a rate independent material. However the number of examples for which comparisons with experiments have been made is too small to allow firm conclusions of this type.

Recently Bodner (1967) at Technion-Israel Institute of Technology has made a new series of tests on mild steel cantilevers with tip masses, similar to the "Impulse Tests" described above (pp. 112-122). The new results were closely comparable. They provide desirable confirmation of the viscoplastic analyses and of the usefulness of the mode approximation technique in this problem. In fact, strain gauge measurements gave quite striking evidence that the actual deformation process closely resembles that assumed in the mode solution, and predicted by the full analysis with strain rate dependence.

4. Experiments of Florence and Firth

Florence and Firth (1965) have reported tests on supported and clamped beams of steel and aluminum alloys, with uniform loads applied explosively. The tests were designed to investigate especially the applicability of rigid-plastic theory. They provide a valuable complement to the tests on cantilevers discussed above. They were comprehensive, well planned and executed tests. Nevertheless they also illustrate the basic difficulties in making and interpreting tests on dynamic plastic deformations of structures.

The elementary rigid-plastic solution for a supported or clamped beam with initial velocity V_o over its span $2L$ is obtainable by simple momentum considerations (Symonds 1955). Writing $V_o = I_1/m$, the results for the final deflection y_f and final angle θ_f as functions of position can be written, for the case of pinned ends, as

$$\frac{y_f}{L} = \frac{I_1^2 L}{6mM_p}\left(3 - \frac{x}{L}\right)\frac{x}{L} \qquad (4.1a)$$

$$\theta_f = \frac{I_1^2 L}{6mM_p}\left(3 - \frac{2x}{L}\right) \qquad (4.1b)$$

where I_1 is the impulse per unit length and x is measured from the end, Fig. III 30. The quantities of main interest are the final central deflection $y_f(L)$ and angle at the support $\theta_f(0)$, which are (for pinned ends) written as

$$\frac{y_f(L)}{L} = \frac{\delta_{th}^{(1)}}{L} = \frac{I_1^2 L}{3mM_p}; \qquad \theta_f(0) = \theta_{th}^{(1)} = \frac{I_1^2 L}{2mM_p} \qquad (4.1c)$$

For clamped ends M_p is replaced by $2M_p$. The notation in equations (4.1c) is that of Florence and Firth; the superscript (1) distinguishes the elementary

rigid-plastic solution from those including corrections for finite deflections and strain-hardening.

As mentioned, end conditions of simple support and clamped ends were used, with design so as to permit free axial motion and enable axial constraints to be negligible. Their materials and properties are listed in Table 10.

TABLE III 10

Material	Yield Stress (psi)	Strain Hardening Modulus (psi)
Al 2024-T4	52,000	0.329×10^6
Al 6061-T6	40,000	0.114×10^6
CR 1018 Steel	54,000	0.2×10^6
Annealed 1018 Steel	43,000	. . . . .

In all tests the beam dimensions were nominally 18 inches in length, 1.0 inches in width, and 0.25 inches in depth.

The loads of impulsive type were applied by detonation of sheet explosive (DuPont EL-506D), over neoprene layers to prevent spalling. The initial velocities, presumed uniform because of the large speed of the detonation wave relative to beam propagation speeds, were measured by streak photography for four aluminum and four steel specimens. In this way a calibration was obtained in terms of impulse per unit volume of sheet explosive. This quantity was found to have constant values for beams of the two materials, namely 2.9×10^6 dyne-sec/cm^3 for aluminum and 3.25×10^6 dyne-sec/cm^3 for steel.

(It is not explained why the values for the two materials are different. For a given geometry, explosive material and burning time, the impulse

should be a constant on a stationary surface. The reduction of impulse for aluminum beams is perhaps associated with the larger velocities attained by these specimens in the "delivery time" of the impulse, given as about 33 micro-seconds. But if this is the explanation, then presumably a similar variation of velocity occurred in the test series, since the thickness of explosive sheet was varied to give the desired range of initial velocities.)

Since the tests were designed to study the validity of rigid-plastic analysis, they covered a range of energy ratio R from less than unity to 6 or 7, (R = initial kinetic energy divided by maximum elastic strain energy). The final deflections ranged from a small fraction of the half-span length L to more than $\frac{1}{2}L$, thus up to about twenty times the beam depth. With deflections as large as these, the precise support conditions are important. The simply supported beams had pins which moved inward on bearing blocks as the beam deflected. The clamped beams had each of the "built-in" ends in a close fitting channel which permitted material to flow into the span. Thus, during the tests on supported beams the span decreased, while in the tests on clamped beams the span remained fixed while the developed length increased.

If appreciable constraints against axial motion were present, these would cause axial forces which (for full constraints) would dominate the motion for deflections appreciably larger than the beam depth (Symonds and Mentel 1958). That such constraints were negligible was indicated by the authors' check on one of the tests (Al 2024-T4 with clamped ends) which showed an absence of longitudinal strain at the middle surface; in this test the strain in the outer fibers reached 4 percent and the deflection was 0.43L.

The authors also gave modifications of the rigid-plastic analysis to take approximate account of finite deflections. These resulted in corrections which were in general small, rarely exceeding 5 percent. The authors seem to have effectively disposed of questions arising from the finite deflections of their specimens.

Florence and Firth presented their results in the form of tables giving the final midpoint deflection and the slope angle measured near the supports. They also displayed results of several test series by means of plots of the midpoint deflection ratio δ/L against the impulse per unit length I_1 ; and of the dimensionless displacement y/L against position x. Typical plots of both kinds are shown in Figures III 31(a,b,c).

These plots show the typical discrepancies between the predictions of equations (4.1) and the test results. The test deformations were smaller, by amounts from about 25 percent to over 50 percent, compared to predictions of the elementary theory. The inclusion of corrections for finite deflection led to minor improvement, while that for strain hardening led to substantially better agreement. Table III 11 summarizes these comparisons.

The corrections for deflection effects and strain hardening will not be discussed here in detail, although they are of great interest. Both involve approximations, but seem quite reasonable. The theory of Florence and Firth which gives their strain hardening correction is based on assumptions similar to those by Cowper and Symonds (1957): the hardening was expressed by a linear moment-curvature relation; the length of the hardening zone was assumed finite but small compared to the span; and the strain hardening was disregarded in the initial phase (in which distributed deformations occur). The accelerations in the plastic zones are taken the

TABLE III 11

Average deflection and slope ratios for R > 2

Tests of Florence and Firth (1965)

Superscript (1) refers to elementary rigid-plastic theory
" (2) " " theory with correction for finite deflections
" (3) " " " " " " strain-hardening

Experiments	$\delta_{ex}/\delta_{th}^{(1)}$	$\delta_{ex}/\delta_{th}^{(2)}$	$\delta_{ex}/\delta_{th}^{(3)}$	$\theta_{ex}/\theta_{th}^{(1),(2)}$	$\theta_{ex}/\theta_{th}^{(3)}$
Pinned; Al 6061-T6 (PB 1-4)	0.558	0.588	0.717	0.488	0.559
Pinned; Al 2024-T4 (PA 1-10)	0.673	0.711	0.920	0.591	0.711
Pinned; 1018 CR steel (PS 1-15)	0.693	0.707	0.837	0.593	0.661
Pinned; 1018 annealed steel (PSA 1-5)	0.770	0.784	. . .	0.653	. . .
Clamped; Al 2024-T4 (CA 1-12)	0.716	0.745	0.798	0.563	0.586
Clamped; 1018 CR steel (CS 1-6)	0.723	0.732	0.767	0.567	0.578

same as in the rotating segments. These and other assumptions avoided the difficult problem of a nonlinear partial differential equation with conditions at moving boundaries. Indications of the magnitudes of the corrections due to strain hardening, in the authors' theory, are shown in Figures III 31(a,b,c), and in Table III 11.

As illustrated in Fig. III 31c, the experimental deflection curves were nearly straight except in central regions. This implies that the first phase of the rigid-plastic theory, in which the general curvatures are produced by travelling hinges, is reduced in importance in the actual behavior. The effect is the same as that predicted by the analysis including rate sensitivity, as discussed in the preceding section. Since Florence and Firth's analysis of strain-hardening does not affect deformation in the first phase, and reduces deflections in the second, it has the opposite effect, tending to increase the general curvature of the specimens.

The same questions raised earlier about experiments must again be asked. The discrepancies between experiment and theory could be attributed not only to strain hardening, but to elastic vibrations (especially for beams of aluminum alloys); strain rate sensitivity (especially for the annealed steel specimens); axial constraints; shear deformations; or to combinations of these. What can be learned from the tests about the relative importance of these?

It is of interest to re-plot the experimental deformations as ratios to the quantities from elementary rigid-plastic theory. As in the similar treatment of test results for the cantilevers, the new plots provide help in answering the question stated above.

Figure III 32 gives a plot of the ratio of experimental angle to

the angle predicted by the theory without strain-hardening, against values of the applied impulse as abscissa. There is a very steep rise in the curves over a relatively short range of impulse values, and the angular ratio tends to become constant at about 0.6 for most plots. The poor agreement in the low impulse range is probably due to elastic vibrations. If the plot is changed to that of the ratio of the experimental angle to the angle predicted by analysis <u>including</u> strain-hardening, no significant change in the shapes of the graphs occurs. The plots of deflection ratios against impulse are shifted upward from those of Fig. III 32 so that the horizontal portions of the curves are at 0.7 approximately.

To further investigate the evidence for a strain-hardening influence, the ratio of the experimental angle to the angle predicted by the elementary theory is plotted against the experimental angle in Fig. III 33. At the large angular deformation values the curves should show a <u>downward</u> slope if strain-hardening influences or axial constraints are important. This does not seem to be the case. It strongly suggests the presence of other influences, in particular of strain rate sensitivity.

Figure III 34 shows the variation of the same angle ratio plotted against R, (the ratio of input energy to the maximum elastic bending energy the beam can absorb). For $R > 3$ the angular ratio is substantially constant for all materials. Taken by itself this indicates that for $R > 3$, approximately, elastic effects are no longer important, in these tests.

In discussing Parkes's solution to the fixed-ended beam problem in Section 2 of this chapter a "mode approximation" solution was described (Martin and Symonds 1966). This proceedure was applied to the present problem with the effects of strain hardening introduced into the analysis,

using the linear relationship between moment and curvature and the same coefficient λ as used by Florence and Firth. The technique was described by Symonds (1965) for the impact cantilever test. Fig. III 35 shows a comparison between the elementary rigid-plastic solution, the solution of Florence and Firth with strain hardening only, and the mode solution for various values of the parameter z/h where h is the beam depth and z is the length of the plastic region. The great advantage of the mode solution is the ease with which approximate final deformation values are obtained, when strain-hardening or other secondary effects are put into the analysis. It has the disadvantage that one must guess a suitable value for the parameter z/h, although for a considerable range of z/h the shift of the deformation curves is slight. The fact that the final deformed shapes of the test specimens were relatively straight makes it plausible to expect the mode approximation method to be valid. The curves given in Fig. III 35 do show better agreement than the curves from the elementary or the strain-hardening-corrected theory of Florence and Firth.

This observation suggests the use of a strain rate correction, either in an analysis analogous to Florence and Firth's for strain hardening, or in a mode approximation solution (as by Symonds (1965) and Bodner (1967)). The latter has been done, although the plots are not shown. Using again the power type formula equation (3.1) for the strain rate - overstress dependence, with constants $D = 40$, $p = 5$ for steel; $D = 6500$, $p = 4$ for aluminum, leads to the surprising result that the corrections are too large for steel (both cold rolled and annealed) and too small for the aluminum alloys. This is opposite to what would be expected from the known

strain rate behavior of these metals; annealed mild steel would be expected to exhibit stronger rate sensitivity than any of the others. It is notable also that the general extent of disagreement with the uncorrected rigid-plastic theory, as indicated by Table III 11, is about the same for all the test metals: aluminum alloys, cold rolled steel, and annealed steel. Since the strain-hardening slopes (Table III 10) of all the materials are not widely different, the lack of strong variations in these disagreements with elementary theory here is an argument for strain-hardening as the leading secondary effect, contrary to the indications from Fig. III 33.

It is seen that the analysis of Florence and Firth's experiments leads to conclusions rather different from, but less clear, than those deduced from analyses of experiments on cantilevers in the previous Sections. The comparisons with elementary rigid-plastic analysis show that this approach, in the authors' words, "serves as a reasonable first-order theory". The plots of Fig. III 34 would indicate that the neglect of elastic deformations is permissible for loads such that the energy ratio $R > 3$. On the other hand the plots of Fig. III 33 by themselves suggest that strain-hardening is not the main source of discrepancies even for rotations larger than 0.5 radians; if it were, the agreement with an analysis neglecting strain-hardening would get worse and the trend of the plots would be downward. It is also possible that <u>both</u> elastic deformations and strain-hardening remain important, and that the two phenomena counterbalance each other in the region where the impulse and deformation angle are large. Similarly an interaction between elastic deflections and strain rate effects may be occurring.

To sum up, while the experiments on cantilevers with tip masses of

Parkes, Bodner and Symonds, and recently Bodner (1967), have given definite indications of the dominant role of strain rate sensitivity, and of the applicability of mode approximation techniques, the experiments on supported and clamped beams of Florence and Firth indicate that the discrepancies between predicted and observed deformation magnitudes in their tests stem rather from interactions between two or more secondary effects. Further research is needed to fully distinguish the roles of elastic deformation, strain-hardening, and strain rate sensitivity, without neglecting attention to the possibility of important axial constraint effects and plastic shear deformations.

Figure Captions for Chapter III

Figure	Caption
III 1	Summary of calculated and experimental results for cold-rolled steel beams, adapted from Duwez, Clark and Bohnenblust(1950).
III 2	Comparison of angular deformations measured in tests of Duwez, Clark and Bohnenblust (1950) with predictions of elastic-plastic analysis and of rigid-plastic analysis with inclusion of several secondary effects.
III 3	Impact of a mass on a long beam: diagrams for rigid-plastic analysis.
III 4	Experiments of Parkes and typical final shapes of specimens: (a) tests on cantilevers (Parkes, 1955); (b) tests on fixed-ended beams (Parkes, 1956, 1958). The falling weight has mass G, initial velocity V_o.
III 5	Parkes's cantilever test: diagrams for rigid-plastic analysis. The striking mass G is assumed to stick to the beam after impact, but is omitted in sketches (b) and (d).
III 6	Results from Parkes's (1955) tests on mild steel cantilevers, shown in comparison with deformation angle predicted by rigid-plastic analysis using static fully plastic moment. θ_o is given by Equation (2.10); $\beta = mL/2G$.
III 7	Parkes's (1955) tests on mild steel cantilevers: test deformation angles are shown in comparison with magnitude predicted by elementary rigid-plastic analysis, with dynamic plastic moment substituted for the static value.
III 8	Parkes's (1955) tests on mild steel cantilevers: comparison of test angles with elementary rigid-plastic theory. Each pair of test points joined by a line has same β (same specimen geometry) but different velocity and final deflection. If rigid-plastic analysis is valid except for omission of strain-hardening, agreement with theory would be worse at larger strains; in fact, agreement is better at larger strains.
III 9	Parkes's (1956, 1958) tests on fixed-ended beams: patterns of deformation in elementary rigid-plastic analysis. Sketch of test arrangement does not show the actual end-fixing devices, which prevented rotation but permitted axial motion.
III 10	Pattern of configuration assumed in the "mode approximation" solution, with one degree of freedom.
III 11	Results of Parkes's tests on fixed-ended beams (parkes 1956, 1958), and comparisons with theory. Displacement y in inches of impacted point is plotted against length ratio $r = L_1/L_2$ with constant L_2 as shown. Curves were calculated from rigid-plastic "mode approximation" theory; full curves use static fully plastic moment,

Figure	Caption
III 11 (cont.)	dashed curves use dynamic plastic moment, corresponding to strain estimated from Equation (2.29), hinge length taken as 0.5 in. in all cases.
III 12	Results of Parkes's tests on fixed-ended beams: ratio of test deflection to deflection predicted by rigid-plastic (mode approximation) solution using static fully plastic moment.
III 13	Evidence from Parkes's tests on mild steel fixed-ended beams concerning influence of strain rate sensitivity of fully plastic moment. Pairs of test points joined by lines have same input kinetic energy but different velocity. Plot is of ratio of test deflection to that predicted by rigid-plastic analysis (mode solution) using static fully plastic moment. (Compare Fig. III 16).
III 14	Lower yield stress dependence on strain rate of mild steel according to tests of Manjoine (1944). (See Fig. I 6 for comparison with other strain rate test results). Curve of dynamic plastic moment was derived by Parkes (1955) from Manjoine's stress curve (method not specified).
III 15	Curves used by Parkes (1956, 1958) for dynamic plastic moment of duralumin and brass as functions of strain rate. Dynamic yield stress data for duralumin attributed to Klinger (1950), Evans (1942) and Whiffin (1948); for brass to Jones and Moore (1940). (But see Fig. III 18 for actual curves of Evans for duralumin and brass, showing these metals as rate insensitive up to about $\dot{\varepsilon} = 6$ sec^{-1}.)
III 16	Parkes's test results for mild steel fixed-ended beams: comparison with rigid-plastic analysis (by mode approximation solution) using dynamic plastic moment. Compare this plot with that of Fig. III 13 using static plastic moment.
III 17	Static moment-curvature test diagrams of metals used in Parkes's tests.
III 18	Tensile impact test curves of Evans (1942): σ_o = "yield point stress"; σ_m = "tensile strength".
III 19	Comparison of (a) mild steel and (b) 6061-T6 aluminum impulse test results of Bodner and Symonds (1962) with elementary rigid-plastic theory and with theories taking account of strain rate sensitivity. Curves (A) and (D) take M_p as constant with respectively the static and appropriate dynamic magnitude; curves (B) and (C) take M as a function of local strain rate.
III 20	Impulse test results of Bodner and Speirs (1963) on 3003-H14 aluminum at (a) room temperature; (b) at 212°F; (c) at 400°F.

Figure	Caption
III 21	Notation for "impact"problem: cantilever with imposed base acceleration. Beam may be taken as initially moving with constant velocity V_o; then base is brought to rest in a specified short time t_o.
III 22	Patterns of deformation for the impact problem; regions of plastic deformation of opposite signs are indicated in (C).
III 23	Curves summarizing how the initial deformation pattern in the impact problem depends on the base acceleration V_o/t_o and the mass ratio $k = G/mL$. The curves show where the negative moment has its largest magnitude for a given a and k. The acceleration plotted is dimensionless, $a = mL^2V_o/M_pt_o$ (From Ting and Symonds, 1962).
III 24	Comparisons of impact test results on (a) mild steel and (b) 6061-T6 aluminum with predictions of elementary rigid-plastic analysis. Also shown are a curve representing the approximate viscoplastic solution due to Ting and Symonds (1962) and one result from the "complete" viscoplastic solution of Ting (1963). Test deformation angles are shown for the test points.
III 25	(a) Representative computed curves for the impulse problem of $A = (\dot{k}m/B)^{1/P}$ and A/z as functions of time, from Ting (1964). Note that 1 + A is the ratio of dynamic moment at the base to the static fully plastic moment; M_pA/z is the shear force at the base. (b) Representative computed curves for the impulse problem of the length z of the plastic zone and the curvature rate $\dot{k}m$ at the base, as functions of time (from Ting, 1964).
III 26	Comparison of viscoplastic theories and test results with rigid-plastic solution of impulse problem.
III 27	Representative computed curves for the impulse problem from Ting (1964); note nearly linear decrease of angular velocity $\dot{\theta}_1$.
III 28	Representative computed curves for the impact problem, from viscoplastic solution of Ting and Symonds (1962); curves are for dynamic moment at base M_m/M_p and shear force at base q.
III 29	Typical curves for impact problem from Ting and Symonds's (1962) viscoplastic solution. (a) shows plastic zone length z and curvature rate at base $\dot{k}m$ as functions of time. (b) shows nearly linear decrease of angular velocity $\dot{\theta}_1$ as function of time, $t > t_o$.

Figure	Caption
III 30	Notation for tests and analyses of Florence and Firth (1965).
III 31	Typical results of Florence and Firth (1965): (a) and (b) show central deflection as functions of impulse per unit length; (c) shows final deformation curves. Superscripts have the following meaning: (1) designates elementary rigid-plastic solution; (2) designates rigid-plastic solution with correction for finite deflections; (3) designates rigid-plastic analysis with strain hardening included.
III 32	Plots from results of Florence and Firth's tests (1965); comparison of deformation angle (near support) observed in test with uncorrected rigid-plastic theory plotted against unit impulse. If this type of analysis is valid, and disagreement is attributed to strain hardening, the discrepancy should increase as the load impulse increases; plots show opposite trends.
III 33	Plots from results of Florence and Firth's (1965) experiments. Values of test deformation angle divided by prediction of uncorrected rigid-plastic theory are plotted as function of experimental angle.
III 34	Plots from results of Florence and Firth's (1965) experiments. Values of test deformation angle divided by prediction of uncorrected rigid-plastic theory are plotted against energy ratio F.
III 35	Comparison of deformation angles observed in Florence and Firth's (1965) tests with elementary rigid plastic solution, with Florence and Firth's solution correcting for strain hardening, and with "mode approximation" solution considering strain hardening.

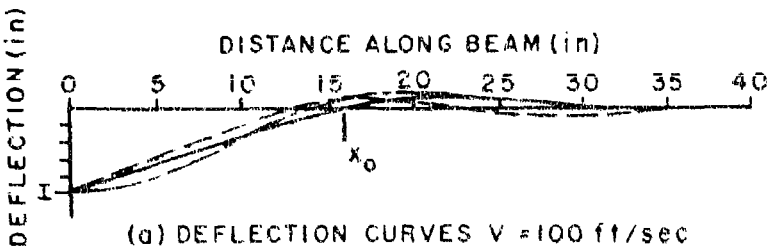

(a) DEFLECTION CURVES V = 100 ft/sec

IMPACT DURATION 0.87×10^{-3} sec

EXPERIMENTAL CURVE ————

THEORETICAL CURVE – – – – –

THEORETICAL ASSUMING ELASTIC BEAM ——·——

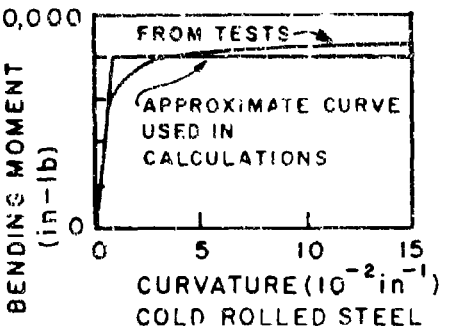

(b) BENDING MOMENT–CURVATURE RELATIONS

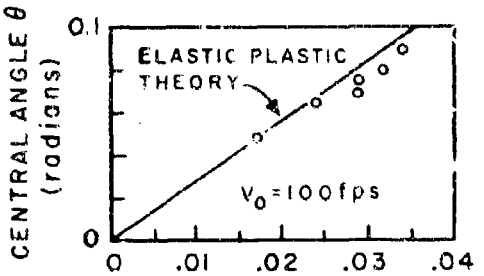

(d) ANGLE θ VS $\sqrt{t}$

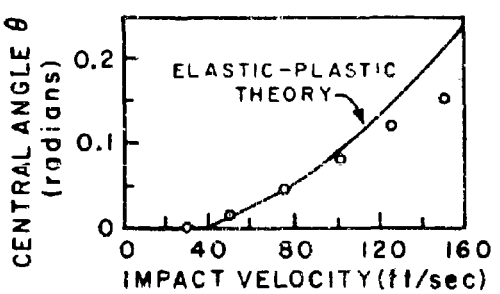

(c) ANGLE θ VS IMPACT VELOCITY V_0

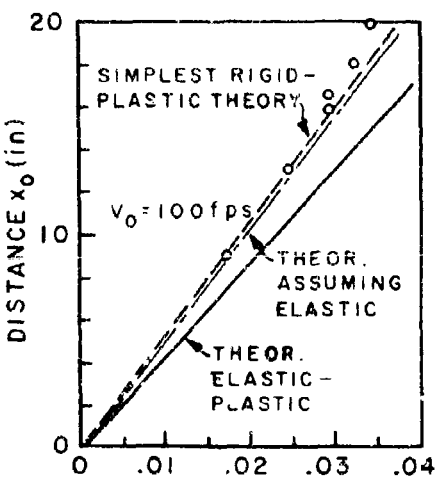

(e) DISTANCE x_0 VS $\sqrt{t}$

TESTS ON COLD ROLLED STEEL BEAMS

DUWEZ, CLARK, AND BOHNENBLUST (1950)

FIG. III 1

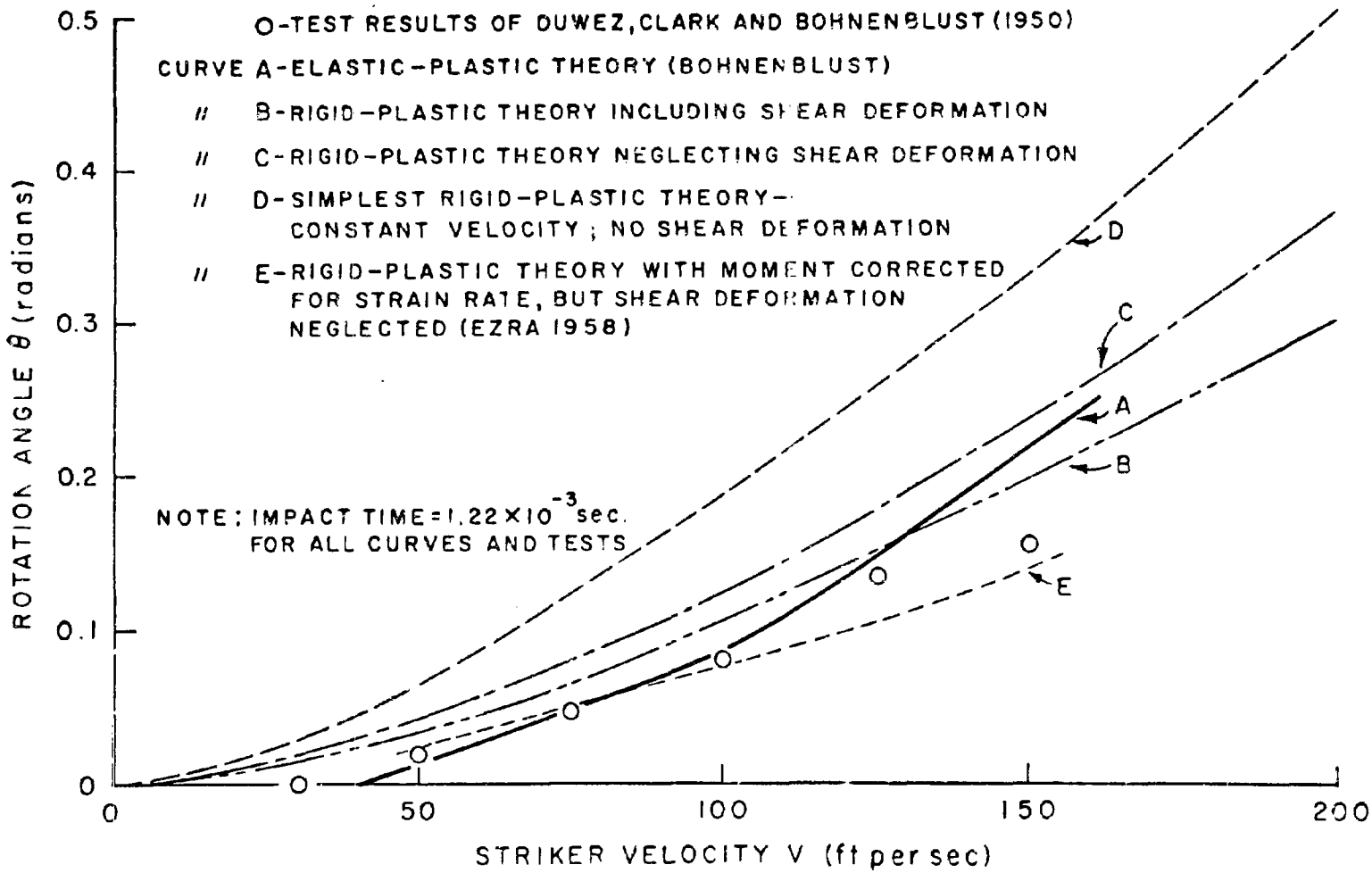
O-TEST RESULTS OF DUWEZ, CLARK AND BOHNENBLUST (1950)
CURVE A-ELASTIC-PLASTIC THEORY (BOHNENBLUST)
// B-RIGID-PLASTIC THEORY INCLUDING SHEAR DEFORMATION
// C-RIGID-PLASTIC THEORY NEGLECTING SHEAR DEFORMATION
// D-SIMPLEST RIGID-PLASTIC THEORY- CONSTANT VELOCITY; NO SHEAR DEFORMATION
// E-RIGID-PLASTIC THEORY WITH MOMENT CORRECTED FOR STRAIN RATE, BUT SHEAR DEFORMATION NEGLECTED (EZRA 1958)
NOTE: IMPACT TIME = 1.22 × 10^-3 sec. FOR ALL CURVES AND TESTS
ROTATION ANGLE θ (radians)
0.5
0.4
0.3
0.2
0.1
0
0
50
100
150
200
STRIKER VELOCITY V (ft per sec)
A
B
C
D
E

FIG. III 2

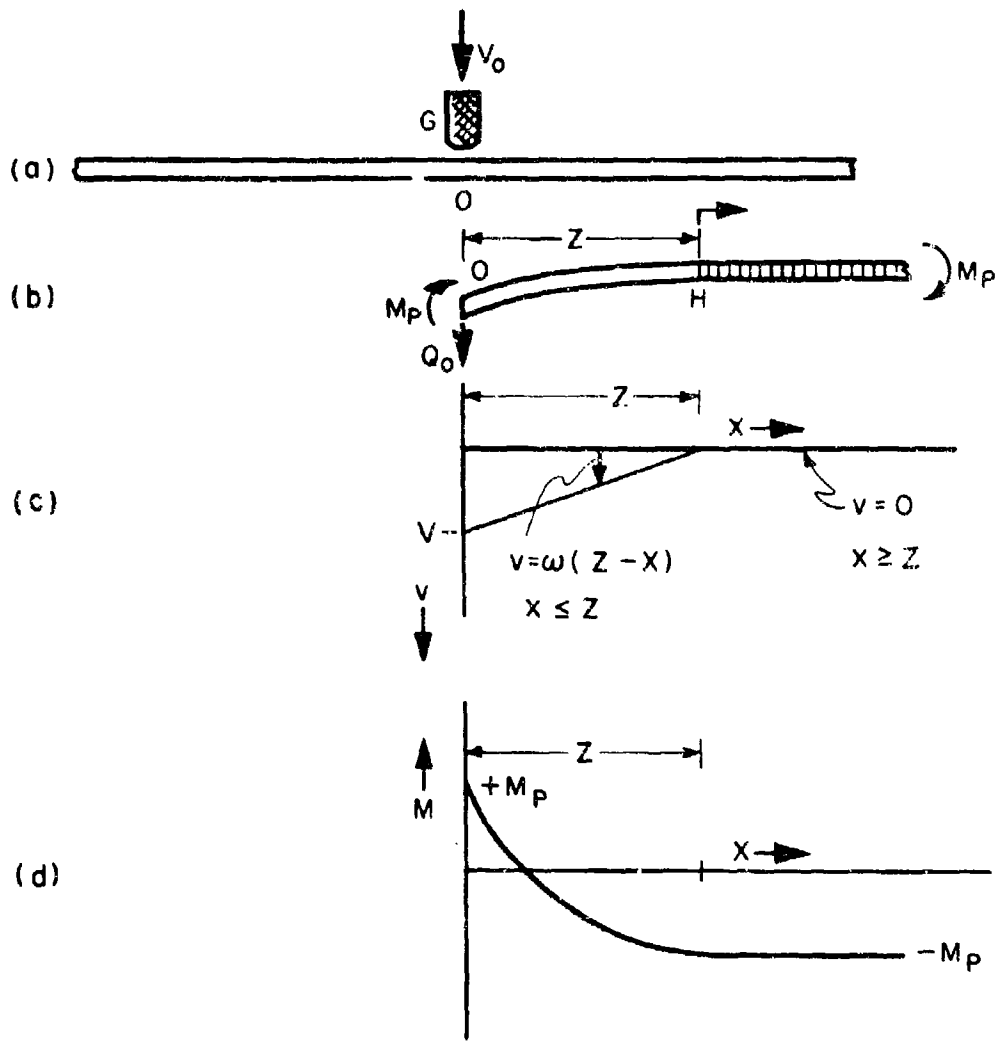

FIG. III 3

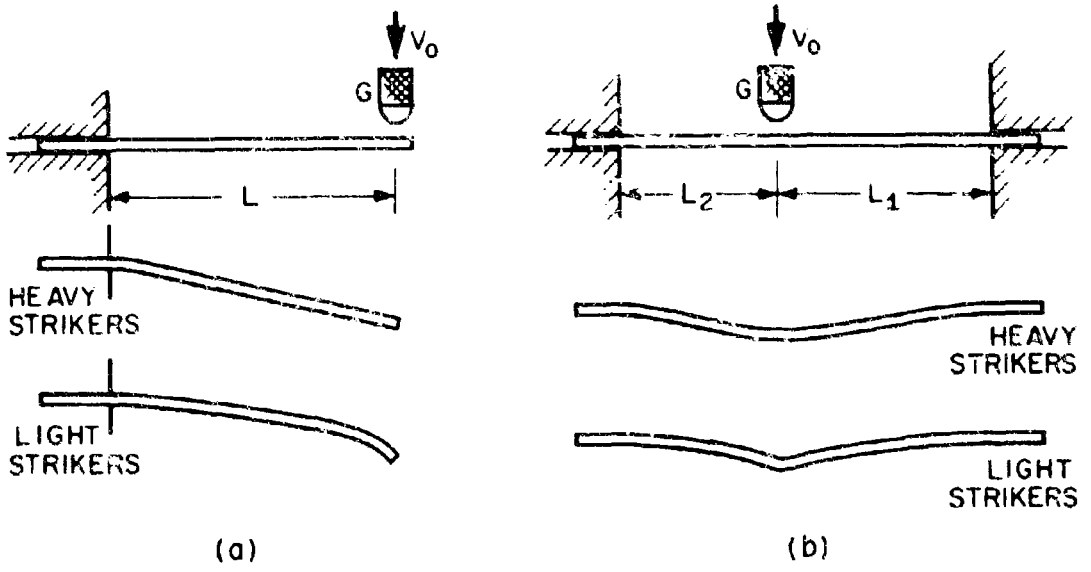

FIG. III 4

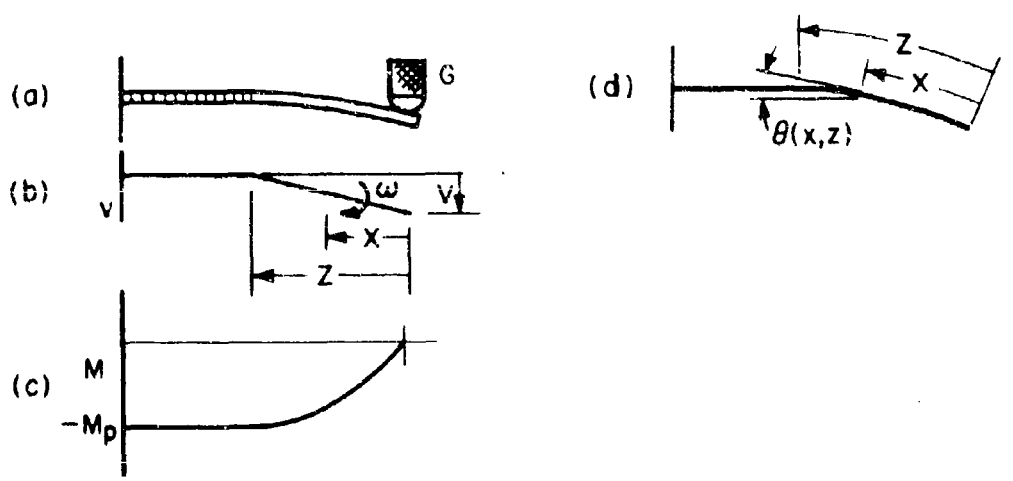

FIG. III 5

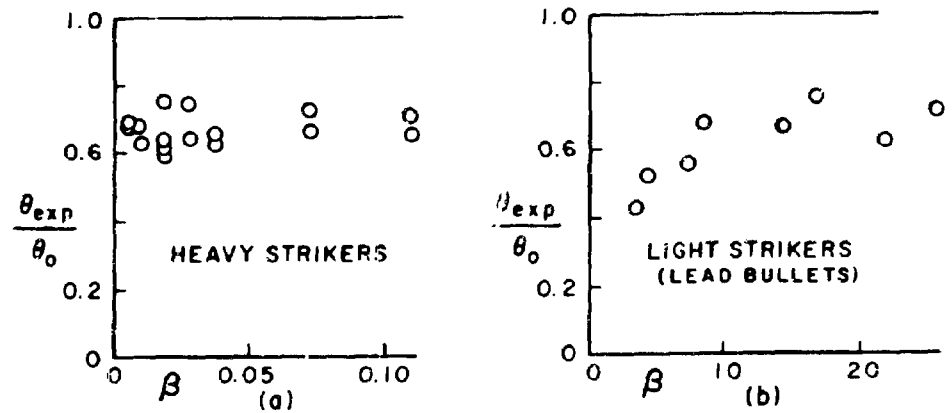

FIG. III 6

θ_0 IS FINAL ANGLE FROM ELEMENTARY RIGID-PLASTIC THEORY - NO STRAIN HARDENING OR STRAIN RATE SENSITIVITY

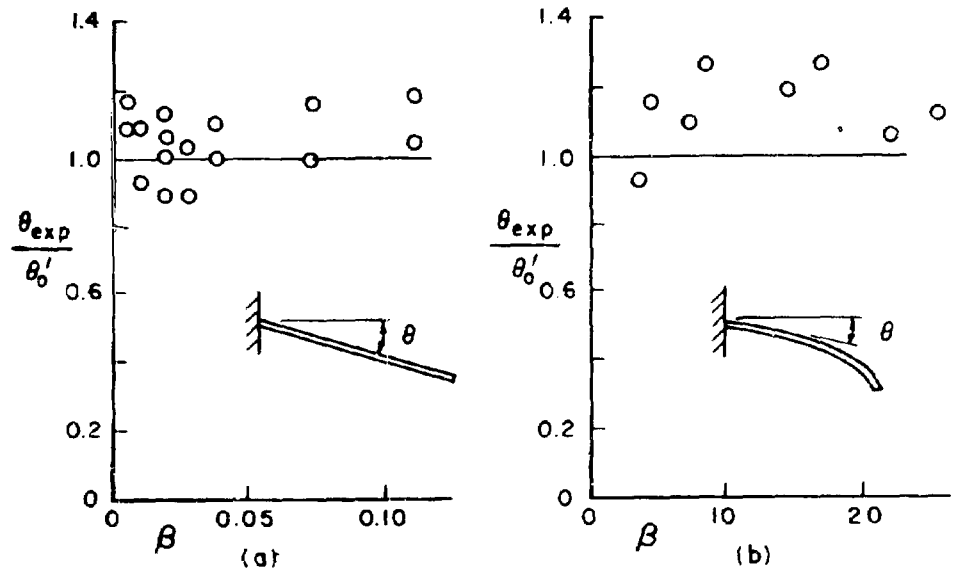

$$\theta_0' = \theta_0 \frac{M(\dot{\epsilon})}{M_p}$$

USING PARKES' STRAIN RATE CORRECTION

IMPULSE (FALLING WEIGHT) TESTS: MILD STEEL
O TEST POINTS, PARKES 1955

FIG. III 7

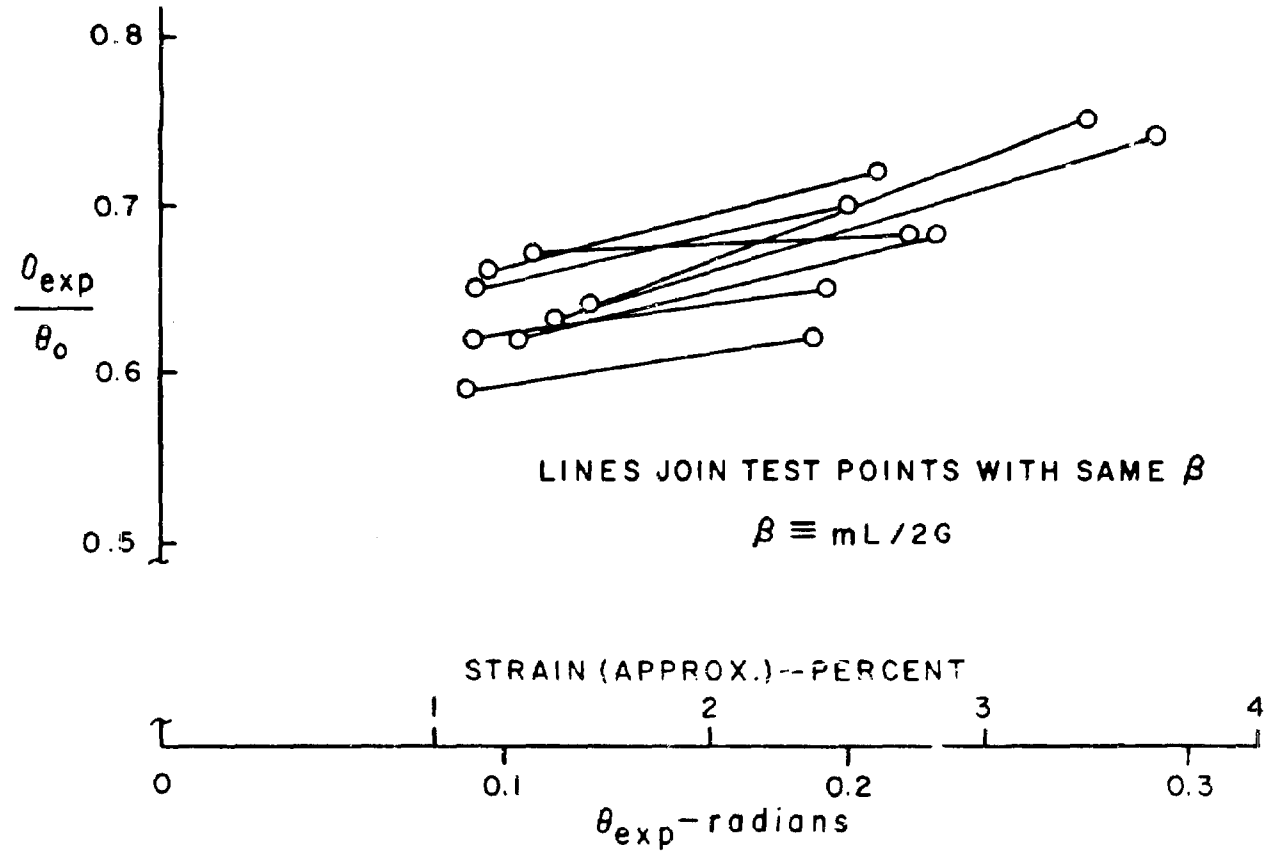

IMPULSE (FALLING WEIGHT) TESTS : MILD STEEL

O TEST POINTS, PARKES 1955.

θ_0 FROM ELEMENTARY RIGID–PLASTIC THEORY

FIG. III 8

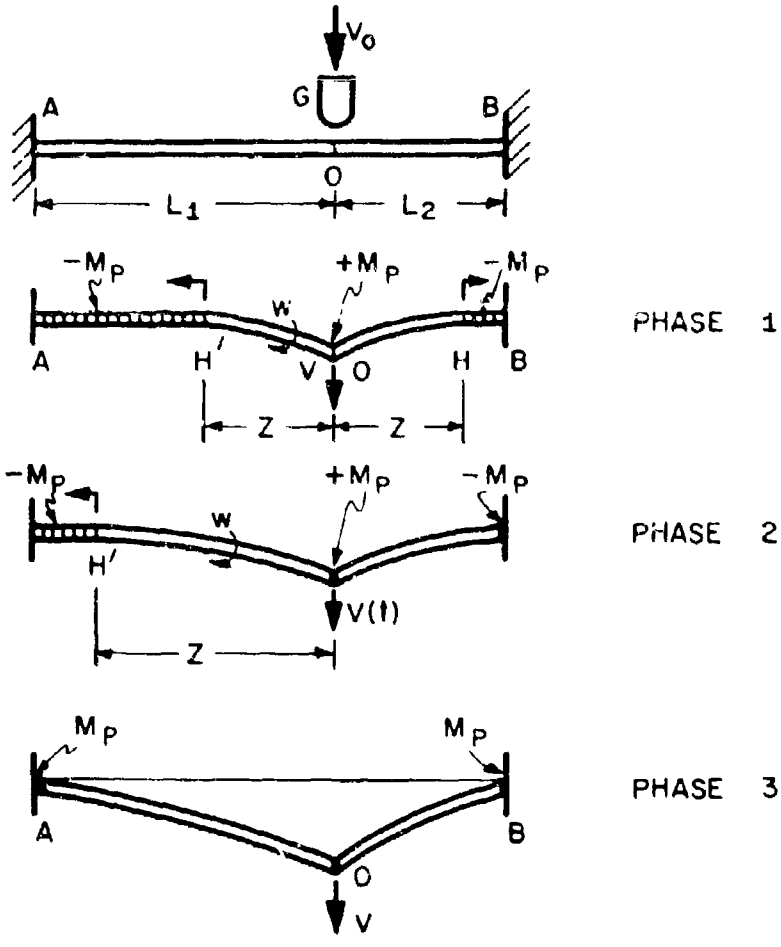

PHASES OF MOTION ACCORDING TO ELEMENTARY RIGID-PLASTIC SOLUTION OF PROBLEM OF CLAMPED – ENDED BEAM UNDER IMPULSIVE LOADING AT AN ARBITRARY POINT. THE STRIKING MASS G IS ASSUMED TO STICK TO THE BEAM AT THE STRUCK POINT O

FIG. III 9

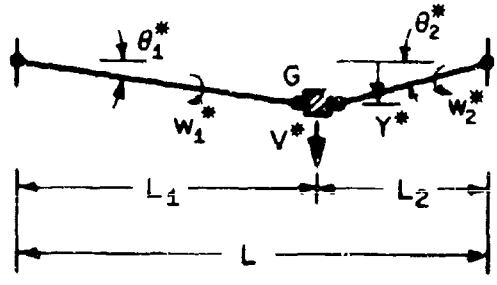

FIG. III 10

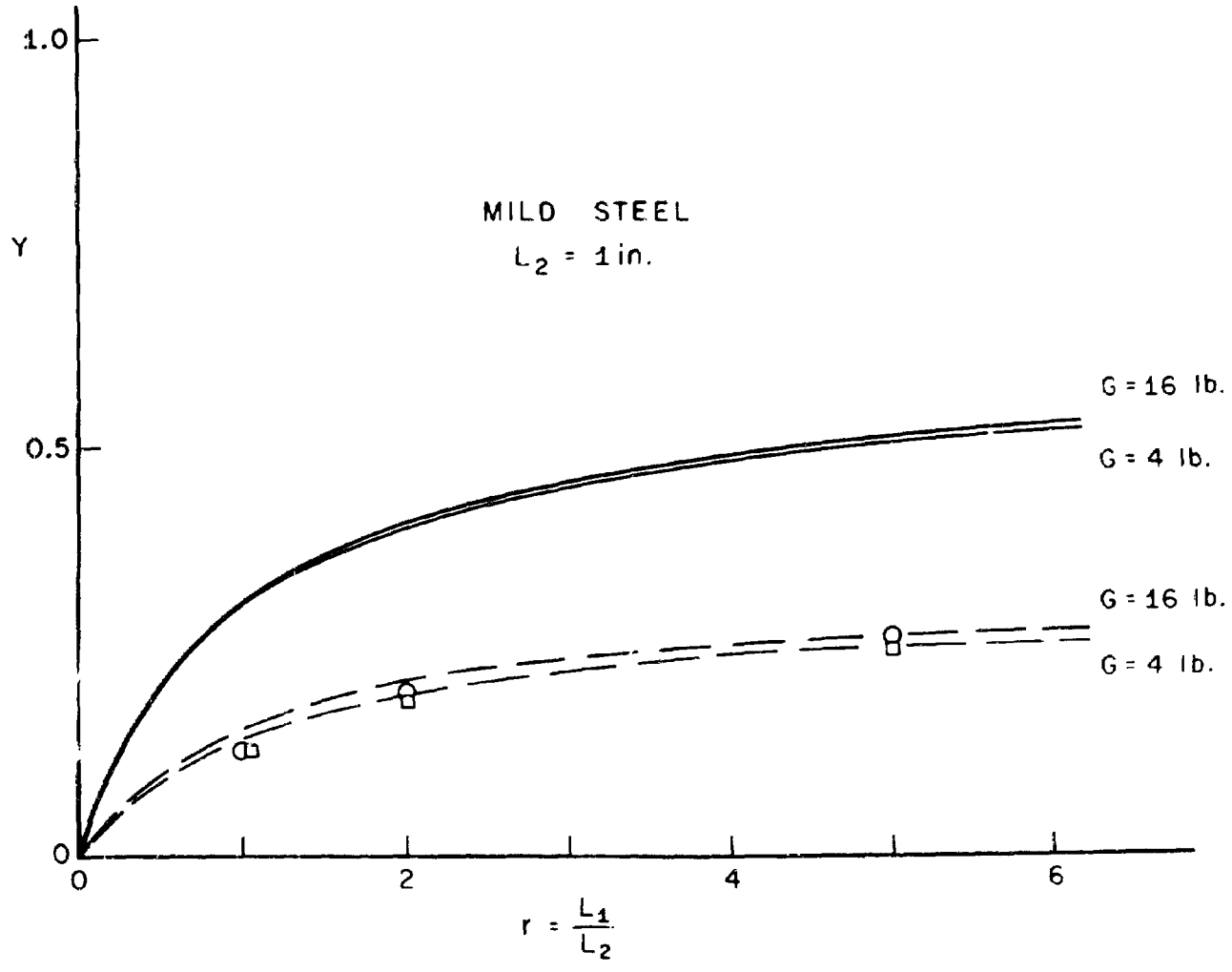
1.0
Y
MILD STEEL
L_2 = 1 in.
0.5
G = 16 lb.
G = 4 lb.
G = 16 lb.
G = 4 lb.
0
0
2
4
6
$r = \frac{L_1}{L_2}$

FIG. III 11(a)

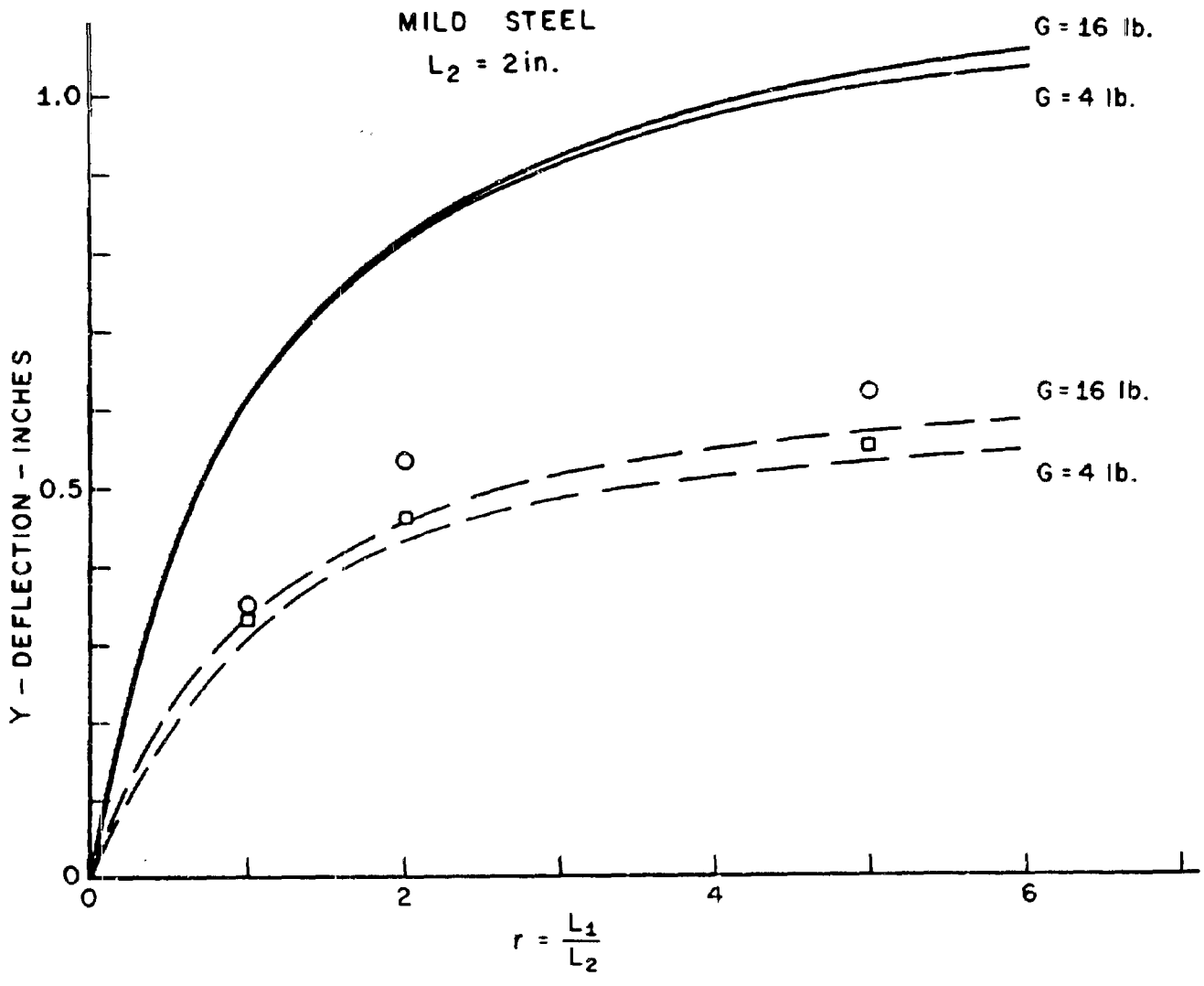
MILD STEEL
L_2 = 2in.
G = 16 lb.
G = 4 lb.
G = 16 lb.
G = 4 lb.
1.0
0.5
0
Y - DEFLECTION - INCHES
0
2
4
6
$r = \frac{L_1}{L_2}$

FIG. III 11(b)

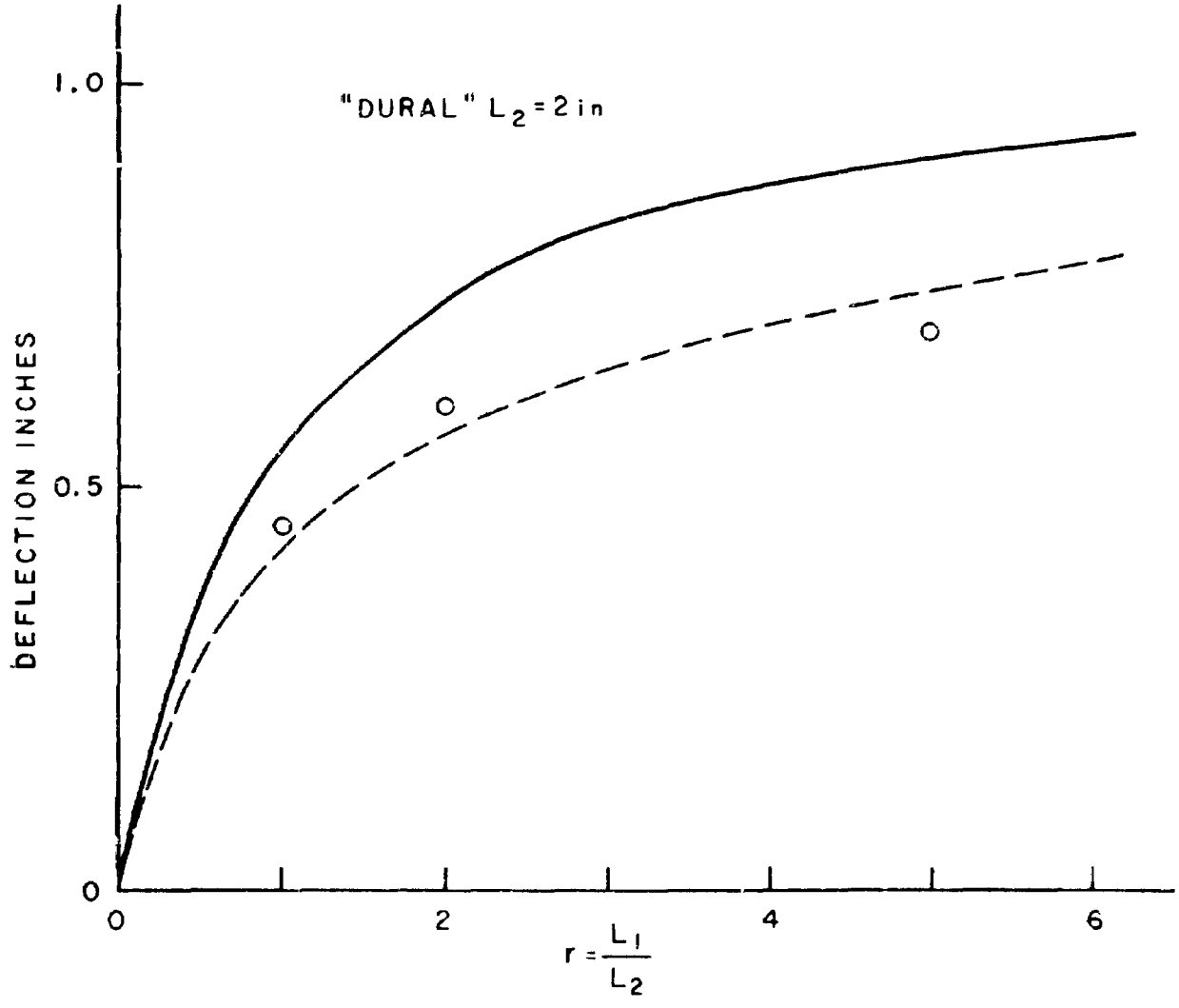

FIG. III 11(c)

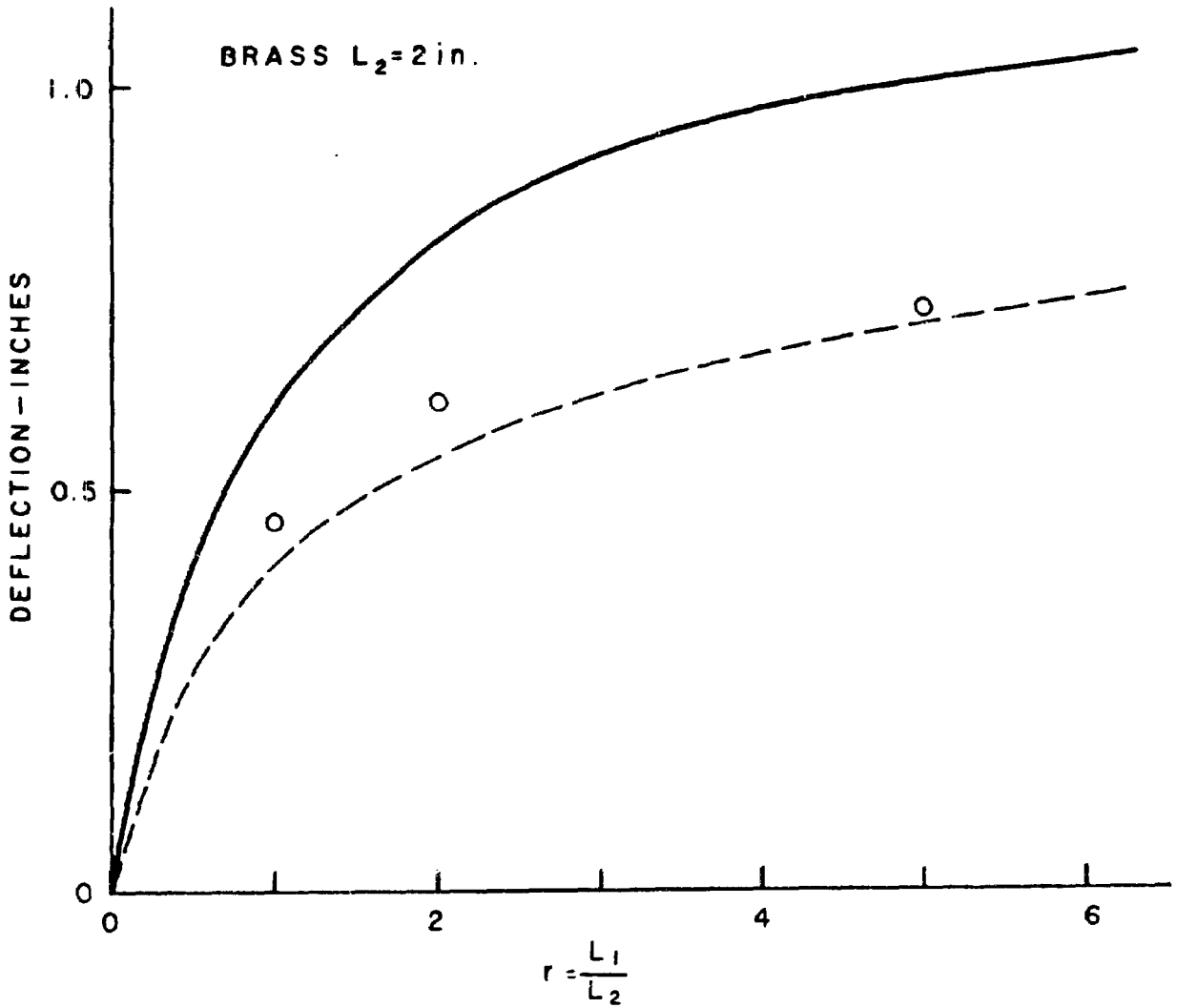

FIG. III 11(d)

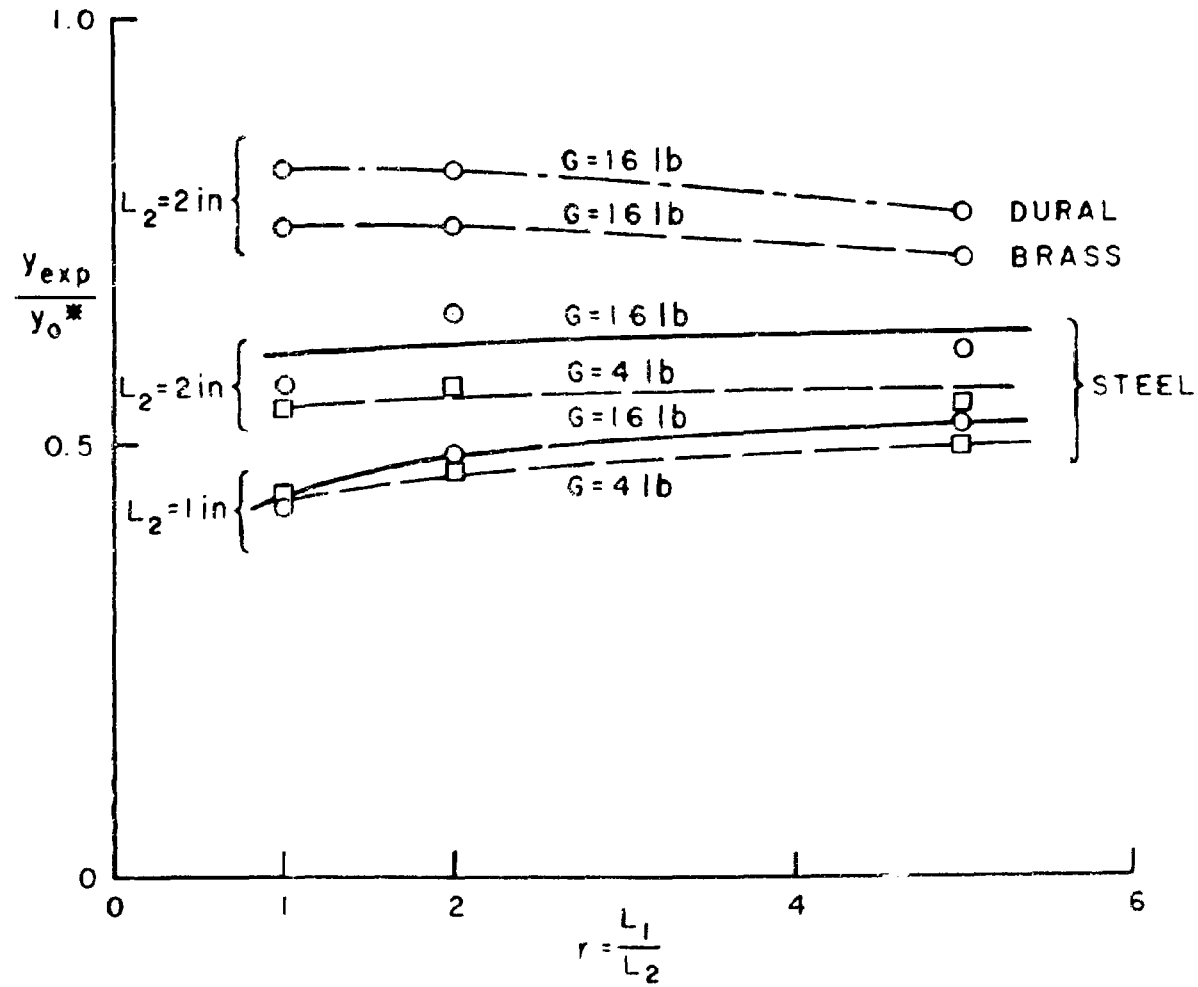
1.0
0.5
0
$\frac{y_{exp}}{y_o^*}$
L_2=2 in
G=16 lb
G=16 lb
DURAL
BRASS
G=16 lb
L_2=2 in
G=4 lb
G=16 lb
STEEL
L_2=1 in
G=4 lb
0
1
2
4
6
$r = \frac{L_1}{L_2}$

FIG. III 12

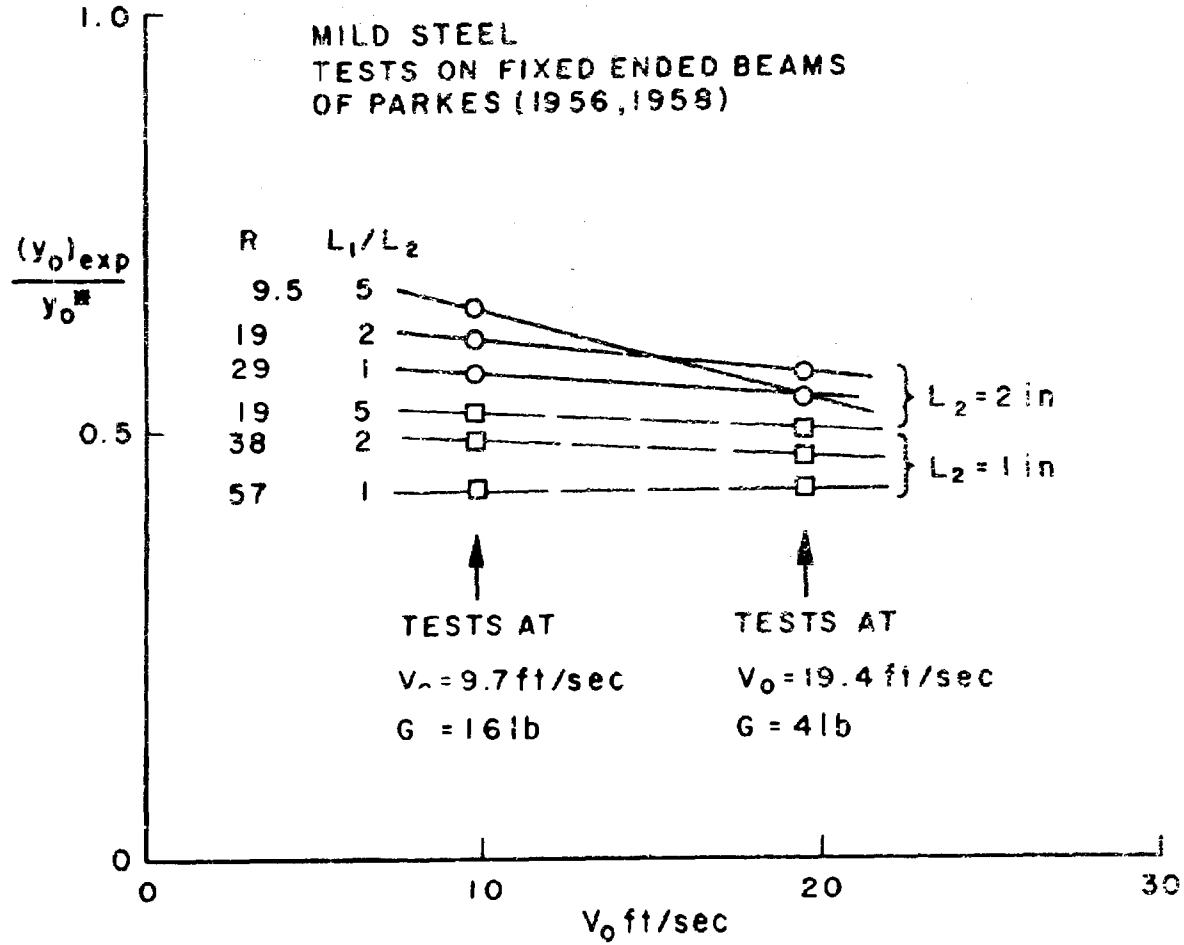
MILD STEEL
TESTS ON FIXED ENDED BEAMS
OF PARKES (1956, 1958)
$\frac{(y_0)_{exp}}{y_0^*}$
1.0
0.5
0
R
L_1/L_2
9.5
5
19
2
29
1
19
5
38
2
57
1
L_2 = 2 in
L_2 = 1 in
TESTS AT
V_0 = 9.7 ft/sec
G = 16 lb
TESTS AT
V_0 = 19.4 ft/sec
G = 4 lb
0
10
20
30
V_0 ft/sec

FIG. III 13

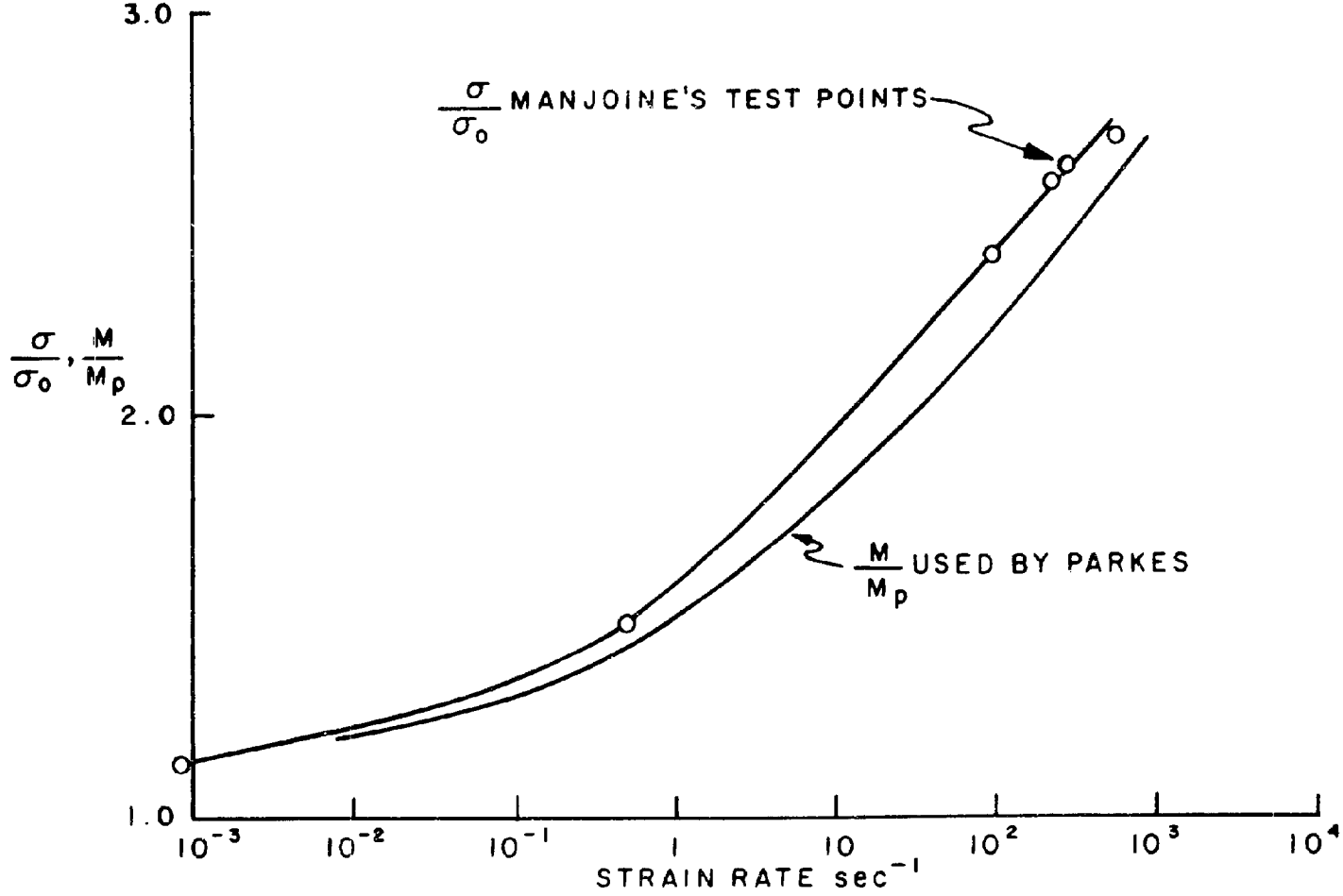

DYNAMIC PLASTIC MOMENT USED BY PARKES (1955, 1956) FOR MILD STEEL

FIG. III 14

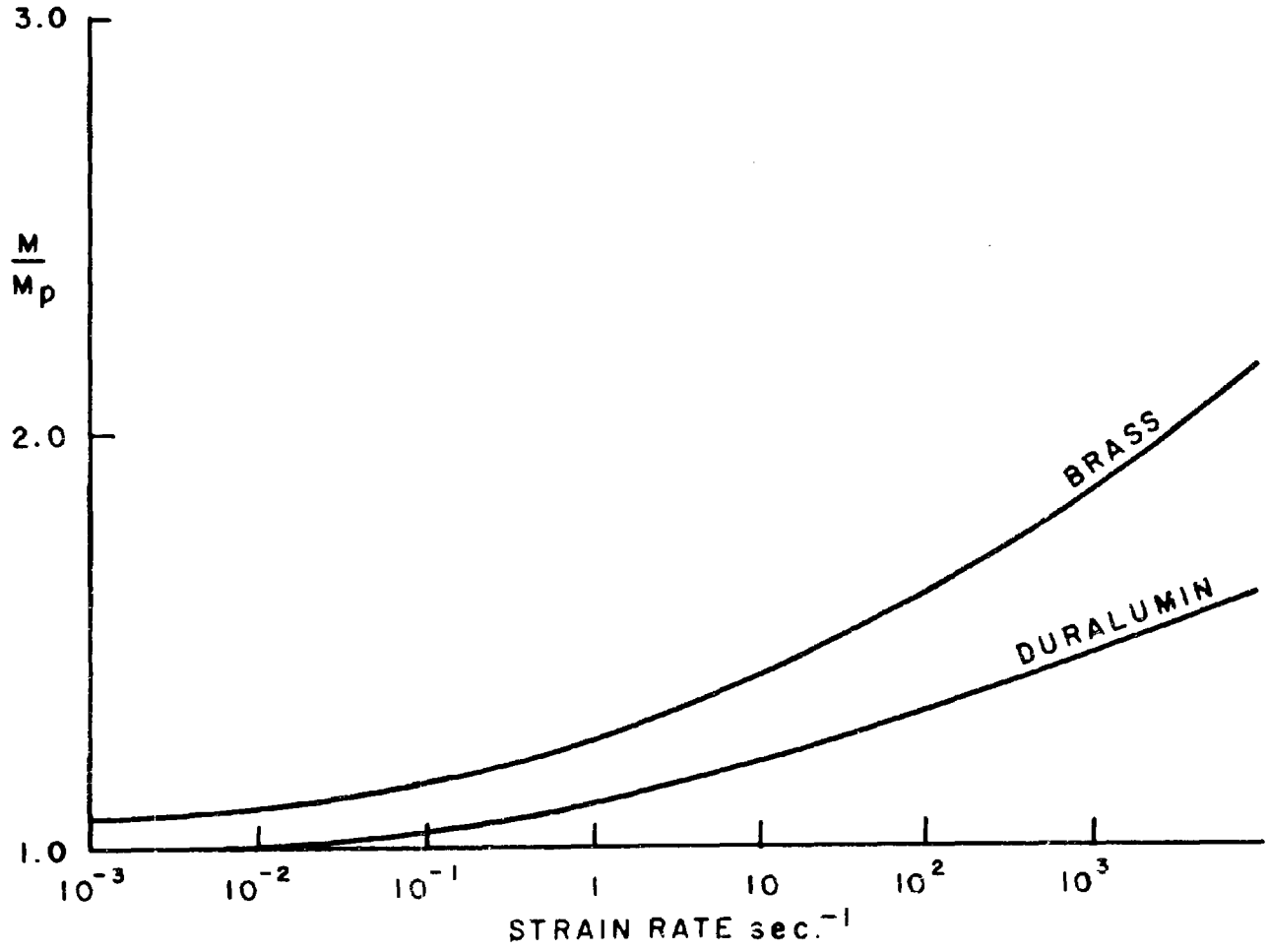

DYNAMIC PLASTIC MOMENT RATIOS FOR BRASS AND DURALUMIN
USED BY PARKES IN ANALYZING FIXED-END BEAM TESTS (PARKES, 1958)

FIG. III 15

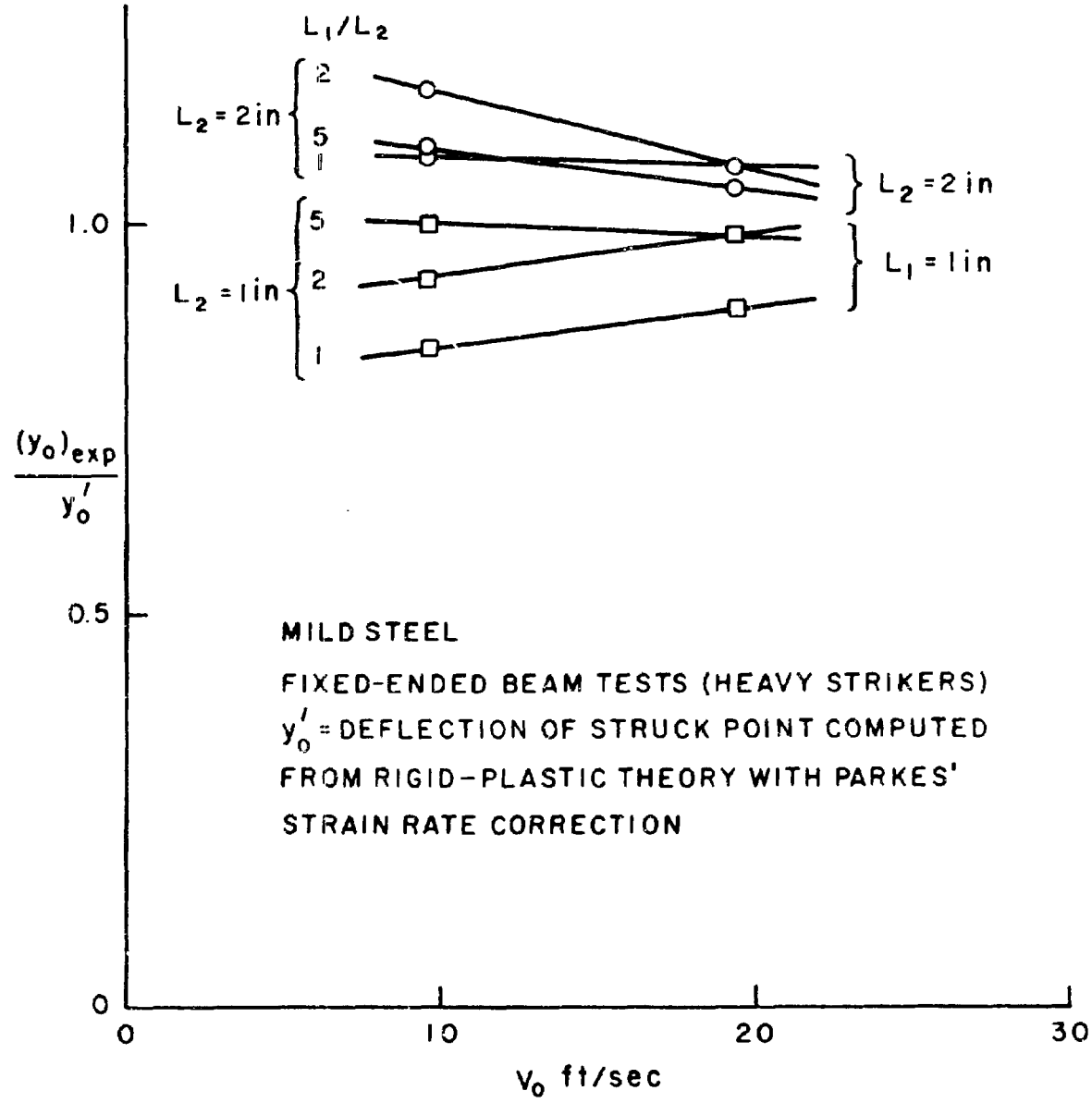
L_1/L_2
$L_2 = 2$ in
2
5
1
$L_2 = 2$ in
$L_2 = 1$ in
5
2
1
$L_1 = 1$ in
1.0
$\frac{(y_o)_{exp}}{y_o'}$
0.5
MILD STEEL
FIXED-ENDED BEAM TESTS (HEAVY STRIKERS)
y_o' = DEFLECTION OF STRUCK POINT COMPUTED
FROM RIGID-PLASTIC THEORY WITH PARKES'
STRAIN RATE CORRECTION
0
0
10
20
30
V_o ft/sec

FIG. III 16

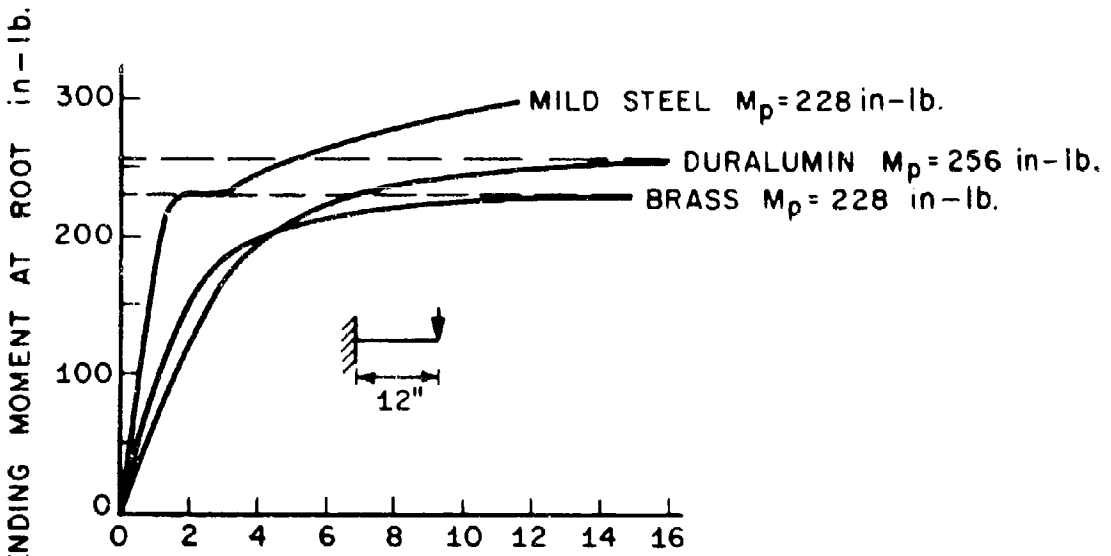

STATIC TESTS ON CANTILEVERS

(PARKES, 1958)

FIG. III 17

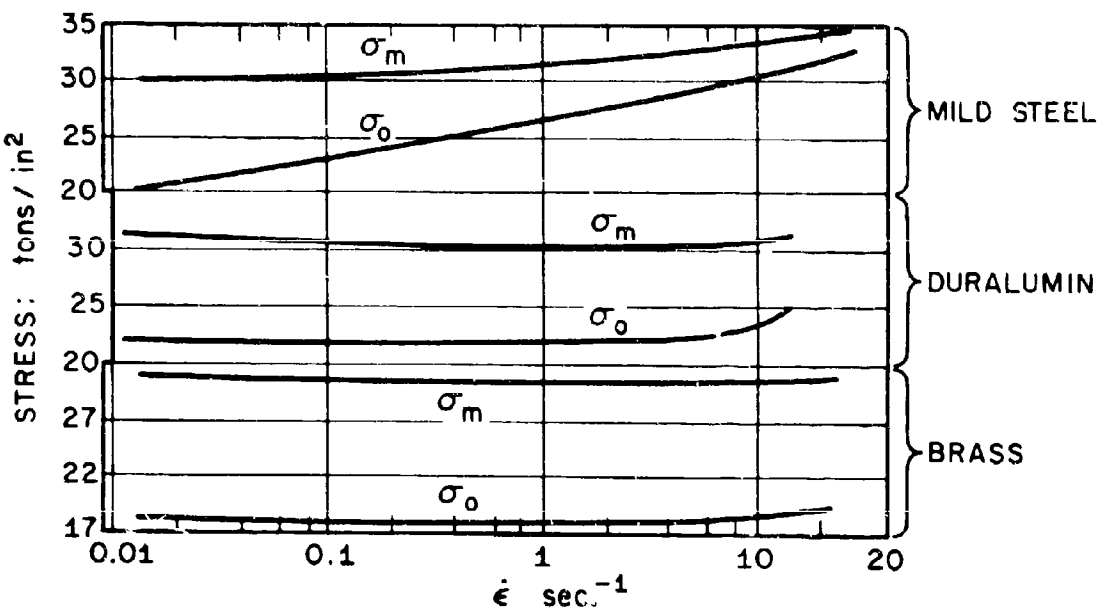

EVANS (1942) TENSILE IMPACT TESTS

FIG. III 18

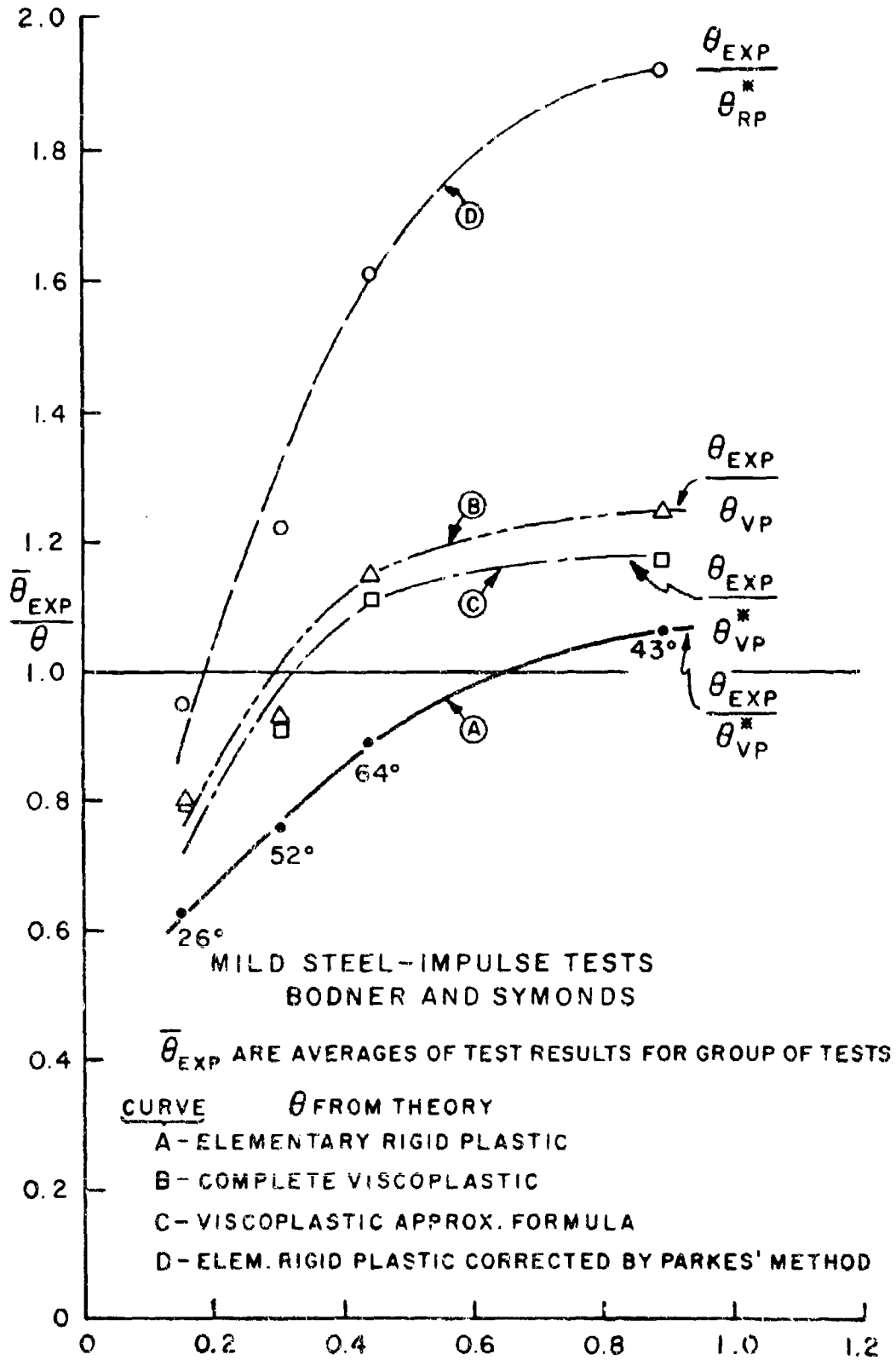
2.0
1.8
1.6
1.4
1.2
1.0
0.8
0.6
0.4
0.2
0
0
0.2
0.4
0.6
0.8
1.0
1.2
$\frac{\bar{\theta}_{EXP}}{\theta}$
$\frac{\theta_{EXP}}{\theta^*_{RP}}$
$\frac{\theta_{EXP}}{\theta_{VP}}$
$\frac{\theta_{EXP}}{\theta^*_{VP}}$
$\frac{\theta_{EXP}}{\theta^*_{VP}}$
A
B
C
D
26°
52°
64°
43°
MILD STEEL - IMPULSE TESTS
BODNER AND SYMONDS
$\bar{\theta}_{EXP}$ ARE AVERAGES OF TEST RESULTS FOR GROUP OF TESTS
CURVE θ FROM THEORY
A - ELEMENTARY RIGID PLASTIC
B - COMPLETE VISCOPLASTIC
C - VISCOPLASTIC APPROX. FORMULA
D - ELEM. RIGID PLASTIC CORRECTED BY PARKES' METHOD

FIG. III 19 (a)

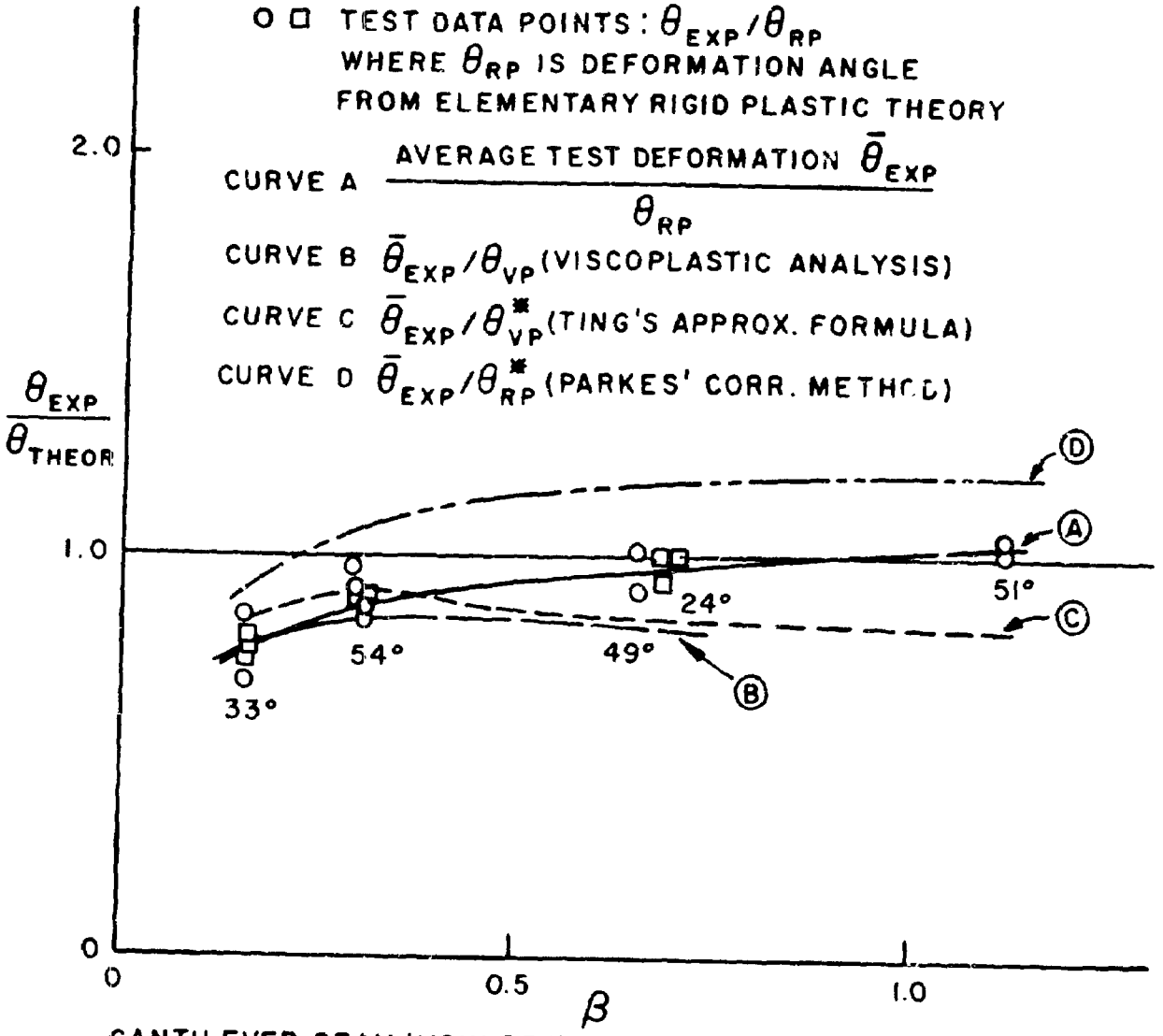

CANTILEVER BEAM IMPULSE TESTS ON 6061-T6 (BODNER & SYMONDS 1962)

FIG. III 19 (b)

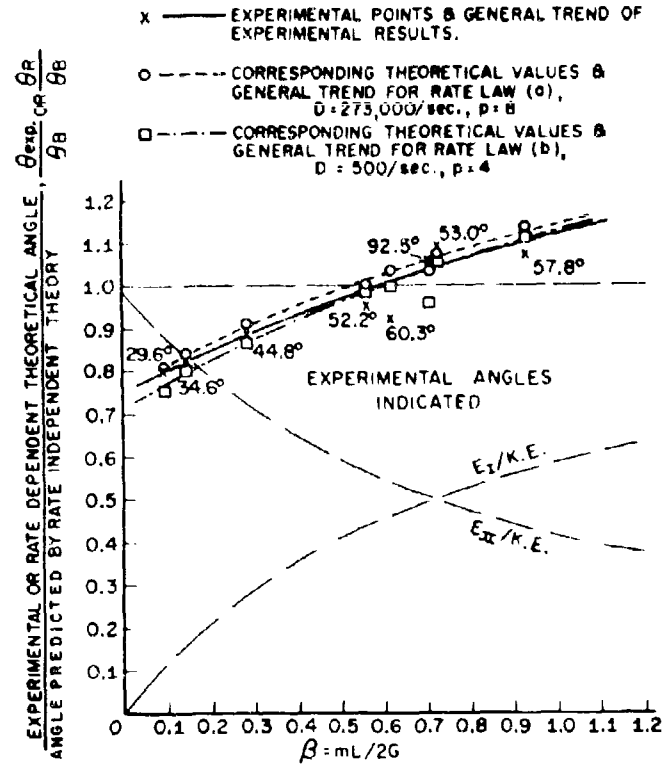

IMPULSE TEST RESULTS AT ROOM TEMPERATURE

FIG. III 20 (a)

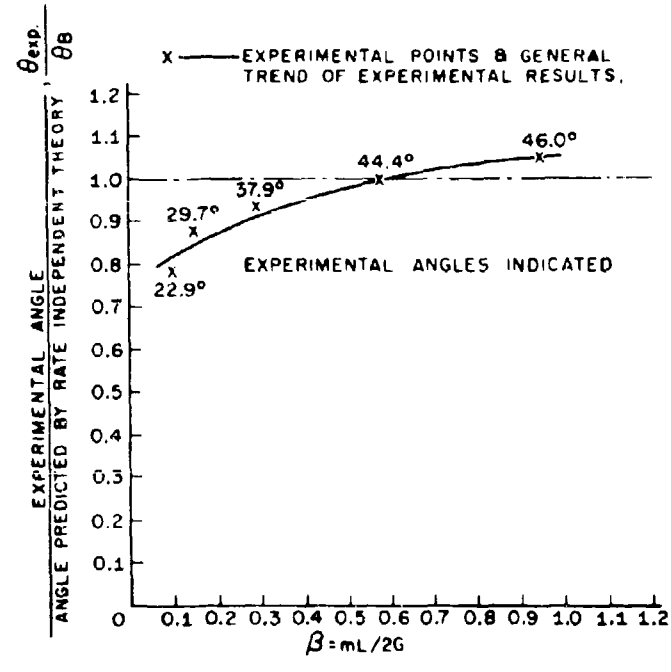

IMPULSE TEST RESULTS AT 212°F

FIG. III 20(b)

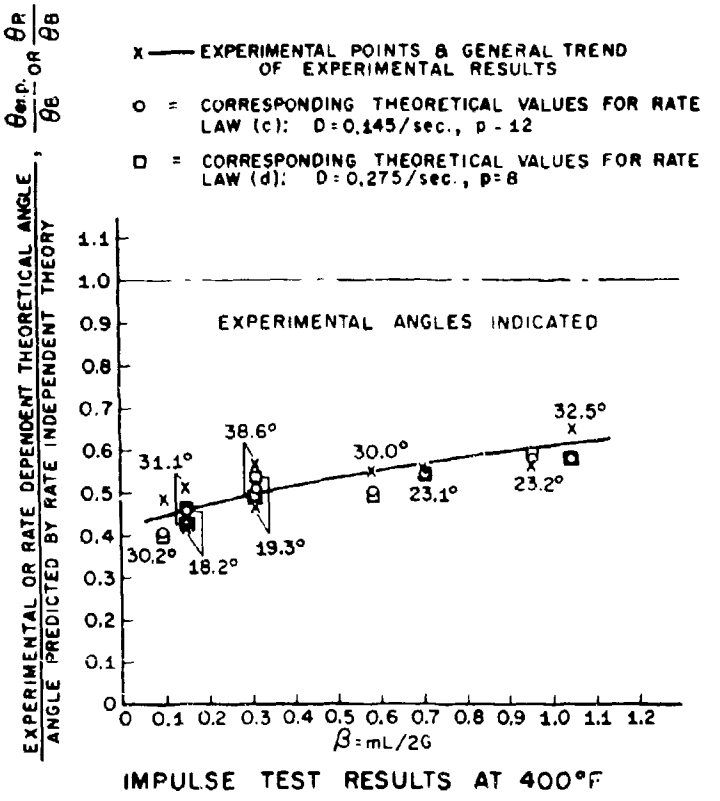

IMPULSE TEST RESULTS AT 400°F

FIG. III 20(c)

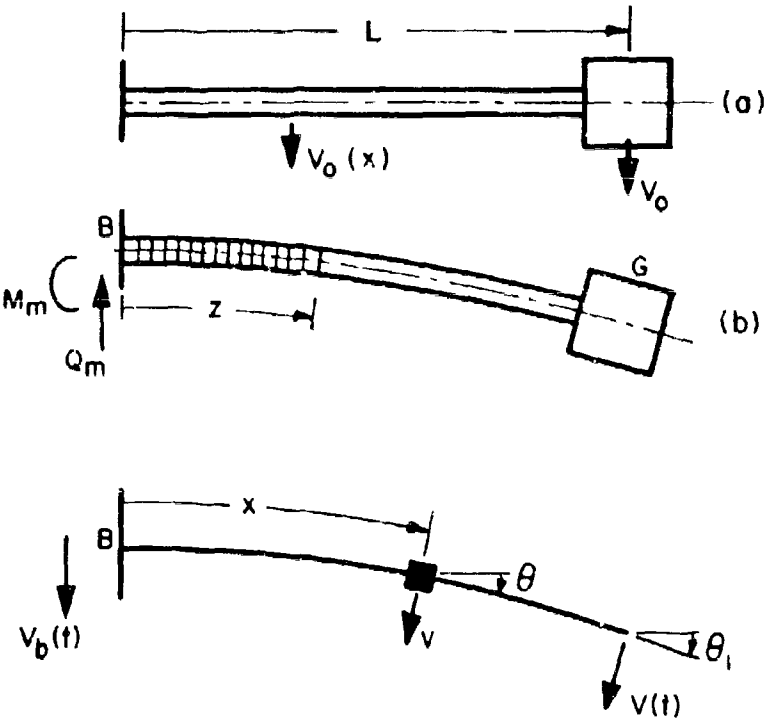

FIG. III - 21

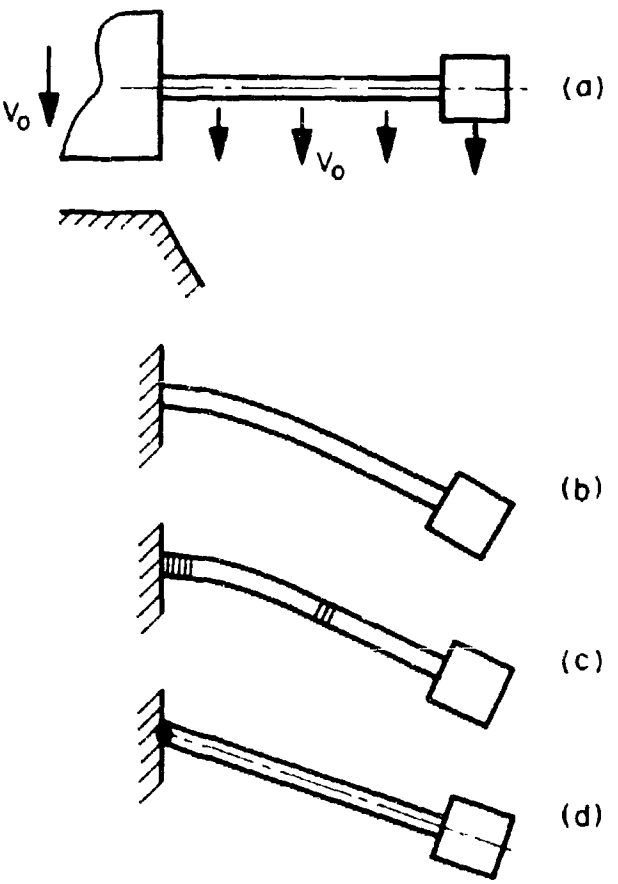

FIG. III 22

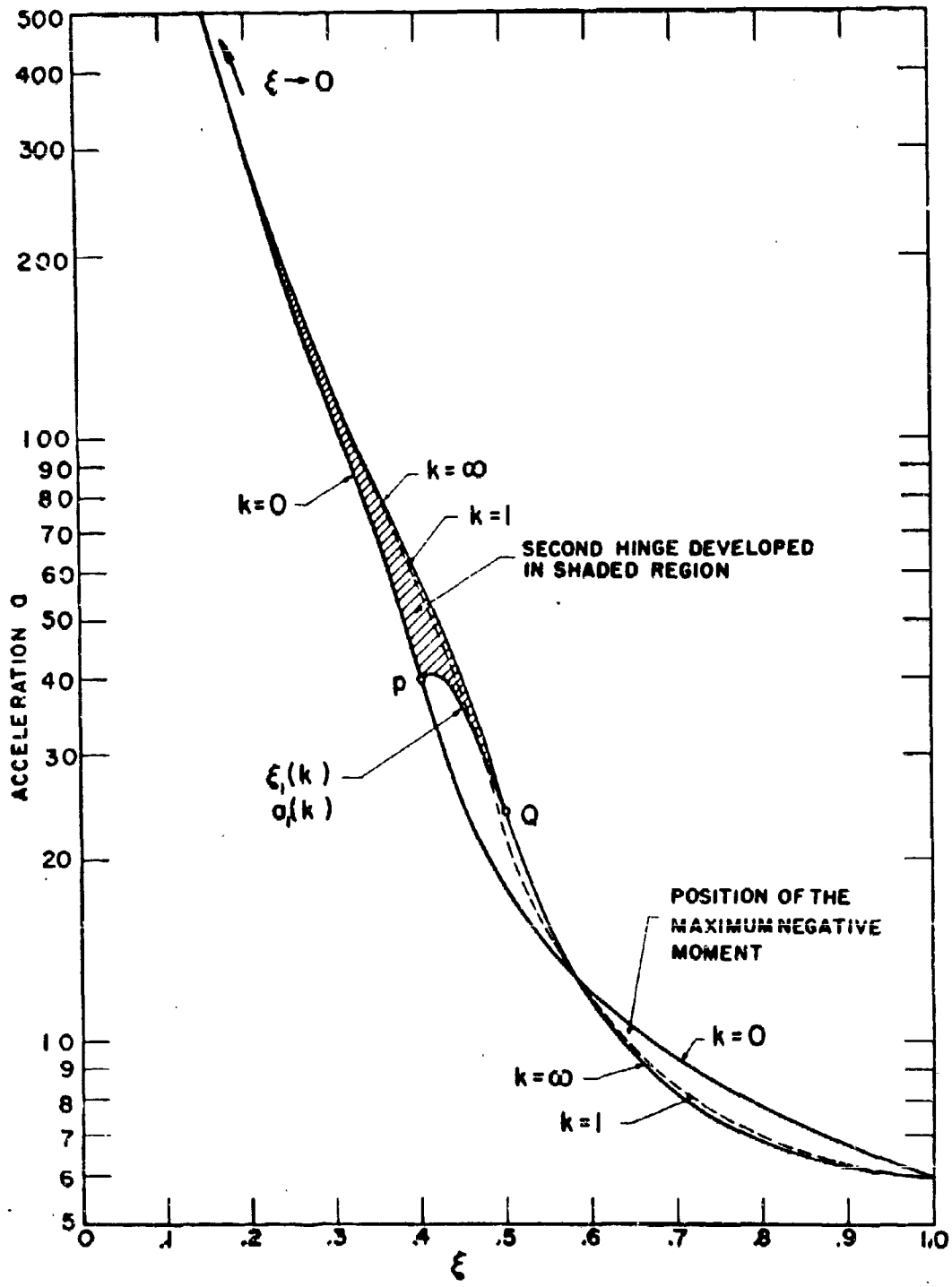
500
400
300
200
100
90
80
70
60
50
40
30
20
10
9
8
7
6
5
ACCELERATION α
ξ→0
k=0
k=∞
k=1
SECOND HINGE DEVELOPED
IN SHADED REGION
P
Q
ξ1(k)
α1(k)
POSITION OF THE
MAXIMUM NEGATIVE
MOMENT
k=0
k=∞
k=1
0
.1
.2
.3
.4
.5
.6
.7
.8
.9
1.0
ξ

FIG. III 23

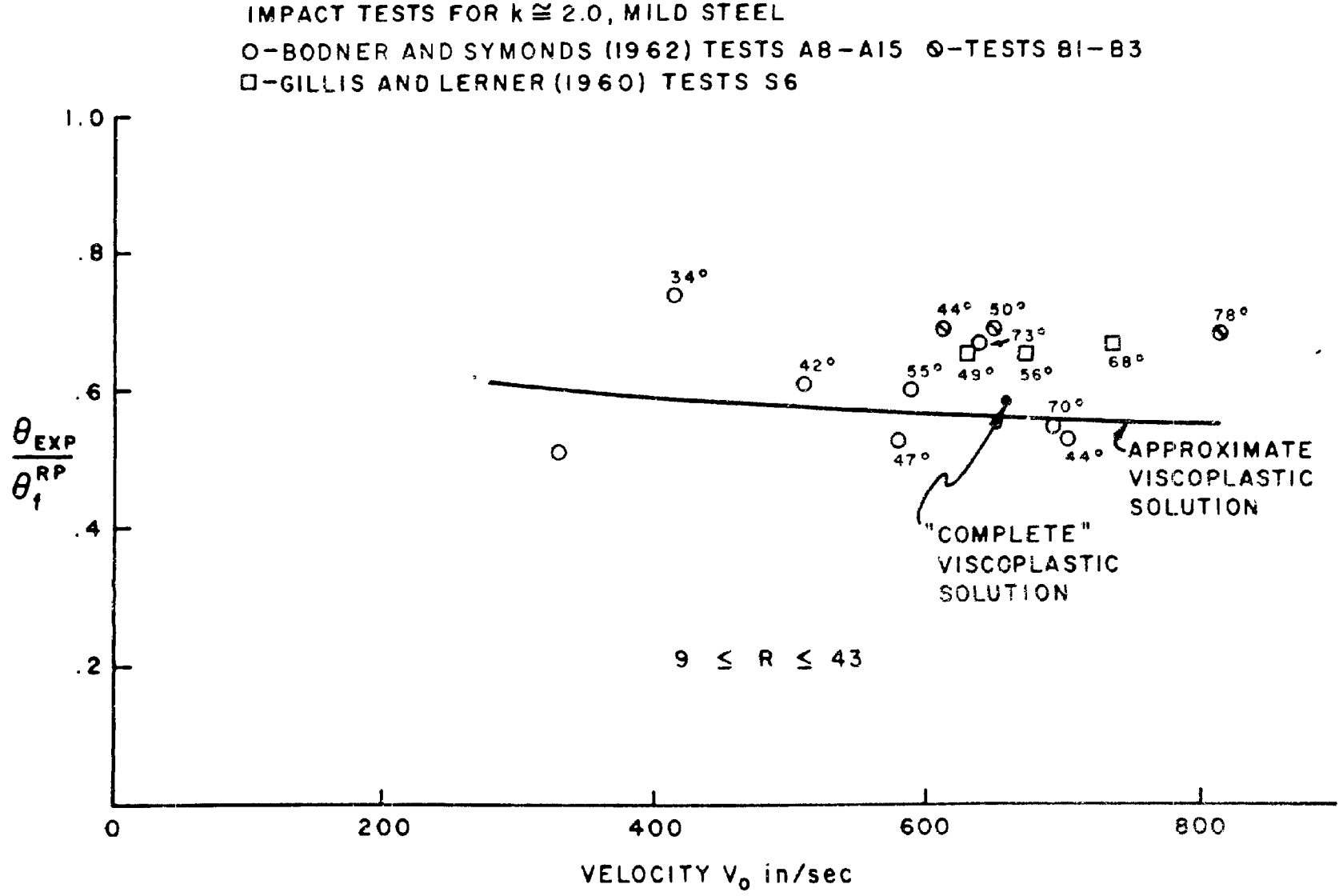
IMPACT TESTS FOR k ≅ 2.0, MILD STEEL
O-BODNER AND SYMONDS (1962) TESTS A8-A15 ⊘-TESTS B1-B3
□-GILLIS AND LERNER (1960) TESTS S6
1.0
.8
.6
.4
.2
θEXP / θ1RP
34°
42°
55°
47°
44° 50°
73°
49°
56°
68°
78°
70°
44°
APPROXIMATE VISCOPLASTIC SOLUTION
"COMPLETE" VISCOPLASTIC SOLUTION
9 ≤ R ≤ 43
0
200
400
600
800
VELOCITY V0 in/sec

FIG. III 24 (a)

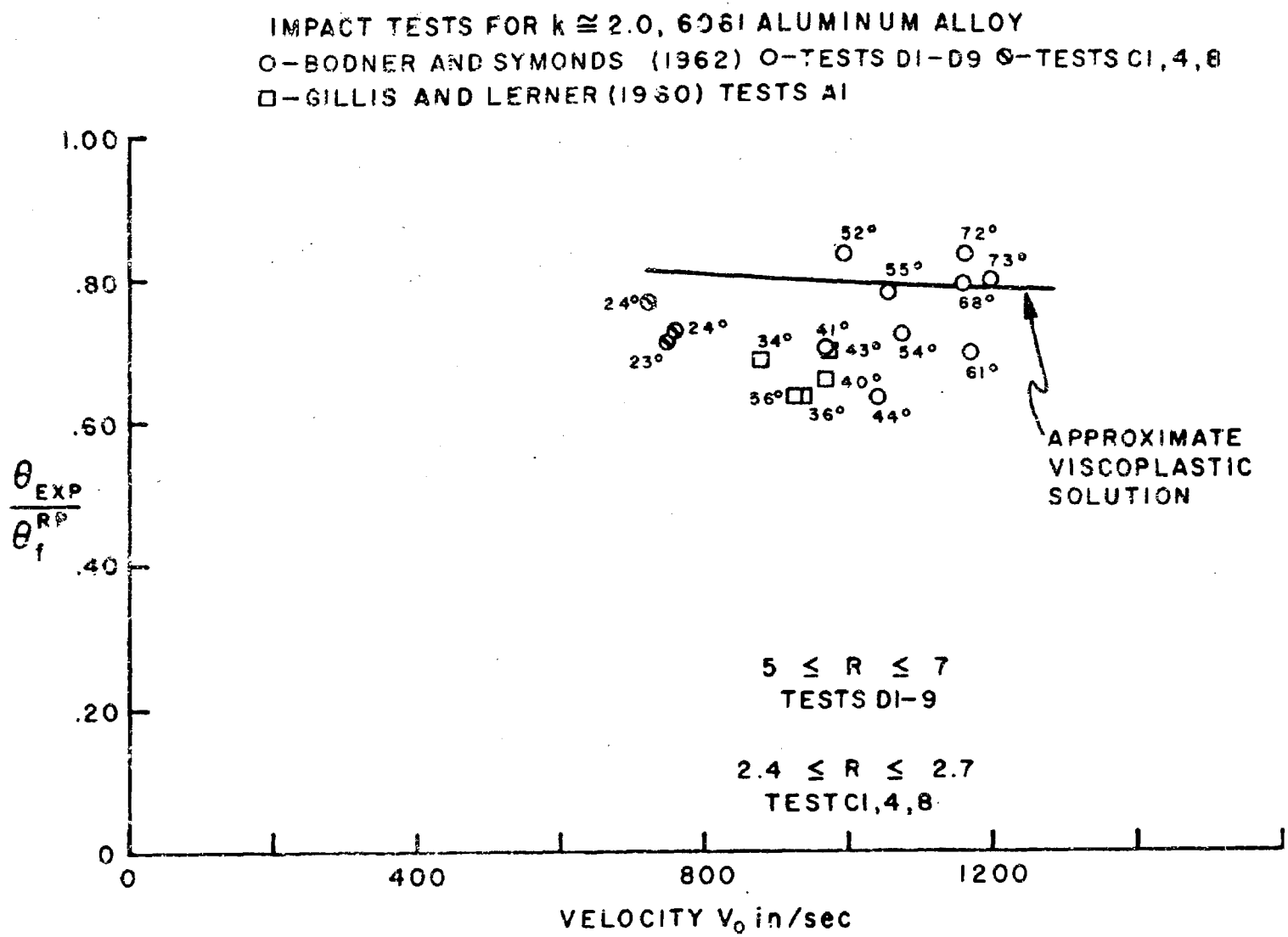
IMPACT TESTS FOR k ≅ 2.0, 6061 ALUMINUM ALLOY
O–BODNER AND SYMONDS (1962) O–TESTS D1–D9 ⊗–TESTS C1,4,8
□–GILLIS AND LERNER (1960) TESTS A1
1.00
.80
.60
.40
.20
0
$\frac{\theta_{EXP}}{\theta_f^{RP}}$
0
400
800
1200
VELOCITY V_0 in/sec
52°
72°
73°
55°
68°
24°
24°
23°
34°
41°
43°
54°
61°
40°
56°
36°
44°
APPROXIMATE VISCOPLASTIC SOLUTION
5 ≤ R ≤ 7
TESTS D1–9
2.4 ≤ R ≤ 2.7
TEST C1,4,8

FIG. III 24(b)

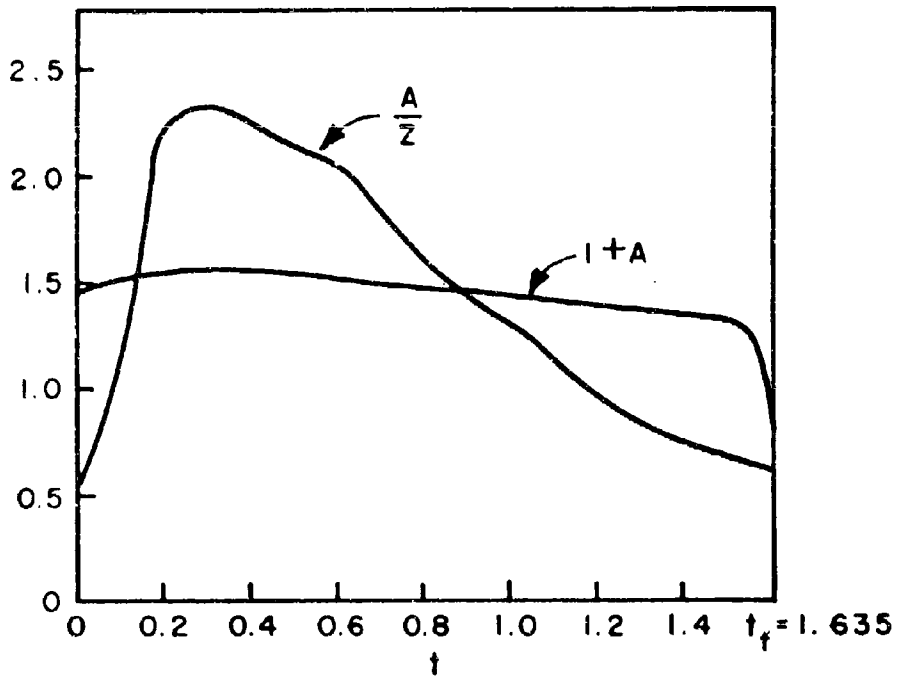

FIG. III 25(a)

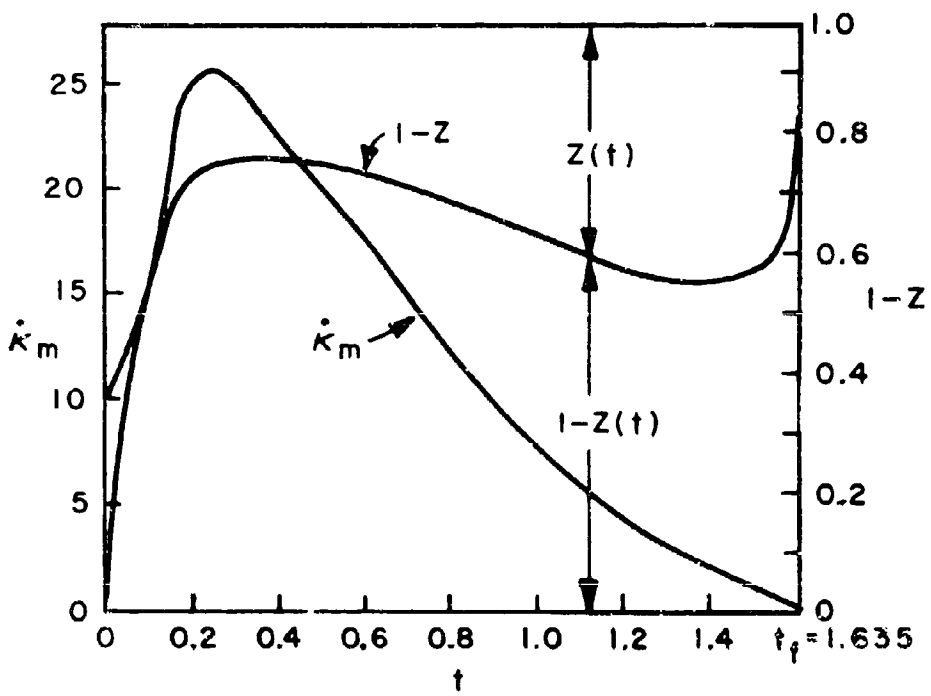

CALCULATED RESULTS—MILD STEEL BEAM
CIMEN E5. IMPULSE TESTS OF BODNER
SYMONDS (1962): k≃1.7

FIG. III 25(b)

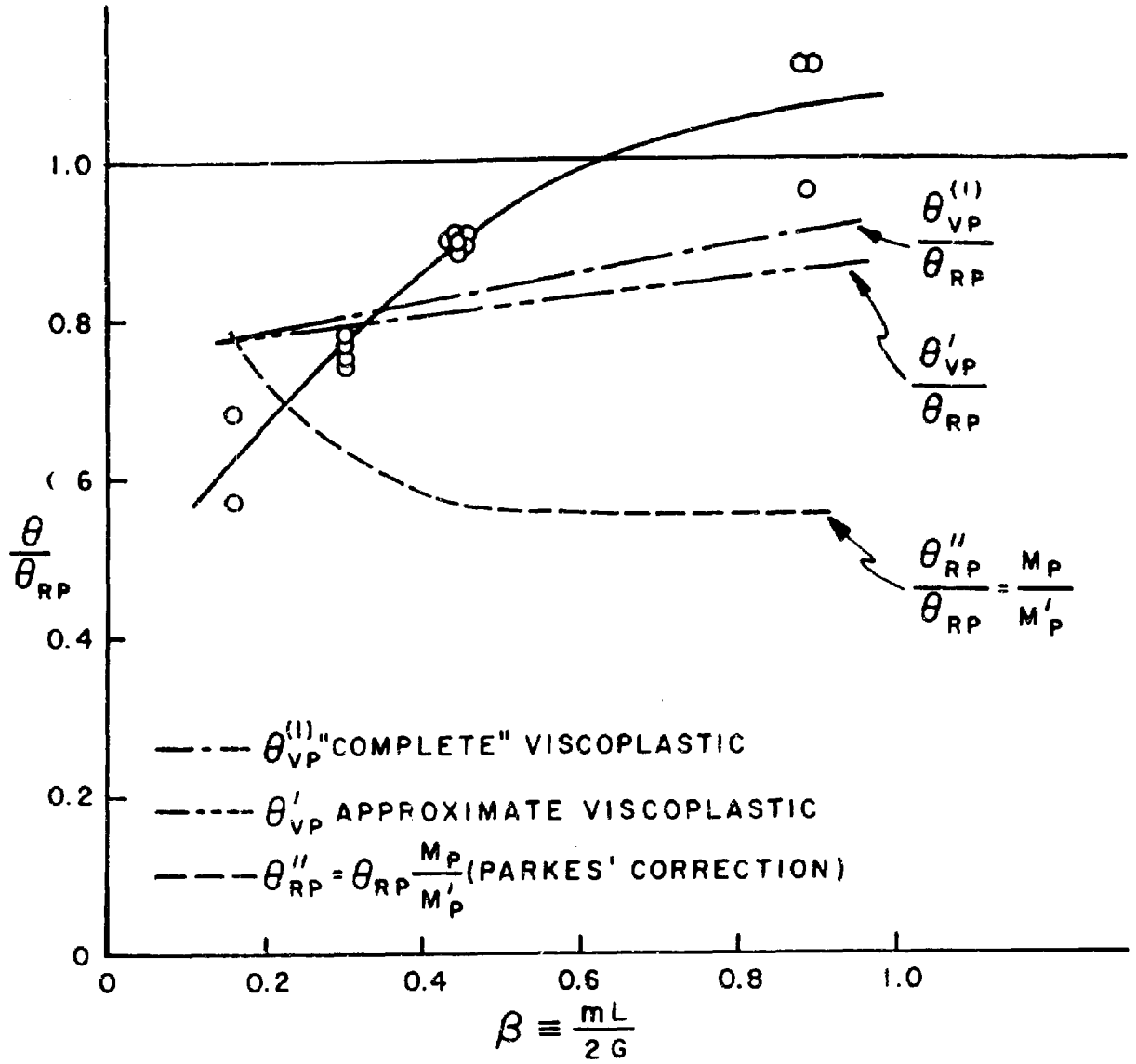

BODNER AND SYMONDS "IMPULSE" EXPERIMENTS ON MILD STEEL

FIG. III 26

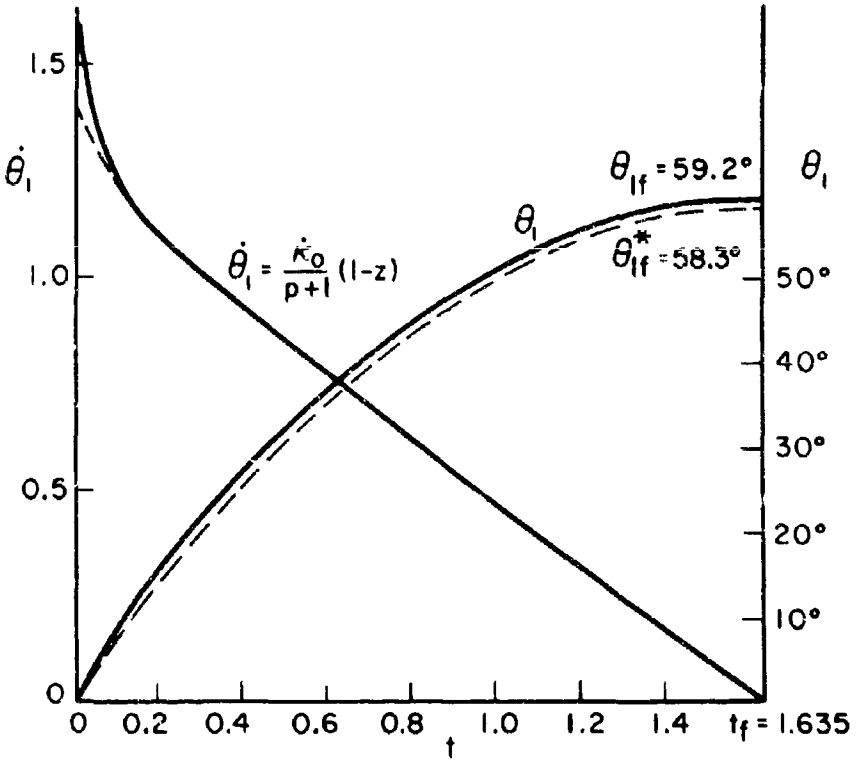

FIG. III 27

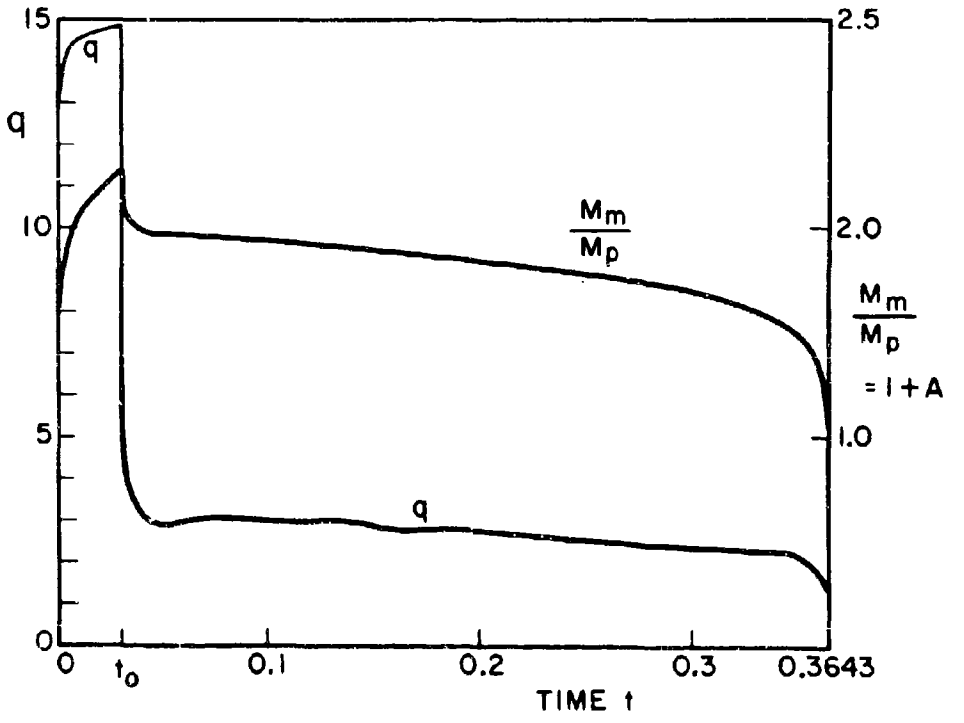

FIG. III 28

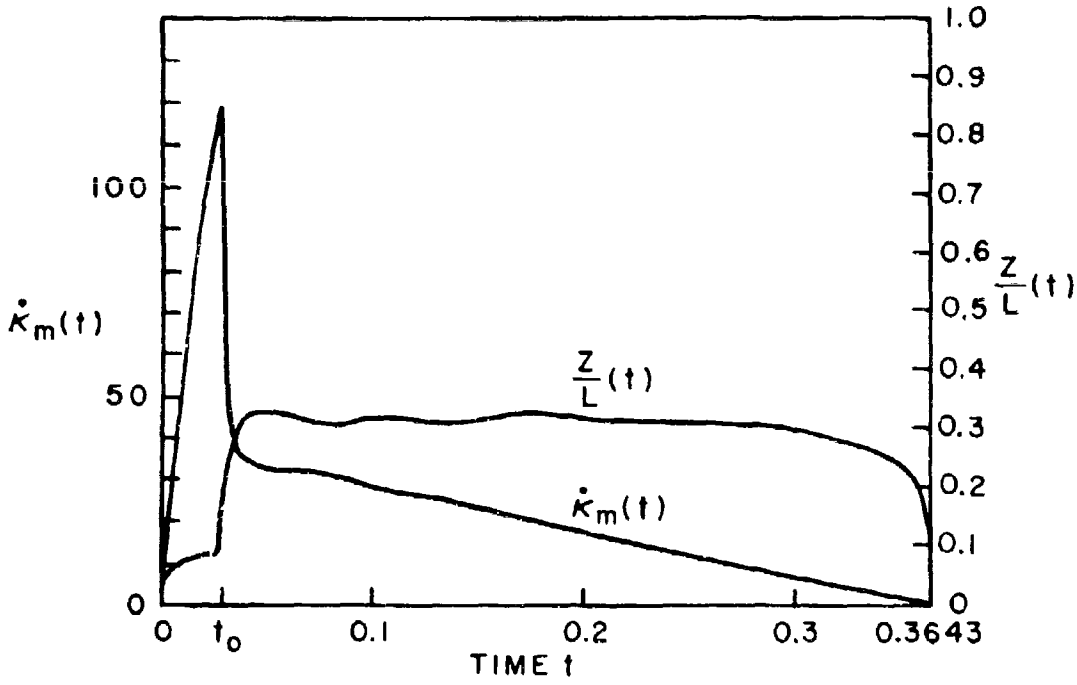

FIG. III 29 (a)

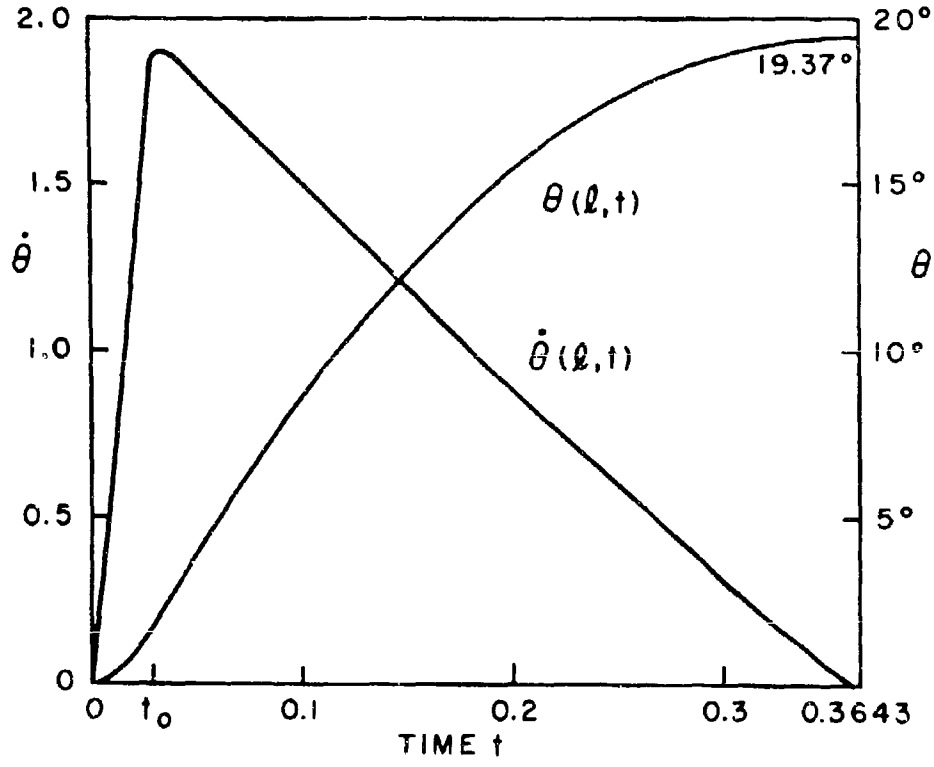

FIG. III 29 (b)

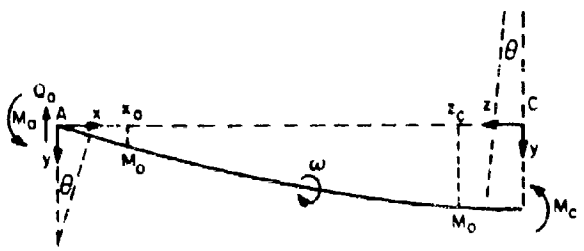

CLAMPED HALF-BEAM DURING PHASE 2

FIG. III 30

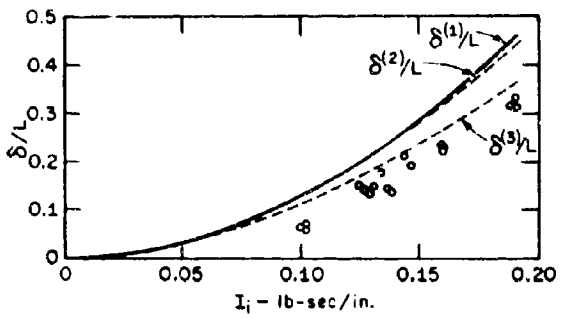

IMPULSE VERSUS CENTRAL DEFLECTION – PINNED (PS) C.R. 1018 STEEL

FIG. III 31(a)

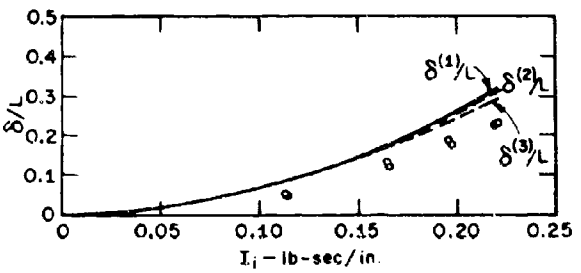

IMPULSE VERSUS CENTRAL DEFLECTION-CLAMPED (CS) C.R. 1018 STEEL

FIG. III 31(b)

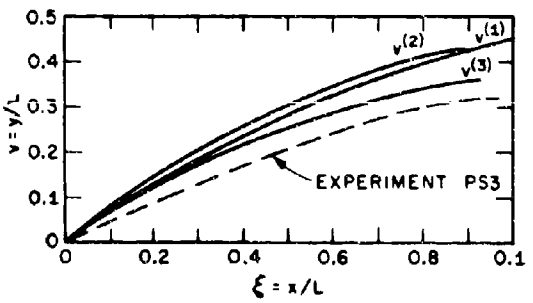

PERMANENT DEFORMATION CURVES – PINNED C.R. 1018 STEEL

FIG. III 31(c)

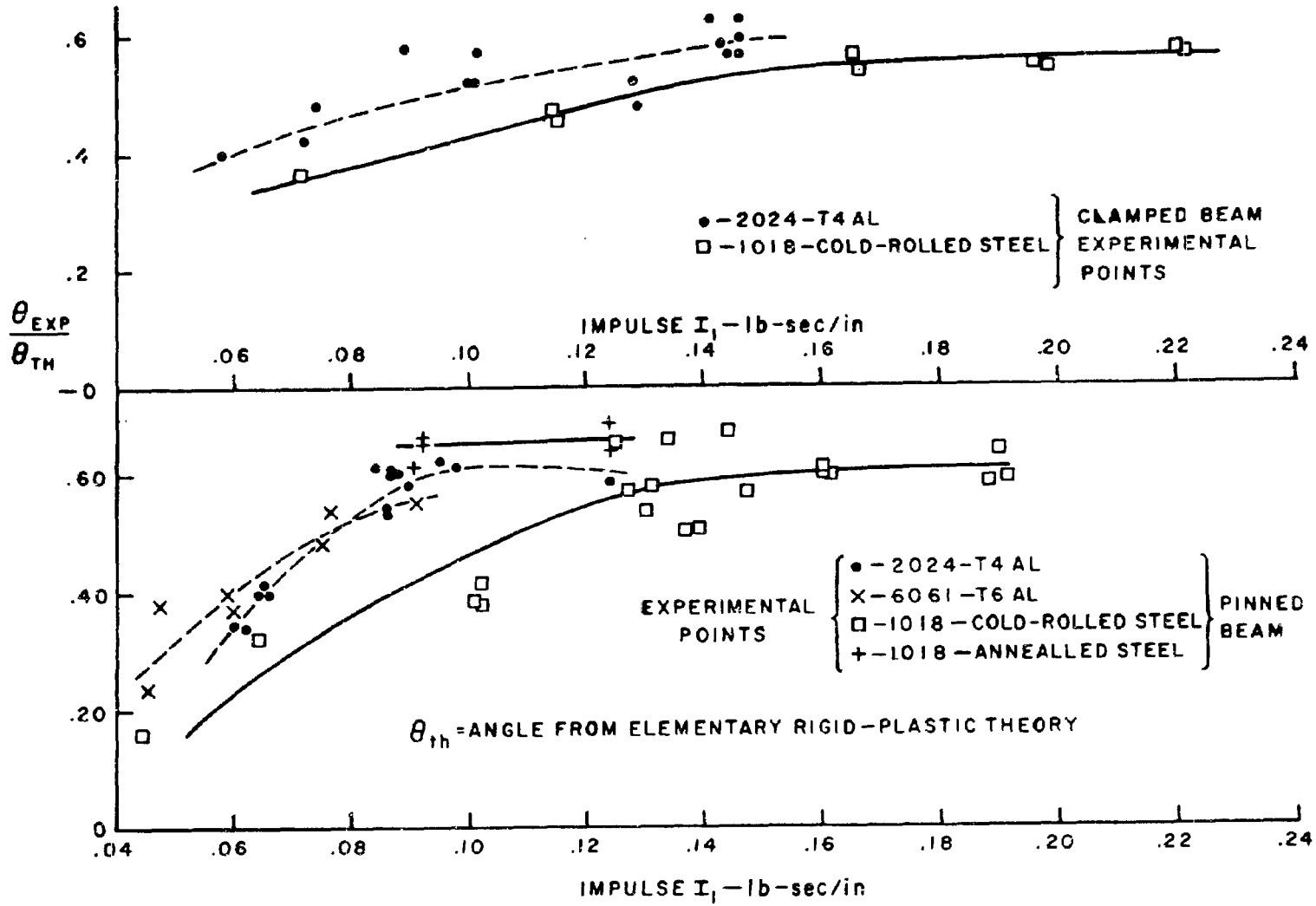
.6
.4
.2
$\frac{\theta_{EXP}}{\theta_{TH}}$
0
.06
.08
.10
.12
.14
.16
.18
.20
.22
.24
IMPULSE I_1 — lb-sec/in
● — 2024-T4 AL
□ — 1018-COLD-ROLLED STEEL
CLAMPED BEAM EXPERIMENTAL POINTS
.60
.40
.20
0
.04
EXPERIMENTAL POINTS
● — 2024-T4 AL
× — 6061-T6 AL
□ — 1018 — COLD-ROLLED STEEL
+ — 1018 — ANNEALLED STEEL
PINNED BEAM
θ_{th} = ANGLE FROM ELEMENTARY RIGID-PLASTIC THEORY
IMPULSE I_1 — lb-sec/in

FIG. III 32

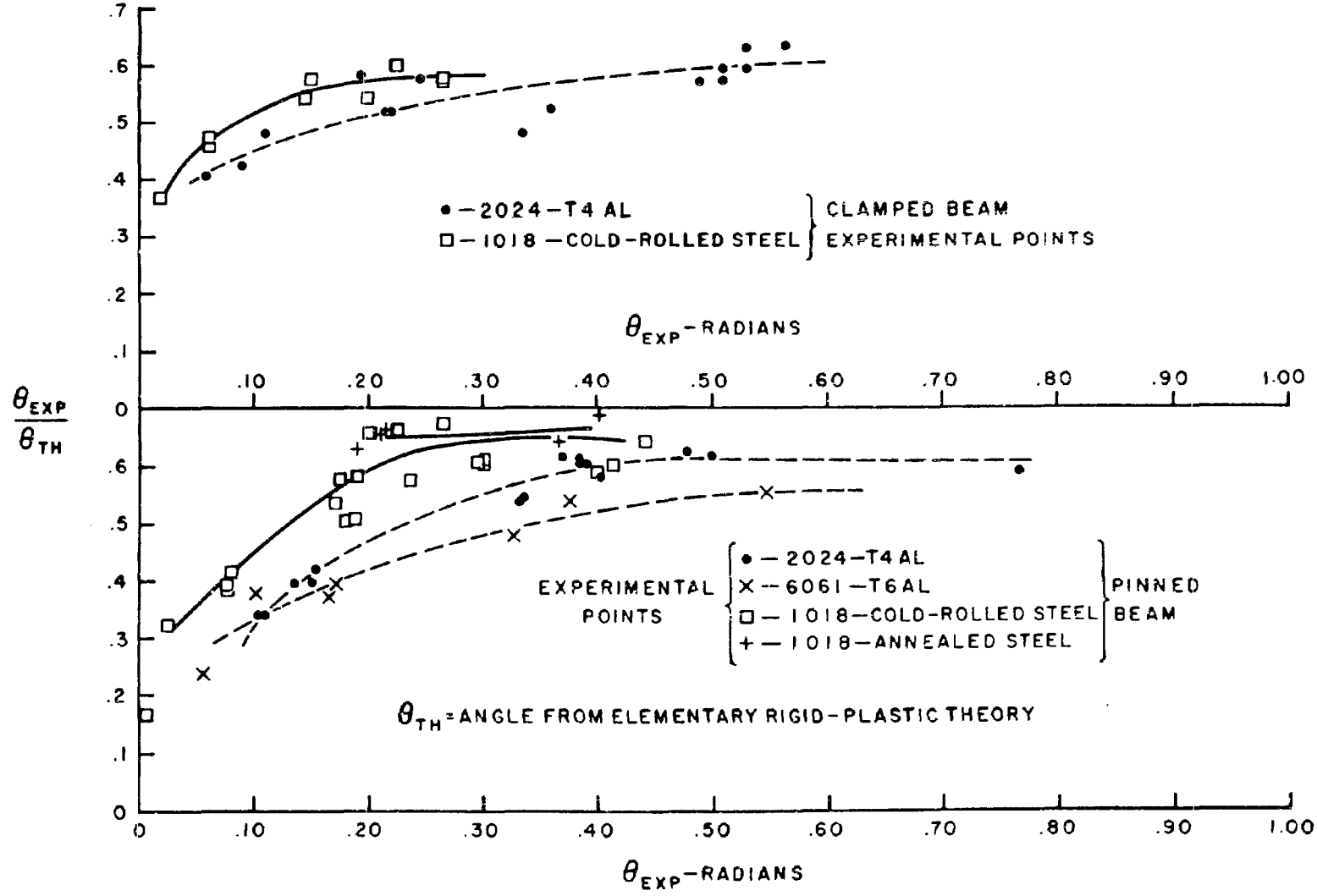
.7
.6
.5
.4
.3
.2
.1
0
• — 2024 — T4 AL
□ — 1018 — COLD-ROLLED STEEL
CLAMPED BEAM
EXPERIMENTAL POINTS
θ_{EXP} - RADIANS
.10 .20 .30 .40 .50 .60 .70 .80 .90 1.00
$\frac{\theta_{EXP}}{\theta_{TH}}$
EXPERIMENTAL POINTS
• — 2024 — T4 AL
× — 6061 — T6 AL
□ — 1018 — COLD-ROLLED STEEL
+ — 1018 — ANNEALED STEEL
PINNED BEAM
θ_{TH} = ANGLE FROM ELEMENTARY RIGID-PLASTIC THEORY
0 .10 .20 .30 .40 .50 .60 .70 .80 .90 1.00
θ_{EXP} - RADIANS

FIG. III 33

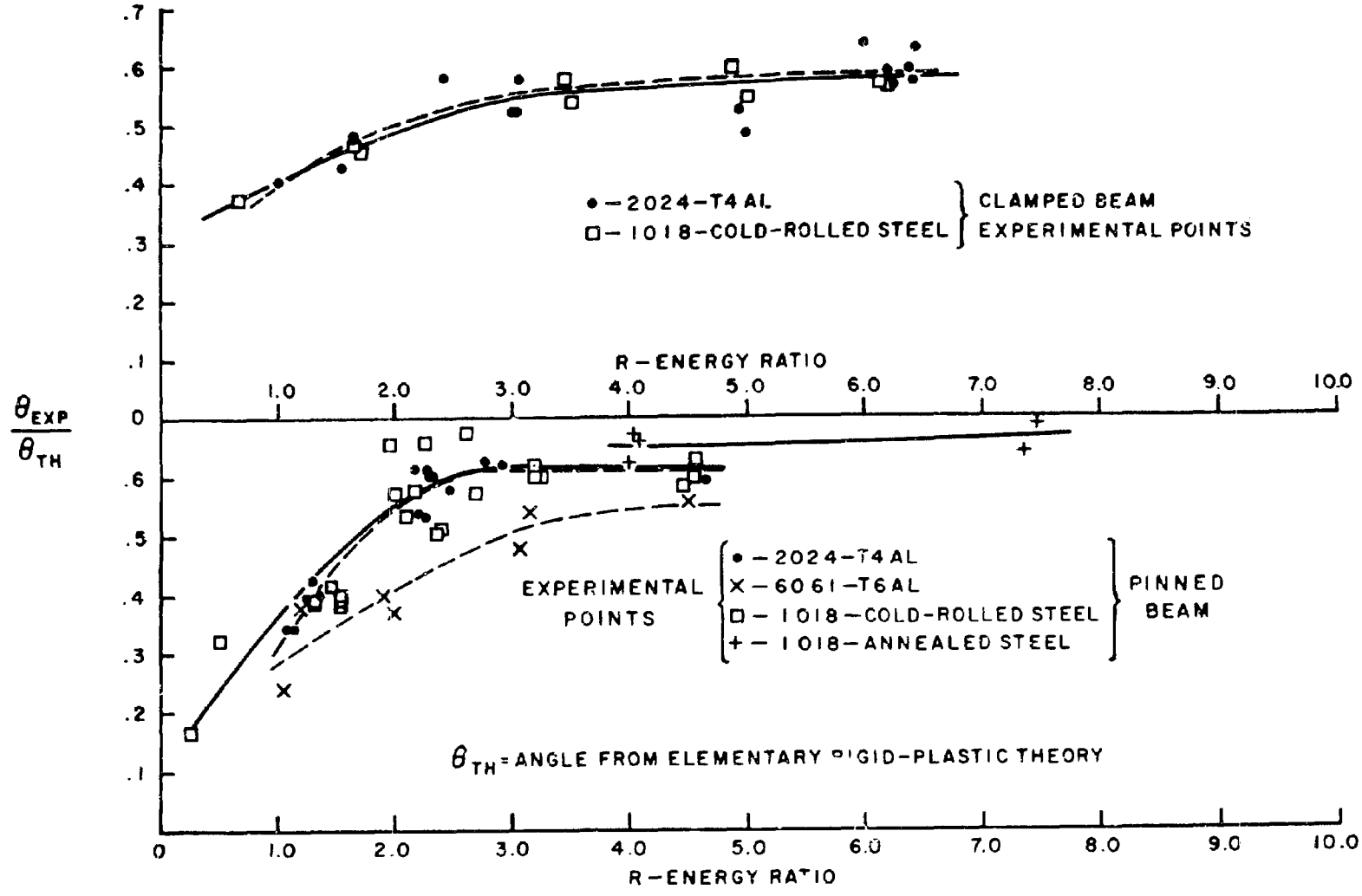
.7
.6
.5
.4
.3
.2
.1
0
$\frac{\theta_{EXP}}{\theta_{TH}}$
• – 2024–T4 AL.
□ – 1018–COLD-ROLLED STEEL
CLAMPED BEAM EXPERIMENTAL POINTS
R – ENERGY RATIO
1.0
2.0
3.0
4.0
5.0
6.0
7.0
8.0
9.0
10.0
EXPERIMENTAL POINTS
• – 2024–T4 AL
× – 6061–T6 AL
□ – 1018–COLD-ROLLED STEEL
+ – 1018–ANNEALED STEEL
PINNED BEAM
θ_{TH} = ANGLE FROM ELEMENTARY RIGID–PLASTIC THEORY
R – ENERGY RATIO

FIG. III 34

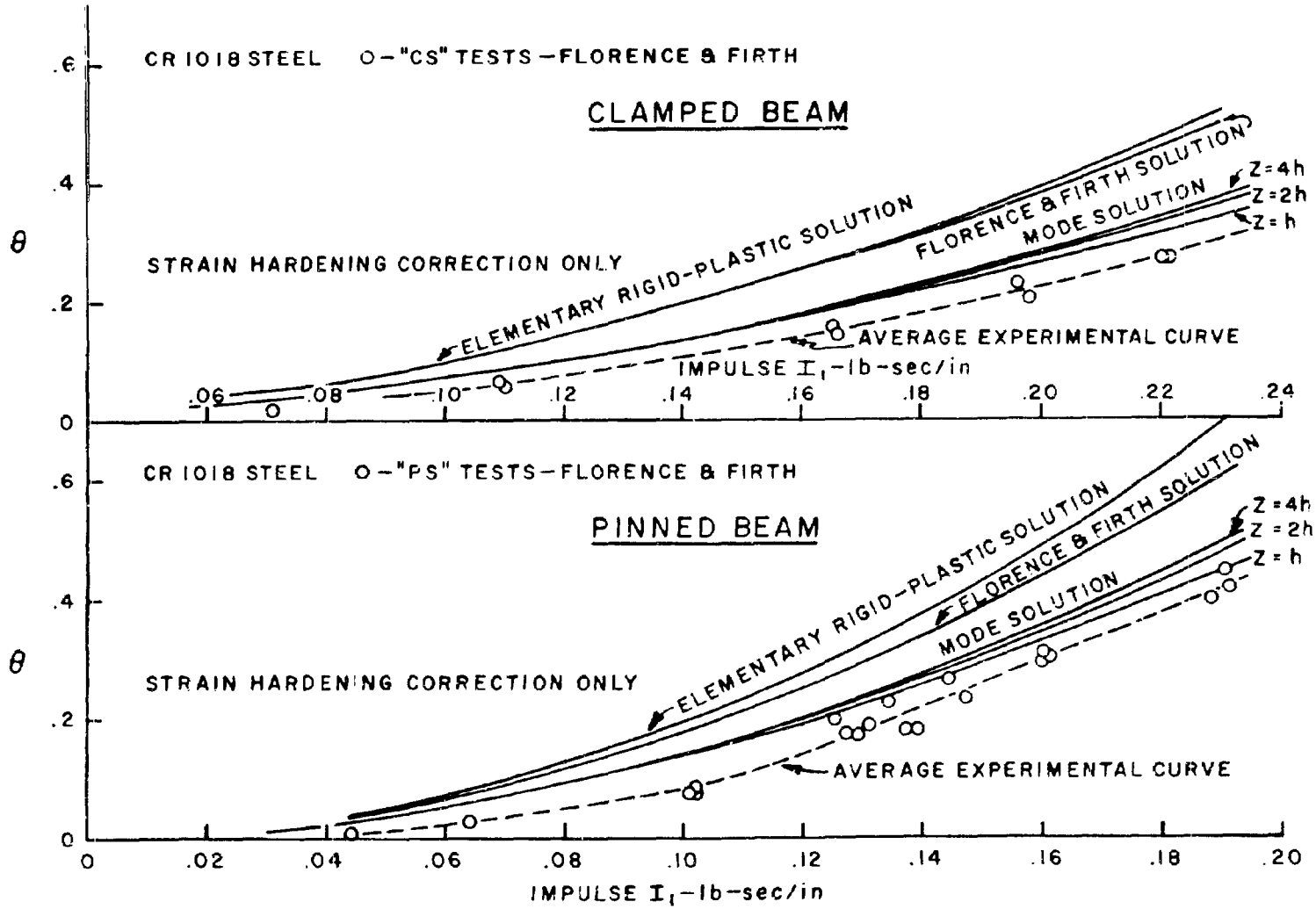
CR 1018 STEEL O-"CS" TESTS-FLORENCE & FIRTH
CLAMPED BEAM
θ
.6
.4
.2
0
STRAIN HARDENING CORRECTION ONLY
ELEMENTARY RIGID-PLASTIC SOLUTION
FLORENCE & FIRTH SOLUTION
MODE SOLUTION
Z = 4h
Z = 2h
Z = h
AVERAGE EXPERIMENTAL CURVE
IMPULSE I_1 - lb-sec/in
.06
.08
.10
.12
.14
.16
.18
.20
.22
.24
CR 1018 STEEL O-"PS" TESTS-FLORENCE & FIRTH
PINNED BEAM
θ
.6
.4
.2
0
STRAIN HARDENING CORRECTION ONLY
ELEMENTARY RIGID-PLASTIC SOLUTION
FLORENCE & FIRTH SOLUTION
MODE SOLUTION
Z = 4h
Z = 2h
Z = h
AVERAGE EXPERIMENTAL CURVE
0
.02
.04
.06
.08
.10
.12
.14
.16
.18
.20
IMPULSE I_1 - lb-sec/in

FIG. III 35

BIBLIOGRAPHY

Allen, F. J., 1955, "An Elastic-Plastic Theory of the Response of Cantilevers to Air Blast Loading", BRL Memorandum Report 886, April.

Alverson, R. C., 1956, "Impact with Finite Acceleration Time of Elastic and Elastic-Plastic Beams", J. Appl. Mechanics Vol. 23, pp. 411-415.

Alverson, R. C., 1958, "Numerical Solutions for Elastic-Plastic Beams by Method of Characteristics", Tech. Rept. 46, Brown University to Office of Naval Research, December.

Aspden, R. J., 1963, "The Effect of Rate of Strain on the Plastic Bending of Beams", Thesis for D. Phil., Oxford University, Engineering Laboratory, December.

Aspden, R. J., and J. D. Campbell, 1966, "The Effect of Loading Rate on the Elasto-Plastic Flexure of Steel Beams", Proc. Roy. Soc. A. Vol. 290, pp. 266-285.

Baron, H. G., 1956, "The Stress-Strain Curves of Some Metals and Alloys at Low Temperatures and High Rates of Strain", J. Iron and Steel Institute, Vol. 182, p. 354.

Baron, M. L., and H. H. Bleich, and P. Weidlinger, 1961, "Dynamic Elastic-Plastic Analysis of Structures", J. Engr. Mech. Div., ASCE, EM-1, February.

Bell, J. F., and Albert Stein, 1962, "The Incremental Loading Wave in the Pre-Stressed Plastic Field", Jour. de Mécanique Vol. 1, No. 4, pp. 395-412, December.

Bell. J. F., 1963, "Single Temperature-Dependent, Stress-Strain Law for the Dynamic Deformation of Annealed Face-Centered Cubic Metals", J. Appl. Physics, Vol. 34, No. 1, pp. 134-141.

Bell, J. F., 1966, "An Experimental Diffraction Grating Study of the Quasi-Static Hypothesis of the Split Hopkinson Bar Experiment", Jour. Mech. Phys. Solids, Vol. 14, pp. 309-328.

Belsheim, R. O., 1954, "Delayed-Yield Time Effect in Mild Steel Under Oscillatory Axial Loads", Naval Research Laboratory, Report No. 4312, March.

Bleich, H. H., and M. G. Salvadori, 1955, "Impulsive Motion of Elasto-Plastic Beams", ASCE, Vol. 120, pp.499-520.

Bleich, H. H., 1956, "Response of Elastoplastic Structures to Transient Loads", New York Academy of Sciences, pp. 135-143.

Bodner, S. R., and P. S. Symonds, 1960, "Plastic Deformations in Impact and Impulsive Loading of Beams", pp. 488-500. "Plasticity" Proc. 2nd Symposium on Naval Structural Mech., E. H. Lee and P. S. Symonds, Eds. Pergamon Press, Oxford and New York.

Bodner, S. R. and P. S. Symonds, 1962, "Experimental and Theoretical Investigation of the Plastic Deformation of Cantilever Beams Subjected to Impulsive Loading", Jour. Appl. Mech., Vol. 29, No. 4, pp. 719-727.

Bodner, S. R. and W. G. Speirs, 1963, "Dynamic Plasticity Experiments on Aluminum Cantilever Beams at Elevated Temperature", J. Mech. Phys. Solids, Vol. 11, pp. 65-77.

Bodner, S. R. and J. S. Humphreys, 1964, "Determination of the Rate Dependence of the Yield Stress from Impulse Testing of Beams", Bulletin No. 33, Shock Vibrations and Associated Environments, pp. 141-147.

Bodner, S. R., 1967, "Deformation of Rate Sensitive Structures under Impulsive Loading", Rep. MML No. 7, Technion-Israel Institue of Technology, Faculty of Mech. Engr., Material Mech. Laboratory.

Boussinesq, M. J., 1885, "Application des Potentiels a l'Étude de l'Équilibre et du mouvement des Solides Élastiques", Gauthier-Villars, Paris, p. 444.

Brown, A. F. C. and N. D. G. Vincent, 1941, "The Relationship Between Stress and Strain in the Tensile Impact Test", Proc. Inst. Mech. Engrs., London, Vol. 145, pp. 126-134.

Campbell, J. D. and K. J. Marsh, 1962, "The Effect of Grain Size on the Delayed Yielding of Mild Steel", Phil. Mag. Vol. 7, pp. 933-952.

Clark, D. S. and P. Duwez, 1950, "The Influence of Strain Rate on Some Tensile Properties of Steel:, Proc.ASTM, Vol. 50, pp. 560-575.

Clark, D. S. and D. S. Wood, 1949, "The Time Delay for the Initiation of Plastic Deformation at Rapidly Applied Constant Stress", Proc. Amer. Soc. Testing Materials, Vol. 49, p. 717.

Conroy, M. F., 1952, "Plastic-Rigid Analysis of Long Beams Under Transverse Impact Loading", J. Appl. Mech., Vol. 19, No. 4, pp. 465-470.

Conroy, M. F., 1956, "Plastic Deformation of Semi-Infinite Beams due to Transverse Impact", J. Appl. Mech., Vol. 23, pp. 239-243.

Costello, E. de L., 1957, "Yield Strength of Steel at an Extremely High Rate", Proc. Conf. on Properties of Materials at High Rates of Strain, London, p. 13-21. Publ. Inst. of Mech. Engrs.

Cowper, G. R. and P. S. Symonds, 1957, "Strain-Hardening and Strain-Rate Effects in the Impact Loading of Cantilever Beams", Tech. Rep. 28, Off. of Naval Research, Contract Nonr-562(10), Nr-064-406.

Drucker, D. C., 1956, "The Effect of Shear on the Plastic Bending of Beams", J. Appl. Mech., Vol. 23, pp. 509-514.

Duwez, P. E., D. S. Clark, D. S. Wood, and H. F. Bohnenblust, 1942, "Behavior of Long Beams Under Impact Loading", NDRC Armor & Ord. Rept A-216, OSRD 1828.

Duwez, P. E., D. S. Clark, and H. F. Bohnenblust, 1950, "The Behavior of Long Beams Under Impact Loading", J. Appl. Mech., Vol. 17, pp. 27-34.

Evans, R. H., 1942, "Effect of Rate of Loading on the Mechanical Properties of Some Materials", J. Instn. Civil. Engrs., Vol. 18, p. 296.

Ezra, A. A., 1958,"The Plastic Response of a Simply Supported Beam to an Impact Load at the Center", Proc. 3rd U.S. Natl. Cong Appl. Mech., ASME, N. Y. pp. 513-520.

Florence, A. L. and R. D. Firth, 1965, "Rigid-Plastic Beams Under Uniformly Distributed Impulses", J. Appl. Mech., Vol. 32, pp. 481-488.

Fox, E. N., 1947, "A Review of Underwater Explosion Phenomena", Underwater Explosion Research, Vol. I, "The Shock Wave", pp. 1-83, Off. of Naval Res., Dept. of the Navy.

Gillis, P. P. and S. Lerner, 1960, "Plastic Deformation of Cantilever Beams Under Impact--Some Experimental Results", Tech. Rep. Brown Univ. to Natl. Science Foundation, Res. Grant No. 8188, Rep. NSF-G8188/5.

Goldsmith, W., 1960, "Impact--The Theory and Physical Behavior of Colliding Solids", Edw. Arnold, Publishers, London.

Green, D. S., 1954, "The Effect of Acceleration Time on Plastic Deformation of Beams Under Transverse Impact Loading", Tech. Rep. NR-041-032 from Brown Univ. to Off. of Naval Res.

Green, S. J., C. J. Maiden and S. G. Babcock, 1966, "Tensile and Compressive Strain Tests on Aluminum and Aluminum Alloys from Rates of 10^{-3} In/In/Sec to 10^{4} In/In/Sec", Proc. U.S. Natl. Cong. Appl. Mech., p. 556, ASME, N. Y.

Hall, W. J. and N. M. Newmark, 1955, "Shear Deflection de Flange Steel Beams in the Plastic Range", Proc. ASCE, Engr. Mech. ., Paper 814, Vol. 81 pp. 814-1 - 814-30.

Harding, J., E. O. Wood, and J. D. Campbell, 1960, "Tensile Testing of Materials at Impact Rates of Strain", J. Mech. Engrg. Science, Vol. 2, pp. 88-96.

Hauser, F. E., J. A. Simmons, and J. E. Dorn, 1961, "Strain Rate Effects in Plastic Wave Propagation", Response of Metals to High Velocity Deformation, P. G. Shewmon & V. F. Zackay, Eds., Interscience Publrs, N.Y., pp. 93-110.

Hoge, K. G., 1965, "The Influence of Strain Rate on Mechanical Properties of 6061-T6 Aluminum Under Uniaxial and Biaxial States of Stress", Presented at 2nd Intern. Cong on Experimental Mechanics, Washington, D. C.

Hopkinson, B., 1904, "The Effects of Momentary Stresses in Metals, Proc. Roy. Soc., London, Vol. 74, p. 498.

Johnson, P. C., B. A. Stein, and R. S. Davis, 1963, "Measurement of Dynamic Plastic Flow Properties Under Uniform Stress", ASTM Special Technical Publication No. 336, (Materials Science Series-5), Philadelphia, pp. 195-207.

Jones, P. G. and H. F. Moore, 1940, "An Investigation of the Effect of Rate of Strain on the Results of Tension Tests of Metals", Proc. ASTM, Vol. 40, p. 610.

Karnes, C. H. and E. A. Ripperger, 1966, "Strain Rate Effects in Cold Worked High-Purity Aluminum", J. Mech. Phys. Solids, Vol. 14, pp. 75-88.

Karunes, B. and E. T. Onat, 1960, "On the Effect of Shear on Plastic Deformation of Beams Under Transverse Impact Loading", J. Appl. Mech. Vol. 27, p. 107.

Keil, A. H., 1960, "Problems of Plasticity in Naval Structures: Explosive and Impact Loading", Proc. of 2nd Symposium on Naval Struc. Mech., Eds: E. H. Lee & P. S. Symonds, Pergamon Press, N. Y.

Kolsky, H., 1966, "Experimental Stress Wave Propagation", Cong. Survey Lecture, Proc. 5th U. S. Natl. Cong. Appl. Mech., ASME, N. Y.

Krafft, J. M., and A. M. Sullivan, 1959, "Effect of Grain Size and Carbon Content on the Yield Delay-Time of Mild Steel", Trans. Am. Soc. Metals, Vol. 51, pp. 643-659.

Lee, E. H. and P. S. Symonds, 1952, "Large Plastic Deformations of Beams Under Transverse Impact", J. Appl. Mech., Vol. 19, pp. 308-314.

Lee, E. H. and S. J. Tupper, 1954, "Analysis of Plastic Deformation in a Steel Cylinder Striking a Rigid Target", J. Appl. Mech., Vol. 21, pp. 63-70.

Lindholm, U. S., 1965, "Dynamic Deformation of Metals", Proc. of Colloq. Behavior of Materials Under Dynamic Loading, (N. J. Huffington, Jr. Ed.) ASME, pp. 42-61, N. Y.

Malvern, L. E., 1965, "Experimental Studies of Strain-Rate Effects and Plastic Wave Propagation in Annealed Aluminum", Proc. Colloq. Behavior of Materials Under Dynamic Loading, pp. 81-92, ASME, N. Y.

Manjoine, M. J., 1944, "Influence of Rate of Strain and Temperature on Yield Stresses of Mild Steel", J. Appl. Mech., Vol. 11, A-211 - A-218.

Marsh, K. J. and J. D. Campbell, 1963, "The Effect of Strain Rate on the Post-Yield Flow of Mild Steel", J. Mech. Phys. Solids, Vol. 11, pp. 49-63

Martin, J. B., 1964, "Impulsive Loading Theorem for Rigid Plastic Continua", Proc. Eng. Mech. Div., ASCE, Vol. 90 (EM5), p. 27-42.

Martin, J. B., 1965, "A Displacement Bound Principle for Inelastic Continua Subjected to Certain Classes of Dynamic Loading", J. Appl. Mech., Vol. 32, pp. 1-6.

Martin, J. B., 1966, "The Determination of Upper Bounds on Displacements Resulting from Static and Dynamic Loading by the Application of Energy Methods", Proc. 5th U.S. Natl. Cong. Appl. Mech., ASME, N. Y., pp. 221-236.

Martin, J. B. and P. S. Symonds, 1966, "Mode Approximations for Impulsively Loaded Rigid-Plastic Structures", Proc. ASCE, J. Engr. Mech. Div., Vol. 92, pp.43-66

Massard, J. M. and R. A. Collins, 1958, "The Engineering Behavior of Structural Metals Under Slow and Rapid Loading", U. of Illinois, Civil Engr. Studies, Structural Res. Series No. 161, Tech. Rep to Off. Naval Res., Contract Nonr 1834(01).

Mentel, T. J., 1958, "The Plastic Deformation due to Impact of a Cantilever Beam with an Attached Tip Mass", J. Appl. Mech., Vol. 25, p. 515.

Nadai, A. and M. J. Manjoine, 1940, "High Speed Tension Tests at Elevated Temperatures" Pt. I, Proc. ASTM, Vol. 40, pp. 822-839.

Nadai, A. and M. J. Manjoine, 1941, "High Speed Tension Tests at Elevated Temperatures" Pts. II and III, J. Appl. Mech., Transactions ASME, Vol. 63, pp. A77-A91.

Newmark, N. M., 1959, "A Method of Computation for Structural Dynamics", Proc. ASCE, Engrg. Mech. Div., Vol. 85, No. EM 3, Part 1, pp. 67-94.

Neal, B. G., 1961a, "Effect of Shear Force on the Fully Plastic Moment of an I--Beam", Jour. Mech. Engrg. Science, Vol. 3, No. 3, pp. 258-266.

Neal, B. G., 1961b, "The Effect of Shear and Normal Forces on the Fully Plastic Moment of a Beam of Rectangular Cross Section", J. Appl. Mechanics, Vol. 28, pp. 269-274.

Nonaka, T., 1964, "Some Interaction Effects in a Problem of Plastic Beam Dynamics", Tech. Rept., Brown University. (Div. of Engineering) to Natl. Sci. Foundation, Report No. NSF GP1115/18.

Nonaka, T., and P. S. Symonds, 1967, "Effects of Shear on a Rigid-Plastic Beam under Blast-Type Loading", In preparation as report from Brown University (Div. of Engineering) to National Science Foundation, Grant NSF GK 1013.

Parkes, E. W., 1955, "The Permanent Deformation of a Cantilever Struck Transversely at its Tip", Proc. Roy. Soc., A, Vol. 228, pp. 462-476.

Parkes, E. W., 1956, "Some Simple Experiments on the Dynamic Plastic Behavior of Mild-Steel Beams", British Welding Journal, Vol. 3, pp. 362-366.

Parkes, E. W., 1958, "The Permanent Deformation of an Encastré Beam Struck Transversely at any Point in its Span", Proc. of the Institution of Civil Engineers, Vol. 10, July, pp. 277-304.

Perrone, N., 1965, "On a Simplified Method for Solving Impulsively Loaded Structures of Rate-Sensitive Materials", J. Appl. Mech., Vol. 32, Series E, No. 3, Sept. pp. 489-492.

Ripperger E. A., and J. W. Turnbow, 1959, "Strain-Rate Effects on Stress-Strain Characteristics of Aluminum and Copper", Proc. 4th Midwestern Conf. on Solid Mech., Univ. of Texas, Austin, pp. 415-440.

Salvadori, M. G., and P. Weidlinger, 1957, "On the Dynamic Strength of Rigid-Plastic Beams under Blast Loads", Proc. Amer. Soc. Civil Engrs, Vol. 83, EM 4, (J. Engrg. Mech) Paper 1389, pp. 35.

Seiler, J. A., 1954, "On Elastic-Plastic Deformation in Beams Under Dynamic Loading" Report A11-109, Contract N7onr - 35801, Brown University to ONR.

Seiler, J. A., B. A. Cotter, and P. S. Symonds, 1956, "Impulsive Loading of Elastic-Plastic Beams", J. Appl. Mech., Vol. 23, pp. 515-521.

Smith, R. C., T. E. Pardue, and I. Vigness, 1956, "The Mechanical Properties of Certain Steels as Indicated by Axial Dynamic Load Tests", Proc. Soc. Exp. Stress Anal. Vol. 13, No. 2, pp. 183.

Stallybrass, M. P., 1960, "The Elastic-Plastic Deformation of a Cantilever Beam Due to Transverse Impact Loading", M. Sc. Thesis to Brown University.

Steidel, R. F. Jr. and C. E. Makerov, 1960, "The Tensile Properties of Some Engi-Engineering Materials at Mod rate Rates of Strain", ASTM Bulletin, pp. 57-64 (TP123-TP130).

Symonds, P. S., 1954, "Large Plastic Deformations of Beams Under Blast Type Loading", Proc. 2nd U.S. Natl. Cong. Appl. Mech., p. 505.

Symonds, P. S. and C. F. A. Leth, 1954, "Impact of Finite Beams of Ductile Metal", J. Mech. Phys. Solids, Vol. 2, pp. 92-102.

Symonds, P. S., 1955, "Simple Solutions of Impulsive Loading and Impact Problems of Plastic Beams and Plates", Tech. Rep. No. 3, Brown Univ. to Norfolk Naval Shipyard, Underwater Explosions Res. Div.

Symonds, P. S. and T. J. Mentel, 1958, "Impulsive Loading of Plastic Beams with Axial Constraints", J. Mech. Phys. Solids, Vol. 6, pp. 186-202.

Symonds, P. S., 1965, "Viscoplastic Behavior in Response of Structures to Dynamic Loading", Proc. of Colloq. on Behavior of Materials Under Dynamic Loading, pp. 106-129, (N. J. Huffington, Jr. Ed.) ASME, N.Y.

Taylor, D. B. C. and A. Z. Tadros, 1956, "Tension and Torsion Properties of Some Metals Under Repeated Dynamic Load (Impact)", Proc. Inst. Mech. Engrs. (London),Vol. 170, pp. 1039-1051.

Taylor, G. I., 1948, "The Use of Flat Ended Projectiles for Determining Dynamic Yield--Part I--Theoretical Considerations", Proc. Roy. Soc. London, Vol. 194, Ser. A, p. 289.

Thomson, W. T., 1954, "Impulse Response of Beams in the Elastic and Plastic Regions", J. Appl. Mech., Vol. 21, pp. 271-278.

Ting, T. C. T. and P. S. Symonds, 1962, "Impact of a Cantilever Beam with Strain Rate Sensitivity", Proc. 4th U.S. Natl. Cong. Appl. Mech., ASME, NY, p. 1153-1165.

Ting, T. C. T., 1963, "On the Solution of a Non-Linear Parabolic Equation with a Floating Boundary Arising in a Problem of Plastic Impact of a Beam", Q. of Appl. Math., Vol. XXI, pp. 133-150.

Ting, T. C. T., 1964, "The Plastic Deformation of a Cantilever Beam with Strain Rate Sensitivity Under Impulsive Loading", J. Appl. Mech., Vol. 31, p. 38-42.

Vigness, I., J. M. Krafft, and R. C. Smith, 1957, "Effect of Loading History Upon the Yield Strength of a Plain Carbon Steel", Proc. Conf. on Properties of Materials at High Rates of Strain, London, Publ. Instn. of Mech. Engrs, p.138-146.

Whiffin, A. C., 1948, "The Use of Flat-Ended Projectiles for Determining Dynamic Yield Stress-II-Tests on Various Metallic Materials," Proc. Roy. Soc. Ser. A, Vol. 194, pp. 300-322.

Witmer, E. A., H. A. Balmer, J. W. Leech, and T. H. H. Pian, 1963, "Large Dynamic Deformations of Beams, Rings, Plates, and Shells", AIAA J.,Vol 1, p.1848-1857.

Witmer, E. A., E. N. Clark, and H. A. Balmer, 1967, "Experimental and Theoretical Studies of Explosive-Induced Large Dynamic and Permanent Deformations of Simple Structures", Exper. Mech., Vol 7, p. 56-66.

Unclassified
Security Classification

DOCUMENT CONTROL DATA - R & D

Security classification of title, body of abstract and indexing annotation must be entered when the overall report is classified)

1. ORIGINATING ACTIVITY (Corporate author)
Brown University, Engineering Division
Providence, Rhode Island

2a. REPORT SECURITY CLASSIFICATION
Unclassified

2b. GROUP

3. REPORT TITLE
SURVEY OF METHODS OF ANALYSIS FOR PLASTIC DEFORMATION OF STRUCTURES UNDER DYNAMIC LOADING

4. DESCRIPTIVE NOTES (Type of report and inclusive dates)
Final Technical Report

5. AUTHOR(S) (First name, middle initial, last name)
P. S. Symonds

6. REPORT DATE	7a. TOTAL NO. OF PAGES	7b. NO. OF REFS
June 30, 1967	254	95

8a. CONTRACT OR GRANT NO	9a. ORIGINATOR'S REPORT NUMBER(S)
Nonr 3248(01)(x) b. PROJECT NO.	BU/NSRDC 1-67
c.	9b. OTHER REPORT NO(S) (Any other numbers that may be assigned this report)
d.	

10. DISTRIBUTION STATEMENT
Distribution of this document is unlimited.

11. SUPPLEMENTARY NOTES	12. SPONSORING MILITARY ACTIVITY
	Naval Ship Research & Development Center Washington, D.C. 20007

13. ABSTRACT

Survey provides a critical study of methods for the analysis of metal structures under dynamic loads leading to large plastic deformation. Relevant material behavior and analytical and numerical methods are summarized. Emphasis is put on critical study of experiments, particularly on beams, with consideration of strain rate sensitive plastic behavior.

DD FORM 1 NOV 65 1473 (PAGE 1)
S/N 0101-807-6801

Unclassified
Security Classification

Security Classification

KEY WORDS	LINK A		LINK B		LINK C	
	ROLE	WT	ROLE	WT	ROLE	WT
Structures, Loading (Mechanics)						
Dynamic loading						
Structures, metal						
Rings						
Arches						
Trusses						
Plates, circular and rectangular						
Membranes						
Shells						
Cylinders						
Beams						
Spheres						
Spherical caps						
Experimental data						
Theory						
Literature search						

DD FORM 1 NOV 65 1473 (BACK)
(PAGE 2)

Unclassified
Security Classification